THE CATALYTIC CONVERSION OF LOW CHAIN LENGTH HYDROCARBONS TO LIQUID FUELS USING ION EXCHANGE RESIN

BY

WERNER KARL SCHUMANN

B.Sc. (Cape Town)

B.Sc. (Eng) (Cape Town)

Submitted to the University of Cape Town in fulfilment of the requirements for the degree of Master of Science in Engineering

ACKNOWLEDGEMENT

The author wishes to thank the following people and organizations for their assistance during his research studies:

1) Sasol for its financial and technical assistance and advice. A special thanks goes to Dr M Dry and Mr K Kriel.

2) Dr C T O'Connor for his supervision of the project, and Dr M Kojima for helpful advice, both of the Department of Chemical Engineering at the University of Cape Town.

3) Mr J van der Heyden of Caltex.

4) K.O.P. for supplying catalyst samples. A special thanks goes to Dr P J Ridgwell.

5) Rohm and Haas for supplying catalyst samples.

6) Messrs J C Q Fletcher, M W Rautenbach and D M M McClean for their helpful advice, informative discussions and their assistance. Mr M W Rautenbach is also thanked for making his computer program for data analysis available.

7) Mr K Wheeler and Mr A Barker of the Chemical Engineering Workshop.

8) Miss B Williams for the mass spectroscopic analysis.

9) Mr Hemstedt for the microanalytical analysis.

10) The NMR unit for the NMR analysis.

ABSTRACT

The use of ion exchange resins in the polymerization of a C_4-mixture to liquid fuels has shown that the catalyst is highly active, deactivates at a slow rate and selectively produces mainly dimers. Macropore diffusion resistance strongly influences the overall rate of the reaction. An increase in liquid production rate is obtained with increasing macroporosity, increasing degree of functionalization and decreasing catalyst bead size. A minimum acid strength of $pK_A = -2.4$ is required. The liquid production rate is increased by increasing the reaction temperature and weight hourly space velocity. Moreover, longer chain length product are obtained with increasing reaction temperature and at reaction conditions, which result in the complete conversion of monomers. Recycling liquid product reduces the liquid production and increases the production of trimer at the expense of dimer.

At moderate reaction temperatures ion exchange resins are regenerable but the activity of the catalyst is destroyed at reaction temperatures greater than approximately 130°C. Deactivation occurs parallel to the main reaction and is due to cationic fouling. The liquid product obtained is highly branched. The R.O.N. of the -180°C fraction is approximately 97 and the cetane number of the +180°C fraction approximately 35.

TABLE OF CONTENT

LIST OF FIGURES

CHAPTER 1

CHAPTER 3

CHAPTER 4

CHAPTER 7

LIST OF TABLES

CHAPTER 1

CHAPTER 3

CHAPTER 4

CHAPTER 7

NOMENCLATURE

Terminology

ASTM	American Society for Testing of Materials
DVB	Divenylbenzene
D.W.C.	Dry weight capacity (equivalent/gram)
F.I.D.	Flame ionization detector
G.C.	Gas chromatography
IP	British Institute of Petroleum
LHSV	Liquid hourly space velocity
L.P.R.	Liquid production rate (weight of liquid product/(hour x weight of catalyst))
M.O.N.	Motor octane number
NMR	Nuclear magnetic resonance
PS	polystyrene
R.O.N.	Research octane number
R.R.F.	Relative response factor
T.C.D.	Thermal conductivity detector
T.I.C.	Total ion current
WHSV	Weight hourly space velocity
TR	Reaction temperature
p	Reaction pressure

1. INTRODUCTION

In South Africa the oil-from-coal industry has developed the first commercial process, whereby synthetic fuels are produced from coal via gasification using Fischer-Tropsch catalysts. It started in 1943 when the American rights to the Fischer-Tropsch process were purchased by South Africa. In 1950 the South African Oil, Coal and Gas Corporation (Sasol) was formed. The first plant, Sasol I, with a capacity of 4130 barrels/ day (1) went into operation in 1954. It uses two types of reactors, namely the Arge fixed bed and the Synthol fluidized bed reactors. Two further plants, Sasol II and III, which are improved and enlarged versions of Sasol I, were later built, each having a capacity of 35900 barrels/ day (1). In both of these plants only Synthol reactors are used. Tables 1.1 and 1.2 show a typical hydrocarbon product spectrum for the Arge and the Synthol reactors respectively (2), as well as that of a typical crude oil (4). It is readily seen that Sasol also produces significant quantities of light hydrocarbon gases. The latter fraction, which amounts to approximately $1.5 \times 10^6 m^2$/ day (1), is partly reticulated to local industry and partly converted, via a catalytic polymerization process, to liquid fuels, thereby increasing overall production in terms of barrels of liquid fuel produced per ton of coal processed. Currently Sasol I can more than satisfy the local gas demand and therefore the light hydrocarbons from Sasol II and Sasol III represent excess supply.

The catalytic polymerization process referred to in the above uses the conventional phosphoric acid catalyst to polymerize the light hydrocarbons to liquid fuels. This process, however, produces relatively little diesel and a relatively poor quality of petrol and diesel. In addition, the catalyst is corrosive.

Figure 1.1 shows some figures on the South African demand for petrol and diesel (1). From this figure, it can be seen that while demand for petrol rose by 3% over the period 1973 to 1976, the demand for diesel rose by 22% over the corresponding period. Further, diesel

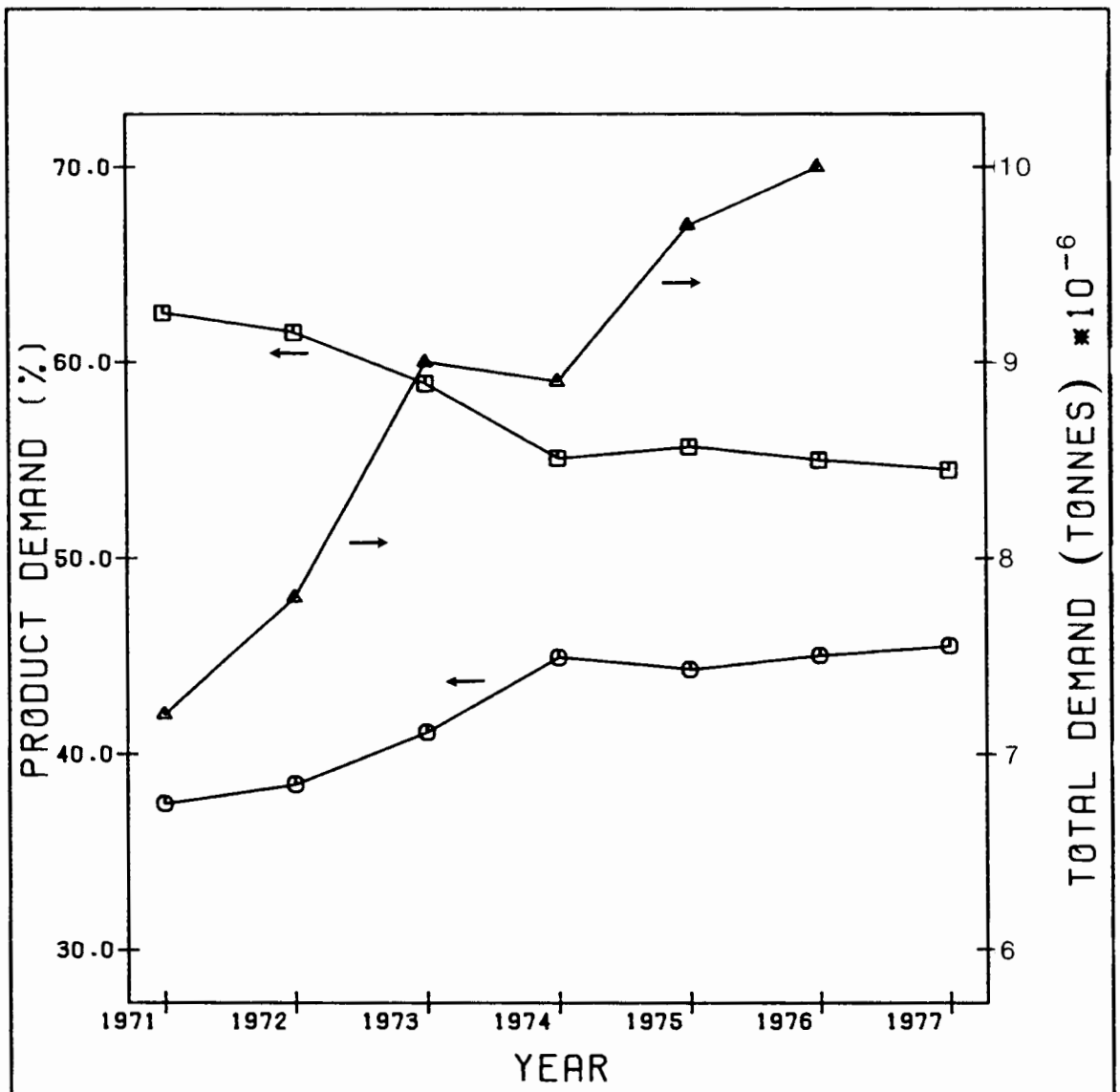

FIG.1.1 RSA FUEL CONSUMPTION

Selectivities, %	Fixed bed		Synthol	
CH_4	5.0		10.0	
C_2H_4 C_2H_6	2.6		10.0	
C_3H_6 C_3H_8	4.8		14.0	
C_4H_8 C_4H_{10}	5.2		9.0	
Petrol C_5-C_{12}	22.5		39.0	
Diesel C_{13}-C_{18}	15.0		5.0	
Heavy oils C_{19}-C_{21}	6.0		1.0	
C_{22}-C_{30}	17.0		3.0	
wax C_{31}^+	18.0		2.0	
NAC	3.5		6.0	
Acids	0.4		1.0	
	C_5-C_{12}	C_{13}-C_{18}	C_5-C_{10}	C_{11}-C_{14}
% Paraffins	53	65	13	15
% Olefins	40	28	70	60
% Aromatics	0	0	5	15
% Alcohols	6	6	6	5
% Carbonyls	1	1	6	5
% n-Paraffins	95	93	55	60

Table 1.1 : Typical hydrocarbon product spectrum obtained from a fixed bed and Synthol reactor

Fraction	Boiling Point Range (°C)	Yield (vol %)
light naphtha	20 - 100	10.0
heavy naphtha	100 - 150	8.7
kerosene	150 - 235	18.7
light gas oil	235 - 343	21.2
heavy gas oil	343 - 565	30.3
residual oil	565^{+}	9.0

Table 1.2 : Assay of a typical crude oil, Arabian light (Berri) (4)

consumption is often a reflection of a country's economic growth and, while South Africa might be in a temporary recession, future economic development will increase diesel consumption. Therefore one may assume that the petrol consumption remains fairly constant, and that the diesel consumption continues increasing. This suggests that currently there is an imbalance in the South African fuel supply.

The present study has investigated an alternative catalyst for the catalytic polymerization of the light hydrocarbons to liquid fuels. In using organic ion exchange resins as heterogeneous catalysts, one has detailed knowledge about the number and chemical nature of the catalytically active groups as well as their physical environment, all of which can be easily altered. The main objective of this study has been to increase the quality and quantity of the liquid fuels, resulting from the polymerization reaction.

The experimental work was carried out in a high pressure fixed-bed reactor. The activity and selectivity of the catalyst as well as the qualities of the liquid product were analysed using, inter alia, gas chromatography(G.C.), mass spectroscopy, nuclear magnetic resonance (N.M.R.), standard fuel tests and other analytical techniques.

1.1 The Catalyst

Organic ion exchange resins consist of an irregular, macromolecular, three-dimensional network of hydrocarbon chains. These are made up of linear hydrocarbon macromolecules, which are bound together by crosslinks. This structure forms the matrix to which fixed ionic groups are added. The charge of these groups is balanced by mobile counter ions, and they, together with the fixed ionic group, form the active sites of the ion exchange resins (Fig. 1.2).

While the matrix of ion exchange resins is hydrophobic, the ionic groups are hydrophilic. Both the hydrocarbon polymer and the ionic groups,together, are soluble in water. This solubility is removed by interconnecting the polymers with crosslinks. Although this makes the ion exchange resin insoluble, it allows a certain amount of swelling of the matrix. Since the matrix is random, the pore sizes are not uniform. This polydispersed pore structure can be characterised by the following three variables:

- porosity, which is the ratio of pore volume to total volume of a porous structure;
- specific pore surface area; and
- mean pore diameter and pore size distribution.

Ion exchange resins can sorb solvents and expand. The extent of swelling is determined by the balancing of osmotic and electrostatic forces, on one hand, and the tendency of the expanded matrix to contract, on the other. At equilibrium, the swelling is favoured by a number of factors:

- polar solvent, i.e. large dielectric constant;
- low degree of crosslinking;
- strong solvation tendency of the fixed ionic group;
- high capacity;
- large and strongly solvated as well as low valence counter ion; and
- low concentration of external solution.

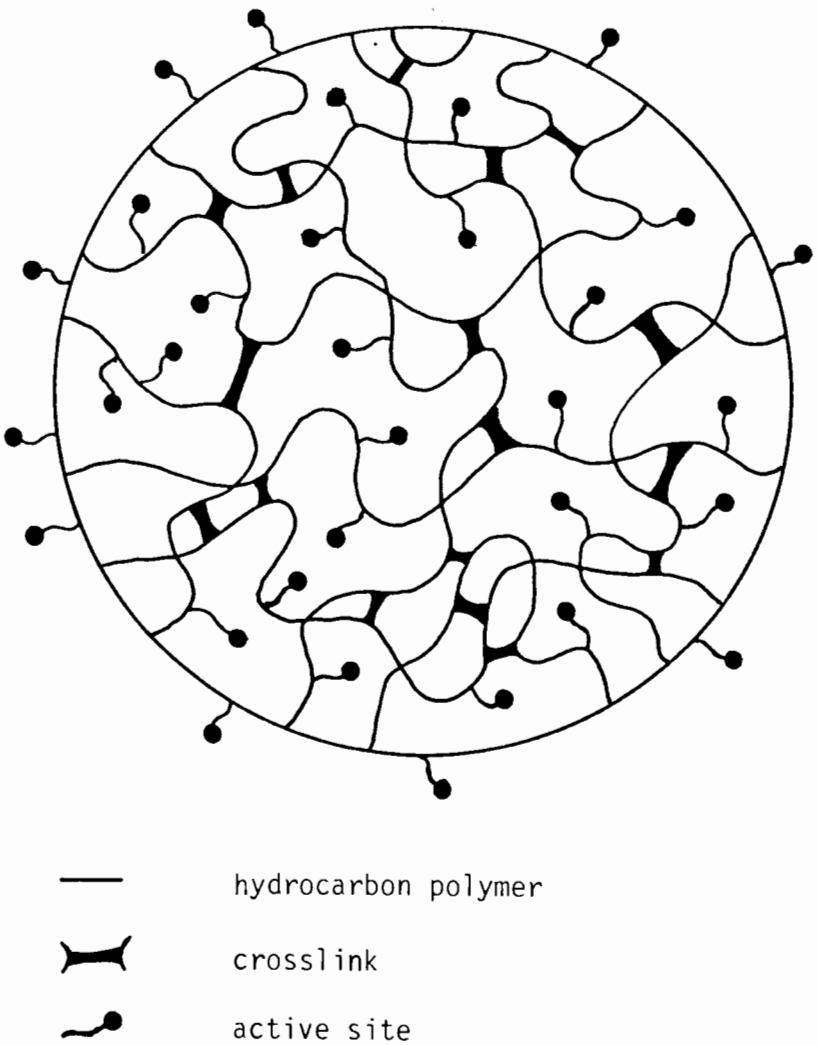

Fig. 1.2 : Pictorial presentation of ion exchange resin

While the uptake of solvents is called swelling, the uptake of solutes is called sorption. Sorption is a result of a distribution of the solute between the pore liquid and the solution. For every sorbed counter ion, a co-ion has to be sorbed in order to balance the charge.

The stability of ion exchange resins depends mainly on the structure, the degree of crosslinking of the matrix, and the nature and number of the fixed ionic groups. The higher the crosslink density of the resin, the harder and more resistant is the structure to breakdown and attrition. The limited chemical and thermal stability of resins is a frequent cause of the degradation of the matrix, e.g. by oxidation, or of the loss of the fixed ionic groups, e.g. by thermal hydrolysis.

The ion exchange behaviour of resins is determined by the fixed ionic groups. The number of ionic groups gives the ion exchange capacity. The nature of the ionic groups affects the ion exchange equilibrium. The extent of this equilibrium depends on the selectivity of the resin. Some of the empirical rules of ion exchange selectivity are given below (7):

- at low aqueous concentrations and ordinary temperatures, the extent of exchange increases with increasing valence of the exchanging ion, ($Na^{+} < Ca^{++} < La^{+++}$);
- at low aqueous concentrations, ordinary temperatures and constant valency, the extent of exchange increases with increasing atomic number, (Li <Na <K <Rb);
- at high concentrations the extent of exchange of different valences diminishes and, in some cases, the ion of lower valence has the higher exchange potential;
- at high temperatures, or in non-aqueous media, or at high concentrations, the exchange potentials of ions of similar valence do not increase with increasing atomic number but are very similar, and level off or even decrease;
- the exchange potentials of various ions may be approximated from their activity coefficient. The higher the activity co-efficient, the greater is the extent of exchange;

- the exchange potential of the hydrogen ion or the hydroxide ion depends upon the strength of the acid or base formed between the functional group and the hydrogen or hydroxide ion. The stronger the acid or base formed, the lower is the extent of exchange;
- organic ions of high molecular weight and metallic anionic complexes exhibit unusually high extents of exchange;
- as the degree of crosslinking or the fixed ionic concentration of any ion exchanger is lowered, the exchange equilibrium or selectivity coefficient approaches unity.

Ion exchange resins can be divided into four types which are analogous to common acids and bases and which undergo similar reactions. However, the primary difference between them is that ion exchange resins are insoluble and actually exchange constituents from solution by the formation of a resin salt, while common acids and bases form water soluble salts in solution. These four types are the following:

- strongly acidic cation exchange resin;
- weakly acidic cation exchange resin;
- strongly basic anion exchange resin;
- weakly basic anion exchange resin.

Strongly acid cation exchange resins and strongly basic anion exchange resins show the typical salt splitting properties of common strong acids and bases, while weakly acidic and weakly basic exchangers do not. Nor do these remove extremely weak acids and bases.

Any of the abovementioned resin types can be further sub-divided into two groups having major structural differences, viz. gelular and macroreticular resins. This structural difference has catalytic significance, as will become apparent below.

The matrix of gelular ion exchange resin is a homogeneous structure with no discontinuities. In the dry stage, the gelular matrix is totally collapsed and the polymeric chains are as close as atomic

forces will allow. Unless the matrix is swollen by a medium, the interior of the bead is impervious to any molecule. Catalytic activity would be due only to active sites on the bead surface. The number of active sites on the bead surface, however, are few relative to those in the bead interior. Therefore catalysis by gelular resins requires a swelling medium, unless one or more of the reactants acts as a swelling medium. This swelling is required to expand the hydrocarbon chains in order to create the solvent-filled spaces which form the microporous structure of gelular resins and through which the diffusion of molecules takes place to achieve a high degree of reactant/catalyst contact (Fig. 1.3). Generally gelular resins contain low crosslink densities ($< 12\%$), since increasing crosslink density is equivalent to decreasing microporosity. Gelular ion exchange resins are rigid transparent spherical beads.

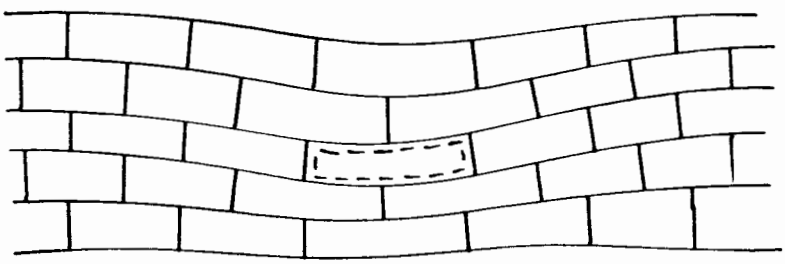

micro porosity of gel-type ion exchange resins

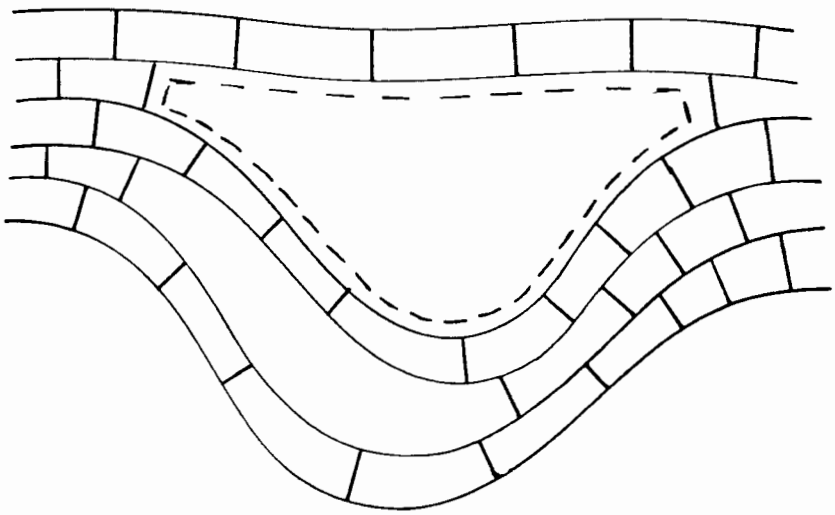

macroporosity of macroporous ion exchange resin

Fig. 1.3 : Matrix of ion exchange resin in two dimensional representation

In macroreticular ion exchange resins the necessity of matrix expansion has been eliminated. They have a heterogeneous structure, which consists of agglomerates of very small microspheres. These microspheres have the same matrix as gelular resins, but are much smaller. In the process of fusing, these microspheres form macrospheres of ordinary bead sizes. These macrospheres contain dispersed rigid macropores, which are much bigger in size than the micropores of the gelular phase (Fig. 1.3). Through these macropores molecules can easily diffuse into the interior of the bead and make contact with the active sites on the macroporous surface, without a swelling medium being present. Macroporous resins are rigid opaque beads. Table 1.3 compares the pore sizes of the two types of resins with those of activated carbon (12).

Type	Pore Size (Å)
gel-type polymerization resin (swollen)	5 - 20
activated carbon	20 - 50
macroporous polymerization resin	100

Table 1.3 : A comparison of the porosity of ion exchange resin and activated carbon.

These pore diameters can be compared with the critical diameter of an isobutene molecule, 5.4Å, where the critical molecular diameter is the smallest opening through which the undeformed molecule will pass (6).

Macroreticular resins are generally defined as follows: "Macroreticular ion exchange resins do not differ from the gel type varieties in their resin matrix. However, the skeletal structure is interspersed with pores, the diameter of which ranges above the molecular radii by several orders of magnitude.

An ion exchange resin is considered macroporous if the following criteria are applicable:

- the appearance in moist condition is opaque to turbid;
- there is a difference between apparent and true density;
- the internal surface area is greater than $5 m^2/g$; and
- the pore diameter is greater than 100Å. "(12)

The production of macroreticular resins is carried out via a polymerization reaction in the presence of an inert material, which is added prior to polymerization and which dissolves only the monomer. During polymerization this inert material, which remains in the liquid phase, is submicroscopically distributed through the bead. After the reaction it is removed by extraction or evaporation, leaving an open-pore structure and a freely accessible inner surface.

The most common crosslink and hydrocarbon polymer chain used for strongly cationic exchange resins are divinyl benzene (DVB) and polystyrene, respectively. The active group, most commonly sulphonic acid, is usually added to the aromatic ring in the para-position, but may also go into the ortho- or meta-position. Monosubstitution occurs in general (Fig. 1.4).

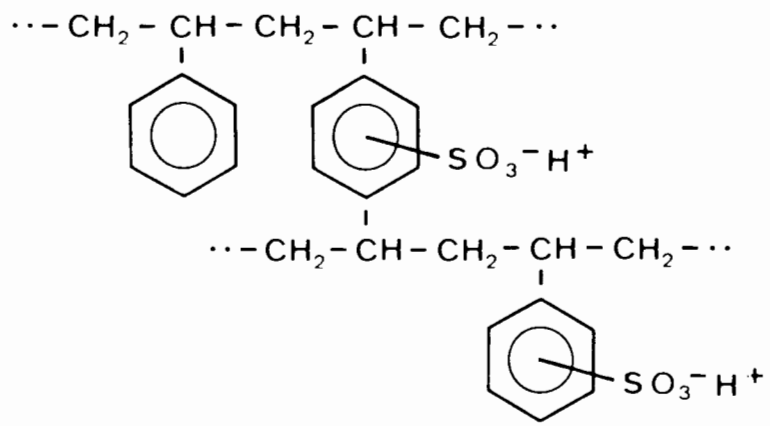

Fig. 1.4 : Chemical structure of a typical macroporous acidic ion exchange resin.

Practical experience has shown that sulphonic acid resin catalysts can be divided into four types. This classification is based on two factors which affect catalytic efficiency. Firstly, the presence or absence of low levels of water establishes whether the catalytic agent will be the solvated proton or the undissociated sulphonic acid group, respectively. Gates (15) has shown the undissociated sulphonic acid group to be more active catalytically than the solvated proton by a factor of forty. Secondly, the distribution of reactant between bulk solvent and resin matrix also affects catalytic efficiency. The influence of solvent varies depending on whether it is pure water, water/organo-solvent, or pure organic solvent. Polar or non-polar solvents exert different influences as well. Therefore the two major types and their respective subdivisions are :

Type A: Sufficient water is present to solvate all the protons in the sulphonic acid resin, i.e. the solvated proton is the catalytically active species. This type can be further subdivided, according to whether or not an organic solvent has been employed to solubilize a water insoluble reactant.

Type B: The absence of water leaves an undissociated sulphonic acid group. The sub-types are determined by the presence or otherwise of water in the reaction product. The generation of water of reaction results in an eventual transition from a Type B to a Type A reaction.

Catalysis by completely water swollen resins in aqueous or polar solvents resembles homogeneous acid catalysis within the pore liquid in the bead, i.e. quasi-homogeneous catalysis. This is because the counter ions are mobile and solvated and therefore, in principle, not different from ions in a corresponding homogeneous solution. The only difference is that reactant and product diffusion within the matrix has to take place and that there may be an interaction between the reactant and the matrix.

In the selection of the correct ion exchange resin, the following factors are considered:

the ionic functionality is determined by the nature of the system, i.e. whether the reaction is acid or base catalysed and whether a strong or weak species is required.

The porosity is important in two ways. Firstly, the nature of the solvent determines if the presence of physical porosity, i.e. a macroreticular resin, is required. If the solvent does not swell the matrix sufficiently, physical porosity is required. The higher the physical porosity, the less dependent the resin is upon matrix hydration and the more suitable the resin is in anhydrous conditions. Secondly, gel phase porosity (degree of crosslinkage) determines rates of diffusion, kinetics and selectivity of molecular size.

The type of reactor also influences the selection of the most suitable resin. Table 1.4 compares various reactors in terms of resin structure and particle size (12).

Type of Reactor	Beads (200-1250 microns)		Powder (< 50 microns)
	gel type	macro-reticular	
stirred vessel	0	0	
fixed bed	0	0	
closed loop reactor			0

Table 1.4 : A comparison of the type of reactor with resin structure

1.2 Polymerization using Heterogeneous Catalysts

1.2.1 Kinetics of the Overall Process

In the following discussion it is assumed that mass transfer in the bulk solution is instantaneous. For a reaction to occur, the reactants must diffuse into the resin bead, react and then the products must diffuse back into solution (Fig. 1.5) (5). Therefore the overall rate can be influenced by the following:

- diffusion of the reactants and products across the Nernst diffusion layer, a liquid film surrounding the catalyst bead;
- diffusion of the reactants and products into and out of the interior of the resin bead (matrix diffusion); and
- the chemical reaction at the active site.

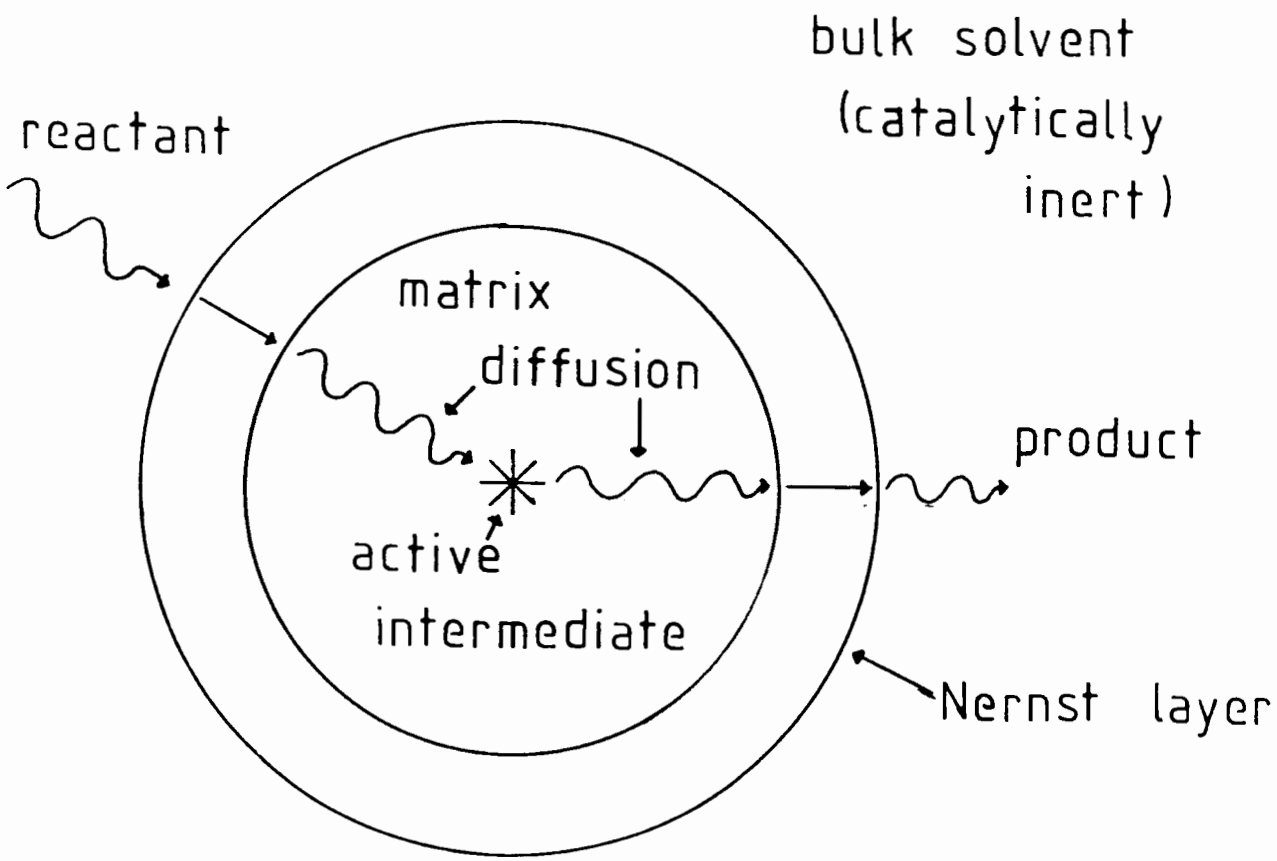

Fig. 1.5 : Schematic representing mechanism of gelular catalysis

Large matrix diffusion resistance results in molecules reacting before they penetrate into the interior of the catalyst particle. The rate is then controlled by either film diffusion or the rate of chemical reaction on the bead surface, whichever is slower. The latter limiting case is when the reaction is surface reaction controlled.

For optimum catalyst utilization, a high matrix diffusivity is desirable. At any given condition, if the rate of chemical reaction is faster than diffusion rates, reactants cannot be supplied to the catalytic sites throughout the beads fast enough to establish an equilibrium concentration. The reaction thus occurs only in the outer shell of the beads and a significant number of active sites inside the bead are unused. The overall rate determining step can be determined experimentally from a consideration of the various rate controlling steps. (Table 1.5):

- if internal reaction is controlling then the overall rate is proportional to the amount of catalyst and is independent of particle size;
- if either film diffusion or surface reaction is controlling then the overall rate decreases with increasing particle size;
- if film diffusion is controlling the overall rate depends on degree of agitation and is independent of the acid site concentration in the resin;
- if surface reaction is controlling then the overall rate is independent of agitation and is proportional to the catalyst ion concentration in the resin.

A theoretical prediction of the rate controlling step can also be made from the activation energy and the order of the overall process (4).

In addition, the overall rate of the reaction can be influenced by, firstly, the reaction temperature. The rate of diffusion increases at a slower rate than that of a chemical reaction with increasing temperature. Therefore high temperatures lead to intraparticular

diffusion limitations or film diffusion controlling mechanism. Secondly, resins with lower degrees of crosslinking swell more strongly, thereby increasing intraparticle mobilities and thus the rate of intraparticle diffusion is higher.

Thirdly, increasing size and/or branching of the reactant molecules causes a decrease in the extent of matrix diffusion. Finally, both inefficient agitation and high viscosity of the solution result in large film thickness and therefore favour a film diffusion controlling mechanism. However this situation is exceptional and arises only if the chemical reaction is very fast.

Rate step of the overall process	Test Variable	Positive	Negative
internal reaction control control	changing reactant/ catalyst ratio	activity unaffected by reactant/catalyst ratio	activity increases with increasing reactant/ catalyst ratio
Film diffusion and surface reaction control	particle size	activity increases with decreasing particle size	activity unaffected by particle size
Film diffusion control	agitation	activity increases with increasing agitation	activity unaffected by agitation
Surface reaction control	catalyst ion concentration	activity increases as catalyst ion concentration increases	activity unaffected by catalyst ion concentration

Table 1.5 : Tests for experimental determination of the rate controlling step

Although for internal reaction control it is desirable to have a small bead size and low crosslink density, mechanical stability and handling considerations require the opposite. Only

macroreticular, and not gelular resins, satisfy these conflicting requirements. The microspheres in the former, when fused, form the large bead particles. Furthermore, macroreticular resins are generally more highly crosslinked and therefore have a higher mechanical resistance. The loss of diffusivity due to the higher crosslink density is more than compensated for by the macroporous structure.

1.2.2 Chemical Reaction

1.2.2.1 Mechanism

Alkenes may undergo two types of polymerization. In true polymerization the product consists of alkenes having molecular weights which are integral multiples of the monomer alkene i.e.

$$x\ C_nH_{2n} \rightarrow C_{xn}H_{2xn}$$

The second type, conjunct polymerization, yields a complex mixture of alkanes, alkenes, alkadienes, cycloalkanes, cyclo-alkenes, cycloalkadienes, and sometimes aromatic hydrocarbons. Of the gaseous olefins, isobutene is the most readily polymerized catalytically and ethylene the least. Butenes, in general, undergo mainly true polymerization. Interpolymerization of two different alkenes is termed copolymerization.

1.2.2.1.1 True Polymerization

The carbonium ion mechanism is the most widely accepted mechanism of polymerization. The following rules indicate the structures expected to arise as a result of this mechanism (18):

- formation of electron deficient carbon according to Markownikoff's rule, i.e. the proton is added to the carbon atom holding the greater number of hydrogen atoms;

- isomerization of carbonium ions to a stable form;
- allowance for absence of products where such products of reaction are prevented by steric hindrance.

In the polymerization of isobutene, for example, the following steps are involved:

i) Addition of a proton from the acid site to the double bond to form a tertiary carbonium ion.

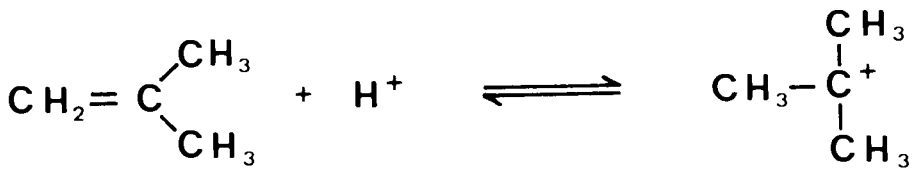

The carbonium ion then undergoes one of the following reactions, which include either union with a negative ion having a complete octet of electrons, elimination of the same or a new proton to give the same or a new olefin, rearrangement of the carbon skeleton followed by the loss of a proton to give a new olefin, or polymerization, i.e. addition of another olefinic molecule.

ii) a) Isomerization

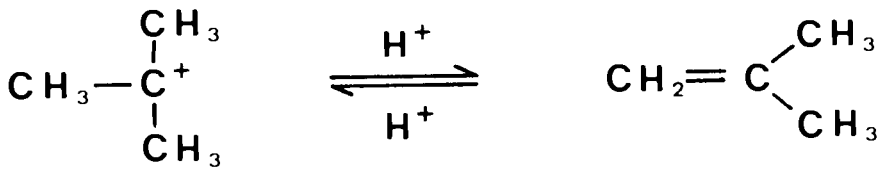

b) Polymerization

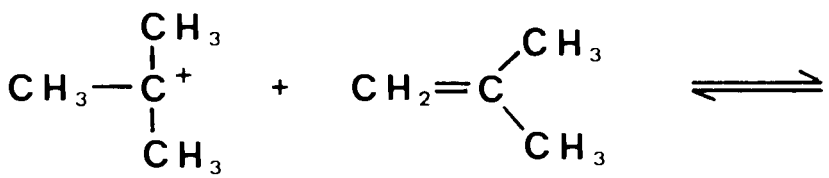

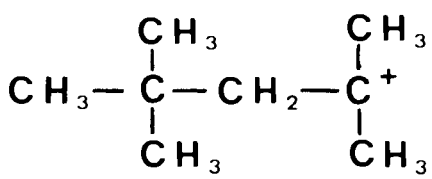

This higher molecular weight carbonium ion may either add to another olefin or lose a proton to give the olefinic polymer to which a carbonium ion may then be added.

iii) Loss of proton to give an olefinic polymer

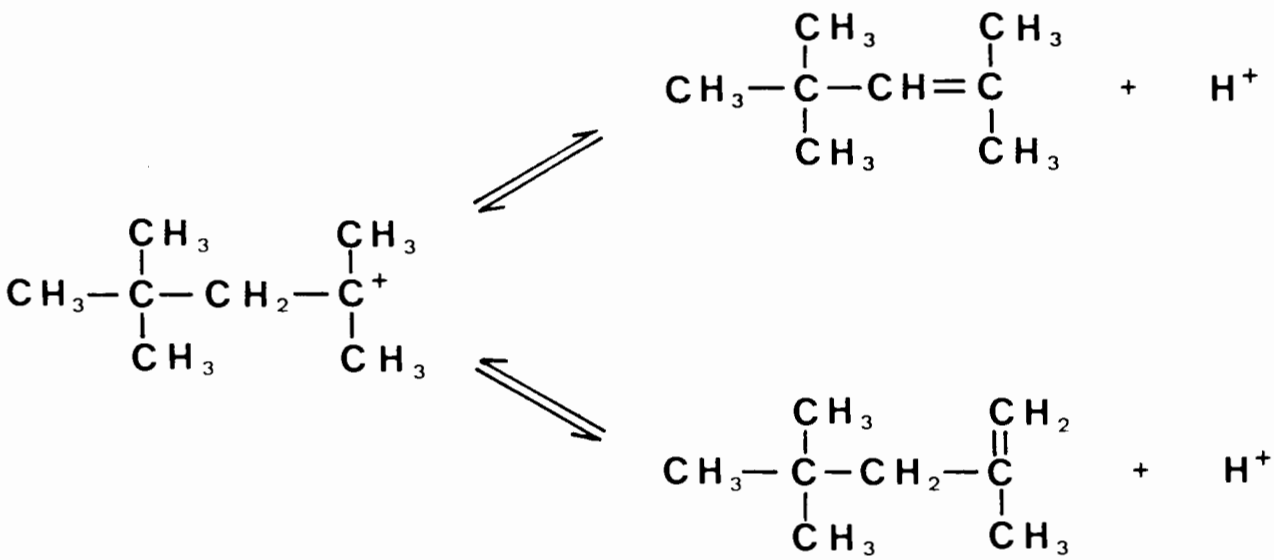

Other mechanisms which have been suggested are the methyl separation mechanism and the hydrogen separation mechanism. Neither of these mechanisms, however, require the presence of protons and are therefore not considered. The hydrogen transfer mechanism can be used to explain the isomerization of 1-butene. The acid approaches the 1-butene molecule in such a way that one of the hydrogen atoms of the acid approaches the end carbon atom of the double bonded pair, while one of the oxygen atoms, which has no hydrogen on it, approaches the hydrogen atom on the third carbon atom in the 1-butene molecule. When the complex, which is so formed, decomposes, the acid may take with it the hydrogen atom on the first carbon atom, the product being 2-butene.

This mechanism can also explain the polymerization of isobutene. However, it does not account for conjunct polymerization and it does not take into account the formation of products having a

carbon skeleton different from that of the primary product.

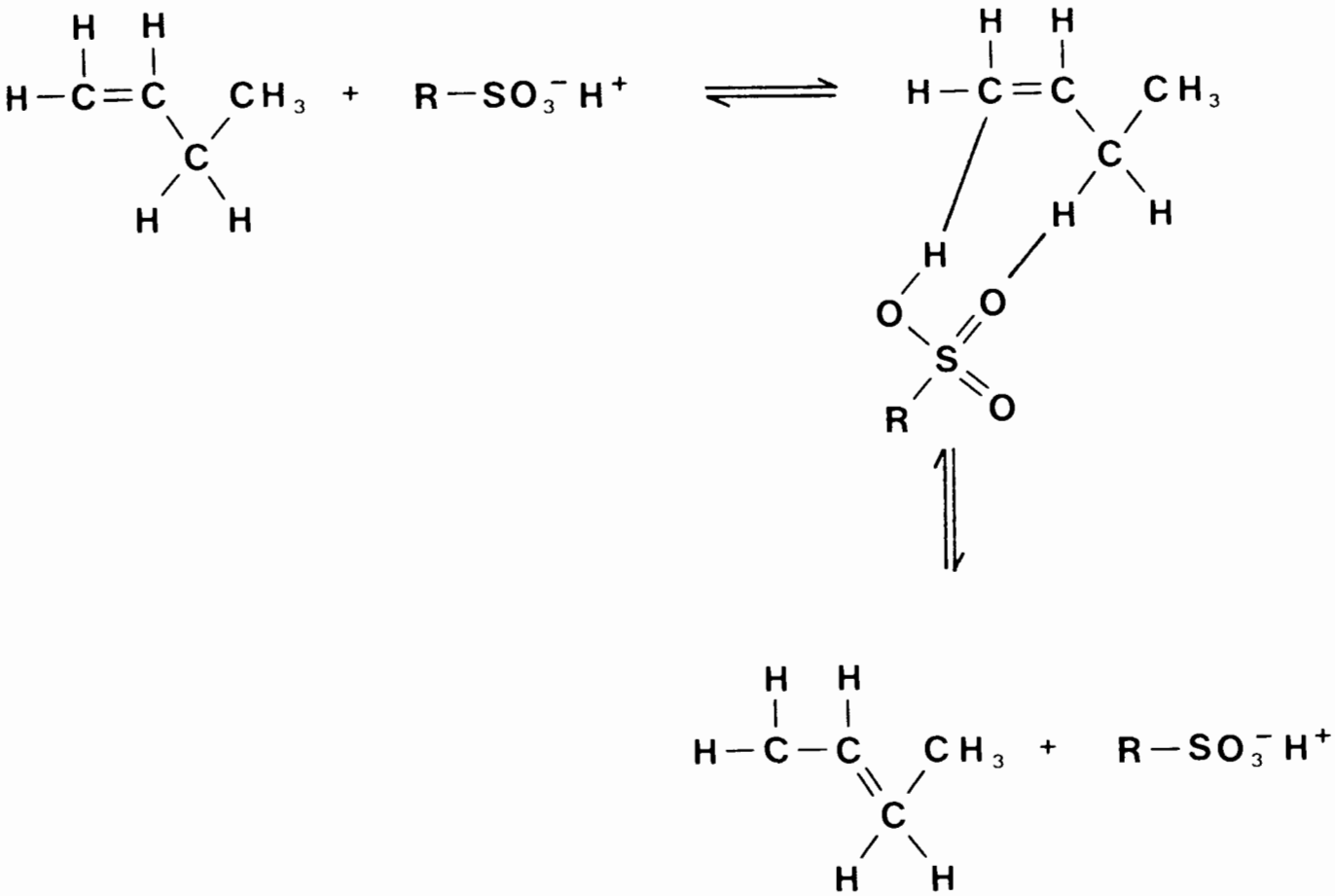

Various acid catalysts have been used to study the dimerization and trimerization of some reactants. These are shown in Table 1.6 (17).

1.2.2.1.2 Conjunct Polymerization

The extent to which conjunct polymerization takes place depends largely on the particular catalyst and on conditions such as temperature and concentration. It results in the formation of saturates. The mechanism may be as follows:

Reactants	Dimer	Trimer
Isobutene	2,4,4-trimethyl -1-pentene (82%) 2,4,4-trimethyl -2-pentene (18%)	4-methylene - 2,2,6,6 tetramethylheptane (55%) 2,2,4,6,6-pentamethyl - 3-heptene (35%) 2,4,4,6,6-pentamethyl - 1-heptene (5%) 2,4,4,6,6-pentamethyl - 2-heptene (5%)
2-Butene	3,4-dimethyl -2-hexene	3,4,5,6-tetramethyl - 2-octene 3,4,5,6-tetramethyl - 4-octene
Isobutene + 2-butene	diisobutene (25%) 3,4,4-trimethyl -2-pentene (40%) 2,3,4-trimethyl -2-pentene (35%)	
Isobutene	2,2-dimethyl hexane * (53%) 2,3-dimethyl hexane (28.4%) 2,2,4-trimethyl pentane (10%) 2,2,3-trimethyl pentane (19.3%) 2,3,4-trimethyl pentane (37%)	

* hydrogenated

Table 1.6 : Polymerization products using various reactants

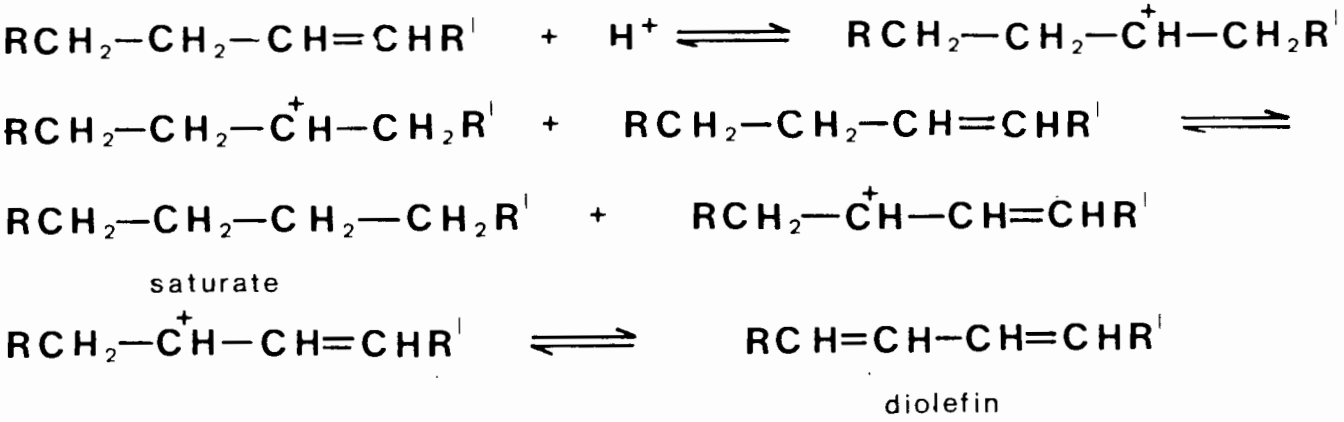

For olefin polymerization the significant reactions are:

- initiation by proton addition;
- propagation by olefin addition;
- chain termination by proton expulsion;
- chain termination by proton transfer;
- chain termination by addition of hydride ion;
- depolymerization to same or other chain length than that of original olefin;
- isomerization;
- hydrogen exchange;
- cyclization, equivalent to self-alkylation or self-polymerization; and
- loss of hydride ion.

1.2.2.2 Kinetics

1.2.2.2.1 Kinetics of n-Butene Isomerization

Early studies showed that the double bond shift in n-butenes over solid acids is reversible, apparently first order in both directions, and surface reaction controlled rather than diffusion controlled (20, 21, 22). Haag and Pines examined the isomerization of n-butenes over alumina (23). They found the reaction to be kinetically rather than thermodynamically controlled and that the thermodynamically less stable cis-2-butene is produced at a faster rate than the trans-isomer. Their results as shown in

Fig. 1.7 (23) indicated a three-component kinetic system with competitive reversible reactions. The stereo-selectivity did not appear to be limited to alumina-catalysed reactions, but was observed with other solid as well as liquid acid catalysts (26).

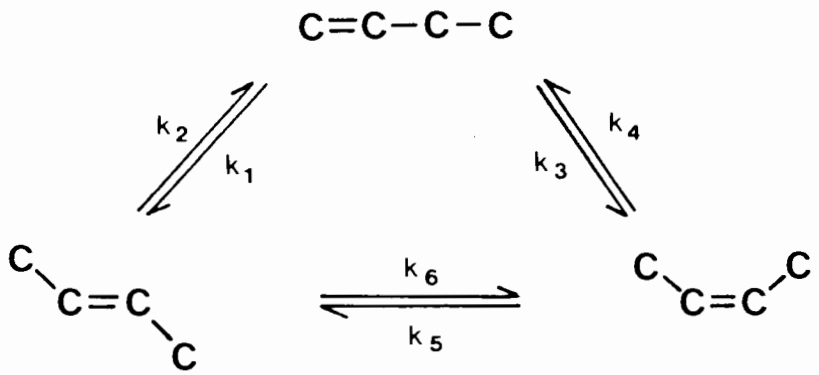

	k_1	k_2	k_3	k_4	k_5	k_6
pellets	3.8	1.0	9.1	4.6	2.4	4.6
powder	3.8	1.0	16.7	8.5	4.4	8.5

Fig. 1.6 : Apparent relative rate constants of butane isomerization

1.2.2.2.2 Kinetics of Oligomerization of Isobutene

Haag studied the kinetics of the oligomerization, such as the influence of monomer concentration, conversion, and temperature on the rate of reaction and the distribution of the oligomers. The catalyst was a macroporous ion exchange resin. He considered the following reaction scheme, and the corresponding kinetics.

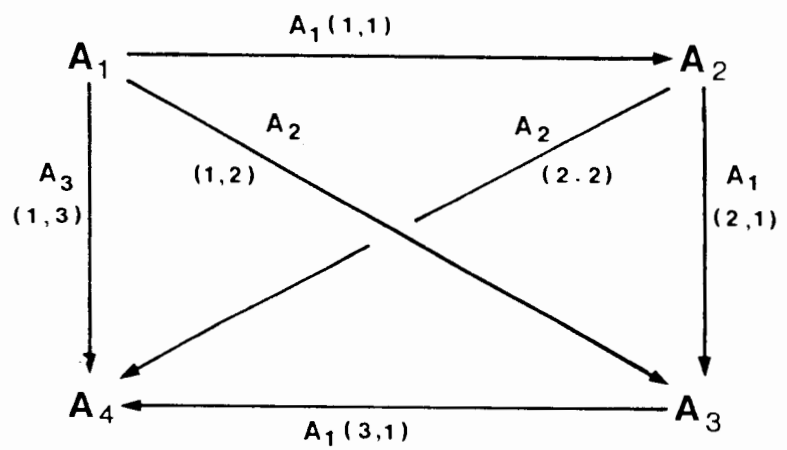

where A_1,A_2,A_3 and A_4 denote the monomer, dimer, trimer and tetramer respectively. His principal findings are described below:

- Dimerization of monomer. This involves the reaction

$$A_1 + A_1 \xrightarrow{(1,1)} A_2$$

The selectivity is 95-99%. The bimolecular dimerization is of first order, both at low (low temp - 2% conversion at 0°C) and high (high temp - 80% conversion at 20°C) conversions. However, at very dilute solutions the conversion follows a second-order rate law.

- Dimerization of dimer. This involves the reaction

$$A_2 + A_2 \xrightarrow{(2,2)} A_4$$

The product was predominantly tetra-isobutene. Again first order kinetics was observed for high and low conversions. However the rate constant for the dimerization of the dimer was about twenty-nine times greater than that for the dimerization of the monomer. Second-order kinetics was again found at low concentrations.

- Kinetic model. A model which successfully described the observed kinetics is the Langmuir-Rideal mechanism according to which the reaction takes place between an adsorbed molecule and one in the gas phase. Adopting this mechanism yields

$$A_1 + S \overset{K_A}{\rightleftharpoons} B_1^*$$

$$B_1^* + A_1 \xrightarrow{K_2} B_2^* \qquad (S = \text{catalytic surface}$$

$$B_2^* \overset{K_B}{\rightleftharpoons} A_2 + S \qquad B^* = \text{intermediate})$$

The rate is then

$$r = K_2' \frac{K_A A^2}{1 + K_A A} \qquad \left(K_B A_2 = 0, \text{ since } K_B < K_A \right)$$

The limiting cases are those of high surface coverage, for which $r = K_2 A_1$ and low surface coverage for which $r = K_2'' A_1^2$.

Hence the above kinetic model is consistent with the observed first- and second-order kinetics at high and low concentrations respectively. This model also supports the carbonium ion mechanism.

Another frequently observed mechanism is the interaction between two adsorbed molecules, such as in alcohol dehydration (25).

- Adsorption constants. From the above rate equation Haag was able to determine the adsorption constants. He found that the monomer was considerably more strongly adsorbed on the catalyst than on the dimer. This also explains the observation that in the oligomerization of isobutene, the very rapid dimerization of the dimer occurs only after the monomer concentration is reduced to very low levels (Fig. 1.7).

- Formation of trimer. The proper decoupling of the trimeric product indicated that the trimer is produced in a consecutive and a parallel reaction (Fig. 1.8). The consecutive reaction involves the addition of free dimer to adsorbed monomer and the parallel reaction the addition of free monomer to adsorbed dimer.

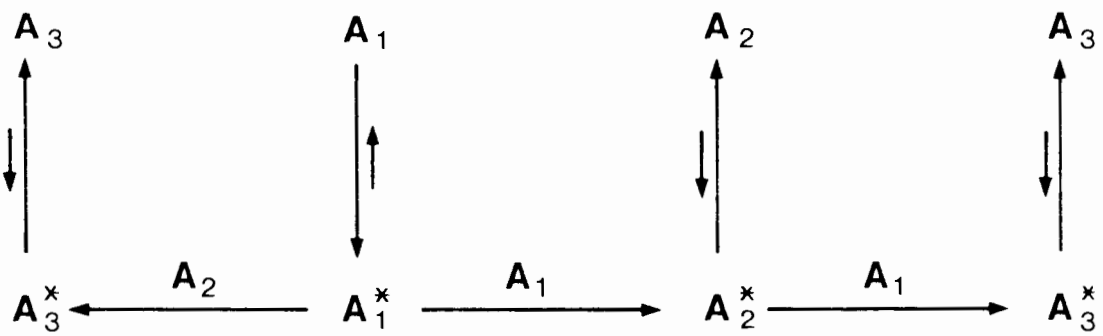

Fig. 1.8 : The reaction scheme for the trimer production

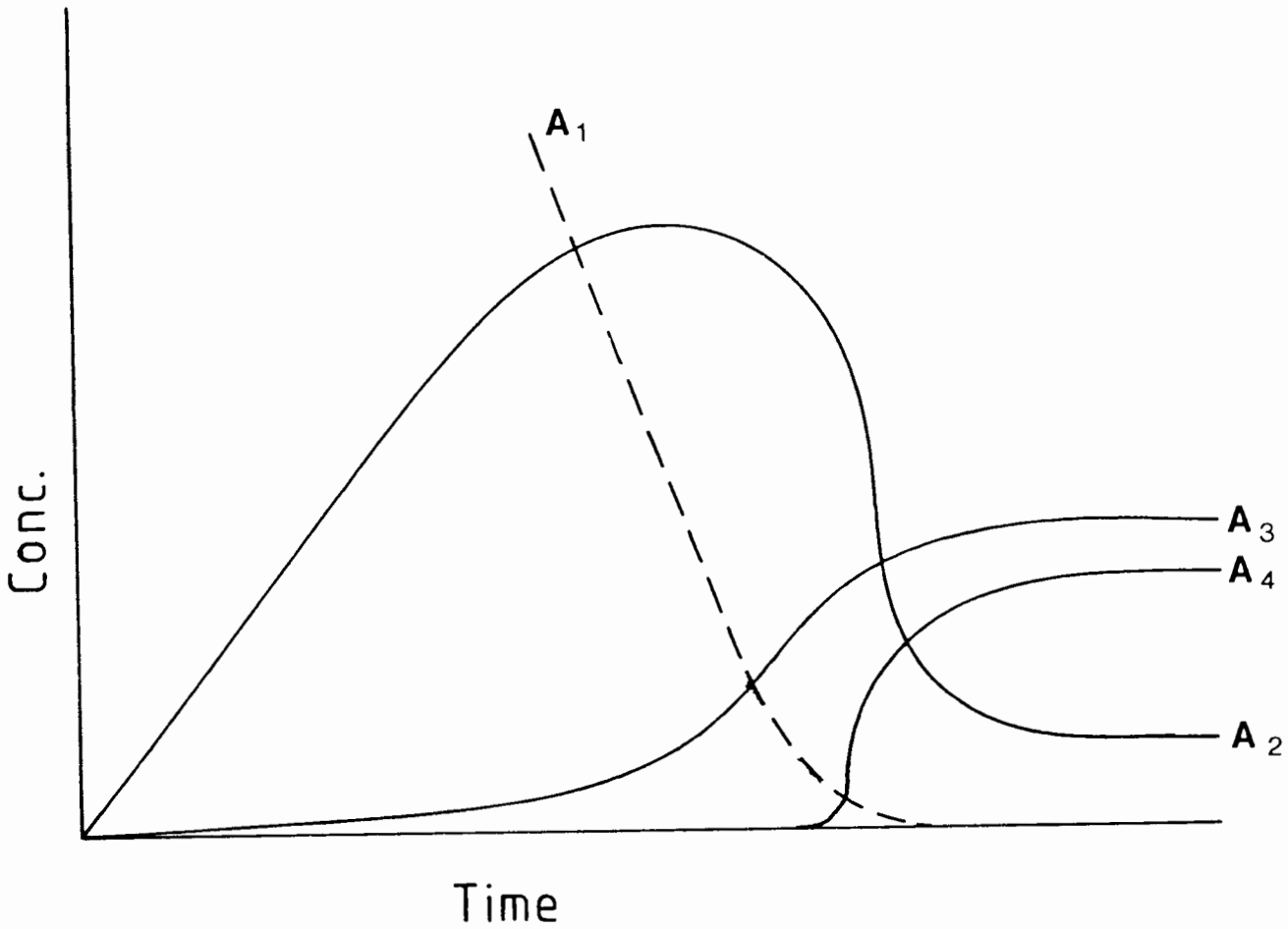

Fig. 1.7 : Concentration profile of the oligomerization of isobutene

The concentration profile of the various species present when the oligomerization of isobutene is carried out in a batch reactor is shown in Fig. 1.7.

1.2.2.3 Thermodynamics of Polymerization

Fig. 1.9 shows the free energy change which occurs during dimerization of C_2,C_4 and C_8 mono-olefins as a function of temperature (18). The dimerization of ethylene to 1-butene is much more favourable at a given temperature than dimerization of any of the other light olefins. Moreover the free energy change for dimerization of α-olefins at a given temperature to form higher α-olefins becomes almost constant above propylene.

Fig. 1.10 shows the free energy change for the dimerization of propylene to isomers of the corresponding higher olefins (18). At a given temperature the isomer of the corresponding higher olefin is more favoured than the normal olefin, since the latter always represents a higher configurational energy. Hence the equilibrium conversion of an α-olefin to a higher α-olefin will always be less than the corresponding conversion of an α-olefin to an iso-olefin. The dimerization of β-olefins or iso-olefins to the corresponding higher olefins will be similar to the α-olefin-α-dimer relationship. However, dimerization of β-olefins or iso-olefins to α-olefins will always be the least favourable reaction.

Figures 1.11 and 1.12 show the free energy change for the formation of higher oligomers as a function of temperature (18) for the monomers propylene and 1-butene, respectively. These figures show that above a certain temperature (about 550°C for both propylene and 1-butene) the reverse reaction, i.e. cracking, occurs. Clearly at higher temperatures the lower oligomers will predominate whereas at low temperatures the higher polymers will predominate at equilibrium.

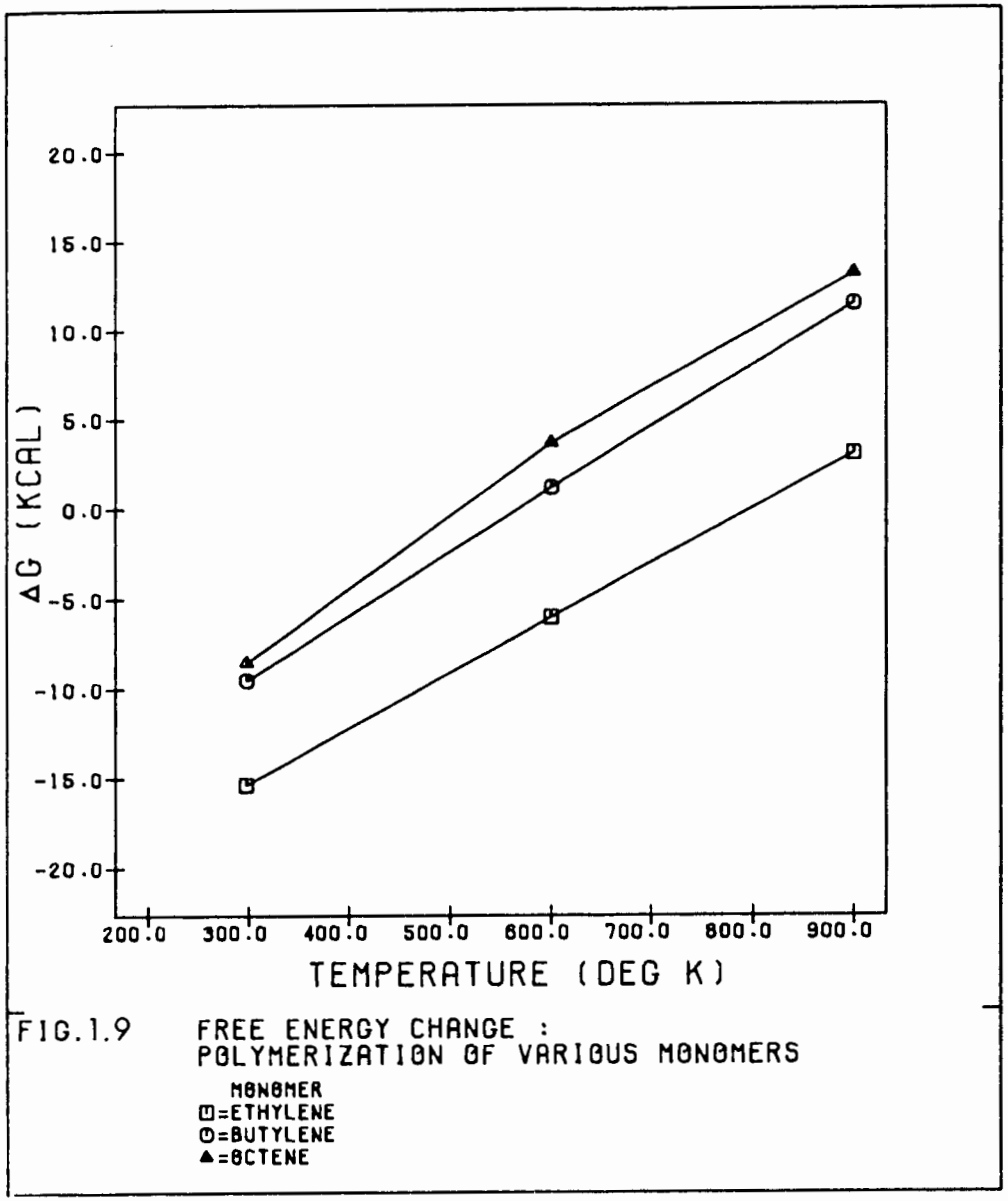

FIG.1.9 FREE ENERGY CHANGE : POLYMERIZATION OF VARIOUS MONOMERS

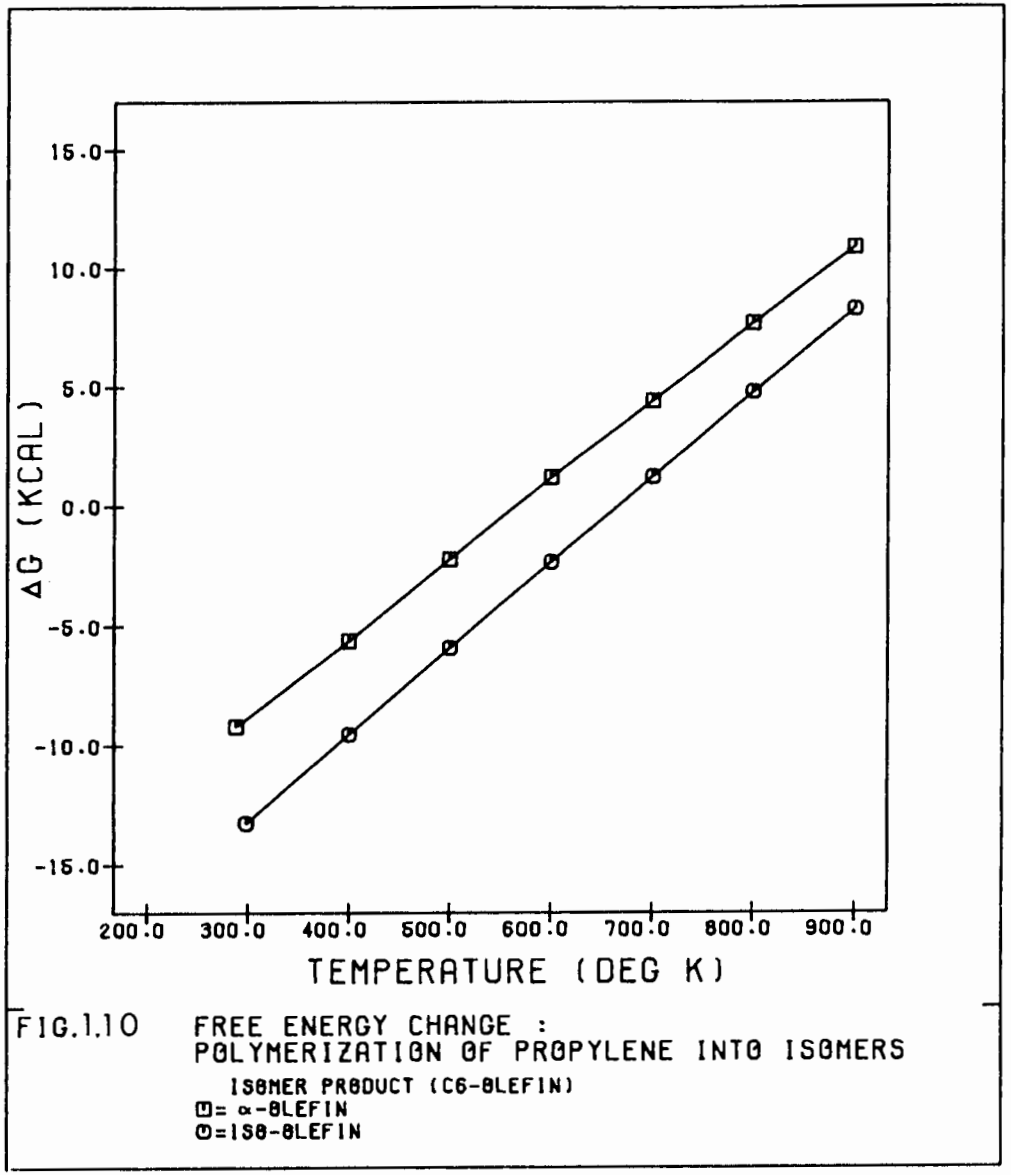

FIG.1.10 FREE ENERGY CHANGE : POLYMERIZATION OF PROPYLENE INTO ISOMERS

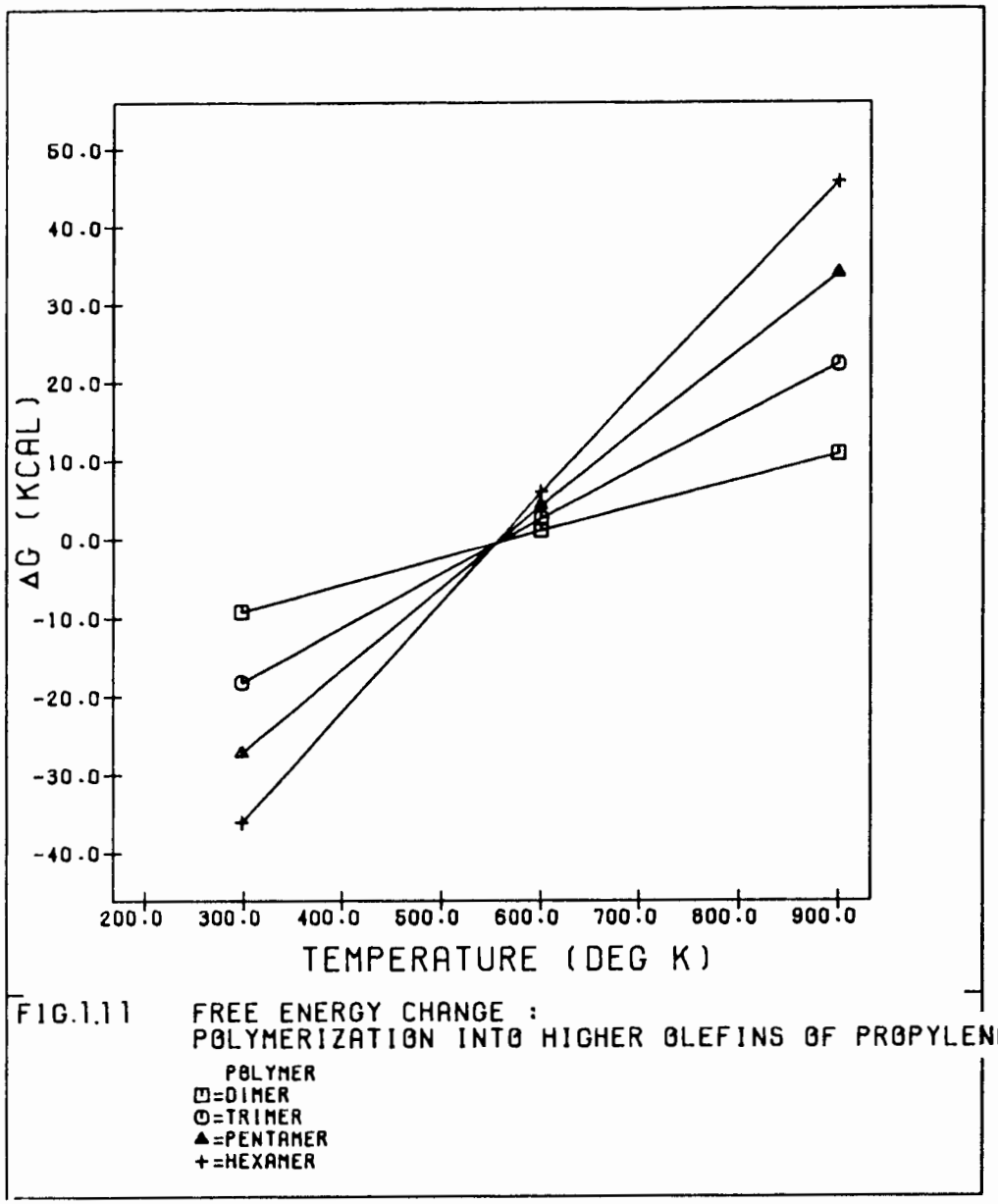

FIG.1.11 FREE ENERGY CHANGE :
POLYMERIZATION INTO HIGHER OLEFINS OF PROPYLENE

POLYMER
□=DIMER
⊙=TRIMER
▲=PENTAMER
+=HEXAMER

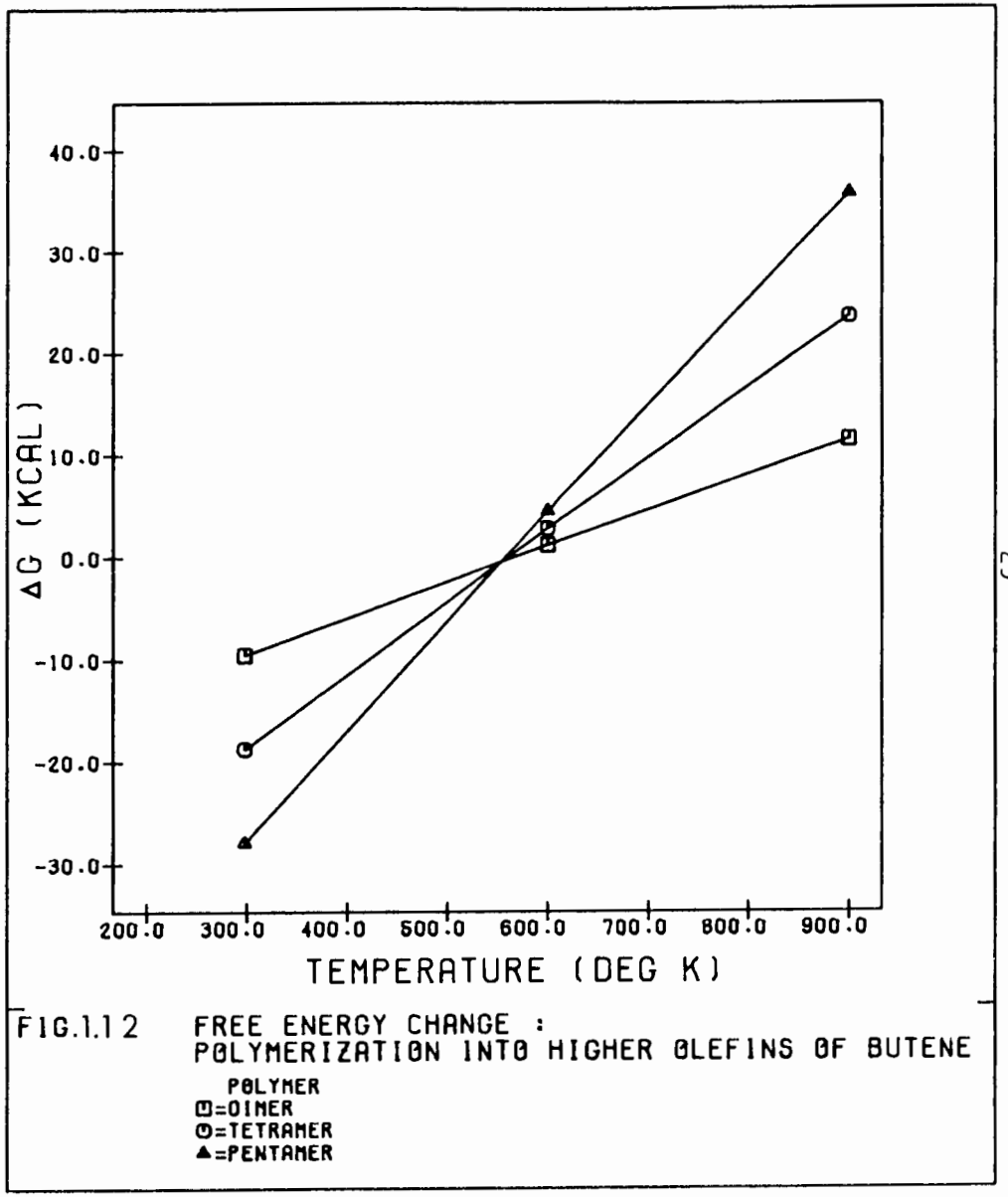

FIG.1.12 FREE ENERGY CHANGE :
POLYMERIZATION INTO HIGHER OLEFINS OF BUTENE

POLYMER
□=DIMER
⊙=TETRAMER
▲=PENTAMER

1.3 Application of Ion Exchange Resin

The ability of ion exchangers to catalyze liquid phase reactions was first observed in 1911 by Tacke and Süchting (29), who found that sucrose in aqueous solution is inverted by acidic zeolites. Similar findings were obtained by Rice (30) and Puri (31), who studied the catalytic properties of soils and clays for the same reaction. They correlated the catalytic activity with the amount of exchangeable hydrogen ions in the exchange complex. Practical applications and plant scale processes using ion exchange resins as catalysts were first developed by the I.G. Farben Industries during World War II (32). Today probably the largest consumer of ion exchange materials as catalysts is the petroleum-refining industry in its cracking and refining processes (16).

The industrial use of ion exchange resin covers a wide field and involves applications in conversion of ionic species, concentrating of ionic species, purification and deionization, fractionation by ion exchange chromatography and catalysis. The latter involves the use of ion exchange resins to promote reactions normally catalyzed by mineral acids and bases. The chemistry is essentially unchanged from that exhibited by free mineral acids and bases in homogeneous catalysis.

1.3.1 Application of Ion Exchange Resins as Catalysts

Resins have been used as catalysts for, inter alia, hydration, hydrolysis, alkylation, esterification, transesterification, dehydration, polymerization, condensation and isomerization reactions. They are well established as economical catalysts in a wide spectrum of industrial processes and the large number of evaluations currently being pursued should result in even wider use. Table 1.7 gives an outline of some of the reactions advantageously catalysed by ion exchange resins. The table shows the type of reaction, its application and the structure of the resin used.

Type of Reaction	Type of catalyst			Application
	Gel type	Macroreticular		
	Beads	Beads	Powder	
acetal formation	0	⊠		acetals
alkylation	0	0	⊠	p-alkyl phenol
chromatography	⊠			fructose/ glucose
condensation	⊠			Bisphenol A
epoxidation	⊠			butyl oleate
ester formation	⊠	0		acetic acid ethyl ester
ester splitting	0	⊠		sorbic acid
ether formation	⊠			alkylaryl ether
hydration	0	⊠		isopropyl alcohol
hydrogenation		⊠		methyl-tert-buthyl ether
hydrolysis	⊠			allyl alcohol
oligomerization			⊠	n-butene
phenol purification		⊠		pure phenol
polymerization			⊠	1,3,5 trioxane
reaction acc. to Prins	⊠			1,3 dioxane
re-esterification		⊠		hydroxyalkyl phosphinic ester

⊠ recommended

0 suitable for application

Table 1.7 : Application of ion exchange resin

1.3.2 Olefin Polymerization Reactions

Historically, polymerization of olefins was carried out using sulphuric acid. However, today the catalyst of choice is solid phosphoric acid which is used in the so-called 'Catpoly' process of U.O.P. The phosphoric acid may either be impregnated on an inert carrier such as kieselguhr, or may take the form of a thin film of liquid on an inert surface, such as quartz chips. The operation may be selective or non-selective. Selective polymerization, which corresponds to the temperature range of 149 to 177°C, applies to the polymerization of normal and isobutene. Only isobutene is polymerized at lower temperatures, while n-butene participates in the reaction at higher temperatures. Non-selective operation is run at 191 to 246°C and results in conversions of 90% of the C_3 and C_4 olefins. Of the C_3-C_4 olefins, propene reacts most slowly, n-butene twice as fast and isobutene much faster than either. However, the polymer from propene has a higher boiling point than the polymer from butene. For propene the rate of polymerization doubles with a 40°C rise in temperature. Fresh catalyst exhibits maximum activity and requires the lowest operating temperatures. These temperatures, however, need to be raised as deactivation occurs. Water must be present in the feed to prevent catalyst dehydration and deactivation. Underhydration favours coke formation whereas overhydration results in catalyst softening and eventual plugging of the bed. High temperatures and low pressures both tend to increase coke deposition. The combination of high pressures and low temperatures gives clean catalyst surfaces and permits non-regenerative operation of sufficient length to make discarding of spent catalyst more economical than re-generation (± every five months at a production rate of 1.25 - 1.67m^3 product/kg catalyst) (18).

The M.O.N. of the product obtained is about 83. The simplicity of the reactor design, the ease of regeneration, and the high mechanical strength of the catalyst are some of the advantages of this process. However, the catalyst is very corrosive, thus requiring special materials of construction and creating problems with the safety and handling of the catalyst. Moreover the catalyst produces relatively little diesel of poor quality and the high boiling point fraction causes rapid deactivation.

Various other systems have been used. These include olefin polymerization with copper pyrophosphate, which proceeds in a manner similar to the phosphoric acid process (18), and the use of zeolites, which have limited attraction because they age rapidly and cannot perform effectively at high olefinic space velocities.

An exception is the synthetic crystalline zeolite ZSM-5. This catalyst is used in the Mobil Olefin-to-Gasoline-and-Distillates (MOGD) process (33). The process converts more than 90 weight percent of the feed olefins to gasoline plus distillates and its value lies in its flexible mode. The product spectrum of the two extreme modes is shown in table 1.8. The gasoline quality is indicated by a R.O.N. of 92 and a M.O.N. of 79. The distillate, after hydrogenation, has a cetane number of 56.

	Maximum distillate mode	Gasoline mode
C_1 - C_3	1	4
C_4	2	5
C_5 - 165°C gasoline	18	-
165°C$^+$ distillate	99	-
C_5 - 200°C gasoline	-	84
200°C$^+$ distillate	-	7

Table 1.8 : Product spectrum of the MOGD process

A relatively new process is the use of ion exchange resins. They have the following advantages (39):

- The support is easily functionalized, allowing a wide range of functional groups to be added and thereby more easily to control the acidity or basicity;

- unlike surfaces of metal oxides, polymeric hydrocarbons are nearly inert and are not expected to interfere in catalysis, which may therefore be associated with a single kind of catalytic group and occur selectively, further reducing by-products;
- polymers having a wide range of physical properties can be prepared, thus enabling control over pore size distribution, internal surface area and number of acid sites.

Severe limitations of ion exchange resins are their limited thermal stability, (Section 1.3.3.4), low mechanical stability, which complicates their use in stirred reactors, and restricted chemical stability towards strong oxidising agents.

Industrially the current aim of the olefin polymerization process using ion exchange catalysts shown in Fig. 1.13, is to separate isobutene from n-butenes by polymerization of isobutene to di-isobutene and tri-isobutene (36, 38).

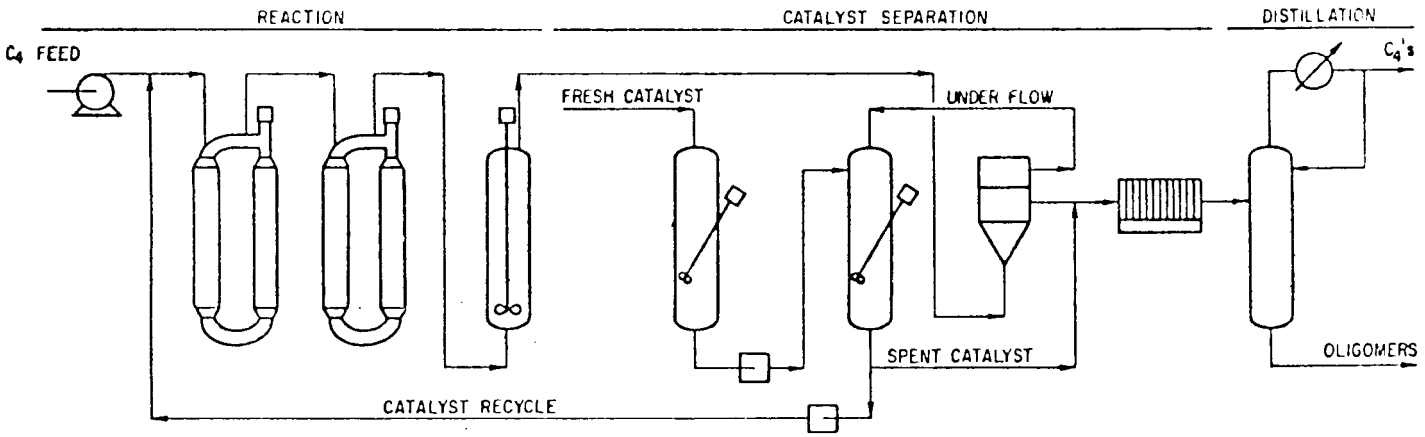

Fig. 1.13 : Ion exchange resin polymerization process

The C_4 hydrocarbon mixture is passed, together with 1% by weight of ion exchange resin at about 100°C and 20 bar pressure, in order to maintain reactant in the liquid phase, through several series of connected reactors. The reactors are designed for the intimate mixing of hydrocarbons and catalyst, and the heat of reaction is removed by circulating condensate. When oligomerization is

completed, the catalyst is mechanically separated from the reaction mixture using a pressure centrifuge and is returned to the first reactor. Catalyst activity is kept constant by adding a small amount of fresh catalyst while removing the same quantity of spent catalyst.

During oligomerization, 1-butene is isomerized to 2-butene. Typically the product contains approximately 57% dimer, 38% trimer and 4% tetramer. However, the process is very versatile and by varying the process conditions, the product distribution can be altered. For example, by first polymerizing isobutene to less than three parts by weight in an isobutene/n-butene mixture, high conversions of n-butene to its polymers can be obtained in a second stage (37). This is not possible in the presence of isobutene, because the co-dimer is more favoured than the polymers of n-butene. The trimer formation can be increased by recycling di-isobutene to the first reactor (40, 41). No particular conditions have to be maintained for this recycle, except that pure di-isobutene is recycled after separating codimers and trimers and tetramers. The conversion of the recycled di-isobutene to trimers is not complete.

The production of tetramers from di-isobutene has to be carried out in a separate process, using a further modified ion exchange catalyst (42). Under these relatively mild conditions, mono-olefins, codimers and tri-isobutene act as inert diluents. The hydrogenated oligomers show a small spread between R.O.N. (100) and M.O.N. (89) which implies a high road performance.

1.3.3 Activity of Ion Exchange Resin

1.3.3.1 Structural Effects on the Activity of Ion Exchange Resin

Many reactions have been studied using ion exchange resins as catalysts. Only a few of these will be mentioned here to demonstrate how the various structural parameters can influence a reaction.

In heterogeneous catalysis using porous, acid catalysts, the reaction rate depends on the basicity of the reactants, the acid strength of the catalytic species and the distribution of the reactants between the resin and the external solution. While the first is fixed by the system, the latter two are influenced by the structure of the catalyst.

A major structural difference arises between gelular and macroreticular resins, the latter showing a difference between the true density of the resin matrix and the apparent density of the resin bead. A characteristic of macroporosity is also the milky to chalky turbidity of the resin substance which indicates the heterogeneous structure of the resin compound. Gelular resins are transparent. Macroreticular resins are envisaged as two phases: the microspheres, and the pore space formed between them. The overall effectiveness, $\emptyset ov$, of such a resin can be expressed in terms of the average micro-effectiveness factor, $\emptyset i$, macro-effectiveness factor, $\emptyset a$, and the fraction, X, of active sites located on the pore walls (45), or

$$\emptyset ov = [X + (1-X)\emptyset i]\,\emptyset a$$

There are three possible cases governing the relative rates of reaction and of microporous diffusion (46). Firstly, in the case of micropore diffusion rate being much slower than the reaction rate, the reaction proceeds only on the walls of the pores of the macroporous ion exchange resin and the activity is proportional to the specific surface area. Selectivity is not affected by micropore diffusion. Secondly, if the rate of micropore diffusion is faster than the reaction rate, the reaction occurs throughout the polymer mass as a whole. Concentration gradients are not formed and the activity does not depend upon the specific surface of the ion exchange resin. The selectivity is not influenced by the micropore diffusion. Thirdly, if micropore diffusion and chemical reaction proceed at comparable rates, then concentration gradients are formed in the polymer mass or only a certain layer of the polymer mass is catalytically active. Selectivity of the reaction can be influenced by micropore diffusion.

The difference in reactivity between the gelular and macroreticular structure was demonstrated by Widdecke and Klein (47), who found in the alkylation of phenols with olefins, very low activity when using gelular resins. By changing the particle size of the beads they also showed that macropore diffusion has no influence on the rate of reaction. Similar observations were made in studies on formic acid dehydration (48) and the re-esterification of esters with alcohols (49). In addition, the latter reaction showed a strong dependency on particle size when using a gelular resin, thus indicating micropore diffusional limitations. All these reactions were carried out in the gas phase.

Another property of ion exchange resins, which affects activity, is the acid strength of the functional group. This has been shown by Widdecke and Klein (47), who found a hundredfold increase in the alkylation of phenol with olefins when using perfluorinated sulphonic acid in place of sulphonic acid. The acid strength of the former is increased due to the neighbouring CF_2 -group. The concept of superacidity will be discussed in section 1.3.3.4. Uematsu(26) studied the acidity of ion exchange resins by n-butylamine titration. Although he found the total capacity to be equal to the total number of ion-exchangeable hydrogen, he also found an apparent heterogeneity in acid strength among the functional groups on the resin catalyst. This heterogeneity of the activity of the functional groups seemed to play a significant role only when non-polar solvents were used or when the catalyst was in an evacuated environment, i.e. the protonic hydrogens were more tightly bonded to the counter group and thus their activities were more affected by the properties of the substrate. The inhomogeneous structure of the substrate resin is known to be produced in the process of polymerization, crosslinking and sulphonation. Heterogeneity can also be induced owing to an interaction (i) between adjacent sulphonic groups (ii) between adsorbed species and neighbouring sulphonic acid groups and (iii) between adsorbed species and substrate resin. A different type of acid form was investigated using the metal salt form of the resin. The order of the catalytic activities and the selectivities correlated strongly with the electronegativity.

A possible active site is the hydrated water molecule or the hydroxy groups co-ordinated to metal cations as these sites are often regarded as protonic sites in cation-exchanged zeolites, metal sulphates and cation-exchanged silica.

An additional parameter often investigated is the extent of functionalization or the number of acid sites. This can be achieved by either preparing a resin with varying numbers of acid sites or by poisoning of acid sites by ion exchange with metal ions. The latter method has been used by Uematsu in butane isomerization (26), by Gates in butanol and formic acid dehydration (48, 52, 53), and in benzene-propylene alkylation (54), and by Sivanand et al in iso-propanol dehydration (56). They observed a non-linear dependence of the reaction rates on the sulphonic acid group concentration, and the former was found to decrease more rapidly than the fall in proton concentration. Three possible explanations were given. Firstly, it was suggested that there is more than one type of acid site and that metal exchange takes place on the more active sites. Secondly, the reaction might take place at more than one acid site and thirdly, Gates et al proposed that a shift to a less effective mechanism occurs. The extent of substitution of aromatic nuclei with sulphonic acid groups has been investigated in the oligomerization of n-butene (37). The results are shown in Table 1.9.

Average content of sulphonic acid groups per aromatic nucleus	1.03	1.45	1.50	1.55	1.74
Conversion (% by weight)	1.78	43,40	80.00	72.00	70.20

Table 1.9 : Effect of numbers of acid sites on the oligomerization of n-butene.

Increasing the distribution constant or the ratio of the concentration of reactants in the pores to that in the external solution is known as matrix enhancement. This results when the matrix acts to increase the number of reactant/catalyst contacts over those obtained in homogeneous catalysis at equivalent reactant/catalyst

concentrations. It may either enhance selectivity as a result of some structural characteristic of the matrix or increase the tendency of reactants to move into the body of the bead. Hammett and Riesz, for example, have found an enhanced ester hydrolysis when exchanging some of the protons with quarternary ammonium ions (57). The ligand groups of the ammonium ion must be similar to those on the ester and by the principle "like dissolves like" it is claimed that a favourable distribution constant is obtained. Similarly an enhanced rate of hydrolysis of olefinic esters is obtained when exchanging some protons with silver ions (58). Silver ions are known to co-ordinate with unsaturated compounds and this favours the distribution of the olefinic ester in the resin (59).

Depending on the reaction system, crosslinking percentage, surface area and average macropore size may affect catalytic activity. These variables are related to each other in that the specific surface area increases with increasing degree of crosslinking, while generally the average pore size increases with decreasing surface area.

The degree of crosslinking influences swelling in microspheres. Gates et al studied four model reactions, involving small polar reactants (methanol dehydration), reactants of intermediate size and polarity (propanol-ethyl acetate re-esterification), larger non-polar reactants (toluene alkylation) and larger polar reactants (t-butyl alcohol dehydration). To date the results of the first two reactions have been published. The methanol reaction (61) showed that swelling and diffusion effects are negligible. It was found that surface sites are less active than sites in the polymer gel interior. The latter observation was also demonstrated for the rate of re-esterification (60). However the reaction rates were strongly influenced by diffusion in the microparticles, but the effect of macropore diffusion and adsorption on microparticle surfaces were negligible. The more highly crosslinked polymers offer greater resistance to diffusion in the microparticles but have the more active catalytic sites within the microparticles. The difference between the two reactions with respect to their

ability to swell the microspheres is based on the molecular size and polarity of the reactant molecules. Higher microparticle surface area does not imply higher catalytic activity. Similarly it was found for the dehydration of isopropanol that surface area had no bearing on catalytic activity, but that activity fell with increasing average pore radius (56). The rate of 1-propanol dehydration decreased with increasing content of divinyl benzene, in spite of the substantial increase in specific surface area in the same direction (46). This indicates that on the less cross-linked ion exchangers the reaction is taking place to a significant extent within the polymer mass.

1.3.3.2 The Effect of External Factors

Factors such as reaction temperature, weight percent, catalyst and reaction time also influence the reaction. Their effects are shown in Tables 1.10, 1.11 and 1.12, respectively, for the case of the batch dimerization of di-isobutene (42).

Temp (°C)	Conversion (wt %)
50	25
60	40
70	60

Table 1.10 : Effect of reaction temperature

Catalyst Conc. (wt %)	Conversion (wt %)
2	25
10	83

Table 1.11 : Effect of weight percent catalyst

Reaction Time (hr)	Conv (wt %)	Reaction Time (hr)	Conv (wt %)
1	27	5	58
2	35	6	63
3	47	20	85
4	53		

Table 1.12 : Effect of reaction time

Similar increases in conversion with increasing reaction temperature were also found by Rothmayer et al who studied the oligomerization of a C_4 hydrocarbon mixture (63). Furthermore, these investigators found that as the reaction temperature increased, less dimers, and more trimers and tetramers were produced.

1.3.3.3 Effect of Water

The major portion of the literature describing acid resin catalysis involves dissociated sulphonic acid in hydrated resins, such as in the hydrolysis of esters using pure water as a solvent (64), (type A_1), or the hydrolysis of methyl and ethyl acetates, ethyl n-butynate and ethyl n-hexanoate dissolved in acetone (65), (type A_2). Gates has published a series of papers describing catalysis by anhydrous sulphonic acid. These papers showed the catalytically active species and the reaction mechanism to be completely different from those observed in the presence of water (48,53).

Zundel showed in infrared spectroscopic studies the structures which exist in hydrous and anhydrous conditions (66). The sulphonic acid groups in a completely anhydrous sulphonic acid resin are paired by the formation of a doubly hydrogen bonded structure, i.e.

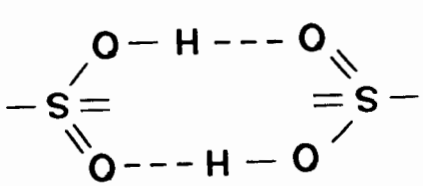

while in the presence of minute quantities of water, the latter molecule is strongly bonded to three sulphonic acid groups

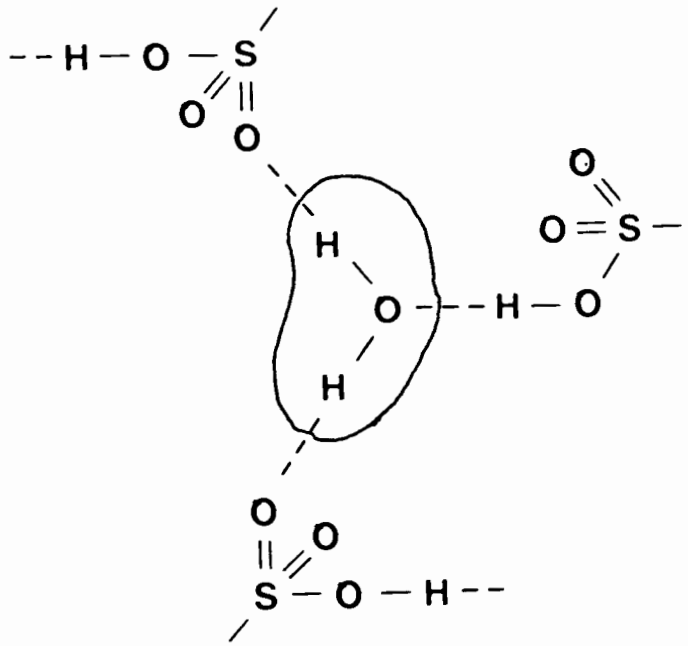

A fourth sulphonic acid group may be similarly bonded to the remaining electron pair of the water oxygen. Gates used Zundel's technique to examine the mechanism of the dehydration of formic acid using anhydrous sulphonic acid resins as catalysts, a type B_2 reaction (48). The study showed that the formic acid was bound to the sulphonic acid sites by hydrogen bonds.

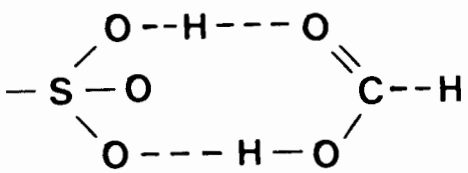

He proposed the following mechanism for the resin catalysed dehydration of formic acid.

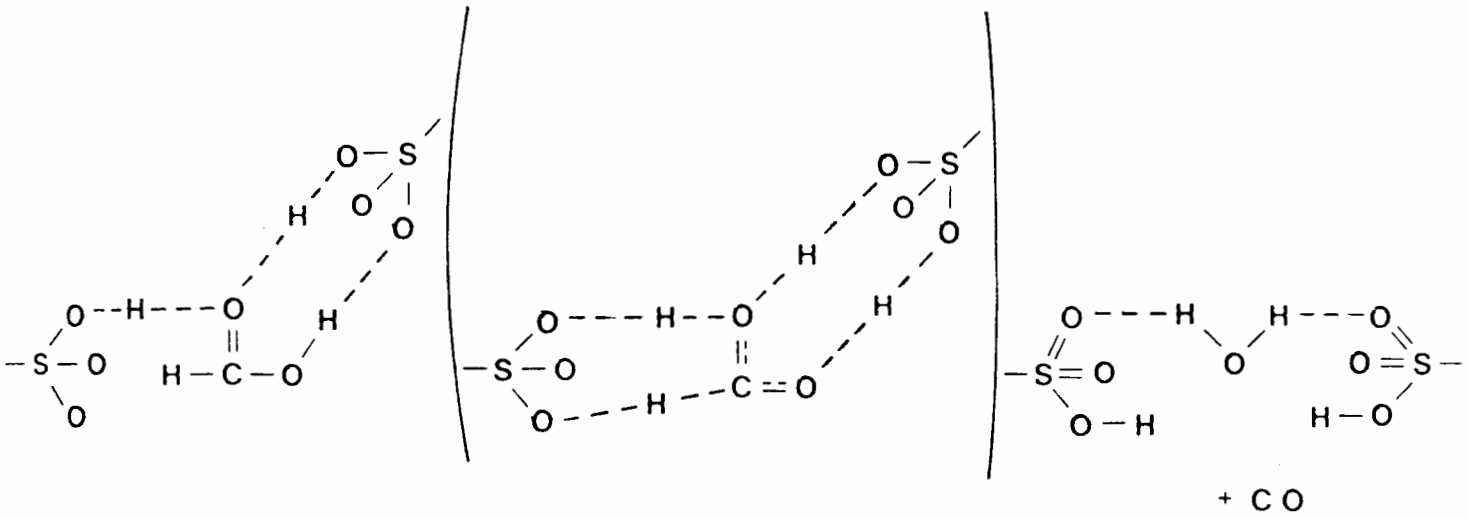

Water in the matrix suppressed the formic acid reaction by binding to the sulphonic acid groups in competition with reactant. Zundel showed that only two water molecules per sulphonic acid group were sufficient to convert all the protons to their solvated state (67). Thornton and Gates followed the type B_1 and B_2 reactions of olefin and paraffin formation from butyl alcohols (53). They found that alcohols could also inhibit reactions by competing with reactants as does water.

Zundel found that the residual water content on drying was a function of the severity of the drying conditions. When hydrated resin is rapidly dried at 150°C all of the water is removed. When drying is slow, water is hydrogen bonded to three sulphonic acid groups and cannot be removed even under severe conditions (67). Similar results were obtained by Krönig and Scharfe. They found that when resin, after being produced, is dried at approximately 100°C and under reduced pressure, about 7% by weight of water remained. Only under more severe conditions, e.g. temperatures between 120 and 220°C, pressures under 100mm Hg and heating times between 2 and 5 hours, can the water content be reduced to less than 2% by weight (42). This drying to a maximum possible extent increases the activities. This was shown by the following example (42). Two catalysts containing 7% and 0.8% by weight of water,

respectively, were used for the dimerization of di-isobutene in a batch system. The catalyst with the higher water content showed a conversion of only 2.6% while the other converted 60% of the feed. A similar need to eliminate the presence of free water in the reaction system was reported by Scharfe for their industrial butene oligomerization process (41) and by Haag in his kinetic studies of the oligomerization of isobutene (24). The latter also found that conversions in batch reactors are lower compared to those in flow reactors, because moisture would remain in batch reactors while it is eliminated quickly from the catalyst in the continuous flow system.

The effect water has on the conversion and selectivity of the polymerization of a C_4 hydrocarbon mixture is shown in Table 1.13 (63). Rottmayer et al found that the amount of dimers formed increased with increasing water content in the feed at the expense of tetramers and longer polymers.

Water content (wt %)	Isobutene conversion (wt %)	1-butene conversion (wt %)	Fractional conversion into dimers
10.0	16	1	0.94
8.0	40	12	0.77
5.5	65	21	0.76
2.0	76	48	0.61
≦ 1.0	81	56	0.59

Table 1.13 : Effect of water content in feed on the polymerization of a C_4 hydrocarbon mixture

1.3.3.4 Improving Thermal Stability and Reactivity

The polystyrene matrix is stable up to temperatures of about 220°C. However, the degradation of the sulphonic acid groups has to be taken into account at temperatures above 130°C. A second order dependence of this degradation on the concentration of sulphonic acid groups was found (69). Further Botha et al showed that the thermal stability of sulphonated styrene divinylbenzene copolymers is limited by the chemical reactivity of the sulphonic acid groups which leads to hydrolytic cleavage of the C-S bond and, in media other than water, to the formation of sulphones. By the use of differential thermal analysis in the gas phase, it was shown that the salt form of an ion exchange resin exhibits a greater thermal stability than the acid form, i.e. thermal splitting of C-S does not occur, and that the strong weight loss of the polymeric acid is not caused by a thermal decomposition of the matrix. Isothermal decomposition in the gas phase showed that the weight and capacity loss was due to chemical reactions. These reactions are the hydrolysis of sulpho groups by traces of moisture after drying, resinification of the polymer under the influence of sulphuric acid (SO_2 formation), and additional crosslinking of the resin due to the formation of sulphones (Resin $-SO_3H$ + HO_3S-Resin → Resin $-SO_2$ - Resin + H_2SO_4) (69).

These authors conclude that the synthesis of polymeric sulphonic acids of higher thermal stability is possible only if the ionic group is not bound directly to the aromatic ring.

Klein and Widdecke reported on the introduction of the substituents X, Y and Z into the polystyrene matrix leading to thermally more stable and/or more active resin catalysts (68).

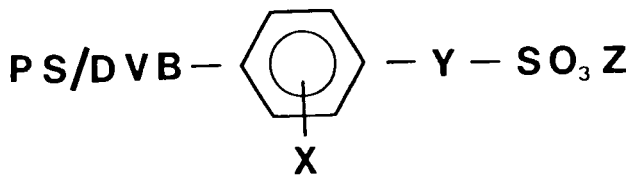

The role of each substituent is discussed below:

i) Substituent X. The introduction of electron withdrawing groups into the aromatic nucleus increases the thermal stability as is reported in the patent literature for the nitro-group (70) and chlorine (71). However, the latter results in the gradual formation of corrosive HCl. To prevent this the aromatic double bond has to be destroyed so that the reversible reaction leading to the loss of the functional group cannot occur. Klein and Widdecke prepared such a perfluorinated polymeric acid (68). Apart from its improved thermal stability at 200°C, it was also chemically more stable towards oxidising agents and more active, because the introduction of the fluorine increases the acidity of the sulphonic acid groups.

ii) Substituent Y. Sulphoalkylation was attempted to obtain a thermally more stable resin, because aliphatic sulphonic acids are much more stable against hydrolysis than aromatic ones. Klein, Widdecke and Döscher synthesised a series of catalysts PS - $(CH_2)_n$ - SO_3 - H^+ (n = 1,2,3) and PS - $CH(CH_2SO_3^-H^+)_2$. They did indeed show a marked increase in thermal stability (71) although their activity was not greatly altered. As one would expect, the catalytic activity of the sulphoalkylated resins was strongly increased by a subsequent fluorination so that highly acidic resin catalysts are obtained.

iii) Substituent Z. Since the rate of desulphonation is proportional to the second power of the H^+ concentration, a significant increase in stability can be achieved by partial substitution with metal cations. The success of this approach very much depends on the availability of a metal ion which combines this effect of stabilization with a retainment of the reaction rate. Surprisingly it was found that in many reactions even an increase in the specific reaction rate was found when the protons were substituted by appropriate metal ions, e.g. by Ag^+ (58) (Ag^+ interacts with double bonds), Al^{3+} or Fe^{3+}. The catalytic activity of a resin can be directly correlated to the acidity.

An alternative approach is the addition of metal halides to the sulphonic acid groups of the resin catalyst. This method combines the Lewis acidity of the halide such as $AlCl_3$ with the Bronsted acidity of the support leading to a highly active catalyst. Because of the high reactivity of the resins the reaction temperatures can be lower so that the thermal stability is no longer the limiting factor. Furthermore reactions which cannot be carried out using commercial sulphonic acid resins are catalysed by these polymeric super acids. These include reactions such as paraffin isomerization, cracking and alkylation.

1.3.3.5 Superacidity

Gates and Magnotta studied these super-acid polymers by synthesising and analysing an $AlCl_3$- sulphonic acid resin complex (73). They were prepared by subliming $AlCl_3$ in a carrier gas stream and reacting it with sulphonic acid resin at 115°C. Evidence for this reaction was the evolution of HCl. Analysis showed that the complex was composed of S, Al and Cl in the ratio of 2:1:2 and that it reacted in a manner characteristic of solid superacids. Uniform distribution of the complex throughout the polymer structure was demonstrated by electron microprobe X-ray analysis. Structures analogous to those existing in solutions of superacids have been suggested for the polymer formed from $AlCl_3$ and sulphonic acid resin. The activity and stability of these polymers have been investigated in separate studies. Gates and Magnotta studied paraffin isomerization and cracking in the presence of $AlCl_3$ - sulphonic acid resin complexes. They found the resin similar to HSO_4AlCl_2, initially converting n-butane into isobutane, and n-hexane into isomerization and cracking products. It was also unstable, rapidly losing HCl during operation. Neither $-SO_3^-H^+$ groups alone nor $AlCl_3$ alone in the polymer caused observable n-butane conversion, but a combination of the two was highly reactive, capable of protonating paraffins, and had a pronton-donor strength comparable to that of a superacid solution. Fuentes, Boegel and Gates showed in

further studies that the presence of HCl in the feed increased the rate of the catalytic reaction (74). Kinetic studies of n-butane isomerization can be described by the Langmuir-Hinshelwood model, the reaction being first order in the concentration of butene. Suggestions of the structure of catalytic sites were made. Fuentes and Gates further claimed that the disproportionation of n-butane over similar catalysts produces propane and pentanes, while the conversion of n-pentane yielded products ranging from methane to hexane, with propane and isobutane being the main products (75). The results were broadly consistent with the classical carbonium ion mechanism.

Other catalyst systems prepared from Lewis and Bronsted acids have been discussed by Kluge and Moore (76), Kelly (77) and Huang and Yurchak (78).

The latter studied the isoparaffin-olefin alkylation over resin/boron trifluoride catalysts to form high octane alkylates (79, 80). Three phenomena were observed in this catalytic system. (i) BF_3 or resin alone is ineffective for alkylation; (ii) the H^+ of the sulphonic acid group of the resin does participate in alkylation; and (iii) polymerization predominates when the equivalent ratio of total BF_3 to $-SO_3H$ is less than 2 while alkylation prevails over polymerization when the equivalent ratio is greater than 2. The above three facts strongly suggest that the active species for hydride transfer, and possibly also methyl group migration, may involve one sulphonic acid group and two BF_3 molecules. Five main process variables were found to affect alkylate quality: temperature, olefin space velocity, external isobutane/olefin ratio, surface area of resin, and resin functionality. The effects were as follows:

- alkylate quality decreased as olefin space velocity increased;
- reducing external isobutane/olefin ratio lowered alkylate quality;

- increasing resin surface area improved alkylate quality;
- alkylate quality increased sharply with decreasing temperature;
- diffusional limitations were overcome at particle sizes of 149 microns and smaller;
- the resin/BF_3 catalyst showed much less difference among various butene feedstocks than conventional HF and H_2SO_4 alkylation catalysts; and
- the catalyst was regenerable via methanol extraction.

2. OBJECTIVES OF THE RESEARCH

The objective of this study was to investigate the polymerization of a mixture of C_4- alkenes using cationic exchange resin. The following factors were studied in particular:

- Intraparticular mass transfer. For this purpose resin beads of different particle size and porosity were used.
- Effects of functional groups. The resin matrix was substituted with sulphonic acid and phosphonic acid groups in order to investigate the effect of different acid strengths.
- Effect of changing the concentration of acid sites. The resin matrix was functionalised to varying extents with sulphonic acid groups.
- Effect of various physical parameters. The effects of reaction temperature, pressure, WHSV, regeneration and co-feeding of dimer were studied.

These variables led to a qualitative determination of the rate limiting step in the reaction. Moreover, the form of the catalyst and the reaction conditions which optimized the catalyst performance were determined. The criteria whereby the effect of each variable was measured was the rate of conversion of feed to liquid product per unit time per mass of catalyst. The quality of the liquid fuel produced was determined using gas chromatography, mass spectroscopy, nuclear magnetic resonance and standard ASTM tests.

3. EXPERIMENTAL METHOD

3.1 The Reactor System

3.1.1 Layout

Experiments were carried out on two identical integral high pressure reactor systems. A diagram of this system is shown in Fig. 3.1.

The feed gas is contained in a number 7 Cadac cylinder, which is mounted in such a way as to ensure that only liquid feed of constant composition emanates from it. The reactants are gravity fed via two purification units and a heat exchanger to a high pressure Lewa diaphragm pump (Type FLM : Q_{theor} =0.848 ℓ/hr or Type HK : Q_{theor} =0.97 ℓ/hr).

One purification unit contained 3Å molecular sieves to remove water from the feed and the other a 60Å filter element to remove impurities from the feed.

The reaction product leaving the reactor is cooled in a condenser and passes through a 60Å filter to remove any entrained catalyst particles before the product is released to atmospheric pressure via a back pressure regulator. The latter is a Grove Mity Mite model S91 XW.

The liquid and gas phases in the product are separated in a catch-pot. The gaseous product passes via a knock-out pot, a gasmeter and a gas sampling tube to an atmospheric vent. The gas meter is a Yazaki V25 gas meter with a nominal capacity of 2.0 m^3/hr. The gas sampling tube enables a sample of tail gas to be isolated and removed from the stream for analysis.

The catchpot is a double-walled glass container and is temperature controlled by means of water recirculating from a thermostatted bath at 50°C. This ensures a relatively low but constant amount

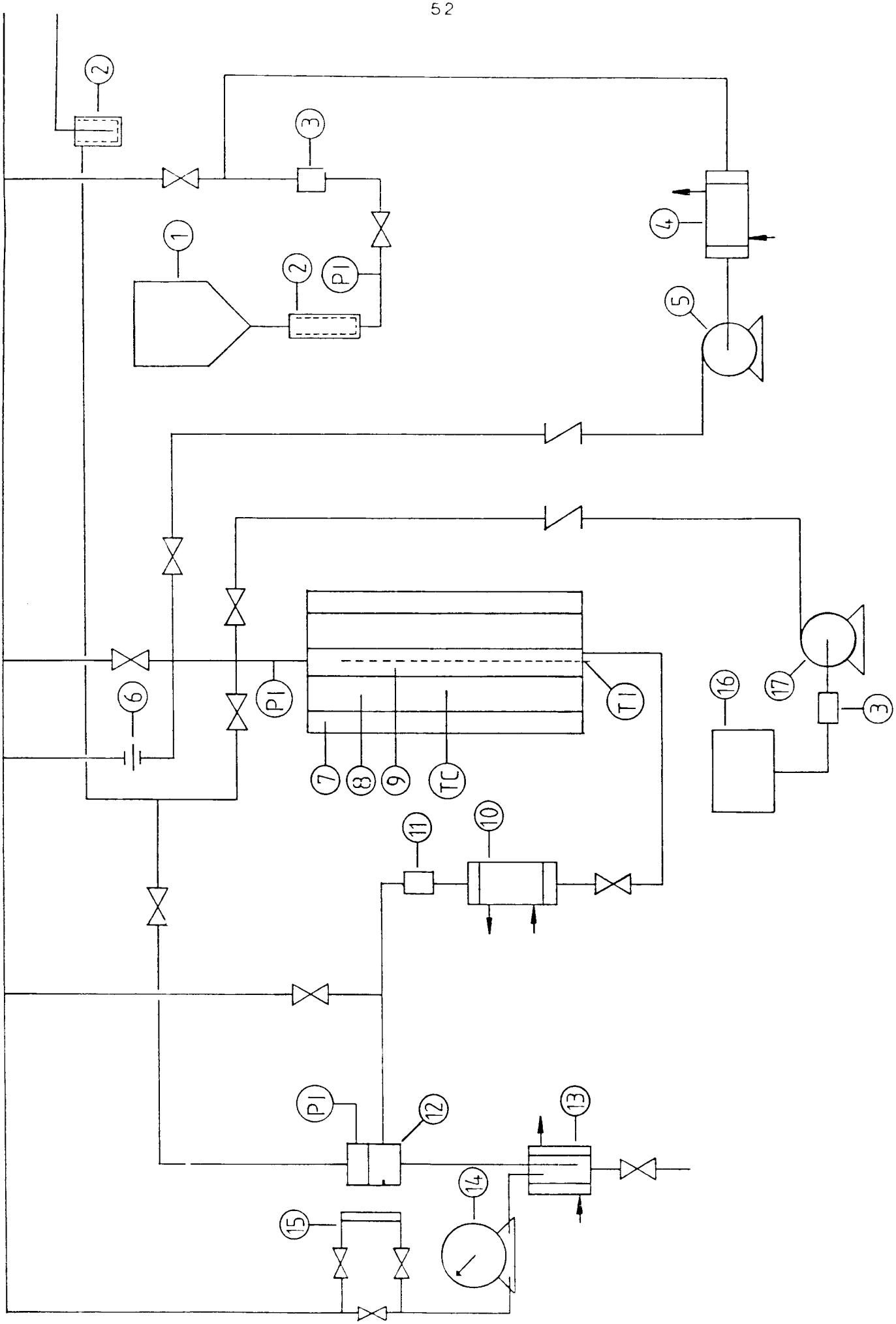

Fig. 3.1 : Diagram of the reactor system

Key to Fig. 3.1

1. Monomer feed cylinder
2. Removable molecular sieve holder
3. Filter, with 60Å element
4. Pump feed cooler, coolant: ethylene glycol/water mixture
5. Monomer feed pump
6. Rupture disc
7. Insulation
8. Heating element & block — integral reactor
9. Catalyst bed
10. Product condenser; coolant : ethylene glycol/water mixture
11. Filter
12. Back pressure regulator
13. Gas/liquid separation vessel; maintained at 50°C by circulating heated water
14. Gasmeter
15. Gas sampling device
16. Recycle feed cylinder
17. Recycle feed pump

of dissolved gases entrained in the liquid product. The liquid product is removed periodically for analysis.

The safety of the line is ensured by the presence of a bursting disc, and a pressure valve in the pump which ensures internal circulation if the delivery side pressure exceeds the setpoint.

Venting lines have been installed to prevent airlocks in the line.

An ethylene glycol/water cooling system cools the feed in a heat exchanger just prior to the pump, the pumphead, and the reactor product in the condenser downstream from the reactor. This serves to prevent cavitation in the pump and ensures adequate condensation of products.

The reactor is made from 316 stainless steel with a diameter of 1 inch and a length of 55cm. The heat is supplied by a heating element coiled around cylindrical aluminium blocks. The aluminium blocks are wrapped around the entire length of the reactor, and serve as a heat sink. These blocks are insulated by fibreglass and asbestos rope. A 2.5mm I.D. thermowell extends up the centre of the reactor enabling the catalyst bed temperature to be measured at various bed depths.

The amount of heat supplied to the reactor is controlled by a Eurotherm proportional temperature controller. The heating element is 12m long and rated at 2kW.

The measuring thermocouple is iron-constantan and is linked to a digital temperature recorder. The controlling thermocouple is chromel-alumel. A separate feed line for co-feeding recycle was also constructed. This consisted of a recycle feed container, a 60Å filter element, and a separate high pressure Lewa diaphragm pump. This separate system was linked to the main system at the inlet to the reactor.

The atmospheric pressure experiments were carried out in a smaller but similar integral reactor system (Ø = 16mm, L = 90mm) (82).

3.1.2 Operation

A detailed description of the operating procedure, including preparations for a run, start-up, steady state operation and shut-down is outlined in Appendix B. Problems of overheating were encountered during start-up while approaching steady state conditions. Due to the high activity of the catalyst, any change of reaction conditions could lead to a runaway reaction. This generated hotspots in the catalyst bed. As the temperature in the reactor was increased, a stage was reached where a phase transition probably occurred. Liquid reactant adsorbed heat from the system, indicated by a sudden, sharp temperature drop (at ± 90°C and 1.5 MPa). This sudden volume

expansion and corresponding pressure increase caused the back pressure regulator to open and a surge of liquid reactant and product occurred, causing a pressure drop in the system to well below operating pressure.

While the reactor pressure built up to its initial value, extensive conversion occurred thus causing marked increases in temperature. Depending on the severity of the overheating, runs were abandoned at this stage and restarted with fresh catalyst. This overheating occurred only in the upper section of the catalyst bed and was mostly of very short duration.

A further problem was encountered in unpacking the reactor subsequent to high conversion runs as a result of the catalyst seeming to fuse in the reactor.

3.1.3 Data Analysis

A computer program was utilized to analyse the data obtained during runs. The following features were available:

- Mass balance. A mass balance calculation was carried out for every run. The percentage loss was determined as follows:

$$\% \text{ loss} = [1 - \{(\Sigma \text{ weight of liquid product}) + (\Sigma \text{ weight of gaseous product})/(\Sigma \text{ weight of reactants})\}] \times 100$$

where the (Σ weight of liquid product) is directly measured by adding the weights of all liquid samples and the (Σ weight of gaseous product) is calculated by the formula:

$$\Sigma \text{ wt of gaseous prod.} = \frac{P\Delta V}{RT} \times M \quad \text{... (ideal gas assumption)}$$

where ΔV = (final gas meter reading - initial gas meter reading)

$T = 288^{\circ}K$

$P = 1$ atm

M = molecular weight based on mean averaged molecular weight over the entire run

and finally the (Σ weight of reactants) is determined from the weight changes of the feed cylinders.

- Cumulative product. This is the sum of liquid product at time t_i collected between $t = 0$ and $t = t_i$. Although this yields averaged as opposed to point data, a more smooth set of results is obtained.

- Specific liquid product flow. This is an indication of the activity of the catalyst and is expressed in terms of liquid product obtained per gram of catalyst per hour.

- Liquid mass % conversion. This is calculated by the formula

$$\text{mass \% conv.} = \frac{\text{mass of liquid product}}{\text{mass of reactant}} \times 100$$

- Liquid sample composition. This is a presentation of the trends of the formation of various polymers with time. It is based on an area % output from the G.C. It can be used to compare polymer production between different runs and variations with time in a particular run.

- Gas sample composition. This data is expressed in terms of mass % and not area %, since the response factors of all components were determined and not assumed to be unity.

- Feed gas mole fraction conversion. This indicates the conversion of the various feed gas components and is expressed as follows : Feed gas mole fraction conversion of component i

$$= 1 - \frac{\text{molar flow of component i in tail gas}}{\text{molar feed rate of component i}}$$

Therefore a positive feed gas mole fraction conversion presents a utilization of the particular component, while a negative value presents a production of that component.

- Gas molar flow rate. This gives the actual component gas flow rates and is obtained from the gas sample composition by the formula:

$$Q_i = \frac{x_i \times \Delta V}{\Delta t}$$

where

Q_i = gas molar flow rate of component i

x_i = mass fraction of component i

ΔV = change in gas meter reading over time Δt

Δt = sampling time interval

Apart from the mass balance data all other methods of analysis could be presented in graphical form as a function of time. A further feature of the program allowed the grouping of data. This was used for gas analysis, because it enabled the classification of the gas components into hydrocarbon types, viz. unsaturates converted, unsaturates produced by isomerization, and saturates.

Although the start-up presented difficulties, these only persisted over a relatively small time fraction of the whole run period and little significant information was obtained therefrom. Hence it was decided to present in the result section only steady state data unless otherwise indicated.

3.2 Catalysts and Catalyst Treatment

3.2.1 Catalysts

In this study only strong, acidic, cationic ion exchange resins of commercial availability were used. Apart from one run, in which a resin with a gelular matrix structure was used, viz. Duolite C20, all other resins were macroreticular. These included Amberlyst 15, Amberlyst 1010 and Duolite C26. Their properties are shown in Table 3.1 (6, 83). The ion exchange resins containing various degrees of functionality were prepared by Klipfontein Organic Products (K.O.P.). The skeletal structure of these samples was the same as that of Duolite C26. Moreover the same matrix was used for the addition of the phosphinic and phosphonic acid groups.

	Ion Exchange Resin			
	Amberlyst 15	Amberlyst 1010	Duolite C26	Duolite C20
Skeletal structure	Styrene-DVB	Styrene-DVB	Styrene-DVB	Styrene-DVB
Ionic functionality	SO_3-H^+	SO_3-H^+	SO_3-H^+	SO_3-H^+
Physical form	Opaque beads	Opaque beads	Opaque beads	Translucent beads
Total capacity eq/ℓ	1.8	1.0	1.85	2.0
Total capacity meq/g	4.6	3.3	-	-
Int.Surf.area m^2/g	55	540	-	nonexistent
Calc. wt capacity of int. surf. meq/g	0.193	1.90	-	nonexistent
Porosity, vol %	36	50	-	nonexistent
Av Macropore diam.Å				

Table 3.1 : Properties of the various ion exchange resins

3.2.2 Catalyst Treatments

3.2.2.1 Pretreatment

The pretreatment procedures were those recommended by various manufacturers (4, 5). The resin was washed with an organic solvent to remove any monomers which remained in the matrix during synthesis. The resin is then sequentially changed from the Na^+- form to the H^+ - form and subsequently either stored in distilled water or dried. The detailed pretreatment procedure is outlined in Appendix D.

Dehydration can be carried out using one of three methods (12).

- heating under vacuum;
- displacement with hydrophilic organic solvents and subsequent removal of the latter by means of heat; or
- azeotropic distillation with organic solvents such as toluene, xylene, methylene chloride, etc.

In the present work the first method was used.

3.2.2.2 Reactivation of Resins

The effectiveness of an ion exchange material is at times reduced by the replacement of H^+ ions with other cations, which adsorb onto the resin surface. Such cation fouled resins are reactivated by treatment with dilute sulphuric acid (10). Appendix D gives a detailed reactivation procedure. In some instances deactivation of ion exchange resins is caused by the accumulation of more complex materials on the surface and in the interior of the ion exchange particles. A batch treatment with concentrated sulphuric acid has been shown to restore the catalytic activity of such an organically fouled catalyst (10). A description of this treatment is given in Appendix D.

3.2.2.3 Determination of Resin Dry Weight Capacity (D.W.C.)

The total acid capacity is determined by adding an excess of sodium hydroxide to a dried, weighed sample of cationic exchange resin. Sufficient time is allowed to exchange all the H^+ ions by Na^+ ions. The excess sodium hydroxide is neutralised by back-titration with HCl. In this way the total number of acid sites can be determined. The exact method is outlined in Appendix D (84).

The method is applicable for strong cationic exchange resins of mono or dual functionality.

3.2.2.4 Preparation of Ion Exchange Resins containing Phosphonic and Phosphinic Functional Groups

The phosphonic acid functional group ($HPO_3^-H^+$) is of intermediate acid strength compared on the one hand to the sulphonic acid functional group, which is highly ionized and acts as a strong acid, and on the other hand to the carboxylic acid functional group, which is only slightly ionized and acts as a weak acid. The phosphinic acid functional group ($PO_3^{2-}(H^+)_2$) has an acid strength of the same order of magnitude as the phosphonic acid functional group, but has two exchangeable protons.

An aromatic resin suitable for use as an ion exchange resin matrix is allowed to react with a phosphorous trihalide in the presence of aluminum chloride to form a halophosphine derivative of the resin matrix, which is then hydrolysed. This causes hydroxyl groups to be substituted for the halogen atoms which are attached to phosphorus in the halophosphine derivative of the resin matrix, and thus provides a cation exchange resin having phosphonic acid functional groups attached to aromatic nuclei of the resin. The cationic exchanging capacity of such exchange resins may be increased by oxidising the trivalent phosphorus in the functional acid groups to pentavalent phosphorus, thereby increasing the number of active acid groups attached to phosphorus which are available for catalysing reactions. A detailed preparation procedure is given in Appendix D (85). The aromatic resin matrix used is that of the commercial resin Duolite C26.

3.2.2.5 Determination of Acid Strength

The acid strength of a solid surface is defined by its proton donating ability. Hammett has derived the following function for the quantitative expression of Bronsted acid sites (86):

$$Ho = pKa + \log\frac{(B)}{(BH^+)}$$

where Ho = acid strength function
pKa = acid strength
(B) = concentration of the base form of the adsorbed indicator
(BH^+) = concentration of the acid form of the adsorbed indicator

Hammett indicators (Table 3.2) are a class of visible indicators, which, when adsorbed on the solid surface, give a measure of this acid strength of the solid as a result of a colour change. If the colour is that of the acid form of the indicator, then the value of Ho of the surface is equal to or lower than the pKa of the indicator. If the colour is that of the basic form of the indicator then the value of Ho of the surface is equal to or higher than the pKa of the indicator. Low values of Ho hence correspond to greater acid strength. The mechanism of interaction of the catalyst with the solid surface is as follows :

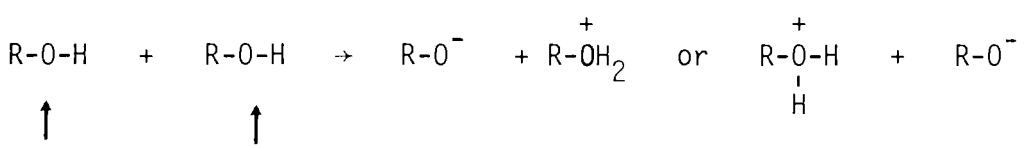

Table 3.2 shows the indicators used, their colour in the acid and base form, their pKa value and the wt% of H_2SO_4 solution corresponding to the respective pKa value.

Indicator	Basic Colour	Acidic Colour	pKa	H_2SO_4 (wt %)
Butter yellow	yellow	red	+3.3	3×10^{-4}
Benzeneazodi-phenylamine	yellow	purple	+1.5	2×10^{-2}
p-Nitrodiphenyl-amine	yellow	orange	-2.4	42
Benzalacetophenone	colourless	yellow	-5.6	71
Anthraquinone	colourless	yellow	-8.2	90

Table 3.2 : Hammett indicators used for solid acid strength determination

3.2.2.6 Determination of the Porosity of the Catalyst

This was done to get a comparison between the pore size distribution and the total pore volume of the various ion exchange resins used. Of primary interest here was the size distribution of the macropores because, as will become evident later, these contained the sites where the actual reaction was taking place. Therefore the size distribution was obtained only down to a pore diameter of 35Å. Pressure penetration volume curves can be utilized to calculate the specific surface area (87) with fair reliability provided sufficiently high pressures are applied to force mercury into the smallest pores and provided there are no bottle-shaped pores. These measurements were carried out by Sasol Technology on a Micro-meritics Pore Sizer 9300 prosimeter. The samples were predried overnight at 50°C and 440mm Hg absolute pressure and then pre-evacuated in the porosimeter to 60 micron by absolute. The data was then obtained by mercury porosimetry at room temperature (ca. 25-30°C)

3.3 Analytical Methods

3.3.1 Gas Chromatography (G.C.)

The gas chromatograph used in this study is a Varian 3700. The response of the G.C. detectors was monitored by a Varian Vista

401 Data system, which can be programmed to give an integral and/or differential analysis of the composition of the sample.

3.3.1.1 Gas Analysis

Both the feed gas, which was obtained from the Sasol I plant, and the tail gas, which was the unconverted feed gas, were analysed using G.C. Two different stocks of feed gas were used. Their compositions are shown in Table 3.3.

Component	Mass Percent	
	Feedstock 1	Feedstock 2
Propane		3.05
Propene	0.15	4.45
Isobutane	1.86	2.45
n-Butane	13.25	12.44
1-Butene	60.81	57.56
Isobutene	6.80	7.07
Trans-butane	8.20	6.41
Cis-Butane	8.03	5.64
C_5 and others	0.50	0.93

Table 3.3 : Feed gas compositions

Feedstock 1 was used for run 01 to run 08
Feedstock 2 was used for run 09 to run 38

The column used for the gas analysis contained an n-Octane/Porasil C packing, was approximately 5.7m long and had an I.D. of 3mm.

The G.C. settings used were as follows:

Detector:	Flame ionization
N_2 pressure:	400 kPa (flowrate : 30mℓ/min)
H_2 pressure:	300 kPa (flowrate : 30mℓ/min)

Air pressure:	300 kPa (flowrate : 300mℓ/min)
Injector temperature:	150°C
Detector temperature:	250°C
Column temperature program:	2 min @ 50°C; 8°C/min to 125°C; 5 min @ 125°C
Column pressure:	47 psig @ 50°C
Sample volume:	0.1 mℓ

A typical chromatogram and the retention times and response factors for the various components are given in Appendix E.

3.3.1.2 Liquid Analysis

Due to the complexity of the liquid product spectrum arising from the large number of isomers of the various polymers formed, it was impossible to identify all the peaks. Instead the analysis of the liquid product was based on the carbon number and since true polymerization of the feed was predominant, the various polymers of the monomer were obvious groupings. A mass spectrometer was used to determine the transition points between successive polymers. However, the cutpoints were not distinct and a certain amount of overlap occurred. This is mainly due to the fact that branched hydrocarbons have much lower boiling points and hence retention times than their straight chain counterparts. In section 4.17 the accuracy of this classification is shown. The various groups and their retention time ranges are given in Table 3.4.

Polymer	Retention time range (mins).
Monomer	0.0 - 1.6
Dimer	1.6 - 4.5
Trimer	4.5 - 10.5
Tetramer	10.5 - 15.0
Pentamer	15.0 - 23.0

Table 3.4 : Polymer G.C. response times

The relative response factors for all these groups have been taken as unity and thus the result is expressed as area %, which is not equal to mass %. It has however been shown that for hydrocarbons the relative sensitivity is approximately 1 (88), and thus the results should be a reasonable representation of the true composition. For accurate quantitative analysis, however, response factors have to be determined.

The analysis based on area % therefore gives information on the variation of the liquid product distribution with time and gives a relative comparison of the formation of specific polymers under different conditions.

For the liquid analysis the packing used in the column was 3% silicone on OV-101. The column had a length of 2.8m and an I.D. of 3mm.

The G.C. settings used were as follows:

Detector:	Flame ionization
N_2 pressure:	400 kPa (flow rate: 30mℓ/min)
H_2 pressure:	300 kPa (flow rate: 30mℓ/min)
Air pressure:	300kPa (flow rate: 300mℓ/min)
Injector temperature:	150°C
Detector temperature:	250°C
Column temperature program:	1 min @ 40°C; 10°C/min to 300°C; 10 min @ 300°C
Column pressure:	17 psig @ 40°C
Sample volume:	1 μℓ

Note that the time during which the temperature of the column is programmed is much longer than the retention time of the longest polymer. This is done to prevent the build-up of high boiling point material on the column, which would cause baseline drift.

3.3.1.3 Determination of the Water Content in the Olefinic Feed

The work in this section was also carried out using the Varian 3700 gas chromatograph and the Varian 401 data system. A thermal conductivity detector (T.C.D.) was used.

The response of a T.C.D. is proportional to the concentration of water in the carrier gas stream. At low concentrations this response is linear with respect to the water concentration. However at high concentrations the detector becomes saturated and the curve plateaus. It is imperative to work in the linear range of the curve.

Hence there were two aims in carrying out this work. Firstly, a correlation was required to related the T.C.D. response to the water concentration in the carrier gas stream. To be of any benefit this correlation had to be linear in the range of concentrations used. Appendix E gives the details for the determination of such a correlation. The results are shown in Fig. 3.2.

Secondly, this correlation was used to determine the water content in the olefinic feed by relating the concentration of water in the carrier gas to the concentration of water in the feed. Appendix E outlines this method and the results are shown in Table 3.5 below.

	Concentration of H_2O in feed (p.p.m.)
Wet feed	597 ± 8.2 %
Wet feed dried over 3Å molecular sieves	152 ± 3.3 %

Table 3.5 : Water content in feed

The apparently limited efficiency of the molecular sieves is in contradiction with generally found trends. This may be due to poor sampling techniques, the possibility of too short a contact time or subsequent saturation of samples and therefore these results are probably not highly accurate.

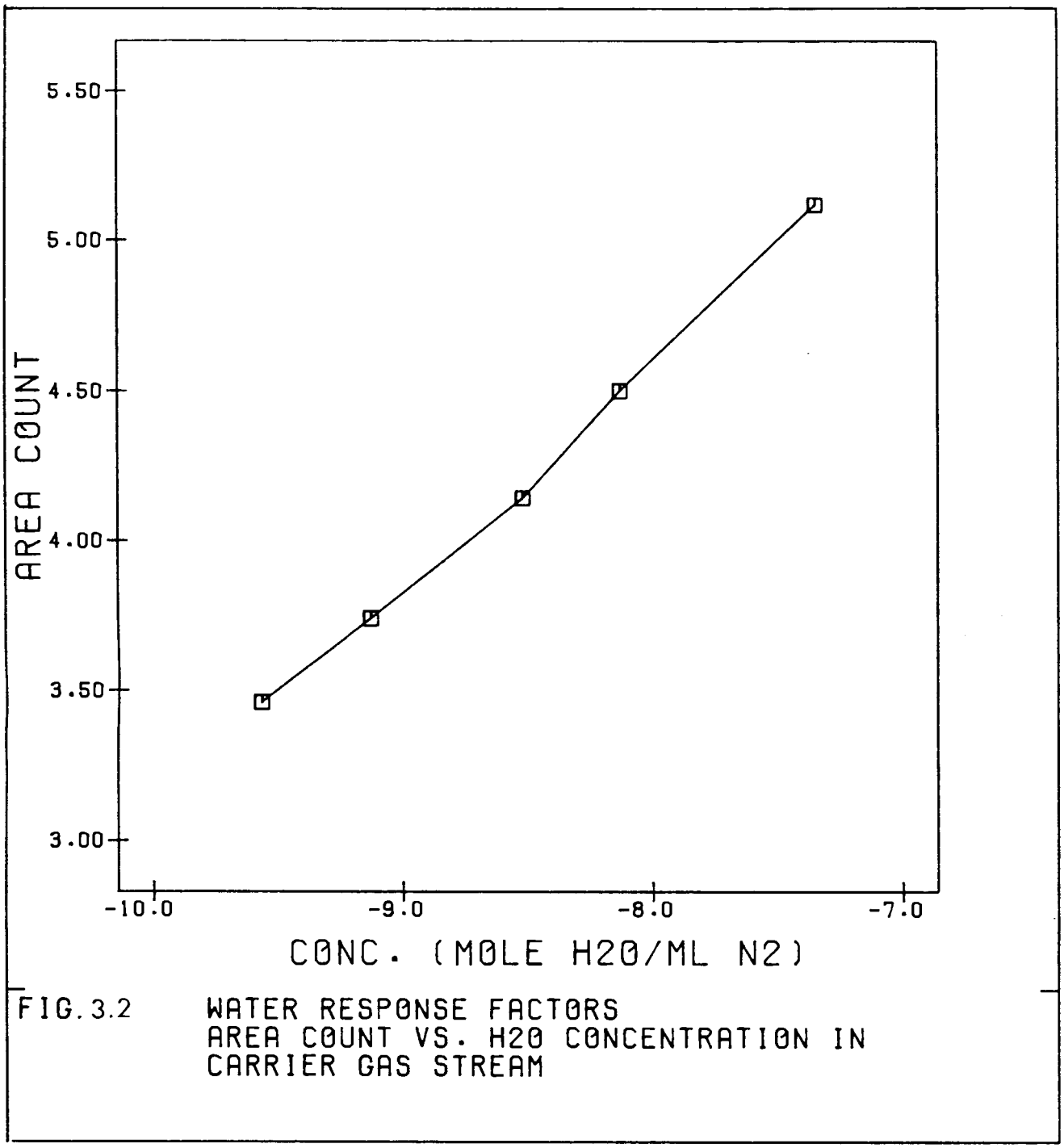

FIG. 3.2 WATER RESPONSE FACTORS
AREA COUNT VS. H20 CONCENTRATION IN
CARRIER GAS STREAM

3.3.2 Mass Spectroscopy

In this study mass spectroscopy was used for two purposes. Firstly it was used to calibrate the G.C. column for liquid product analysis. By separating a complete liquid sample in a G.C., which had an identical column and operated under the same conditions as the G.C. method used for liquid product analysis a chromatogram was obtained in which the molecular weights corresponding to the individual signals could be assigned. This enabled a grouping due to carbon number of the G.C. column to be made. Secondly it was used to determine the presence of saturates in the product.

3.3.3 Nuclear Magnetic Resonance (N.M.R.)

N.M.R. is able to provide the following information:

- the number of signals gives an indication of the different kinds of protons;
- the position of the signals gives information about the electronic environment of each proton;
- the intensity of the signals gives information on the number of protons of each kind; and
- the splitting of the signals into several peaks gives information about the environment of a proton relative to others.

Due to the complexity of the liquid product analysed, only information on the type of protons present, i.e. aromatic, aliphatic, primary, secondary, etc., and on the relative abundance of such groups was obtained. The characteristic proton chemical shifts of the more important types of protons are shown in Table 3.6.

Type of proton		Chemical shift, p.p.m. (S)
Primary	RCH_3	0.9
Secondary	R_2CH_2	1.3
Tertiary	R_3CH	1.5
Vinylic	C = C-H	4.5 - 5.9
Aromatic	Ar-H	6.0 - 8.5
Benzylic	Ar-C-H	2.2 - 3.0
Allylic	$C = C-CH_3$	1.7
	$C = C-CH_2-R$	2.0

Table 3.6 : Characteristic proton chemical shifts

It is obvious from the above table that S values for some groups overlap and this will invariably lead to errors. Nevertheless estimates of the following can be obtained from the spectra:

- the degree of branching, viz. CH_3/CH_2 ratio;
- the volume of aromatics, olefins and saturates present in the gasoline fraction; and
- the hydrogen to carbon ratio.

Myers et al (89) have attempted to correlate the relative amounts of aromatics, saturates and olefins of motor gasoline fuels by the following equations:

$$\text{Aromatics, vol \%} = \frac{(A+C/3)0.97}{(A+C/3)0.97 + (D-2B+E/2+F/3)1.02 + 3.33B} \times 100$$

$$\text{Paraffin, Vol \%} = \frac{(D-2B + E/2 + F/3)1.02}{(A+C/3)\ 0.97+ (D-2B+E/2+F/3)1.02 + 3.33B} \times 100$$

$$\text{Olefin, vol \%} = \frac{3.33B}{(A+C/3)0.97 + (D-2B+E/2+F/3)1.02 + 3.33B} \times 100$$

$$\text{Hydrogen/Carbon} = \frac{A + B + C + D + E + F}{(A+C/3)1.28 + (D-2B+E/2+F/3)1.02 + 3.42B}$$

where A = integral intensity of Aromatic protons
B = integral intensity of Vinylic protons
C = integral intensity of Benzylic protons
D = integral intensity of Tertiary protons
E = integral intensity of Secondary protons
F = integral intensity of Primary protons

These equations have been corrected for average density differences and differences in the ratio of carbons counted to carbons present. This is shown in Table 3.7.

The integration for the olefinic group has to be done very precisely since the correction term is very large.

	Weighted average density (g/mℓ)	Weighted average ratio of carbon counted/carbon present
Aromatics	0.8732	0.7835
Paraffins	0.6612	0.9831
Olefins	0.6808	0.2917

Table 3.7 : Average densities and carbon counts for aromatics, olefins and saturates

An additional correction was the subtraction of 2B from the paraffin term due to the methyl and methane groups α to C=C which resonate in the paraffin methine region.

For the present investigation it was observed that no signal was obtained in the range of 6.0 to 8.5 p.p.m. and therefore no aromatic components appear to be present, i.e. A and C are equal to zero.

Furthermore an attempt was made to reduce the correction term for the olefin content. This was done by assigning two further peaks, namely the peak at 1.7 p.p.m. to the $C=C-CH_3$ group and the peak at 2.0 p.p.m. to the $C=C-CH_2-R$ group. These peaks are significant in the samples due to their high olefinic content. A G.C. analysis was also carried out on the motor gasoline fraction and indicated that it consisted of about 85% by mass of dimer and 15% by mass of trimer. Therefore the ratio of carbons counted to carbons present is recalculated and yields 4/8 x 0.85 x 4/12 x 0.15 = 0.4750. The unaccounted carbons resonate in the paraffinic region and therefore should be subtracted from that region. This was done in the equations below.

$$\text{Aromatics, vol \%} = 0.0$$

$$\text{Paraffins, vol \%} = \frac{(D+E/2+F/3)1.02 - 0.54(B+H/2+G/3) \times 100}{(D+E/2+F/3)1.02 + (2.04-0.54)(B+H/2+G/3)}$$

$$\text{Olefin, vol \%} = \frac{2.04(B+H/2+G/3) \times 100}{(D+E/2+F/3)1.02 + (2.04-0.54)(B+H/2+G/3)}$$

$$H/C = \frac{B + D + E + F + G + H}{(D+E/2+F/3)1.28 + (2.10-0.54)(B+H/2+G/3)}$$

$$CH_3/CH_2 = \frac{(G + F)}{(H + E)} \times 2/3$$

$$\text{Terminal C/ chain C} = 1/3(G + F)/(D + E/2 + B + H/2)$$

where B = integral intensity of C=CH group
D = integral intensity of $R\text{-}\overset{R}{\underset{|}{C}}H\text{-}R$ group
E = integral intensity of $R\text{-}CH_2\text{-}R$ group
F = integral intensity of $R\text{-}CH_3$ group
G = integral intensity of $C{=}C\text{-}CH_3$ group
H = integral intensity of $C{=}C\text{-}CH_2\text{-}R$ group

The above equations will be used to analyse the N.M.R. spectra in the present study. A disadvantage of the correction factor of the olefinic term is that no account has been made for the carbon atoms which do not give an NMR signal, i.e. $-\overset{|}{\underset{|}{C}}-$ and $=\overset{|}{C}-$. This leads to an underestimation of the olefinic content.

3.3.4 Distillation

The bulk liquid product obtained from the reactors was separated into a petrol and diesel fraction in a batch distillation system. This is shown in Fig. 3.3. Up to three litres of liquid product can be treated per batch. The heat is supplied via a power controlled heating mantle. The vapour from the still passes via a column, packed with berl saddles and where contact with the reflux occurs, to a condenser. The condensate from the latter is either returned to the still or is removed as produced. The latter separation is regulated by a plunger which is controlled by a solenoid operating a magnet, fused to the plunger. In turn, the solenoid is controlled by a timing device which enables the total cycle time to be set and the time for the plunger is in the reflux position.

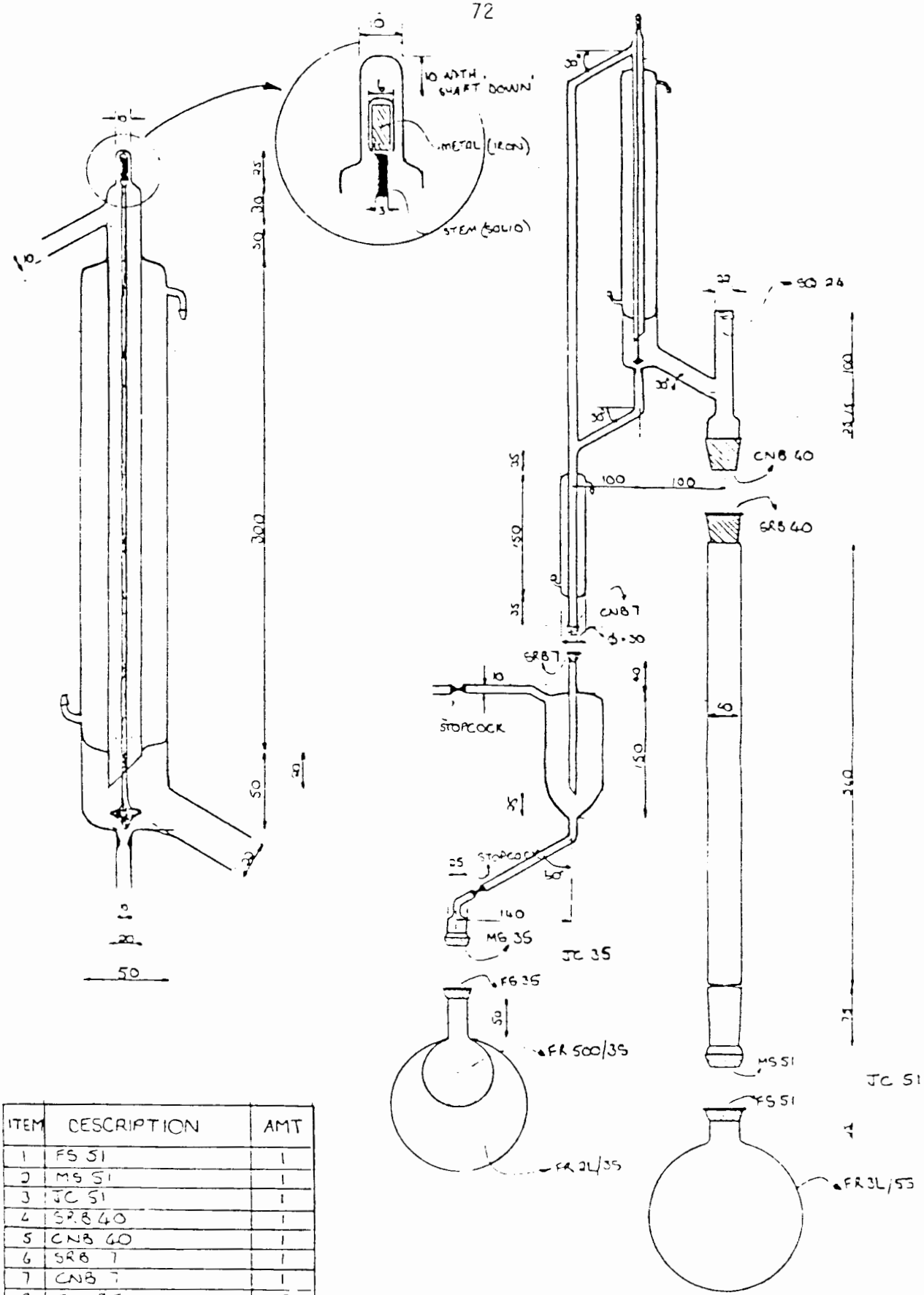

ITEM	DESCRIPTION	AMT
1	FS 51	1
2	MS 51	1
3	JC 51	1
4	SRB 40	1
5	CNB 40	1
6	SRB 7	1
7	CNB 7	1
8	FS 35	5
9	MS 35	1
10	SB 24, QC 24/2 OR 2.9	1 EACH
11	FR. 3L/55	1
12	FR 2L/35	1
13	FR 500/35	5

Fig. 3.3 : Batch distillation system

The reflux ratio is then calculated by the ratio of the time during which the plunger is in the product flow position to the time it is in the reflux position. For all cases, the reflux ratio used was 0.222.

The condenser coolant liquid was water. Hence dissolved gases were not condensed but removed from the system via a gas meter and gas sampling tube to a vent.

The cut-off temperature could be set and was then controlled by a thermostat, which, when the required temperature was reached, switched the reflux ratio to total reflux. The initial cut-off temperature was set at 180°C according to that used by Sasol. However, since differences in barometric pressure causes 180°C inland (av. pressure p.a. ± 85 kPa) to correspond to 187°C at sea level (av. pressure p.a. ± 101.3 kPa), it was decided to use in the final run a cut-off temperature of 190°C.

3.3.5 Microanalysis

Microanalysis was used to determine the ratio of hydrogen atoms to carbon atoms and to confirm that the liquid product was free of oxygen containing components. It can be shown that for an olefin of general formula C_nH_{2n} the mole percent of carbon is 85.71% and the mole percent of hydrogen is 14.29%. For an alkane of general formula, C_nH_{2n+2}, the mole percent of carbon is $100/\frac{(7n+1)}{6n}$ and the mole percent of hydrogen is $100\frac{(n+1)}{7n+1}$.

3.3.6 Standard Fuel Tests

To maintain and control the quality of the great variety of petroleum products, the latter are subjected to a number of tests at various stages of manufacturing, storage and distribution. These tests are of two kinds, firstly, those which are designed to control the quality of the product and, secondly, those which give an indication of its expected performance.

The majority of test methods in use today have been standardized and published either by the American Society for Testing of Materials (ASTM) or the British Institute of Petroleum (I.P.) (90, 91, 92, 93). Appendix E gives the various test methods for motor gasoline and diesel fuel oils, the relevant ASTM/IP code and an explanation of the significance of each test.

4. RESULTS

The criteria whereby the effectiveness of the catalyst was measured was the liquid production rate, expressed in terms of grams of liquid product produced per gram of catalyst per hour and henceforth abbreviated as L.P.R. The term selectivity was used to refer to the relative amount of the various polyers formed. The abbreviations A_1, A_2, A_3 and A_4 are used in diagrams and figures for monomer, dimer, trimer and tetramer respectively. The weight hourly space velocity (WHSV) was defined as the weight of reactant fed to the reactor system per hour per weight of catalyst.

For all experiments a mass balance was carried out. The mass loss in all cases was less than 5%. Catalyst bead sizes between 500 and 850 microns and reaction conditions of 1.5 MPa and 100°C were used for all experiments unless otherwise stated.

4.1 Reproducibility of Data

Two runs were carried out under similar conditions. The catalyst used was Amberlyst 15 with particle size in the range 1000 to 1180 microns.

Figure 4.1 shows the L.P.R. for each run as a function of time. It shows clearly that the largest discrepancies occur during start-up and in the attaining of steady state. However, once steady state is reached the conversions are similar and the reproducibility acceptable.

A study of the variation of the composition of the liquid product with time is shown in Fig. 4.2. It shows that for both runs the composition of the liquid product was reproducible and that in each run approximately the same amount of dimer, trimer and tetramer was produced. The similarity in the liquid product distribution was further indicated by a 100mℓ ASTM distillation, the results of which are shown in Fig. 4.3.

It is thus concluded that at steady state more than adequate reproducibility was attainable, both with respect to selectivity and L.P.R.

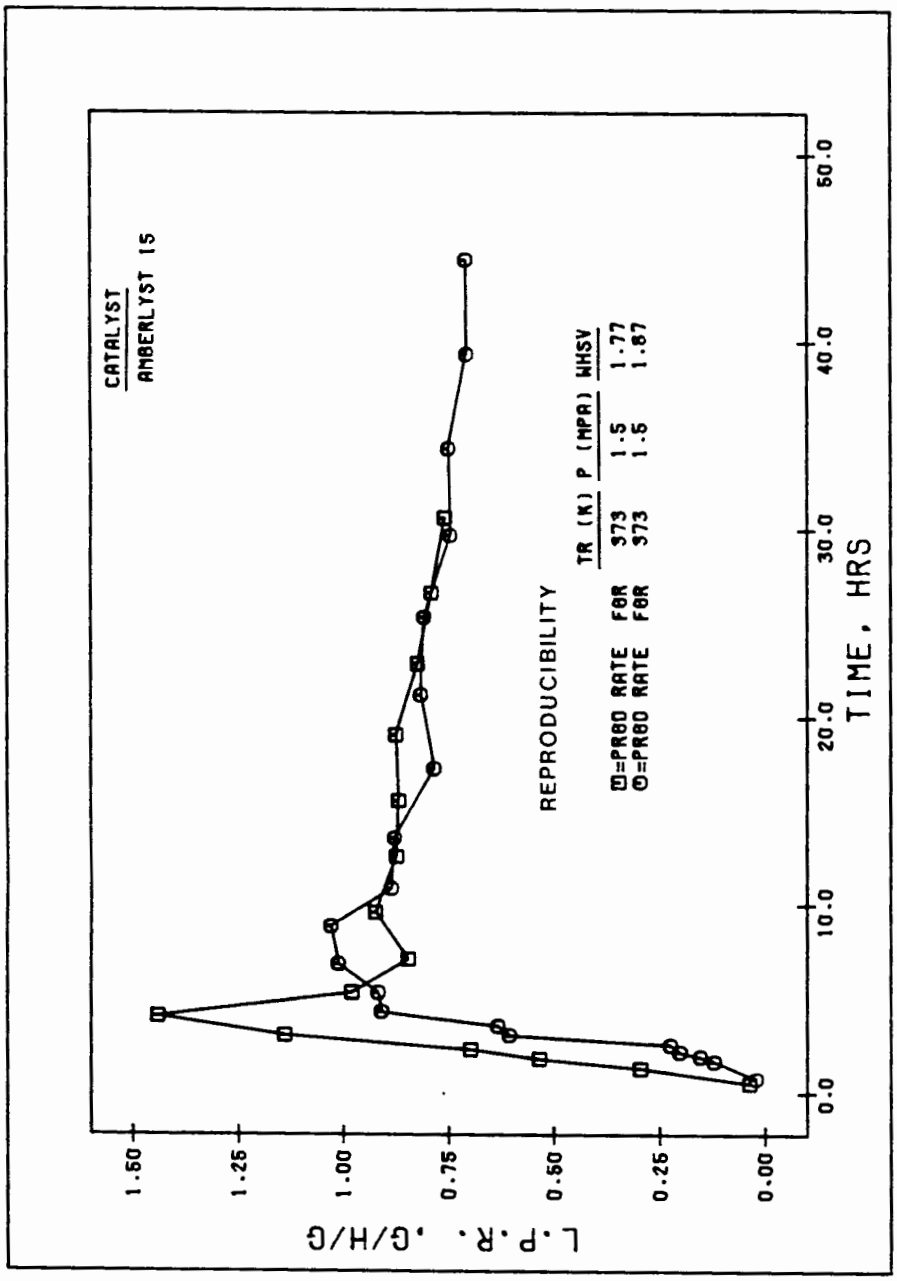

FIG. 4.1 LIQUID PRODUCTION RATE (G/H/G) VS TIME (H)

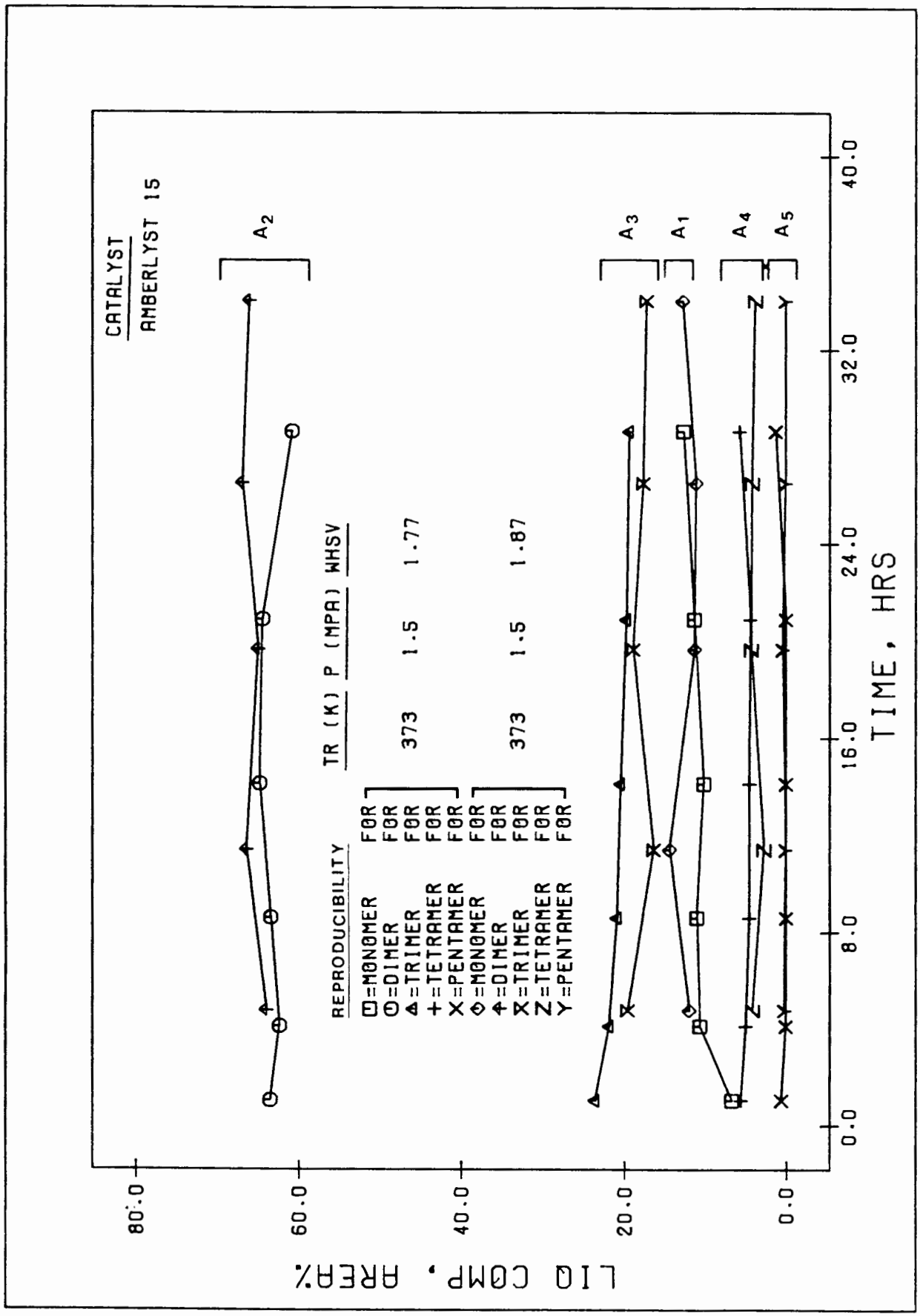

FIG.4.2 LIQ PROD COMPOS (AREA%) VS TIME (H)

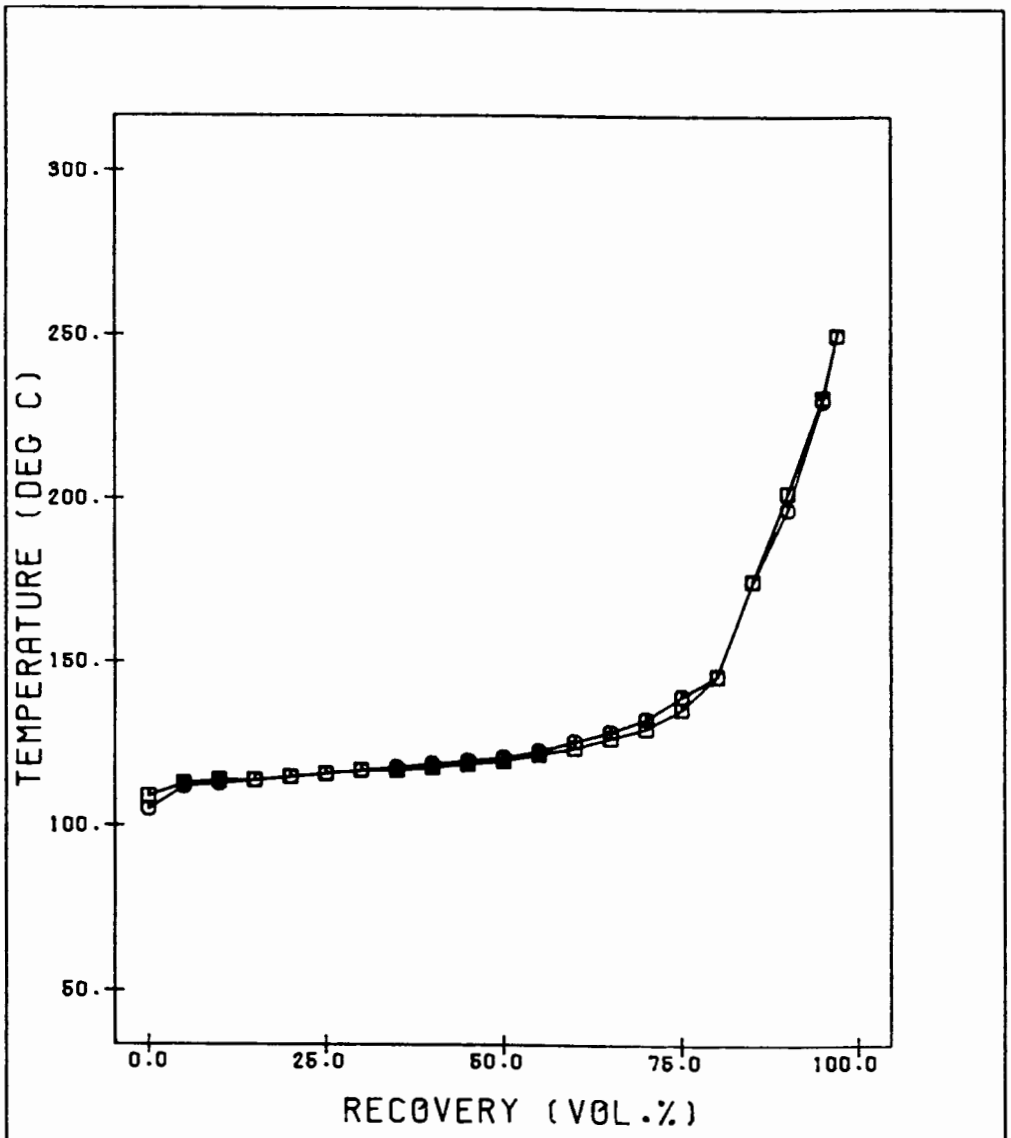

FIG. 4.3 ASTM-DISTILLATION REPRODUCIBILITY OF DATA

4.2 The Effect of Changing Matrix Porosity

For this study reactions were carried out using Amberlyst 15, Amberlyst 1010 and Duolite C26 and a WHSV of approximately 1.78.

Fig. 4.4 shows the pore size distribution of these three resins as determined by mercury porosimetry. While the total volume of pores with diameters bigger than 35Å is the same for Amberlyst 15 and Amberlyst 1010, that for Duolite C26 is much smaller. Amberlyst 15 and Duolite C26 have most of their pore diameters in the range of 100 to 300Å, while those for Amberlyst 1010 are below 100Å.

Specific surface areas calculated from the above pore size distribution are shown in Table 4.1. For this purpose a contact angle of 130° was assumed.

Ion exchange resin	Internal surface area (m^2/g)
Amberlyst 1010	188
Amberlyst 15	84
Duolite C26	68

Table 4.1 : Specific surface areas for resins with different porosities

These values are not similar to those quoted for Amberlyst 15 and Amberlyst 1010 by their manufacturer, viz. 55 and 540 m^2/g respectively.

Fig. 4.5 compares the L.P.R. using these three catalysts with respect to time. Whereas Amberlyst 15 shows a higher L.P.R. it deactivates more rapidly. However after forty hours it still had a higher L.P.R. value than the other two.

The selectivity also proved to be markedly different for the three different resins. This is shown in Fig. 4.6 where the relative trends in the dimer, trimer and tetramer production, respectively, are plotted against time. Amberlyst 15 produces greater amounts of dimer and smaller amounts of trimer and tetramer although to a lesser extent, the same is demonstrated by Duolite C26 and then by Amberlyst 1010, which has the greatest fractions of longer chain length products.

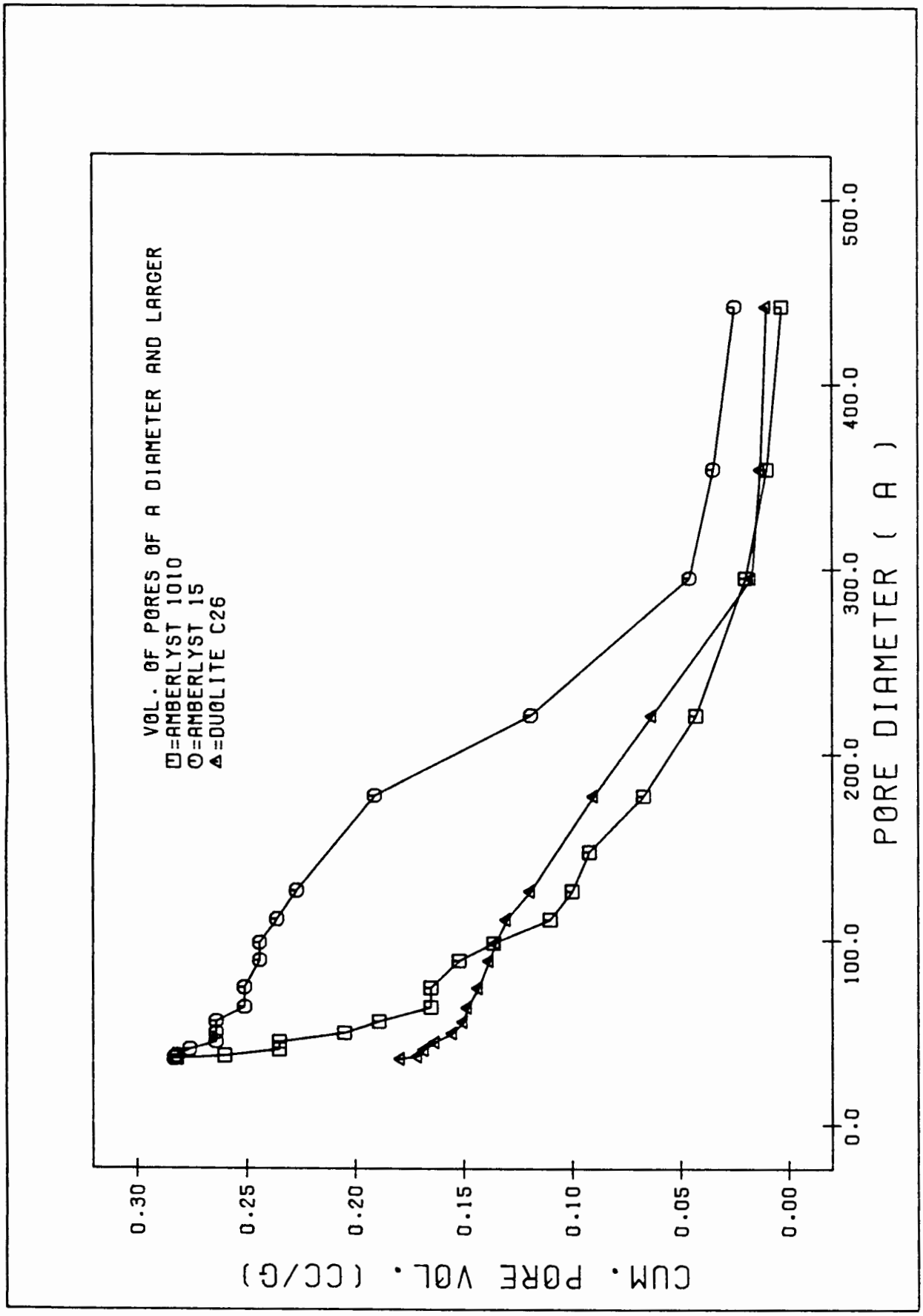

FIG. 4.4 PORE SIZE DISTRIBUTION

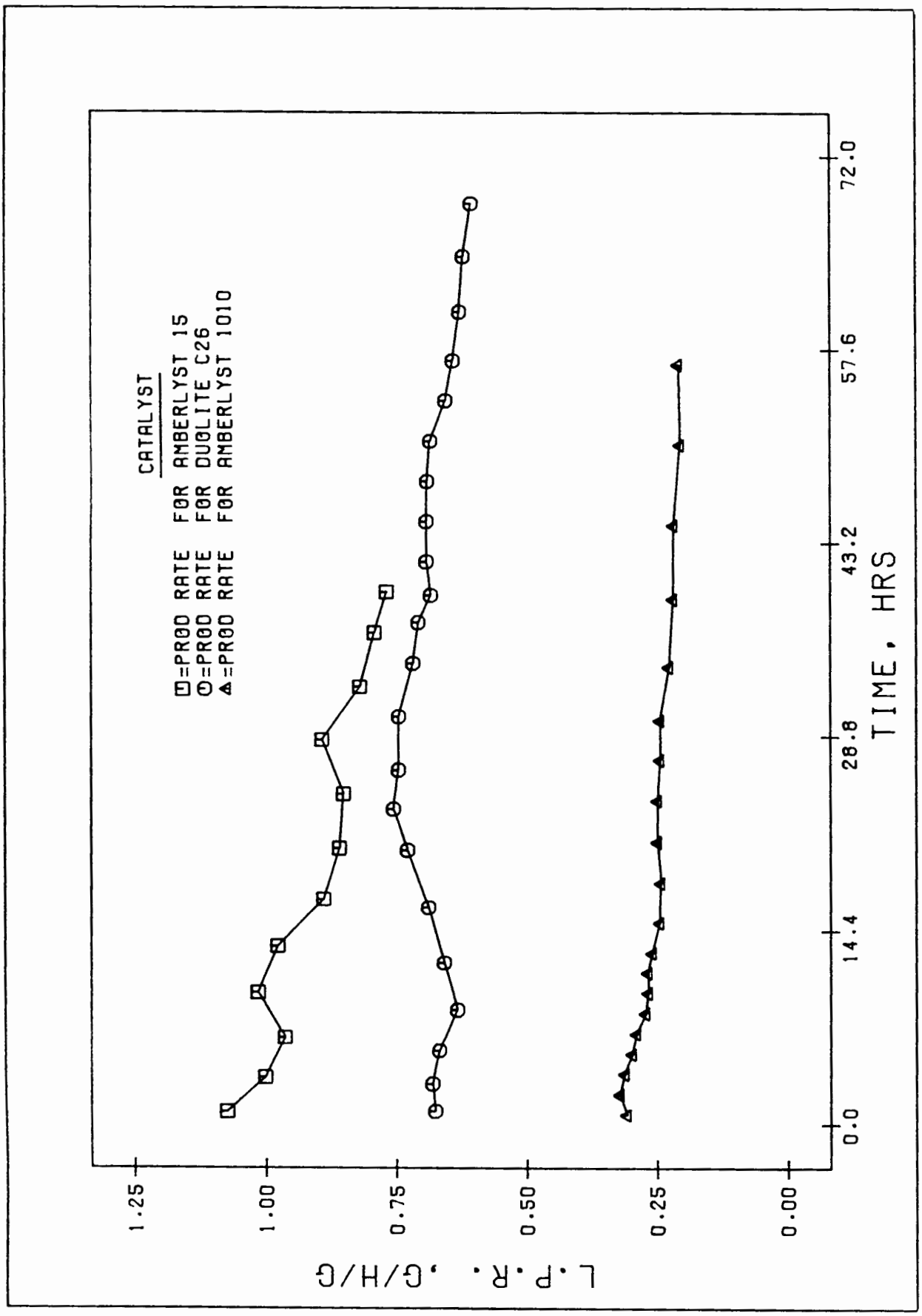

FIG.4.5 LIQUID PRODUCTION RATE (G/H/G) VS TIME (H)

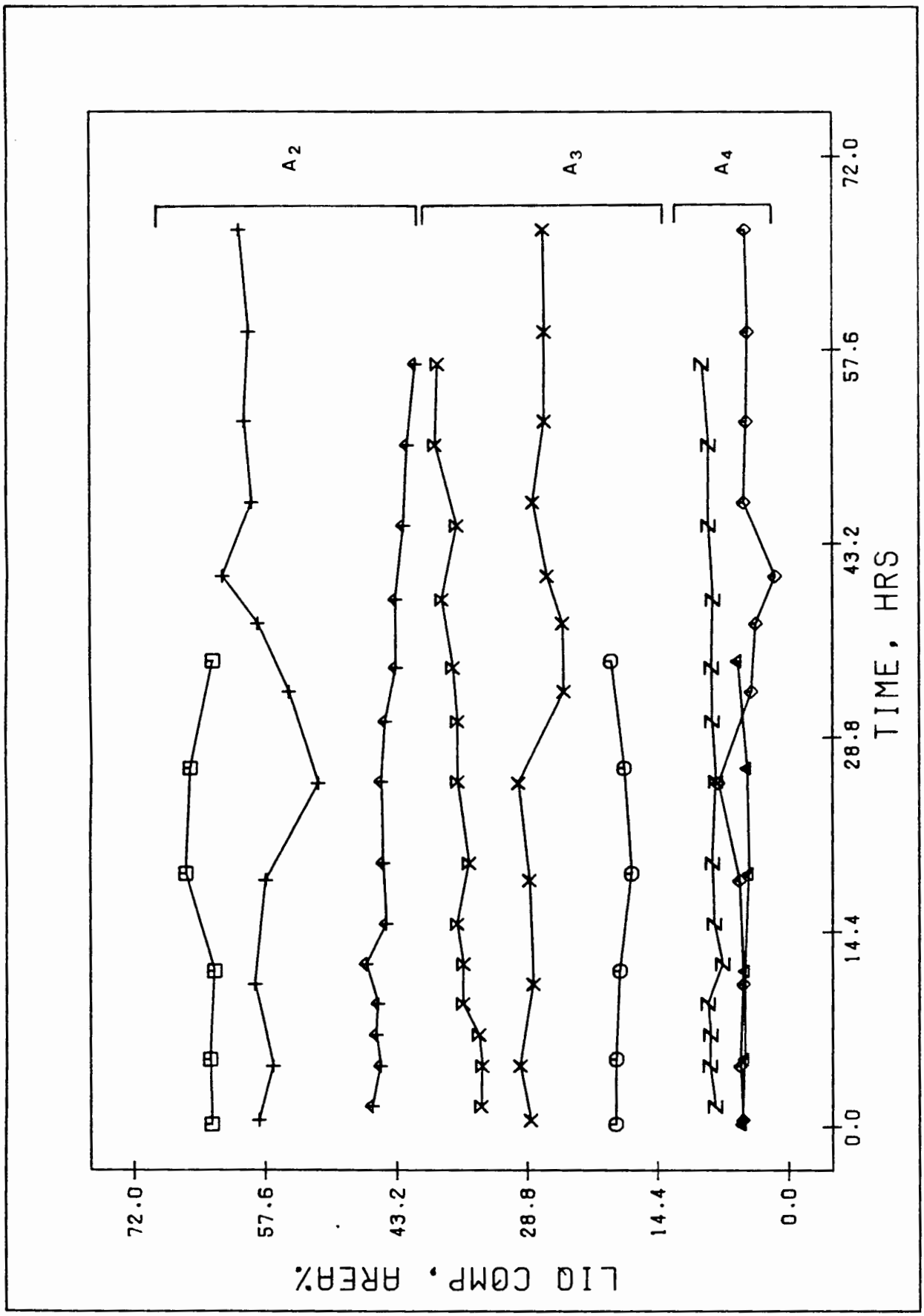

FIG. 4.6 LIQ PROD COMPOS (AREA%) VS TIME (H)

Fig. 4.7 shows a 100mℓ ASTM distillation curve. The superior selectivity of the Amberlyst 1010 resin is clear.

From the above it follows that the resins with larger macropores are more active even though they may have a smaller surface area than resins with small diameter macropores.

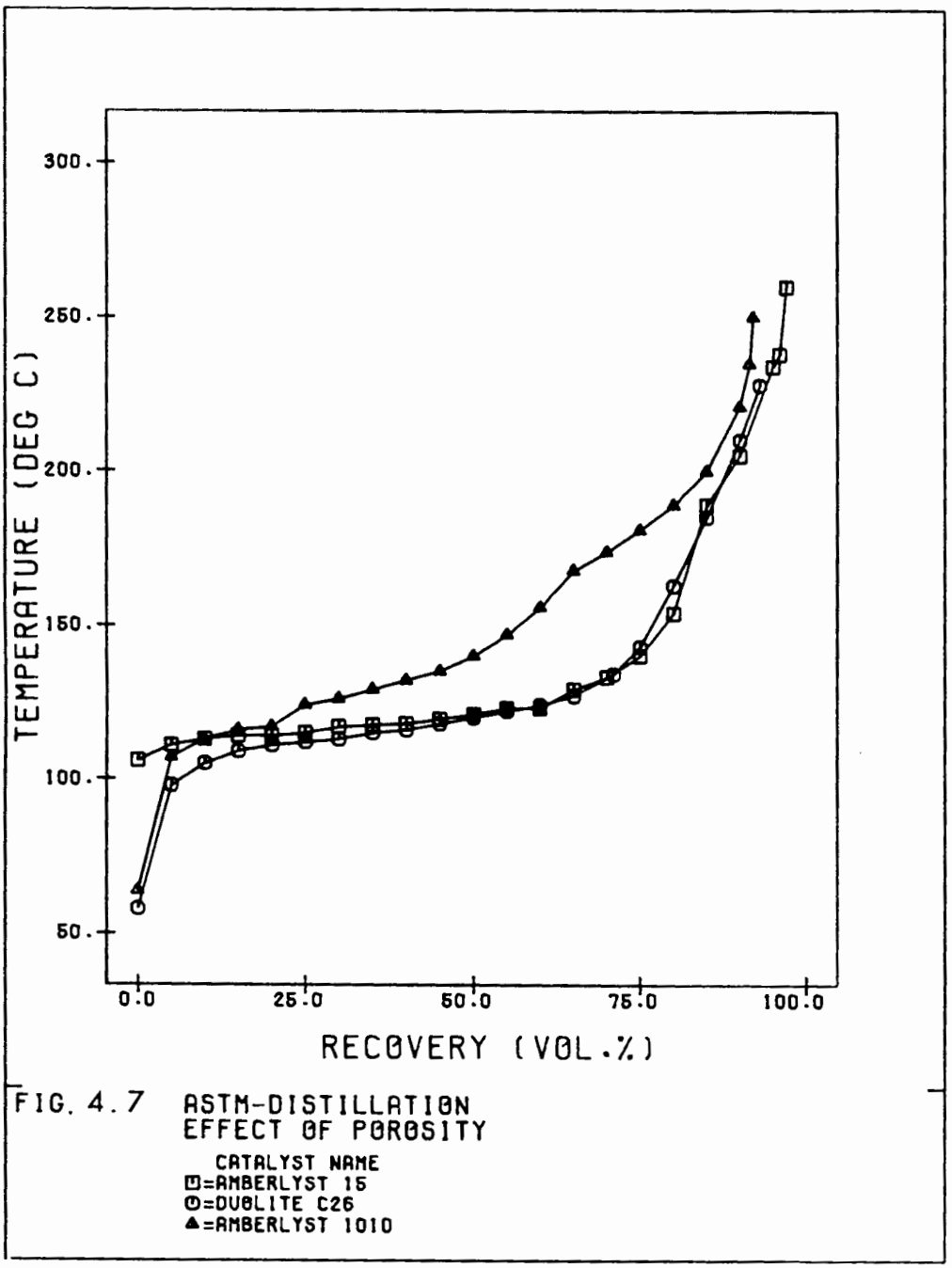

FIG. 4.7 ASTM-DISTILLATION
EFFECT OF POROSITY

4.3 The Effect of Gelular Matrix Structure

A run was carried out using Duolite C20, a strong cationic resin with a gelular matrix structure, as catalyst.

After ten hours at 100°C, 1.5 MPa and a WHSV of 1.7, gas analysis showed no conversion of feed to be taking place. The run was abandoned at this stage.

4.4 The Effect of Changing Particle Size

A batch of Amberlyst 15 was separated into 300-500, 500-850 and 1000-1180 micron size fractions respectively. Reactions were carried out using each fraction at a feed rate of approximately 1.7 WHSV.

Fig. 4.8 shows the L.P.R. using each of these bead size ranges, as a function of time. Although the range of sizes available was relatively narrow, it is clear that the L.P.R. drops as the bead size increases.

Testing a greater range of bead sizes would require crushing of beads. This was not attempted because (i) it is not known what the effect of crushing is on the uniformity of the bead shape and (ii) it would cause problems in supporting the bed without catalyst entrainment in the type of reactor used.

Selectivity data is shown in Fig. 4.9 and Fig. 4.10. The first figure shows that there is no change in selectivity with time and also that the relative amounts of dimer, trimer and tetramer formed in each run do not change with changing bead size. This consistency in selectivity is confirmed by the results of a 100mℓ ASTM distillation of the bulk liquid product shown in Fig. 4.10.

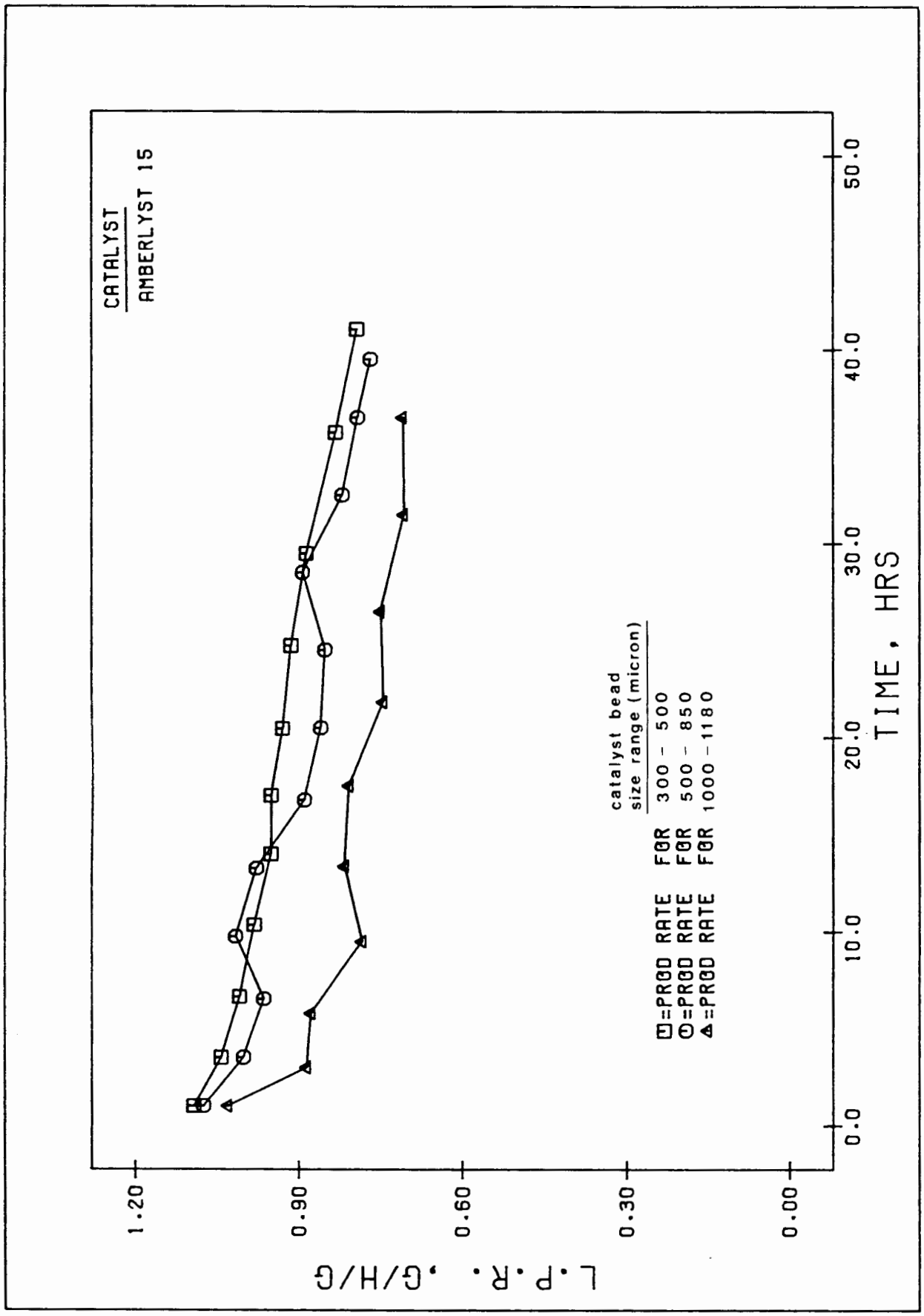

FIG.4.8 LIQUID PRODUCTION RATE (G/H/G) VS TIME (H)

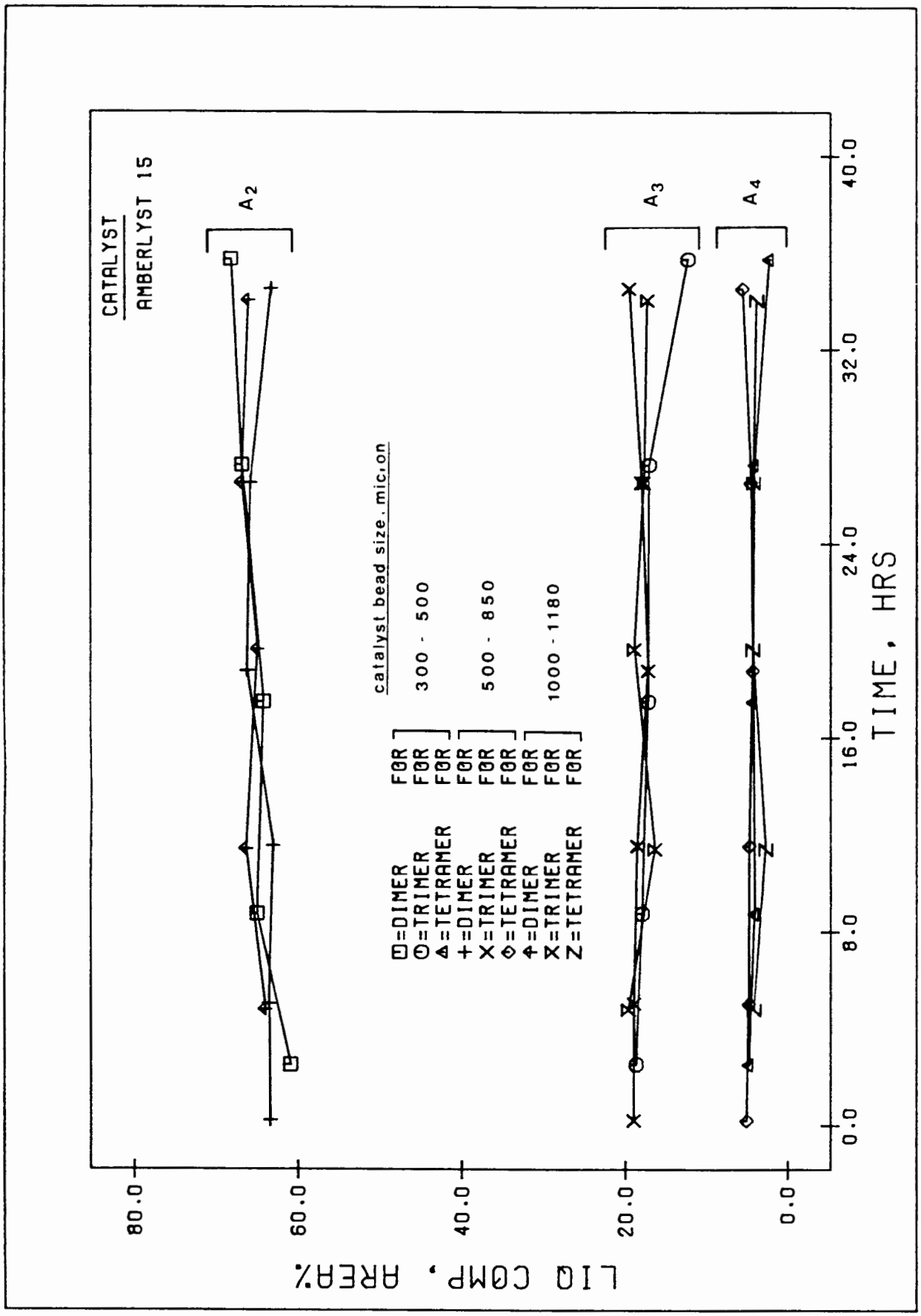

FIG. 4.9 LIQ PROD COMPOS (AREA%) VS TIME (H)

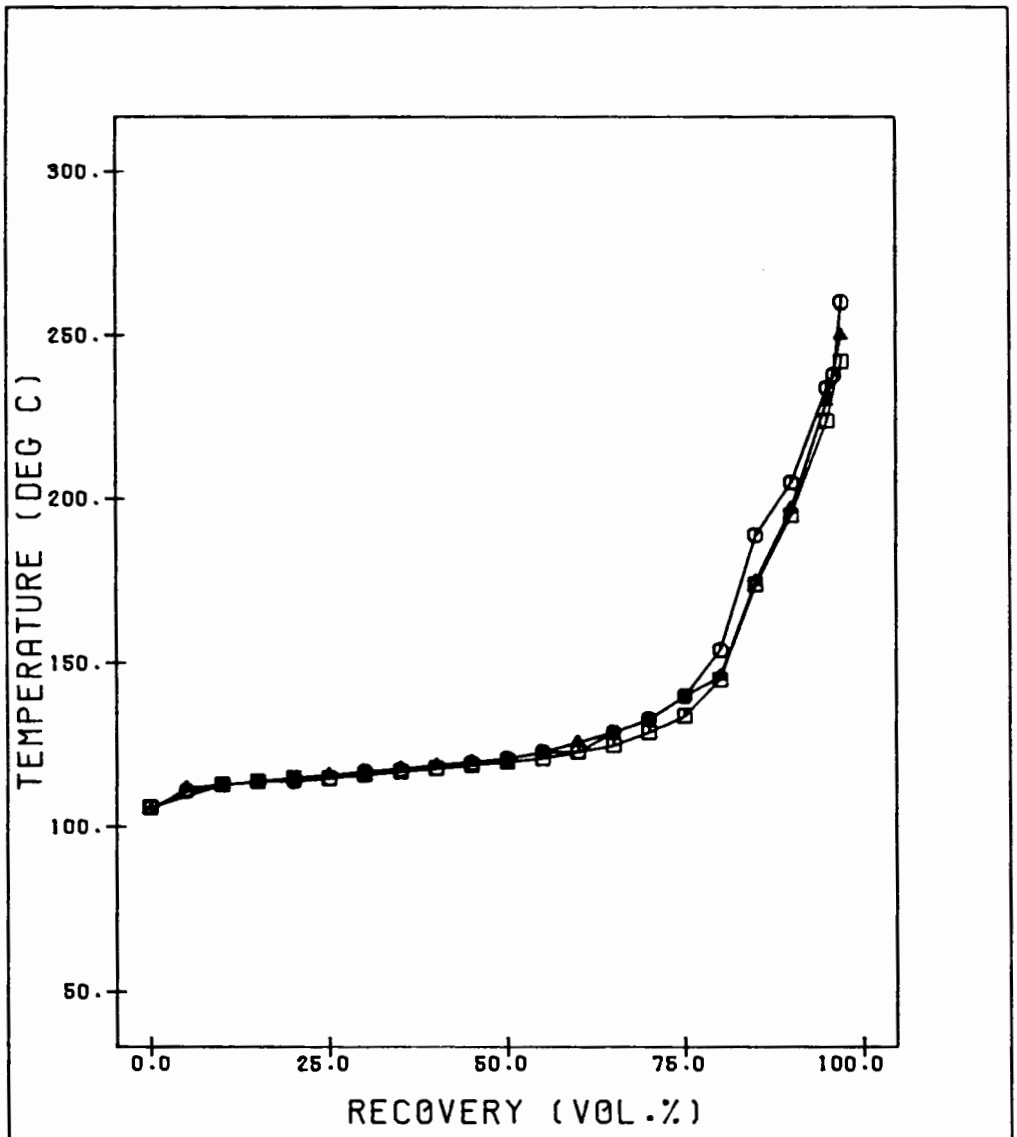

FIG. 4.10 ASTM-DISTILLATION
EFFECT OF CATALYST BEAD SIZE

4.5 The Effect of the Degree of Functionalization

Ion exchange resins with a matrix of the commercial resin Duolite C26 were functionalised to various degrees with sulphonic acid groups by controlling the synthesis reaction temperatures. Reactions were then carried out using these resins at a feed rate of approximately 1.1 WHSV. The determination of the number of acid sites and degree of functionalization is shown in Table 4.10 (Section 4.19).

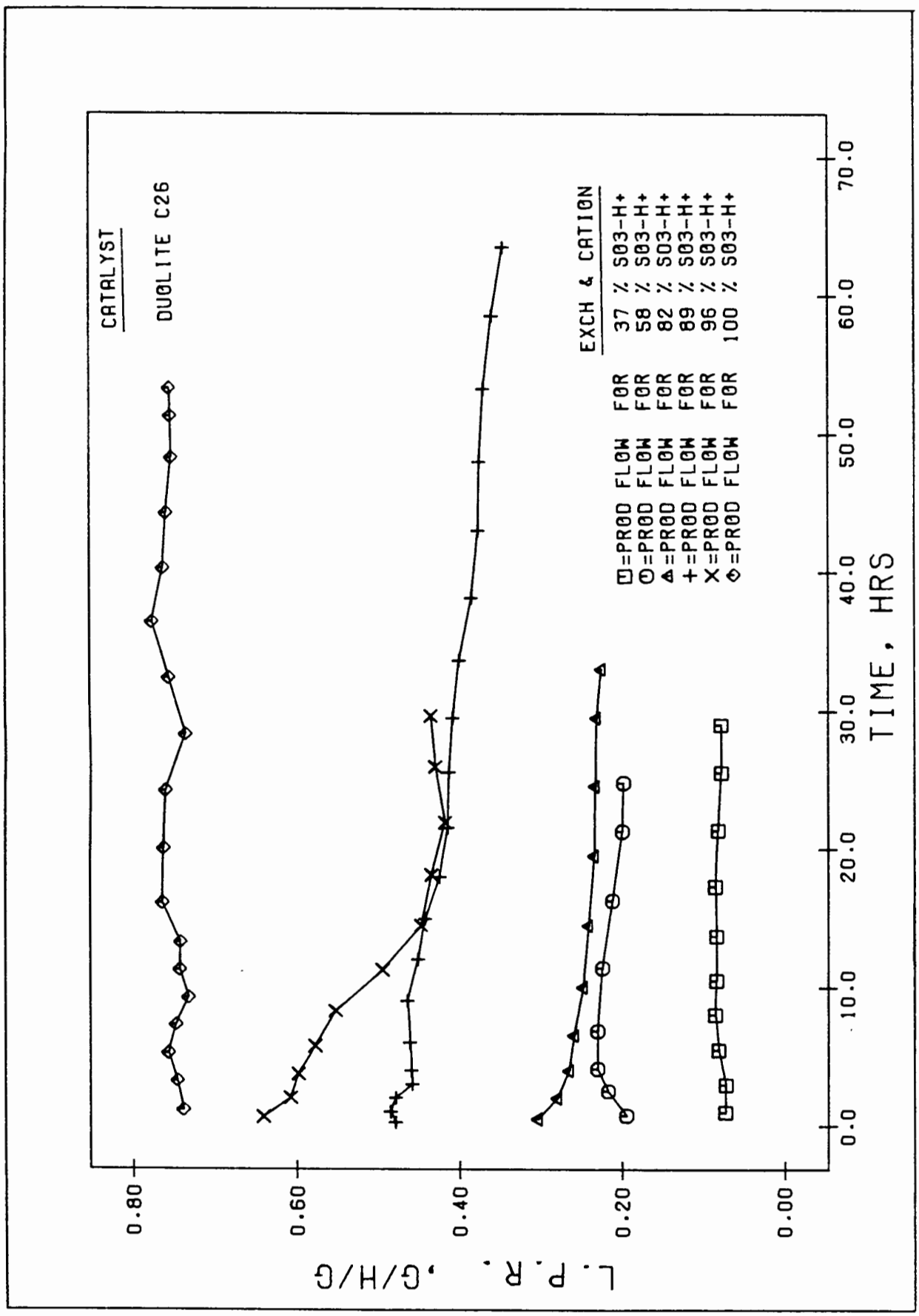

FIG.4.11 LIQUID PRODUCTION RATE (G/H/G) VS TIME (H)

Fig. 4.11 shows the L.P.R. using these resins functionalized to various degrees as a function of time. It is clear that the L.P.R. depends strongly on the number of acid sites and decreases sharply as the percentage of acid sites drops from 100% to 96%, 89% and 82% respectively. The L.P.R. plateaus slightly as the number of acid sites drops further to 60% and 37%. No linear proportionality is observed, with a decrease in L.P.R. much larger than the percentage reduction in the number of acid sites (Fig. 4.12). For example an overall reduction of 63% in the number of acid sites from 100% to 37% caused a drop of more than 85% in the L.P.R. It is not clear why the L.P.R. of the 96% functionalized resin drops markedly with time.

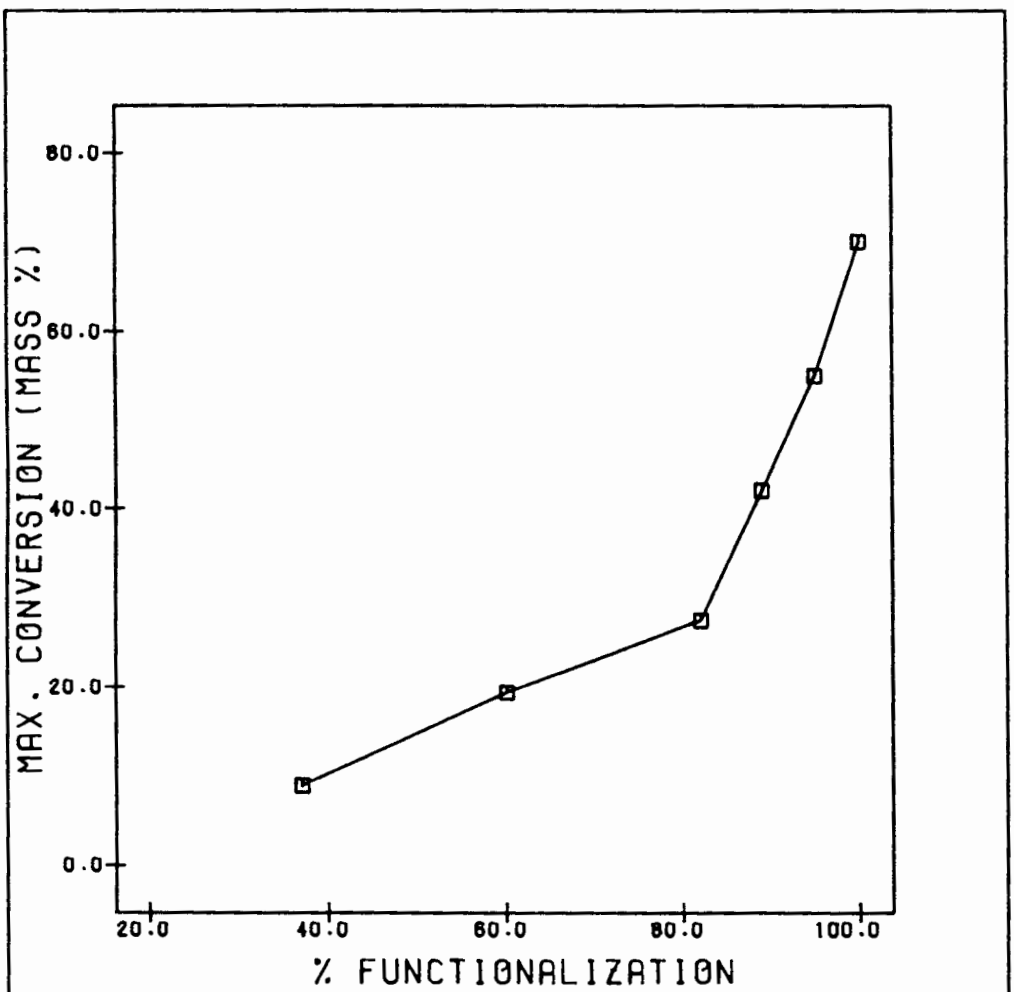

FIG.4.12 MAXIMUM CONVERSION FOR VARIOUS DEGREE OF FUNCTIONALIZATION

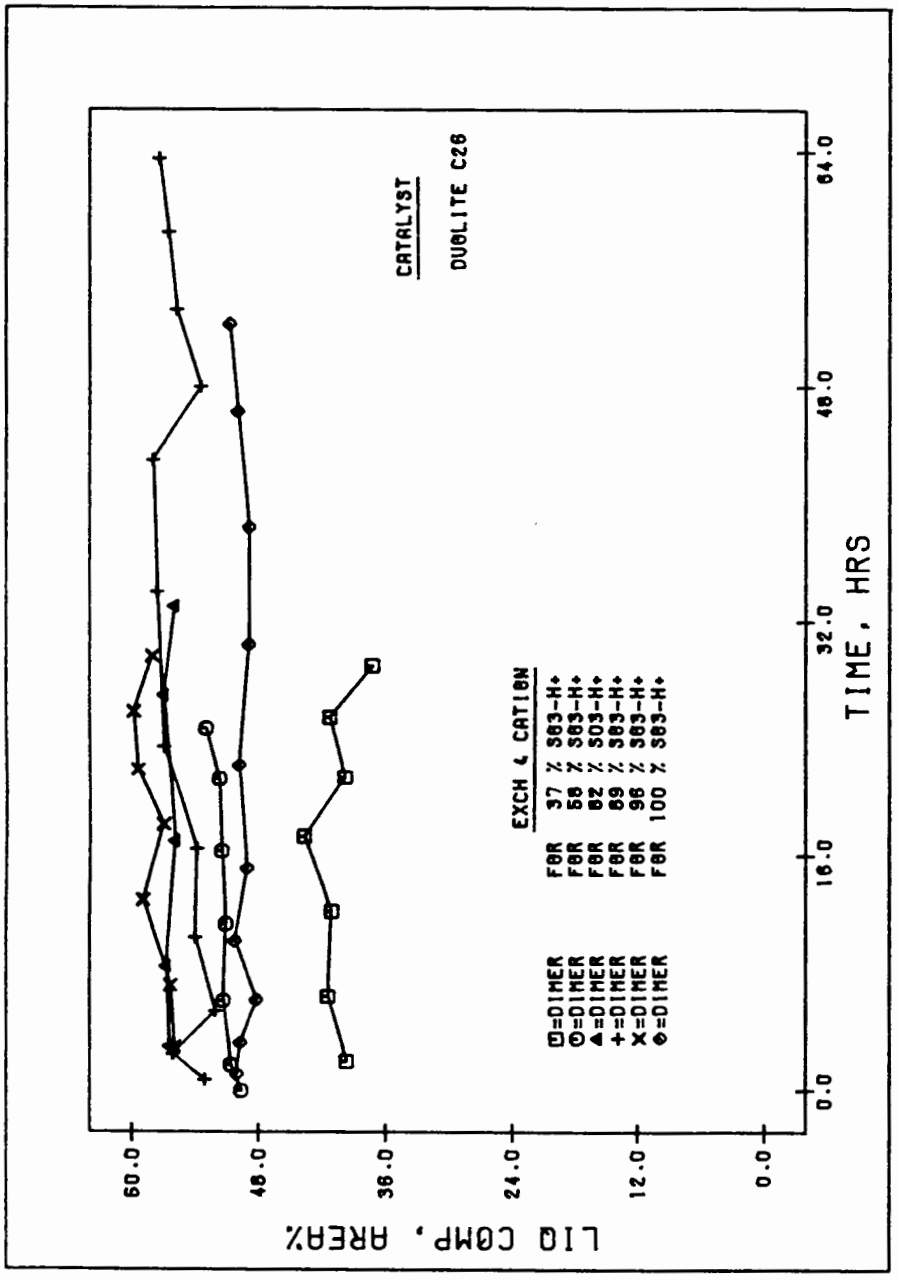

FIG.4.13 LIQ PROD COMPOS (AREA%) VS TIME (H)

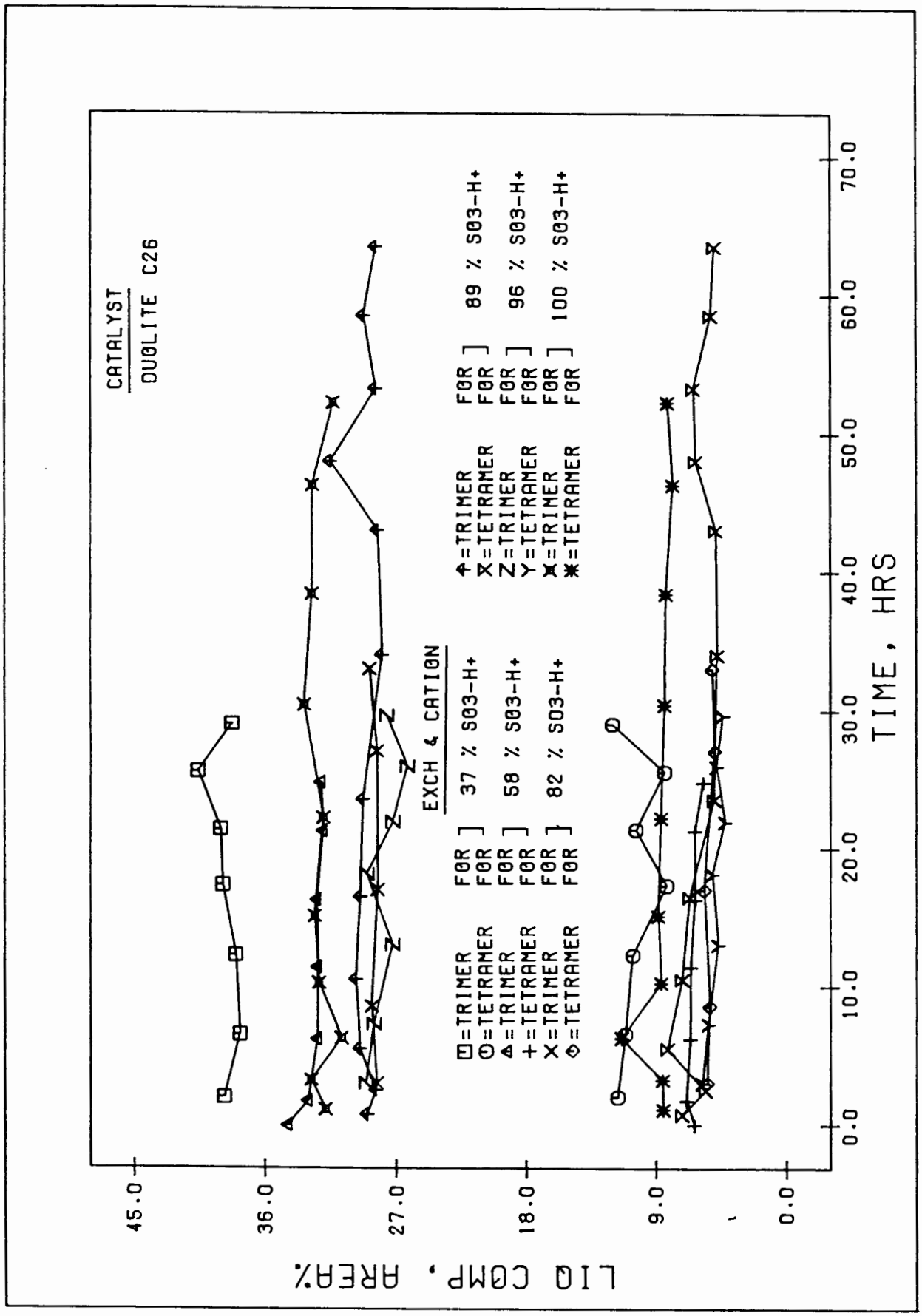

FIG.4.14 LIQ PROD COMPOS (AREA%) VS TIME (H)

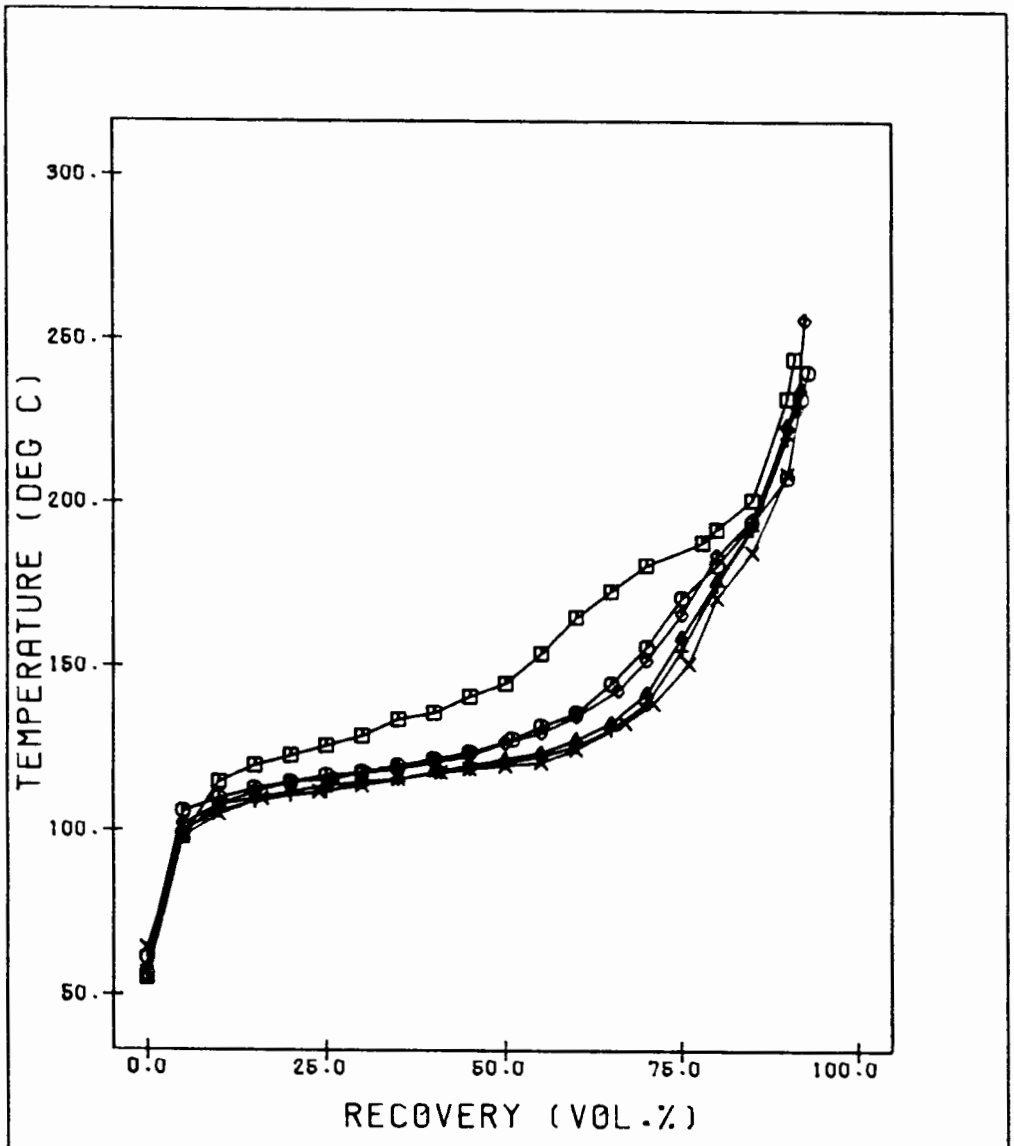

FIG. 4.15 ASTM-DISTILLATION
EFFECT OF DEGREE OF FUNCTIONALIZATION

The change in the selectivity with time is shown in Fig. 4.13 for the dimer and in Fig. 4.14 for the trimer and tetramer. In all cases no significant change was observed with time. With respect to the relative amounts formed, it appears that the amount of dimer decreases and the amounts of trimer and tetramer increase as the number of acid sites per mass of catalyst decreases, i.e. there is a tendency to higher chain length as the degree of functionalization drops. An exception is the 100% functionalized resin, which seems to have the second highest selectivity towards longer chain length.

Fig. 4.15 shows the 100mℓ ASTM distillation results for various degrees of percentage functionalization. The same tendency is observed with the 100% functionalized resin being the exception as before.

4.6 The Effect of Acid Strength

Since ion exchange resins with sulphonic acid groups showed such a high L.P.R., an attempt was made to see whether other acid functionalities of different acid strength would show similar L.P.R. The L.P.R. of resins prepared with phosphonic and phosphinic acid functionalities on a matrix of the same physical properties as Duolite C26 were studied at a WHSV of approximately 1.7.

No conversion was observed after 12 hours under the reaction conditions in which the resins with sulphonic acid groups were highly active.

Acid strength tests using Hammet indicators gave the following results:

Functionality	pKa range	range of equivalent H_2SO_4 wt %
$R - SO_3\text{-}H^+$	-2.4 - 5.6	42 - 71
$R - HPO_2\text{-}H^+$	+1.5 - 2.4	2×10^{-2} - 42
$R - PO_3^{2-}(H^+)_2$	+1.5 - 2.4	2×10^{-2} - 42

Table 4.2 : Acid strength of various functionalities

4.7 The Effect of Changing the WHSV

In order to show the effect of changing the reactant/catalyst ratio, runs were carried out at different WHSV. Amberlyst 15 was used as the catalyst.

Fig. 4.16 shows the L.P.R. for various WHSV's. It shows that this increases as the WHSV increases. However at higher space velocities a greater rate of deactivation is observed. This is clear from the run carried out at a WHSV of 2.53, which has the highest initial L.P.R. but soon drops to a value which is similar to that of the run carried out at a WHSV of 0.85. No higher WHSV values were tested due to the fact that in these cases difficulties were experienced in controlling the reaction temperature during start-up. With respect to lower WHSV, a WHSV of 0.85 represents a condition at which virtually all unsaturated components are converted, and hence lower values were not investigated. This is shown in Fig. 4.17, where the mass % conversion is plotted for three different WHSV's as a function of time.

Fig. 4.18 compares the selectivity for each of these runs. The lowest WHSV gives the least dimers and the most tri- and tetramers. The intermediate WHSV shows the least favourable product spectrum tendencies. As shown in Fig. 4.18 the two runs producing the higher boiling point product, viz. WHSV = 0.85 and 2.53, show a more significant variation of product composition with time. The superior quality of this product obtained in the low WHSV run is also confirmed by the ASTM distillations, the results of which are shown in Fig. 4.19. No marked difference appears between the intermediate and high WHSV runs.

To confirm the increase in L.P.R. with increasing WHSV, studies were carried out using Amberlyst 1010 as a catalyst. The results are shown in Fig. 4.20 where the L.P.R. is shown for two runs at the WHSV values most used in this work. These confirm the previously found trends, viz. the L.P.R. increases with increasing WHSV (Fig. 4.21). The ASTM distillation results are shown in Fig. 4.22 and no marked difference is observed.

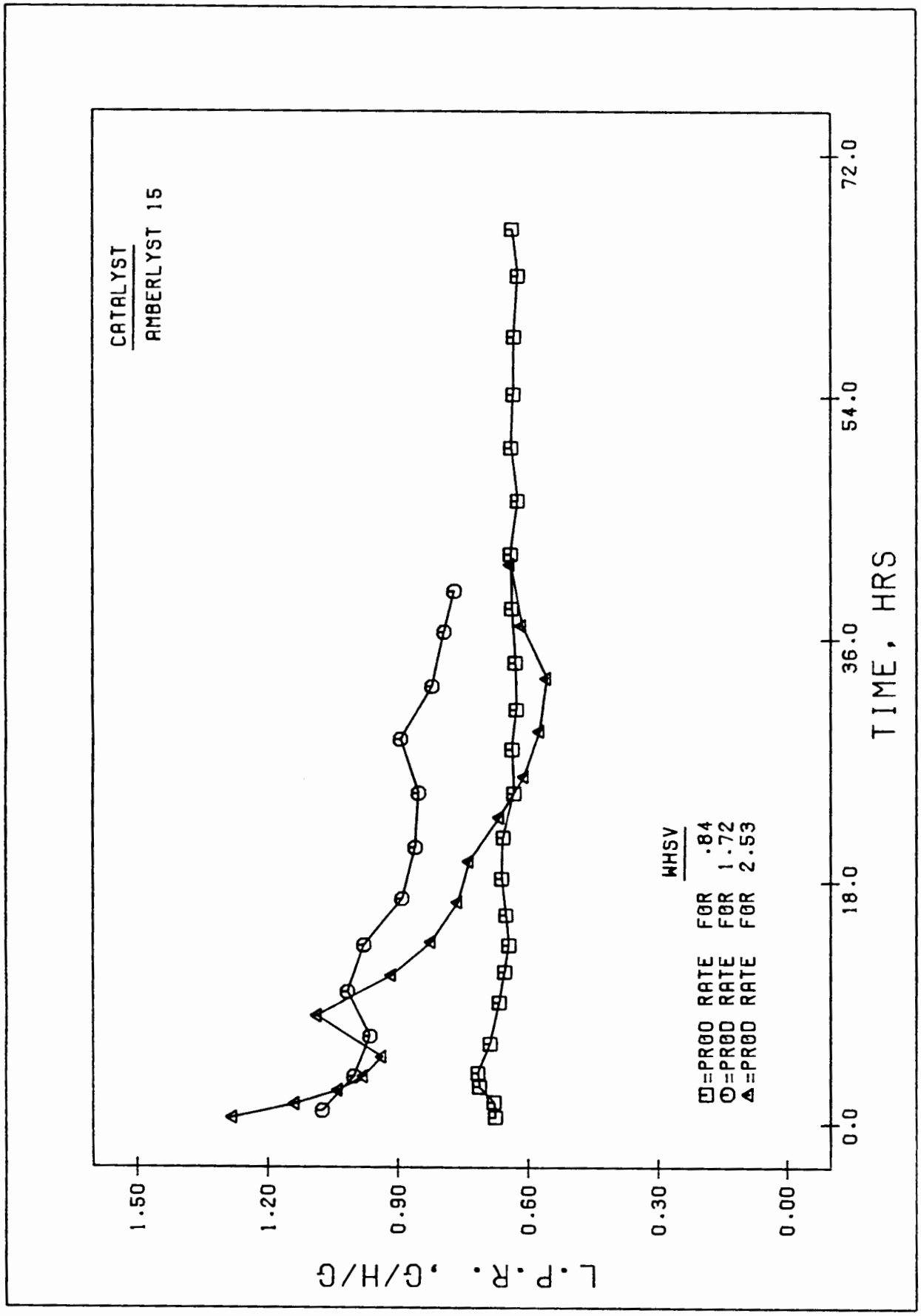

FIG.4.16 LIQUID PRODUCTION RATE (G/H/G) VS TIME (H)

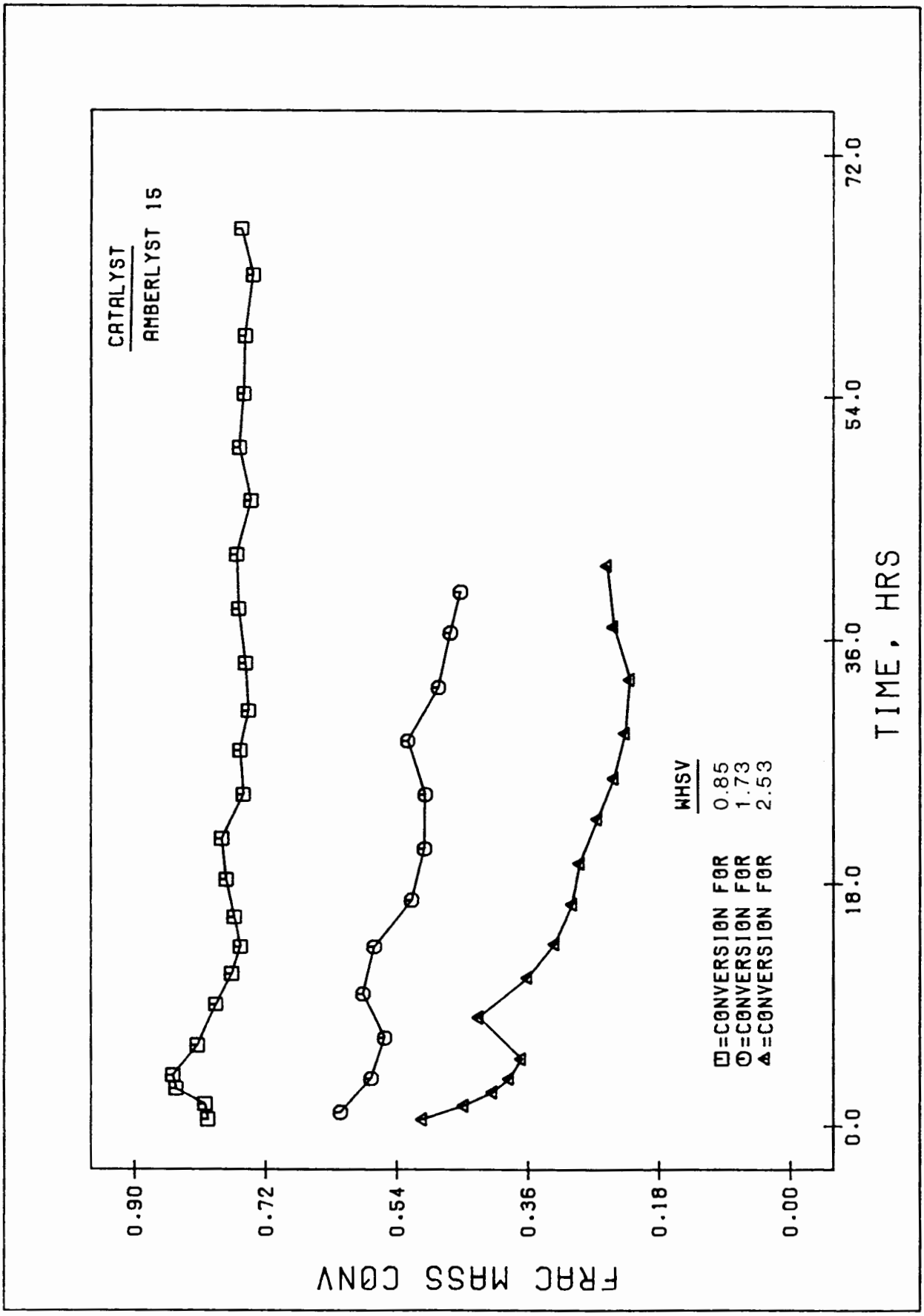

FIG.4.17 FRACT CONV. FEED TO LIQ PROD VS TIME (H)

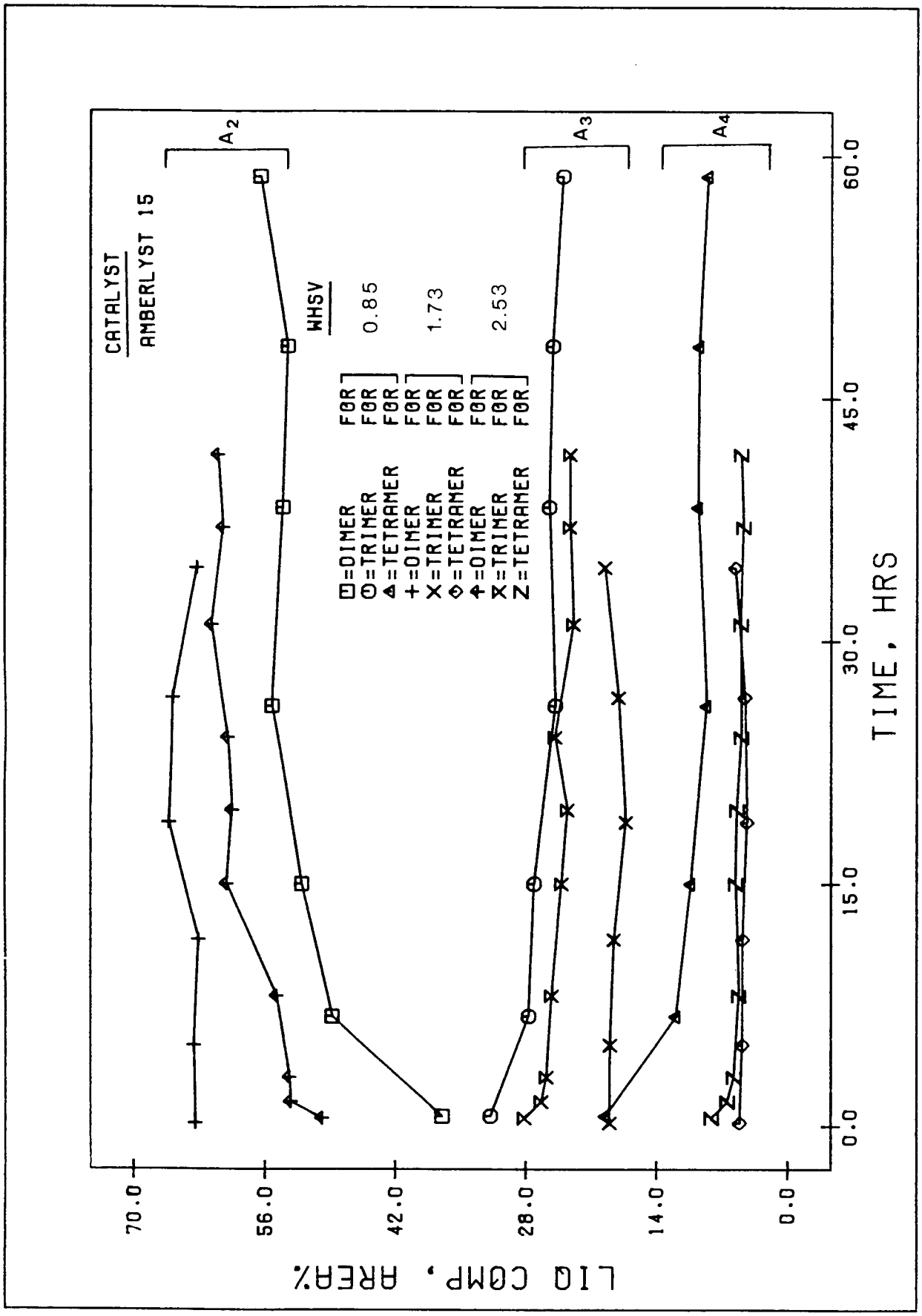

FIG.4.18 LIQ PROD COMPOS (AREA%) VS TIME (H)

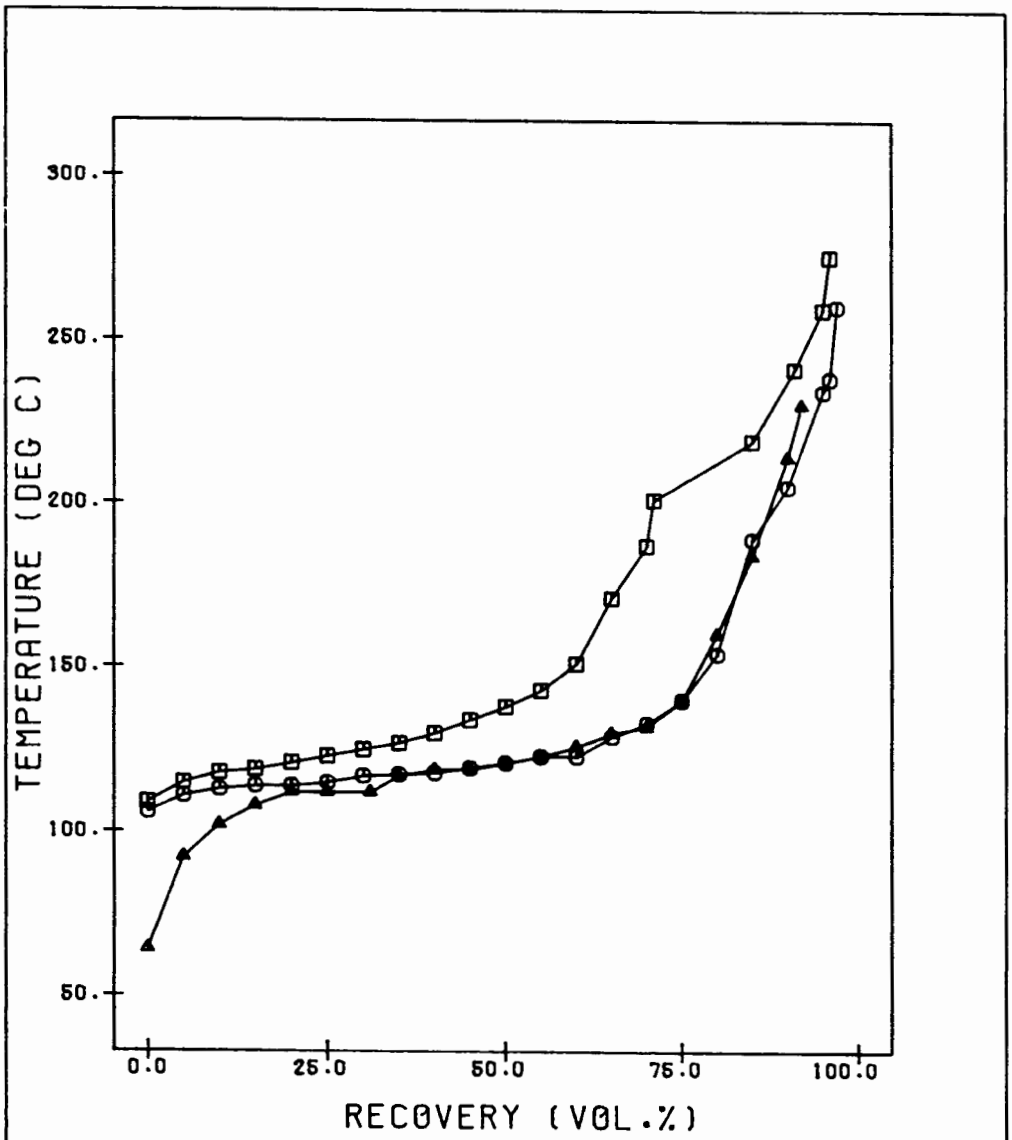

FIG.4.19 ASTM-DISTILLATION
EFFECT OF WHSV USING AMBERLYST 15

WHSV
□=0.65
○=1.73
▲=2.59

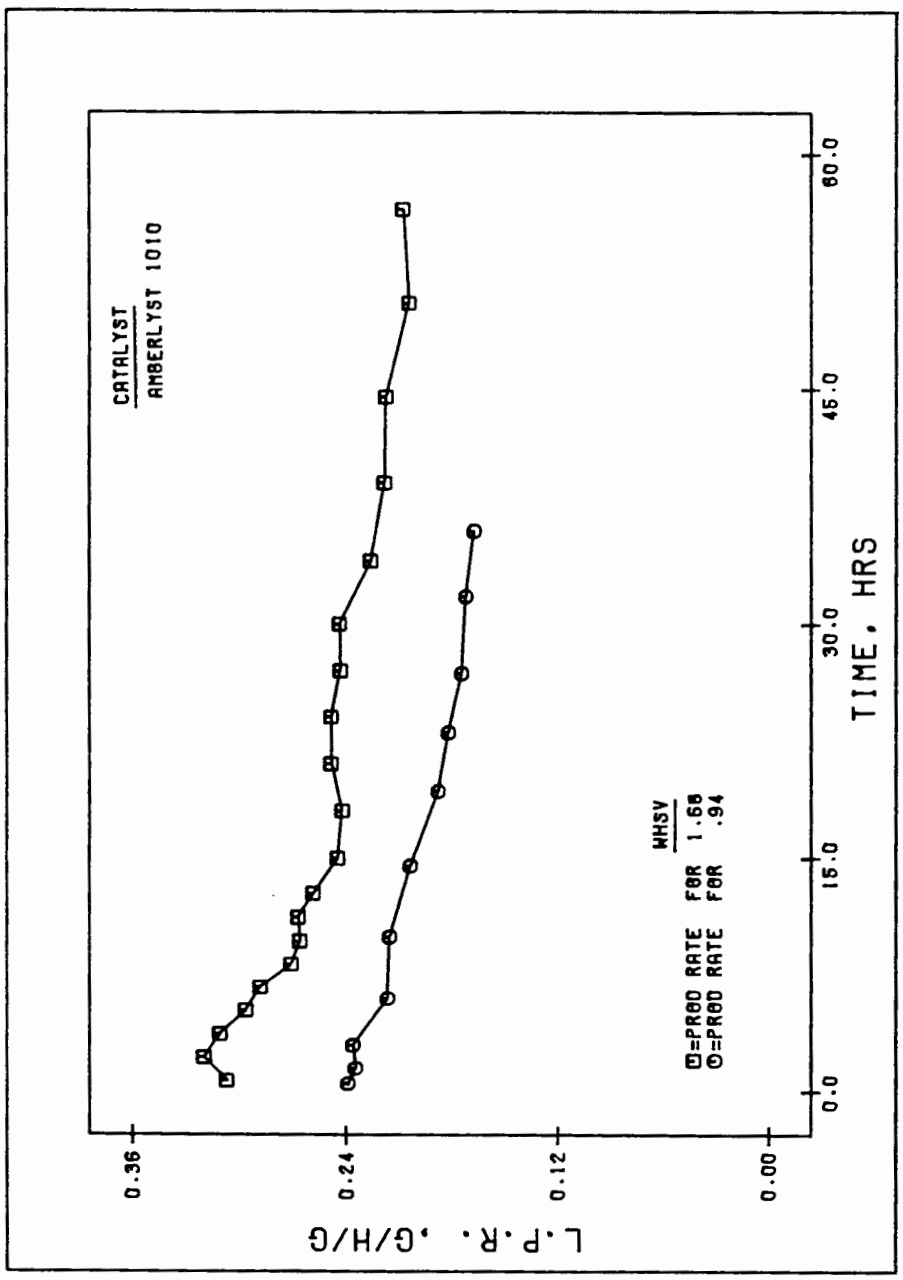

FIG.4.20 LIQUID PRODUCTION RATE (G/H/G) VS TIME (H)

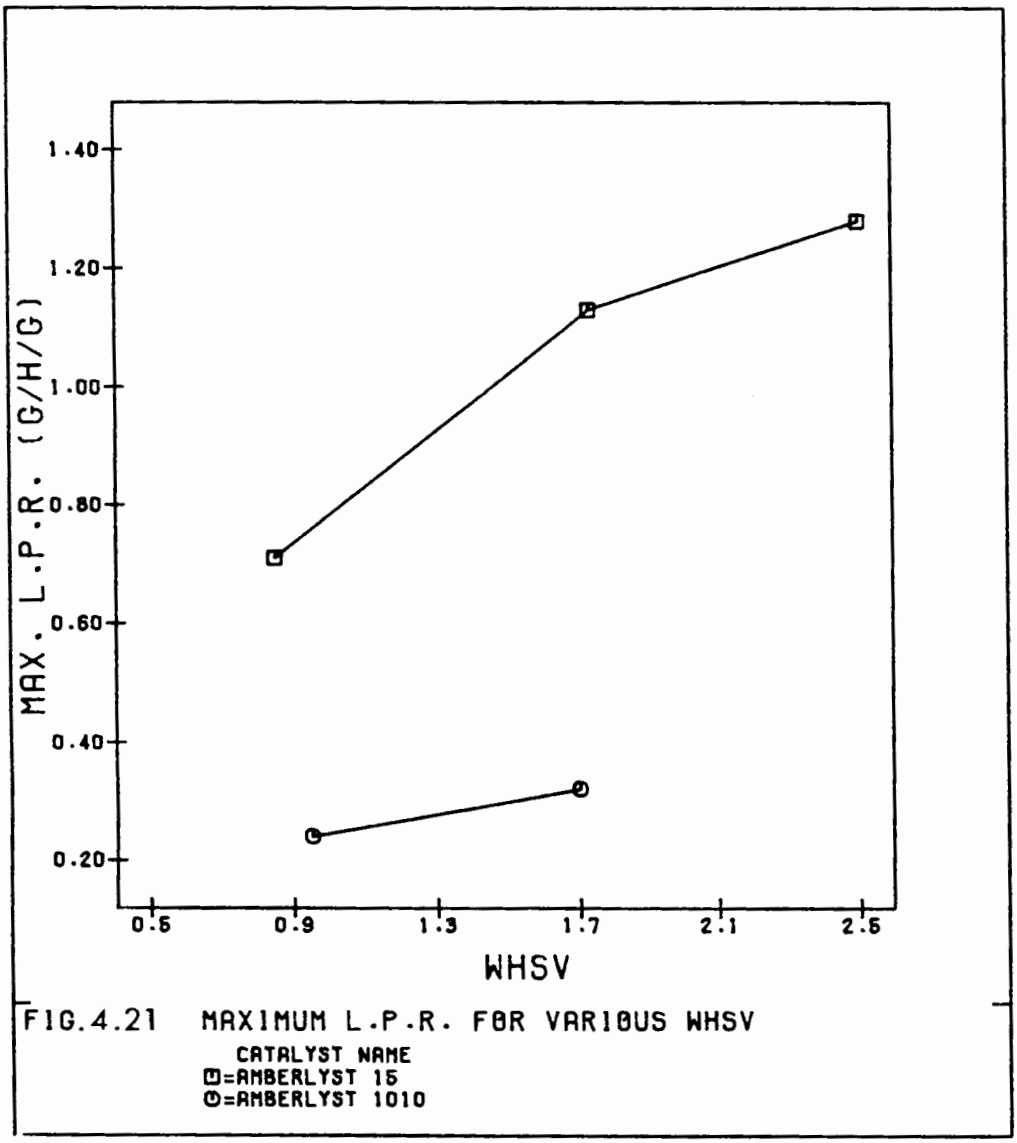

FIG.4.21 MAXIMUM L.P.R. FOR VARIOUS WHSV

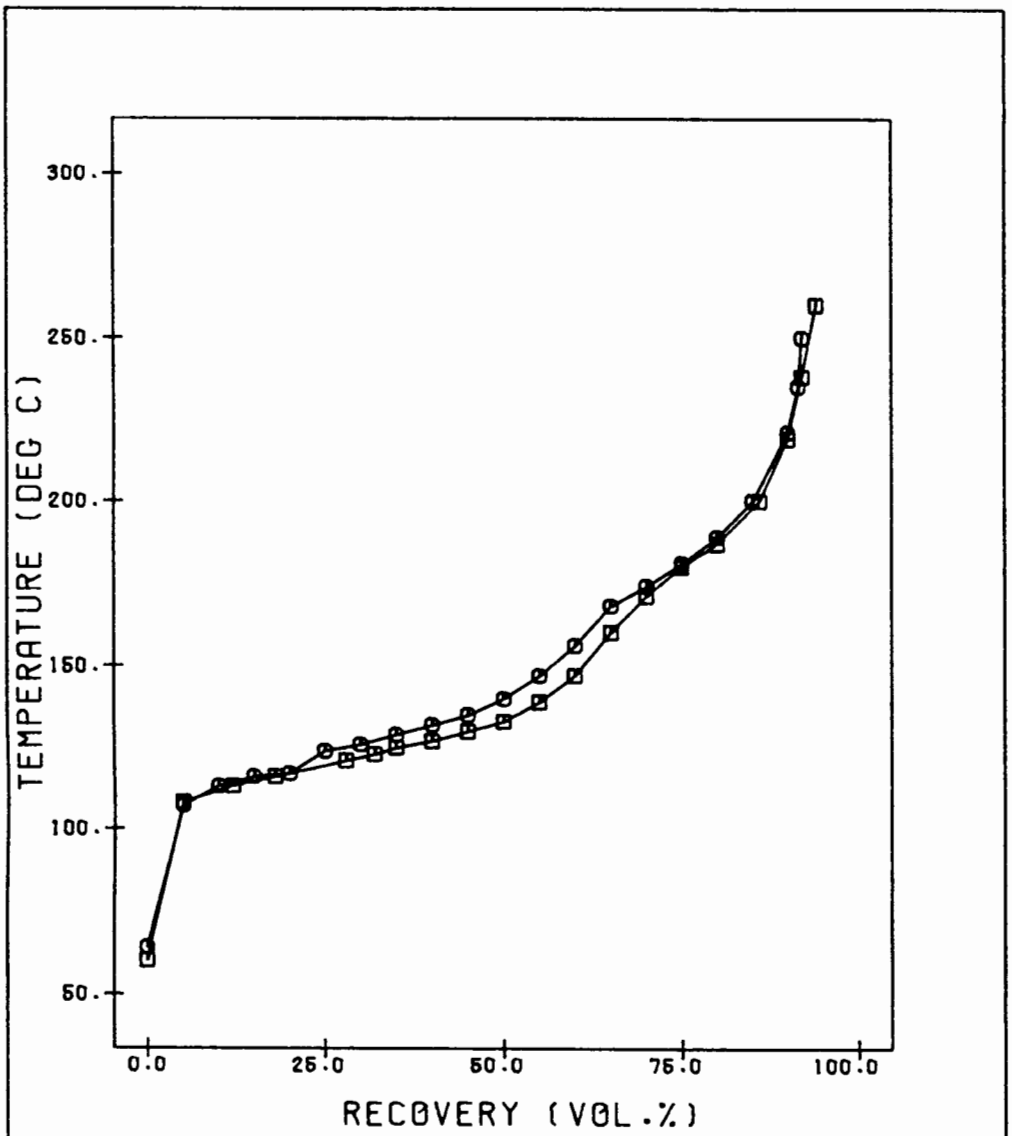

FIG.4.22 ASTM-DISTILLATION
EFFECT OF WHSV USING AMBERLYST 1010

WHSV
□=0.94
○=1.70

In order to show the tail gas analysis for the runs at various WHSV's using Amberlyst 15 as catalyst, the gas components were grouped into three classes:

i) saturates including propane, isobutane and n-butane;
ii) converted unsaturates including propylene, isobutene and 1-butene;
iii) unsaturates produced by isomerization including cis- and trans-2-butene.

The converted unsaturates showed very little difference for the three runs and were virtually completely converted. The unsaturates produced by isomerization showed the largest differences. This is shown in Fig. 4.23 where the fractional conversion is plotted as a function of time. The run with the lowest WHSV and highest feed gas conversion also has the highest utilization of cis- and trans-2-butene. They are both used up and only a slight drop in the rate of utilization is observed with time, similar to that shown in the conversion plot. The run with the second highest feed gas fractional conversion, i.e. WHSV = 1.73, has a negative value for the conversion of cis- and trans-2-butene, indicating that it is actually formed. For the run with a WHSV of 2.53 an excess of cis- and trans-2-butene is produced. This isomerization increases at the expense of polymerization as the catalyst deactivates.

The fractional conversion of the saturates as a function of WHSV is similar to that for the unsaturates produced by isomerization, and decreases with increasing WHSV. For both the higher WHSV runs a continuous drop in saturate conversion is observed, while for the run carried out at a low WHSV only an initial drop is observed and then the rate of utilization remains constant. (Fig. 4.24).

It should be noted that for all except for the very deactivated catalysts the fractional conversion is positive, i.e. that saturates are used up and thus alkylation does occur.

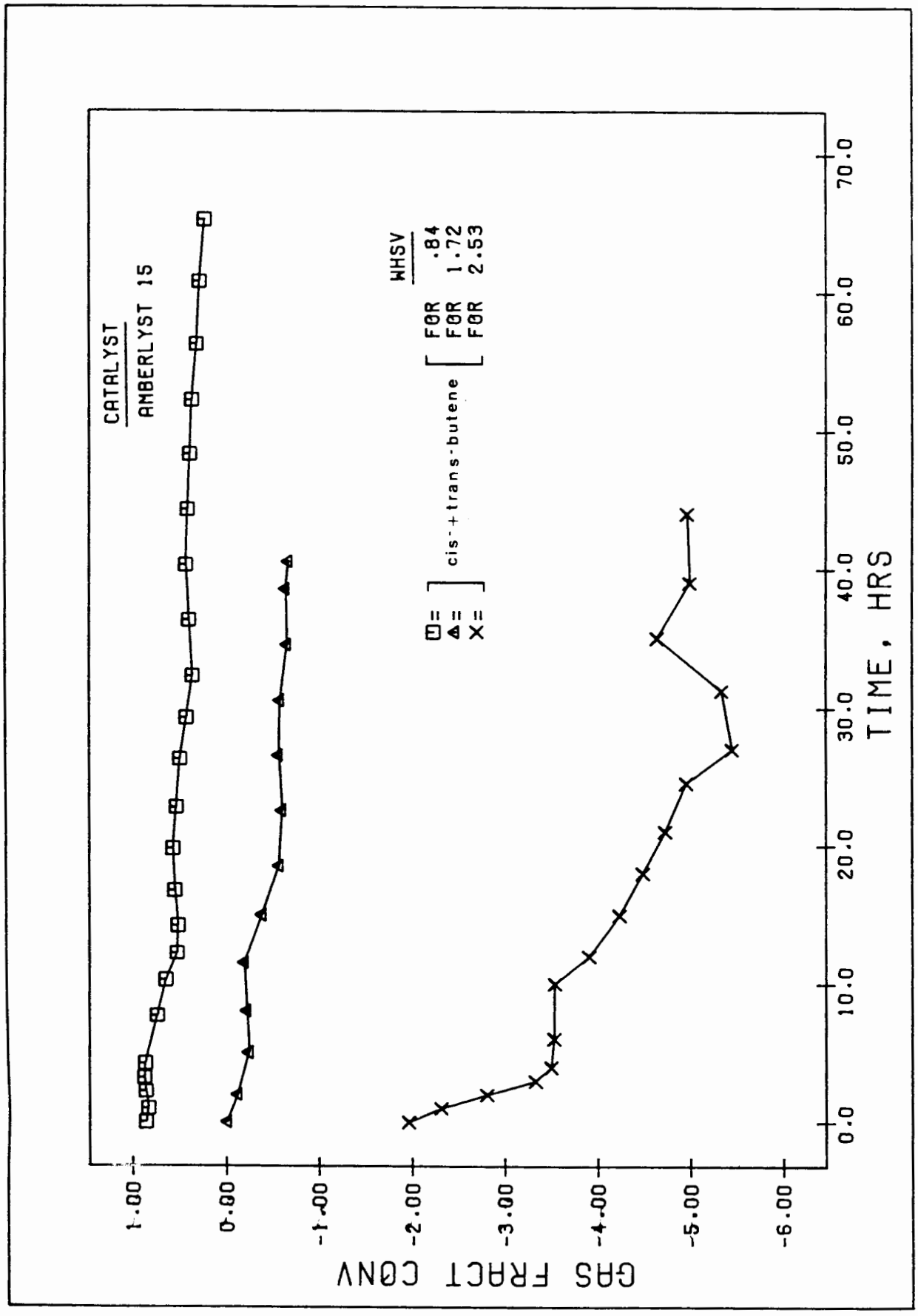

FIG.4.23 FEED GAS FRACT CONV VS TIME (H)

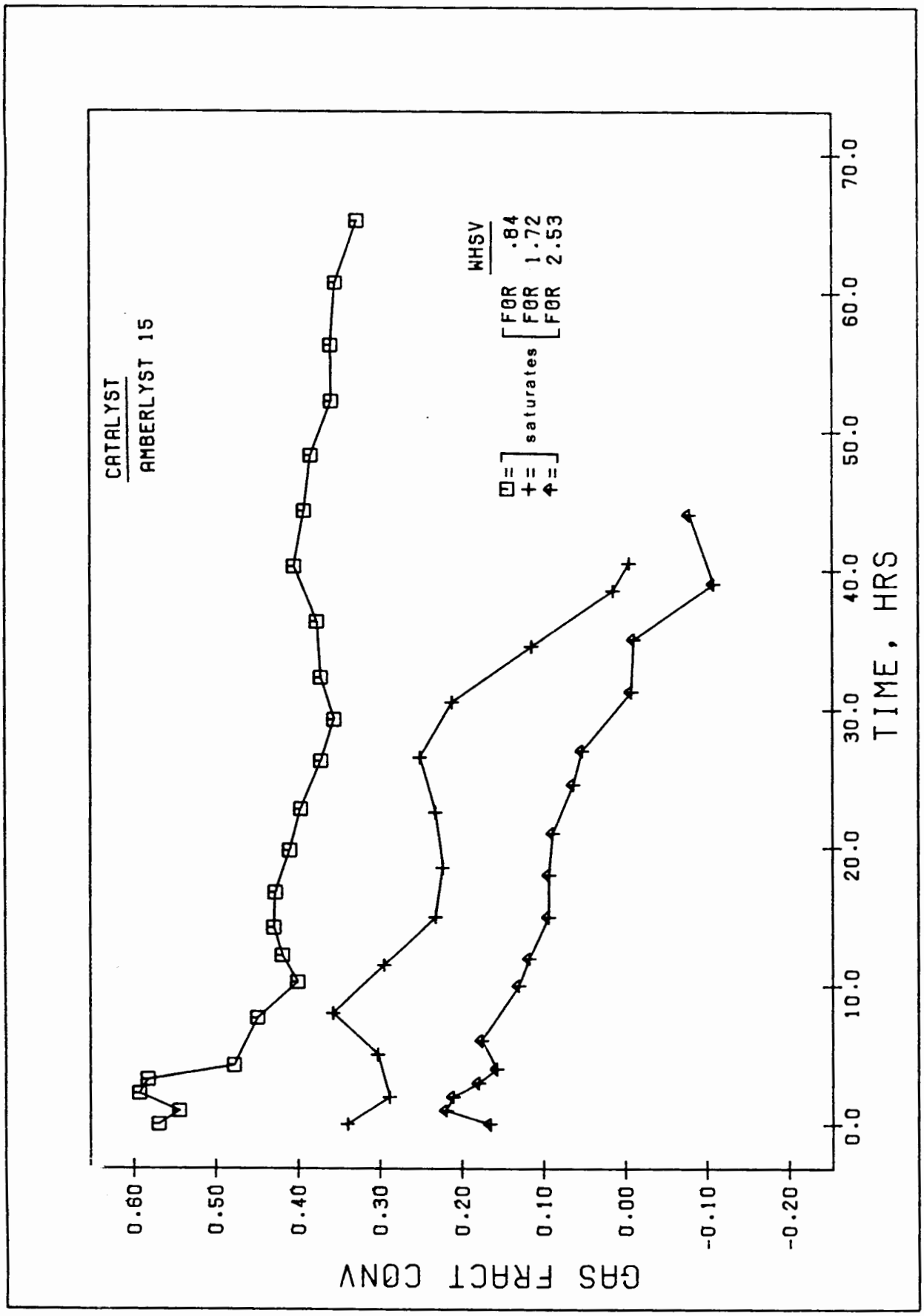

FIG.4.24 FEED GAS FRACT CONV VS TIME (H)

Changing the feed rate has thus shown that:

i) the L.P.R. increases and the conversion decreases with increasing WHSV;

ii) longer polymers are formed, when nearly complete conversion of unsaturates occurs;

iii) alkylation does occur, increasing with increasing conversions

4.8 The Effect of Recycling Liquid Product

This study did not involve an actual recycle where part of the product is returned to the reactor, but a co-feeding of the -180°C boiling point fraction of previous runs to the reactor together with the normal feed. The recycle ratio, R, was defined as follows:

R = mass of -180°C fraction/mass of monomer

The composition of the -180°C fraction in mass % was as follows: dimer 92%, trimer 8%.

The recycle ratio was varied by maintaining a constant -180°C fraction flow rate (Q = 0.718g/min) and changing the monomer flow rate. The various conditions are shown in Table 4.3.below.

Time (min.)	WHSV of gas	Recycle ratio	Gas flow rate (g/min)
0 - 885	0.545	1.496	0.480
885 - 1590	0.866	0.941	0.763
1590 - 2025	1.608	0.507	1.416
2025 - 2445	2.459	0.332	2.166

Table 4.3 : Conditions for various recycle

The catalyst used was Amberlyst 15. A relatively low L.P.R. was observed as shown in Fig . 4.25. Here the L.P.R. is based on the weight of monomer converted and is calculated by the formula :

L.P.R. = mass of gas converted/(time x weight of catalyst)

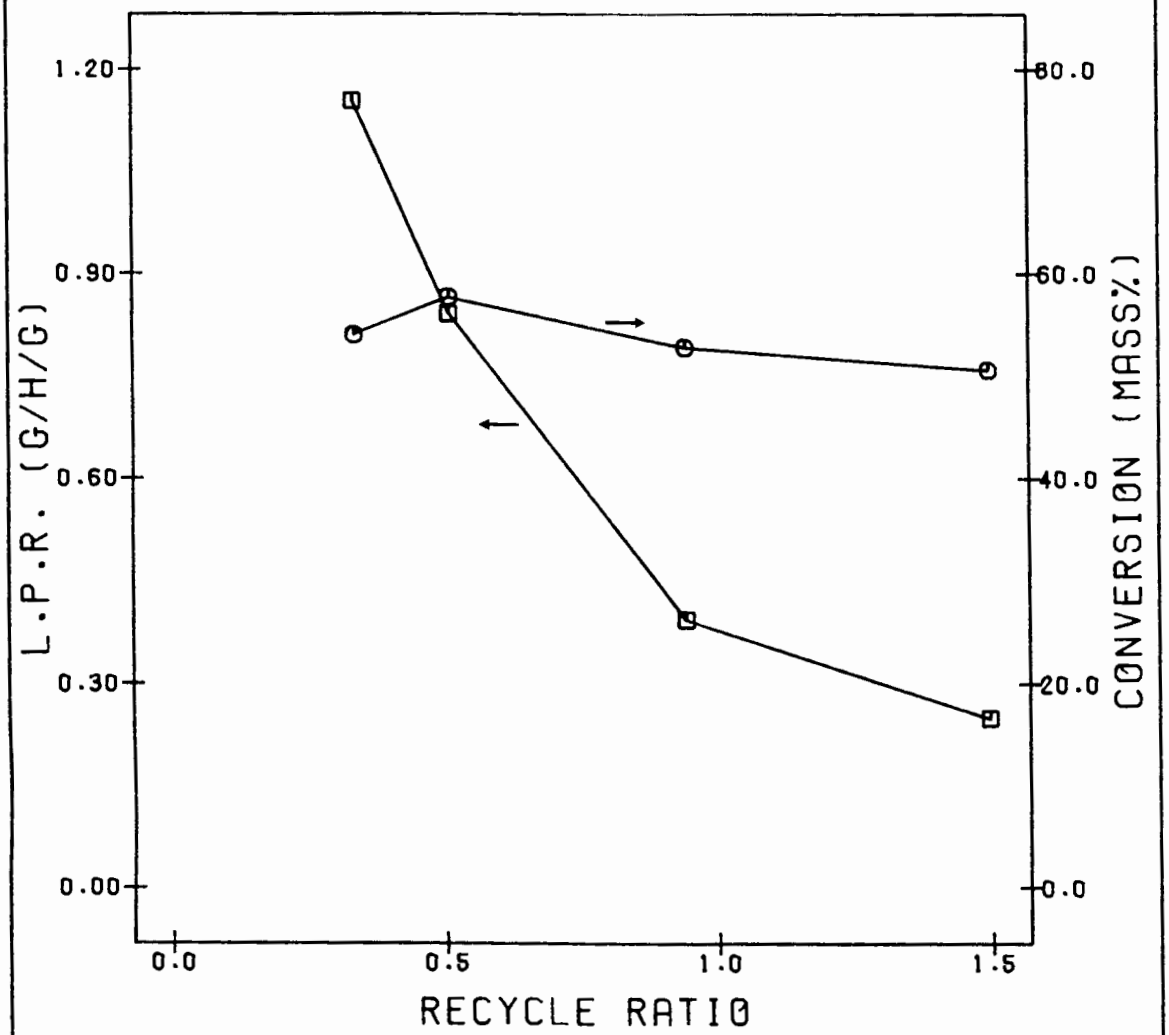

FIG.4.25 L.P.R. AND CONVERSION AT VARIOUS RECYCLE RATIO

□=L.P.R.
○=CONVERSION

The L.P.R. decreased as the recycle ratio increased, i.e. as the amount of monomer was reduced. Also shown in the figure is the mass percent conversion. This was calculated by the formula:

$$\text{mass \% gas converted} = 100\left(1 - \frac{\text{mass of gas unreacted}}{\left[\text{mass of liquid product} - \text{mass of recycle} + \text{mass of unreacted gas}\right]}\right)$$

The conversion did not decrease with time for any recycle ratio nor did it vary much for different recycle ratios.

Comparing these L.P.R. values with those obtained without co-feeding dimer, i.e. only changing WHSV of monomer (section 4.7), a higher L.P.R. was observed in the latter case (Fig. 4.26). Similarly, Fig. 4.27 compares the mass percent conversion between the two situations.

The selectivity of the catalyst with and without co-feeding dimer is shown in Fig. 4.28, for various WHSV's. Significantly more monomers were converted to trimers and less to dimers when co-feeding dimers.

4.9 The Effect of Changing Reaction Pressure

Two runs were carried out in which the reaction pressures were chosen so that in one run the feed was in the gas phase (100°C and 1.5 MPa) and in the other in the liquid phase (100°C and 2.7 MPa). This can be seen from Fig. 7.2.

Fig. 4.29 compares the L.P.R. of the two runs. Although initial L.P.R. is similar, the run carried out with a liquid feed shows a much greater rate of deactivation.

The 2.7 MPa run produced larger amounts of trimer and tetramer and a lesser amount of dimer (Fig. 4.30). Fig. 4.31 shows the results of the ASTM distillation.

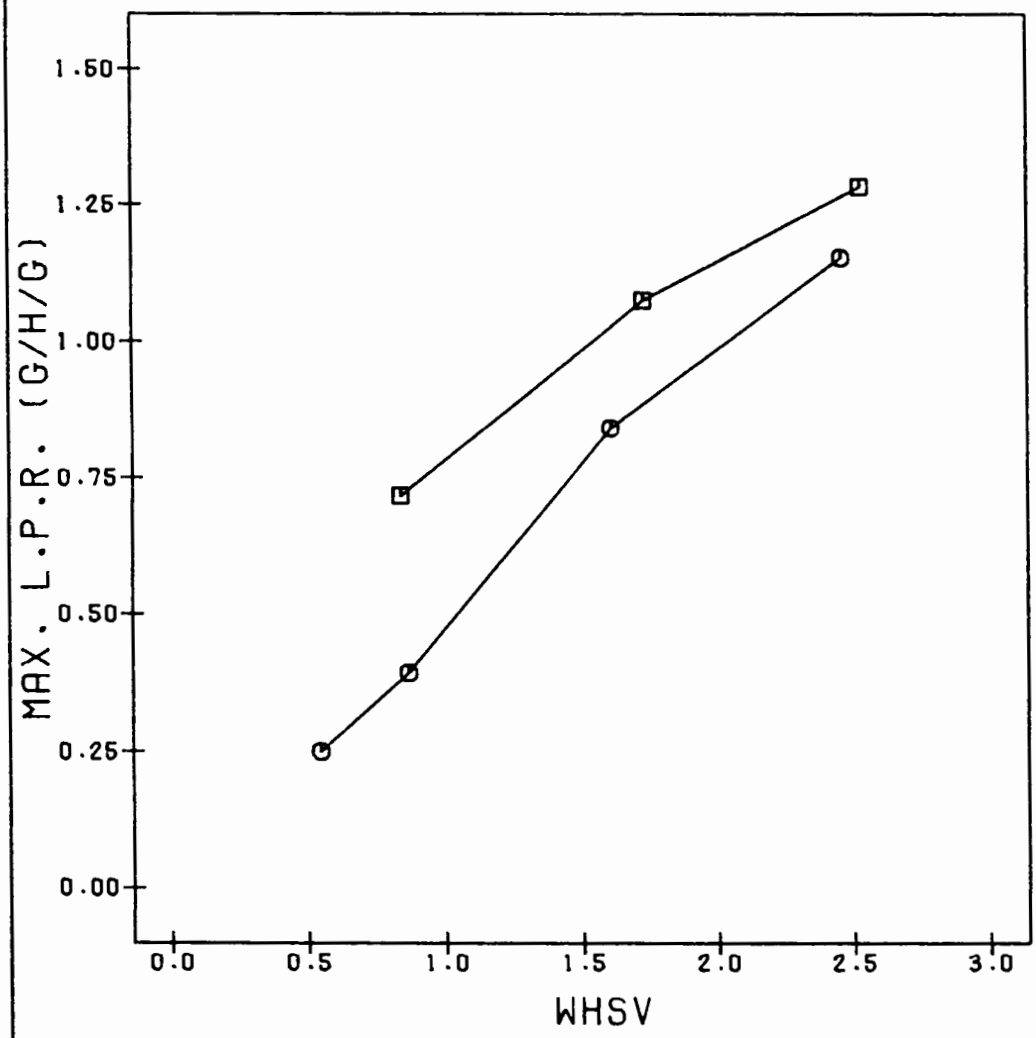

FIG.4.26 EFFECT OF RECYCLE ON L.P.R.

□=NO RECYCLE
⊙=WITH RECYCLE

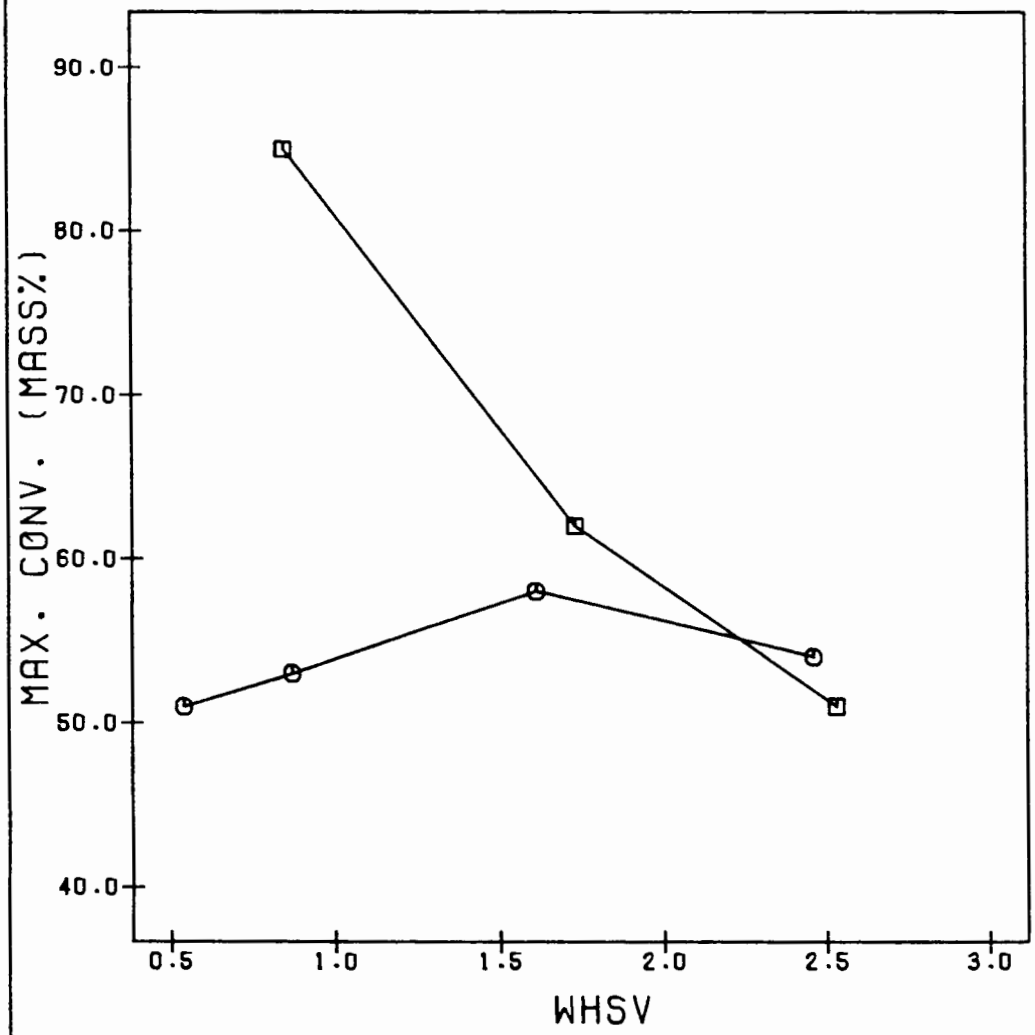

FIG.4.27 COMPARING CONVERSION WITH AND WITHOUT RECYCLE

MAXIMUM CONVERSION
□=WITHOUT RECYCLE
○=WITH RECYCLE

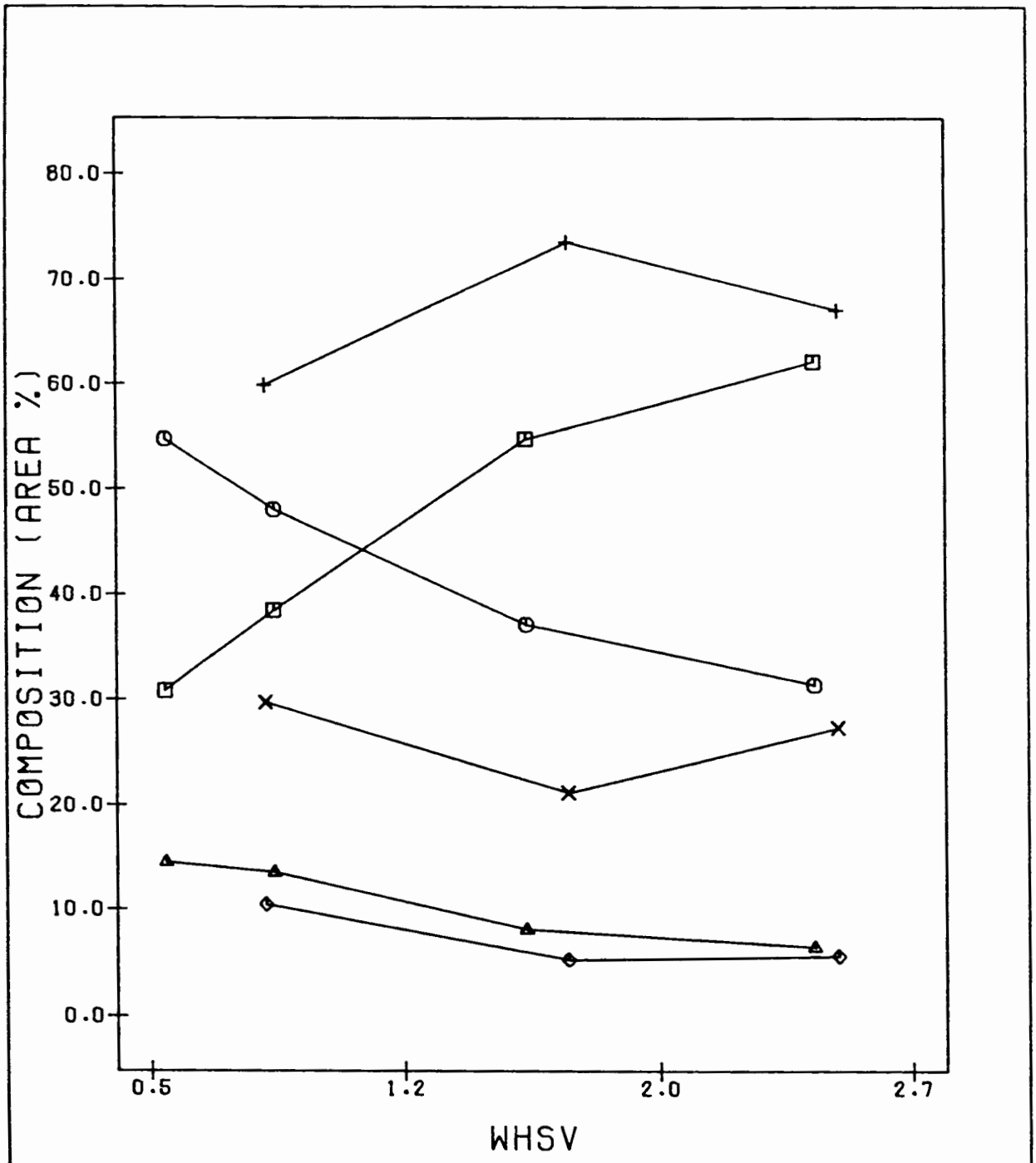

FIG. 4.28 COMPARING SELECT. WITH/WITHOUT CO-FEED

□=DIMER-WITH CO-FEED
○=TRIMER-WITH CO-FEED
△=TETRAMER-WITH CO-FEED
+=DIMER-WITHOUT CO-FEED
×=TRIMER-WITHOUT CO-FEED
◇=TETRAMER-WITHOUT CO-FEED

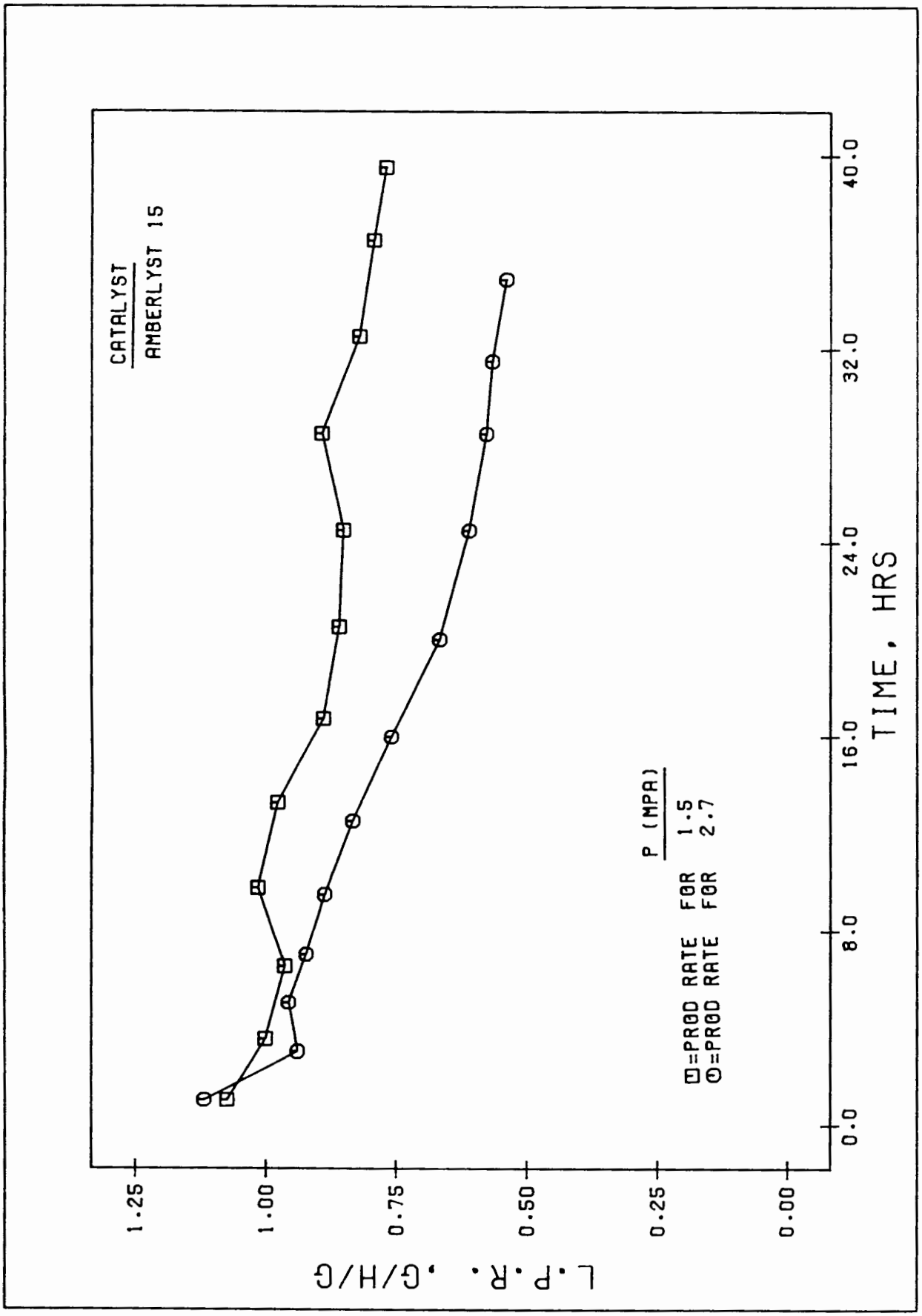

FIG.4.29 LIQUID PRODUCTION RATE (G/H/G) VS TIME (H)

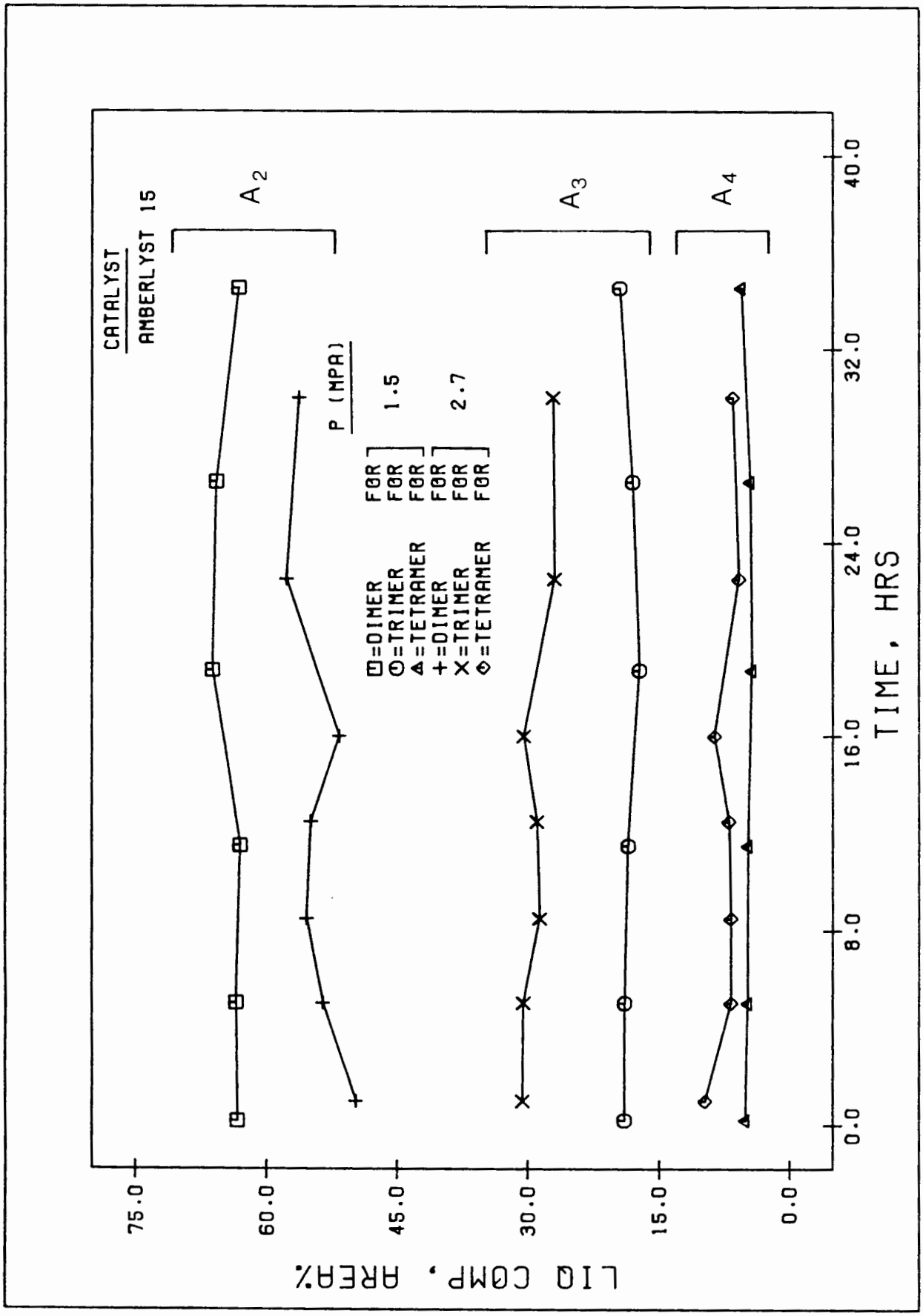

FIG.4.30 LIQ PROD COMPOS (AREA%) VS TIME (H)

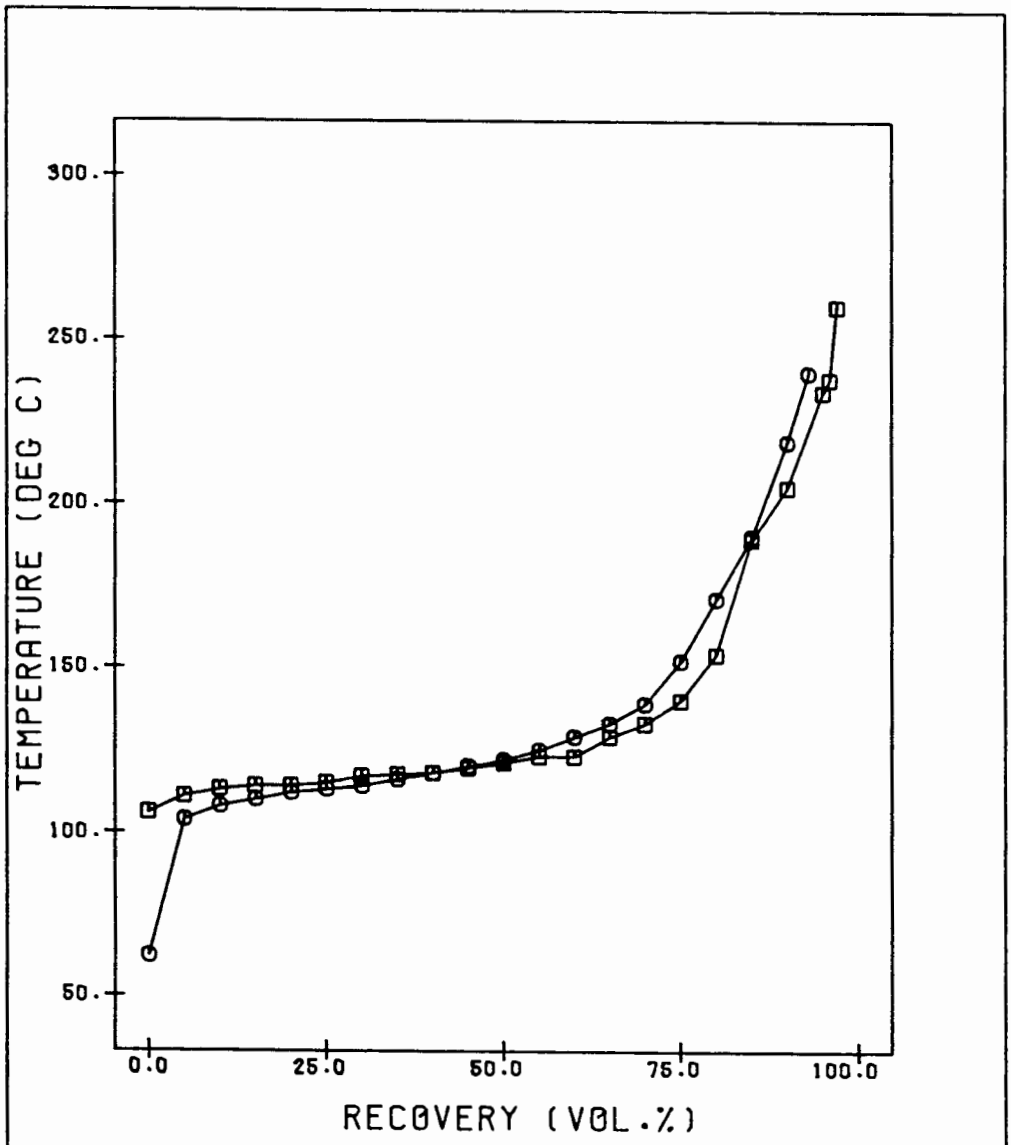

FIG.4.31 ASTM-DISTILLATION:
EFFECT OF REACTION PRESSURE

REACTION PRESSURE
□=P = 1.5 MPA
○=P = 2.7 MPA

4.10 The Effect of changing Reaction Temperature at Atmospheric Pressure

As mentioned in section 3.1.1 this is the only parameter which has been investigated on another reactor system. Three runs, using Amberlyst 15 as a catalyst, were carried out at 1 atm pressure, a WHSV of approximately 1.8 and reaction temperatures of 90, 130 and 160°C, respectively.

Fig. 4.32 shows the L.P.R. data for these runs. As the temperature increases the initial L.P.R. increases as well. However, the L.P.R. at the highest temperature drops rapidly after start-up.

The L.P.R. of the run carried out at 130°C did not seem to drop much faster than that of the run carried out at 90°C. For all 3 runs, exactly the same weight of catalyst was used (5.0g).

Fig. 4.33 shows that the low temperature run yielded a superior product, viz. least dimer, most trimer and tetramer.

4.11 The Effect of changing Reaction Temperature at 1.5 MPa

Amberlyst 15 in the particle size range of 500-850 microns was used for this study. Runs were carried out at a WHSV of approximately 1.7 and reaction temperatures of 100, 130 and 150°C.

Fig. 4.34 shows the L.P.R. as a function of time for these three runs. A significant difference in the initial L.P.R. is seen between the run carried out at 100°C and those carried out at higher temperatures. The latter runs result in a virtually complete conversion of unsaturated reactants and even some saturated material. This is shown in Fig. 4.35 (cf. feed contained about 82% unsaturates).

Therefore no conclusions can be drawn as regards the relative L.P.R. of the catalyst between the runs carried out at 130°C and those at 150°C.

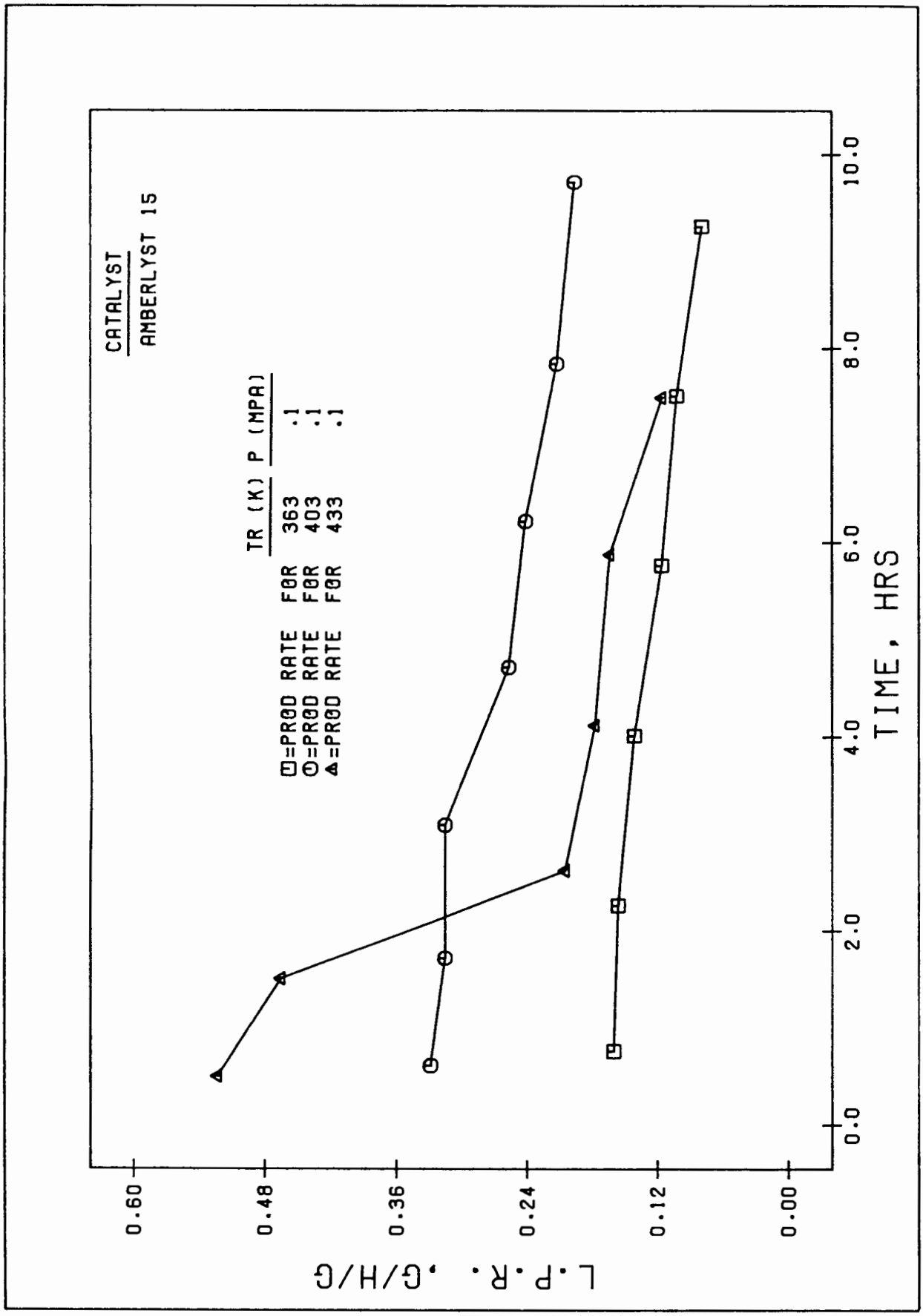

FIG.4.32 LIQUID PRODUCTION RATE (G/H/G) VS TIME (H)

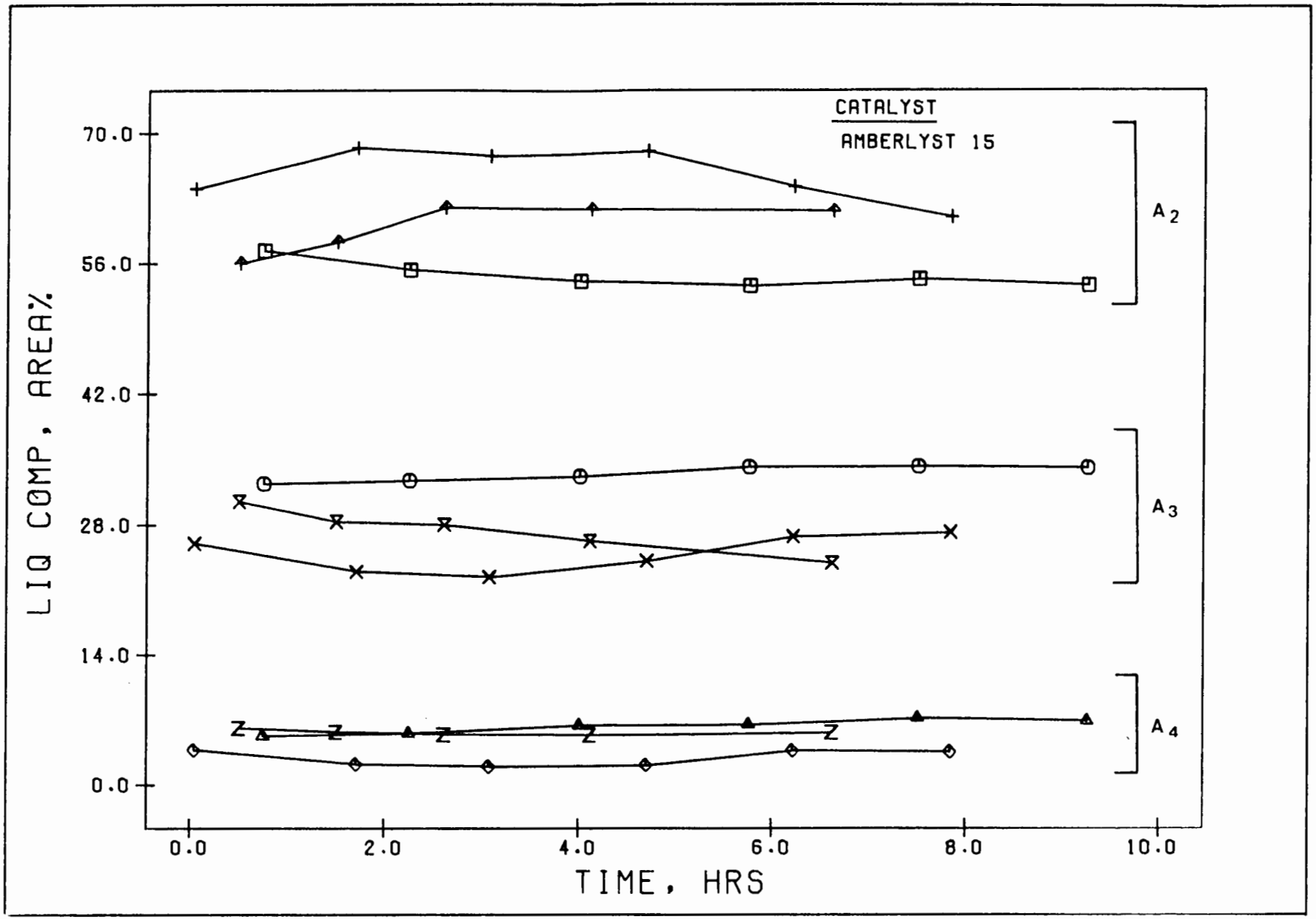

FIG.4.33 LIQ PROD COMPOS (AREA%) VS TIME (H)

		TR (K)	P (MPA)
□=DIMER ○=TRIMER ▲=TETRAMER	FOR FOR FOR	363	.1
+=DIMER ×=TRIMER ◇=TETRAMER	FOR FOR FOR	403	.1
↑=DIMER ⧖=TRIMER Z=TETRAMER	FOR FOR FOR	433	.1

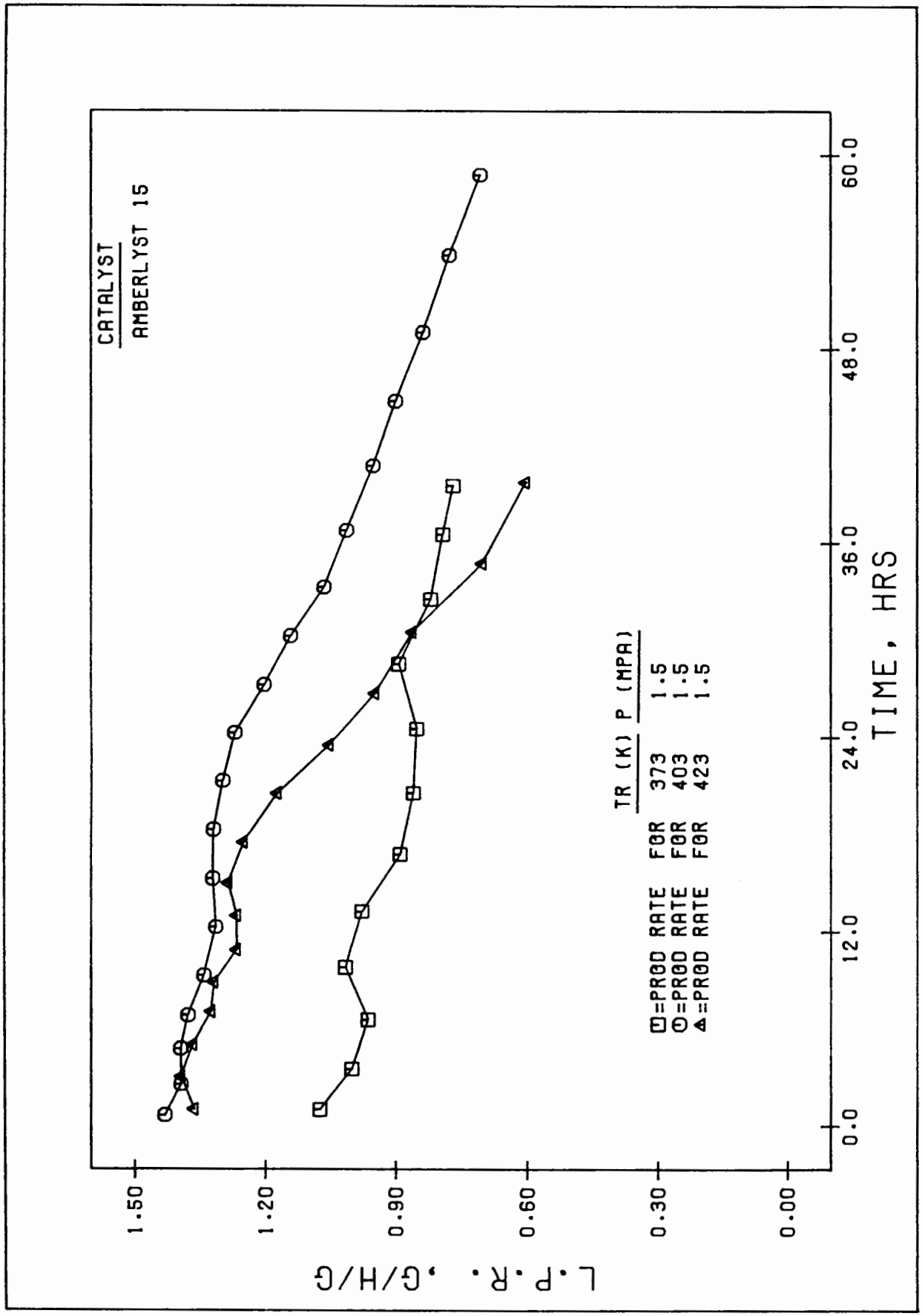

FIG.4.34 LIQUID PRODUCTION RATE (G/H/G) VS TIME (H)

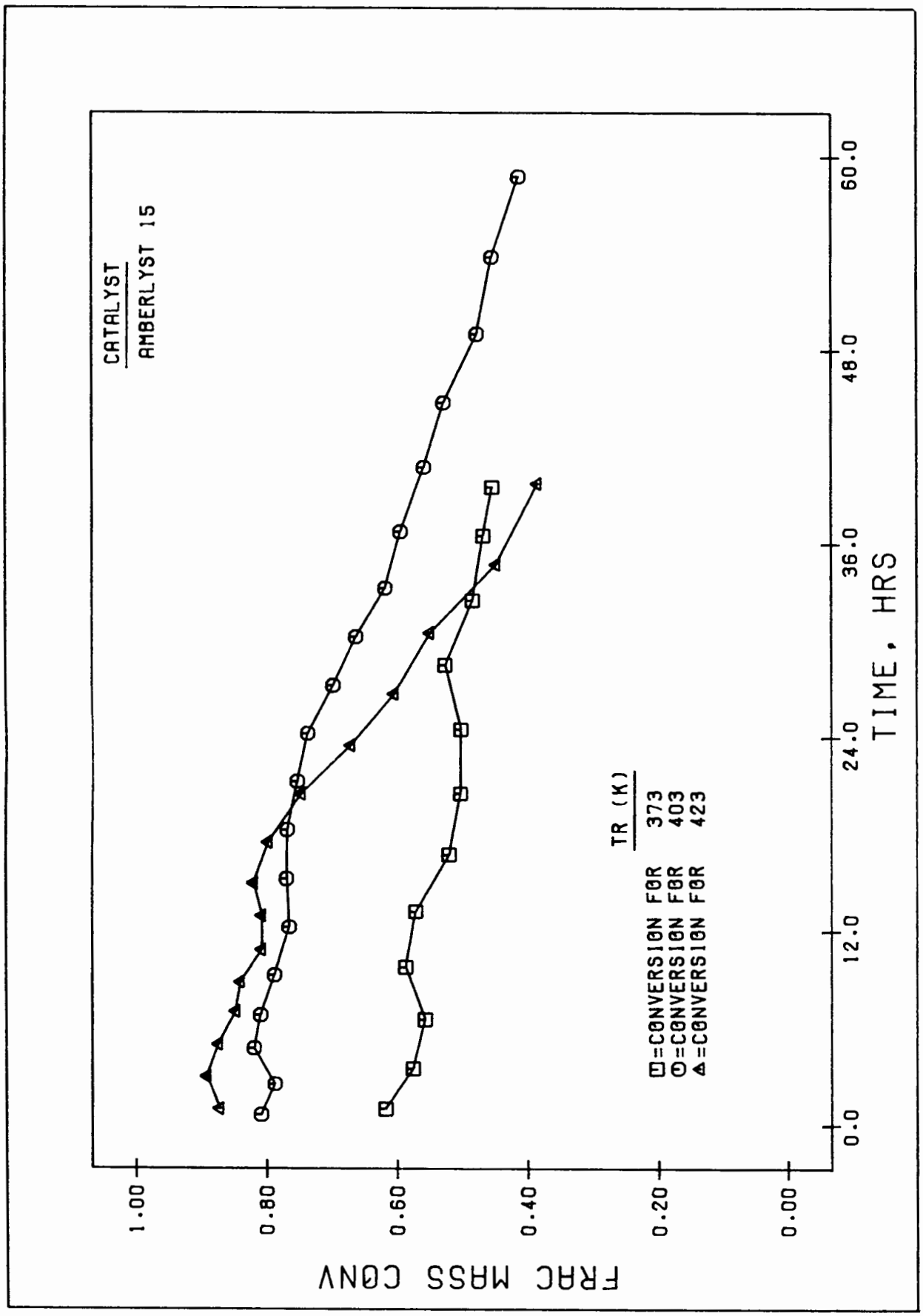

FIG. 4.35 FRACT CONV, FEED TO LIQ PROD VS TIME (H)

Another point to be made about the two high temperature runs is the shape of the curve. The L.P.R. is initially constant but, as seen in Fig. 4.34, drops after approximately 20 hours. This phenomenon is more pronounced for the run carried out at 150°C.

The selectivity was also markedly different for the three runs. This is shown in Fig. 4.36 for the dimer production, in Fig. 4.37 for the trimer production, and in Fig. 4.38 for the tetramer production. The relative amount of dimer decreases with increasing reaction temperature. Moreover, for both of the two high temperature runs, the amount of dimer formed was relatively constant until the time at which the drop in the L.P.R. occurred. At this stage a rapid increase in the amount of dimer produced was observed, as well as a drop in the amounts of the trimer and tetramer formed.

The ASTM distillation results are shown in Fig. 4.39. The significant effect of reaction temperature on the liquid product is evident.

A study of the gas utilization was made for the various reaction temperatures. The unsaturates, propylene, isobutene and 1-butene, were almost completely converted. Fig. 4.40 shows the change in the rate of isomerization of unsaturates with time.

A sharp drop in conversion after about 20 hours at the high temperatures is seen.

Fig. 4.41 shows the behaviour of the saturates. Initially the highest temperature produces the highest extent of alkylation, but as in other cases this drops sharply after about 20 hours.

4.12 The Effect of Regeneration

In order to study the effect of regeneration, a deactivated catalyst sample was divided into two portions and treated separately for organic and cationic fouling, respectively. Reactions were then repeated under the same conditions. The performance of the fresh catalyst and the two regenerated samples for the case in which the

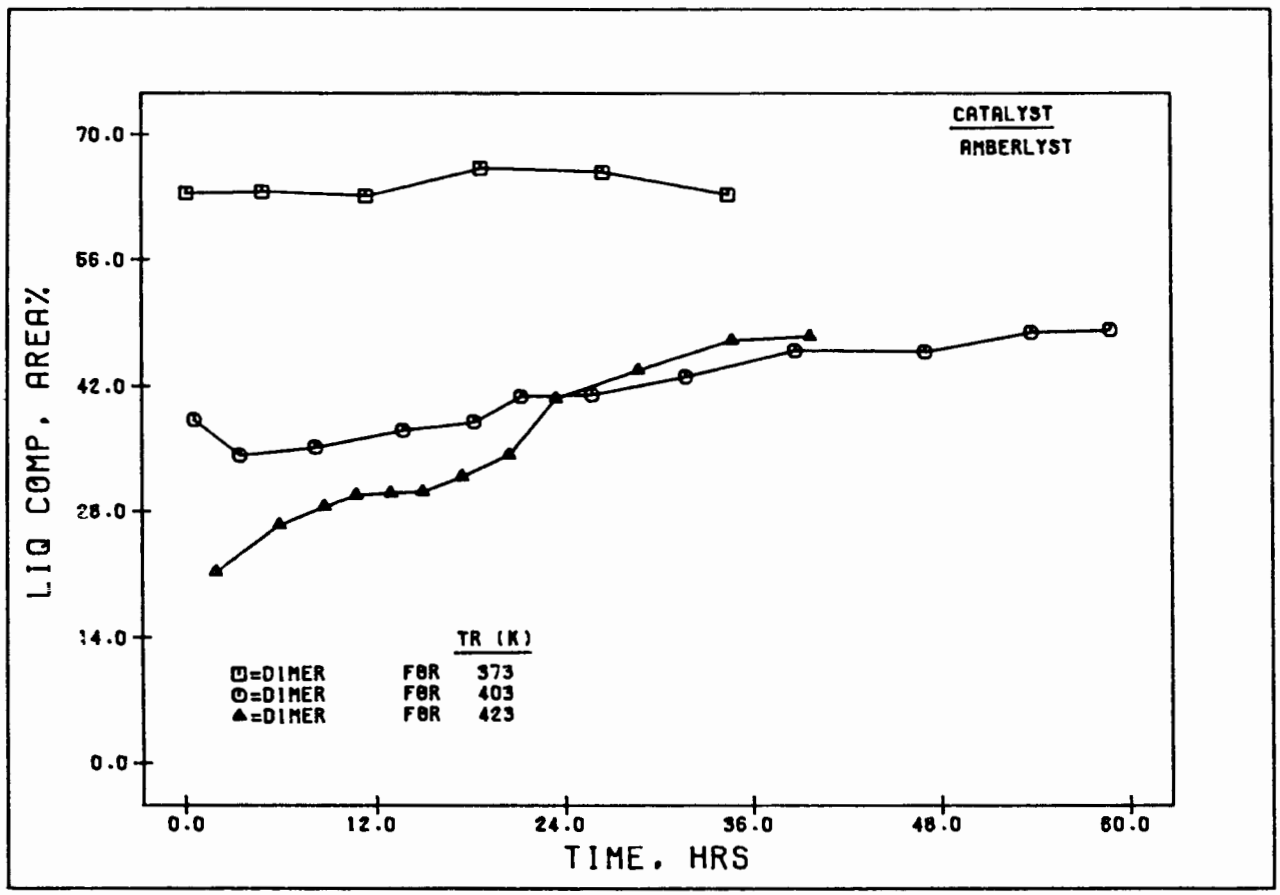

FIG.4.36 LIQ PROD COMPOS (AREA%) VS TIME (H)

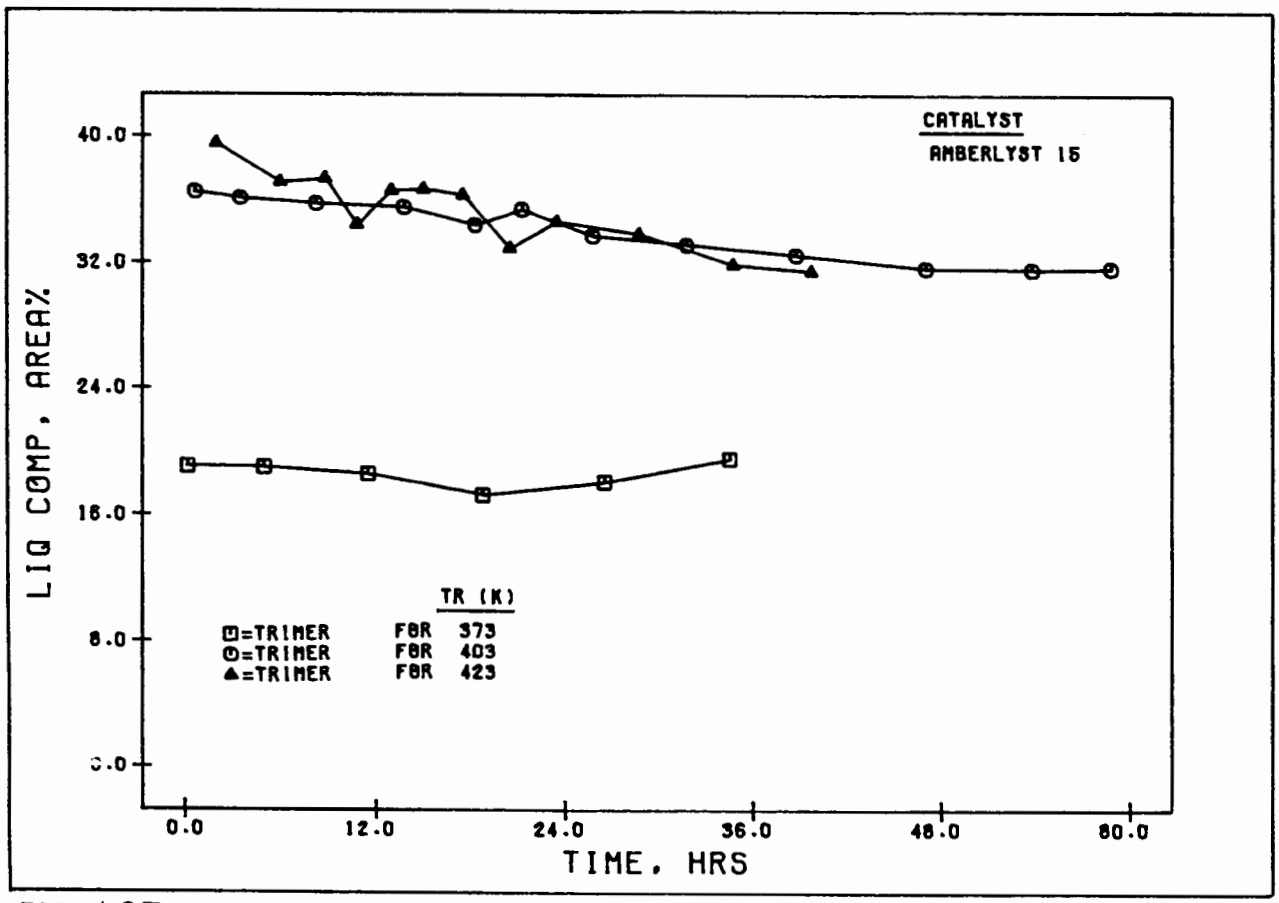

FIG.4.37 LIQ PROD COMPOS (AREA%) VS TIME (H)

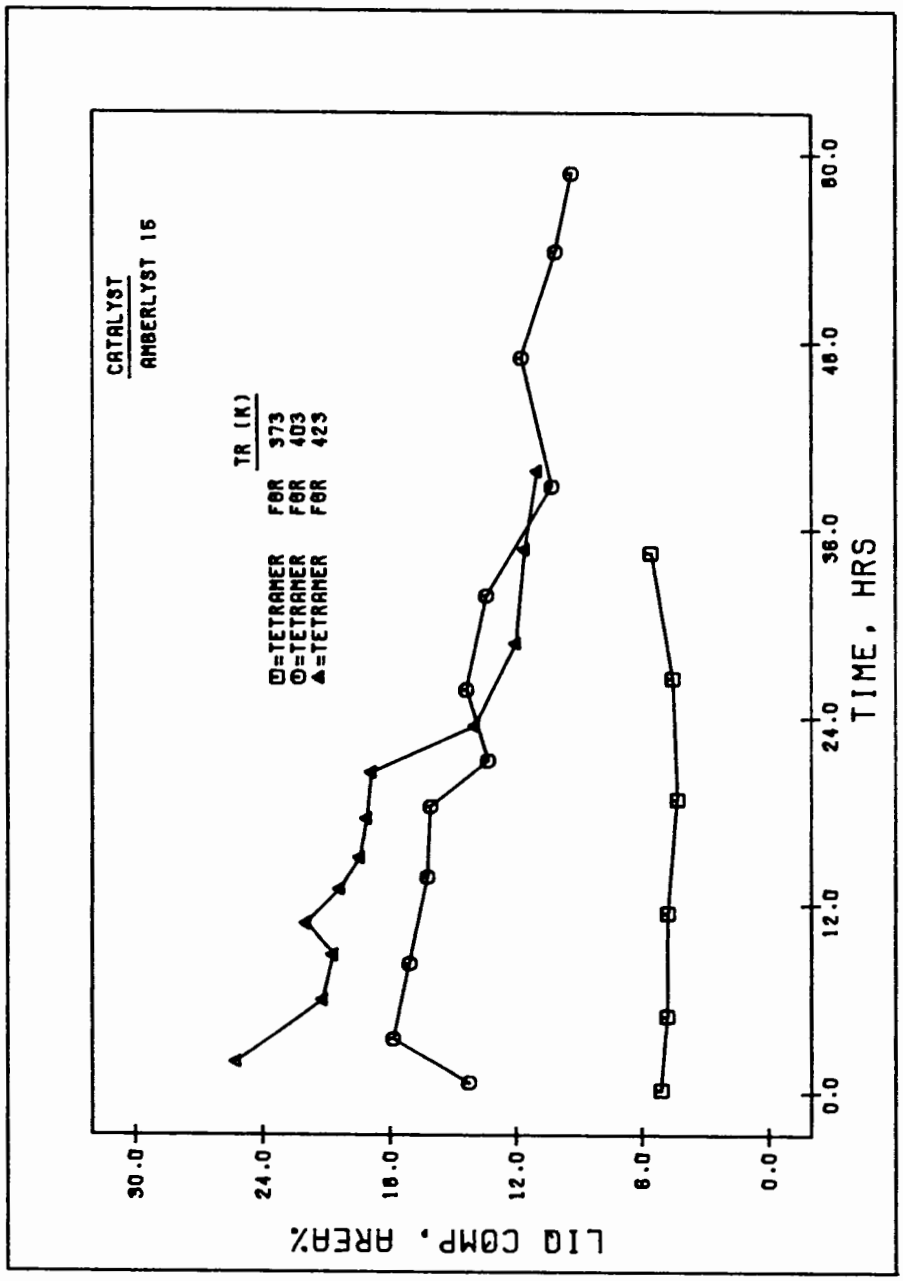

FIG.4.38 LIQ PROD COMPOS (AREA%) VS TIME (H)

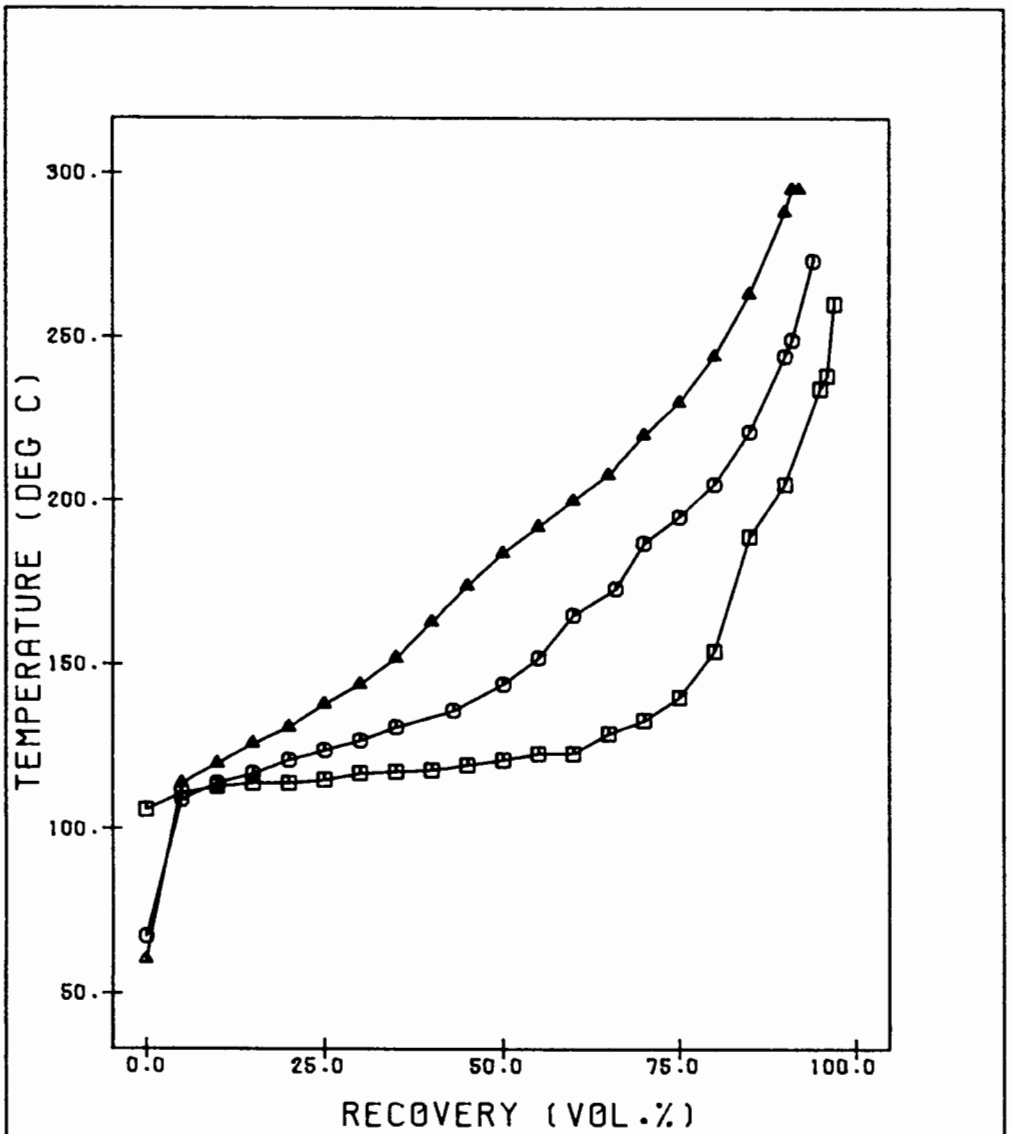

FIG.4.39 ASTM-DISTILLATION:
EFFECT OF REACTION TEMPERATURE

REACTION TEMPERATURE
□=T = 100 DEG C
○=T = 130 DEG C
▲=T = 150 DEG C

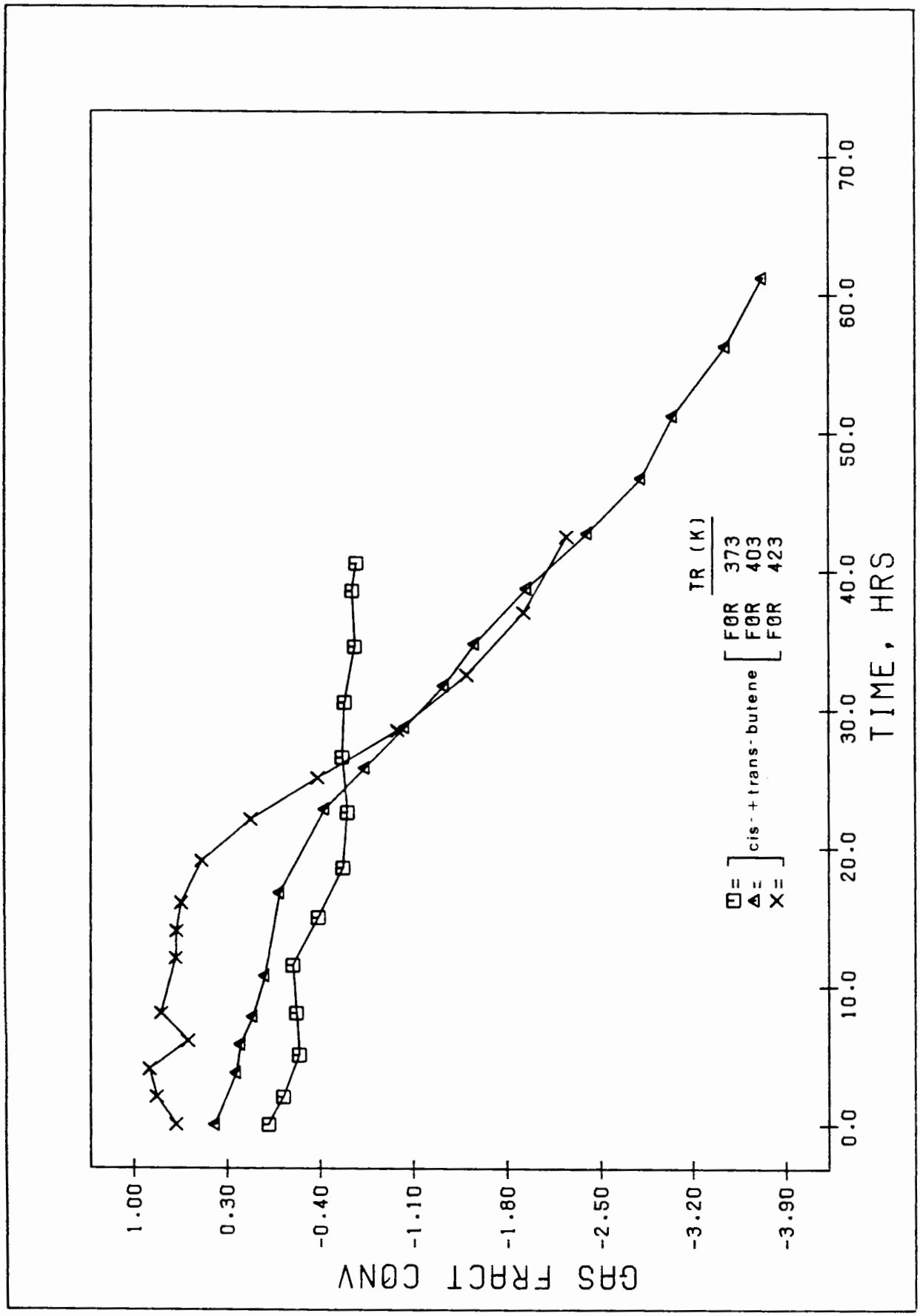

FIG.4.40 FEED GAS FRACT CONV VS TIME (H)

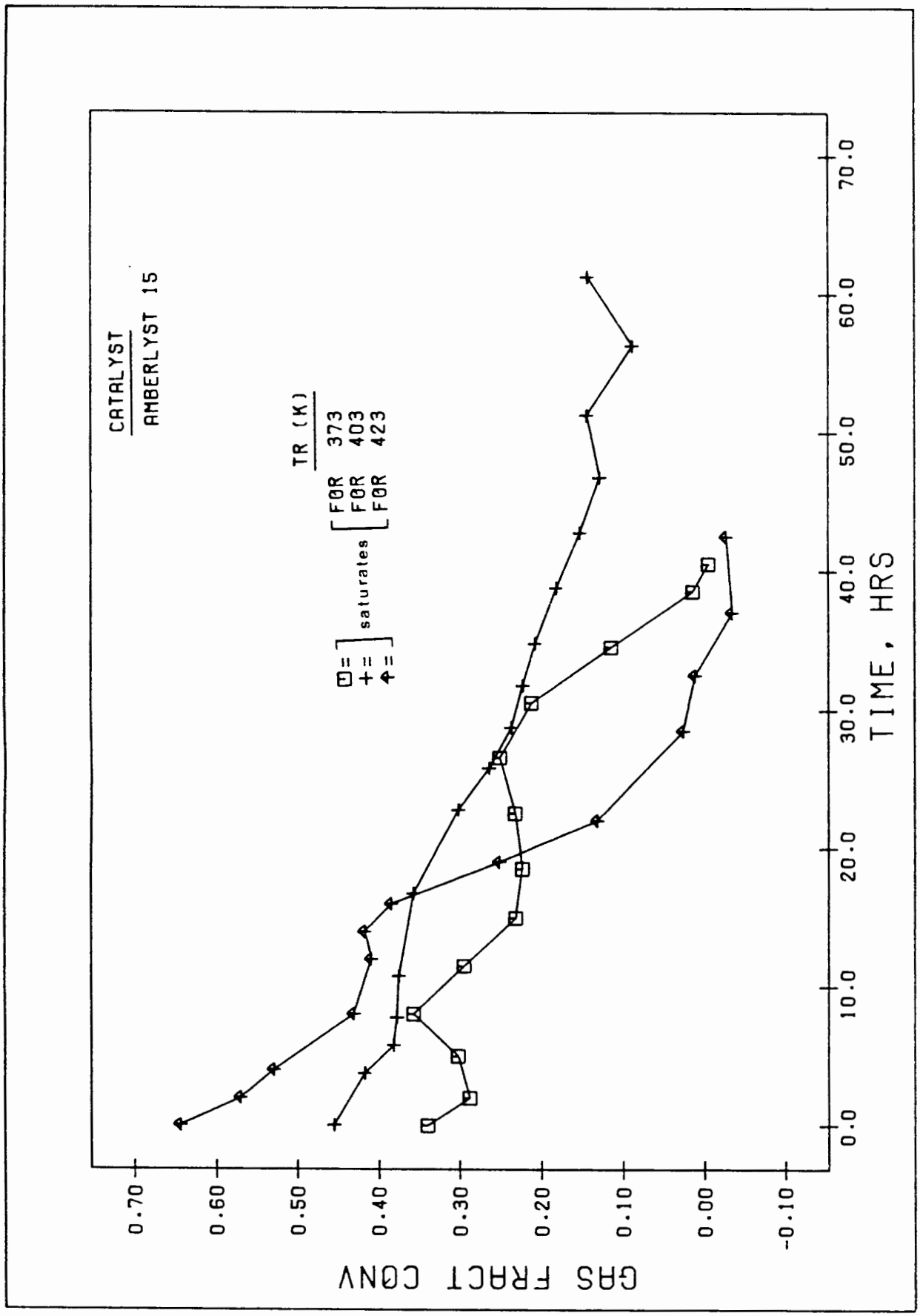

FIG.4.41 FEED GAS FRACT CONV VS TIME (H)

reaction temperature is 100°C are shown in Fig. 4.42. Both of the regeneration techniques appear to have almost completely restored the activity of the catalyst.

The selectivity of the regenerated catalyst was also similar to that of the fresh catalyst. This is shown in Fig. 4.43, where the G.C. analysis is presented, and in Fig. 4.44, where the bulk product is analysed by distillation.

In separate experiments it was shown that at higher temperatures the resin was partially destroyed and could no longer be regenerated. The resin from the high temperature experiments was regenerated for cationic fouling and re-used under the same conditions as the similarly regenerated resin above, viz. reaction temperature of 100°C. Their L.P.R. are compared in Fig. 4.45. The two regenerated resin samples from the high temperature runs did not show nearly the same L.P.R. Both runs had a much lower L.P.R., with the L.P.R. of the run carried out at 150°C being even less than that of the resin from the run carried out at 130°C. Moreover the selectivities are significantly different. Both of the resins undergoing reactions initially at high temperatures produce more trimers at the expense of dimers (Fig. 4.46).

4.13 Long Run at Typical Reaction Conditions

An attempt was made to combine as far as possible the best operating conditions, as determined from the previous sections. The purpose of this run was twofold:

- to make a detailed study of a long run under optimum conditions; and
- to collect sufficient liquid product to carry out a complete set of standard fuel tests.

In choosing the conditions for this run, the criteria of optimum L.P.R. and selectivity were not always consistent. Also the selection of the reaction conditions had to take into account the limitations of the reactor system and of the catalyst used. The reaction conditions chosen were as follows : completely functionalized Amberlyst

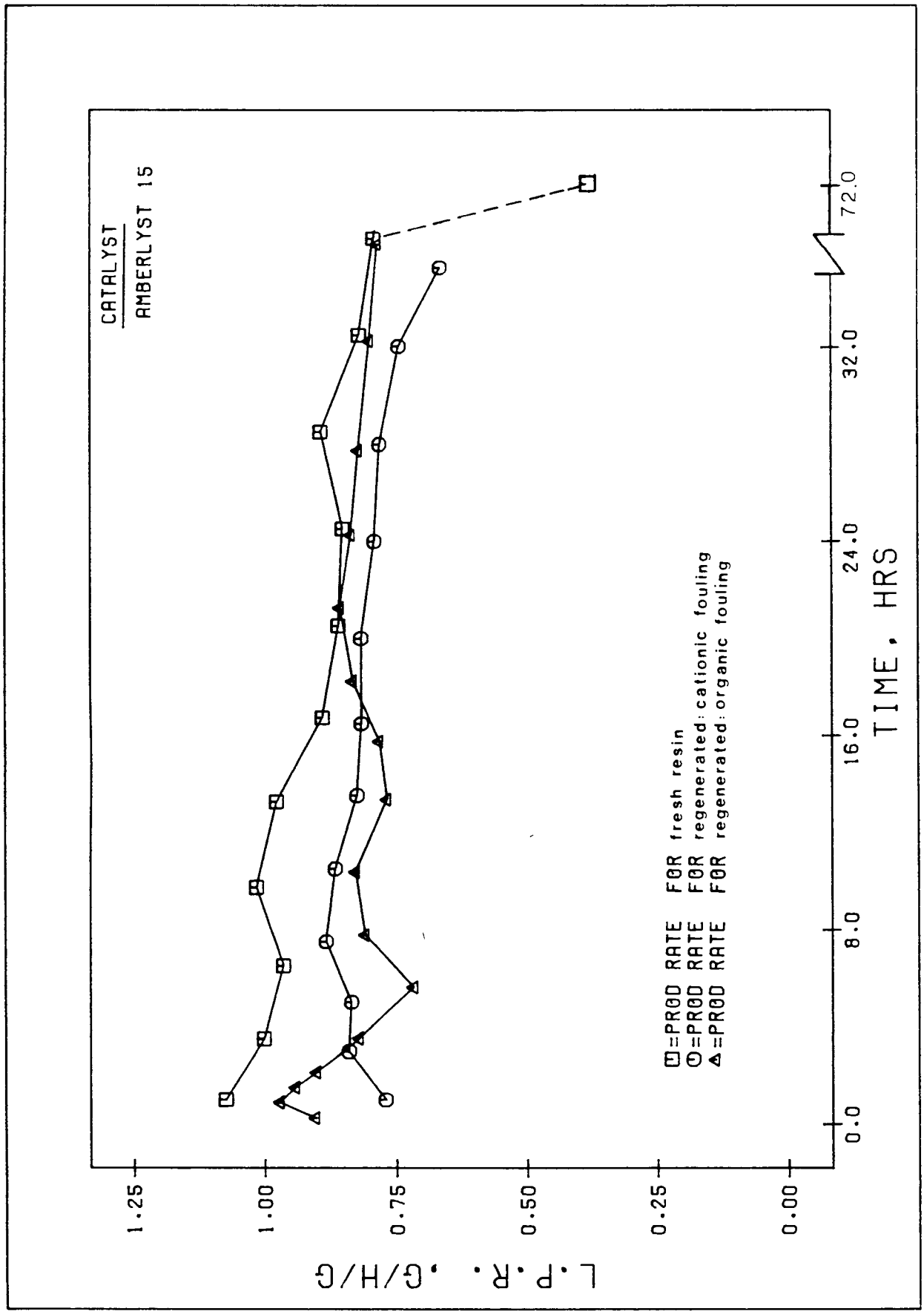

FIG.4.42 LIQUID PRODUCTION RATE (G/H/G) VS TIME (H)

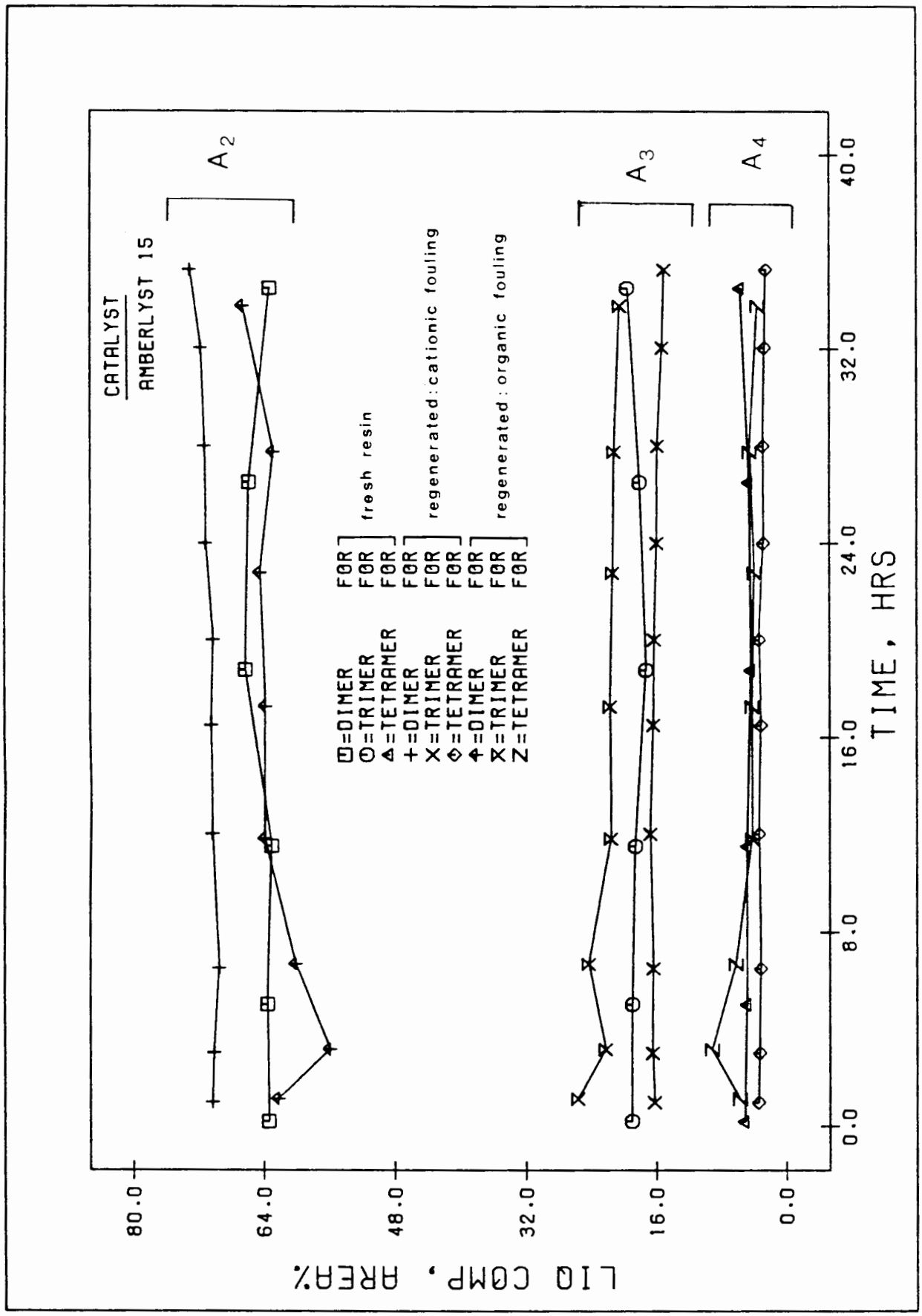

FIG.4.43 LIQ PROD COMPOS (AREA%) VS TIME (H)

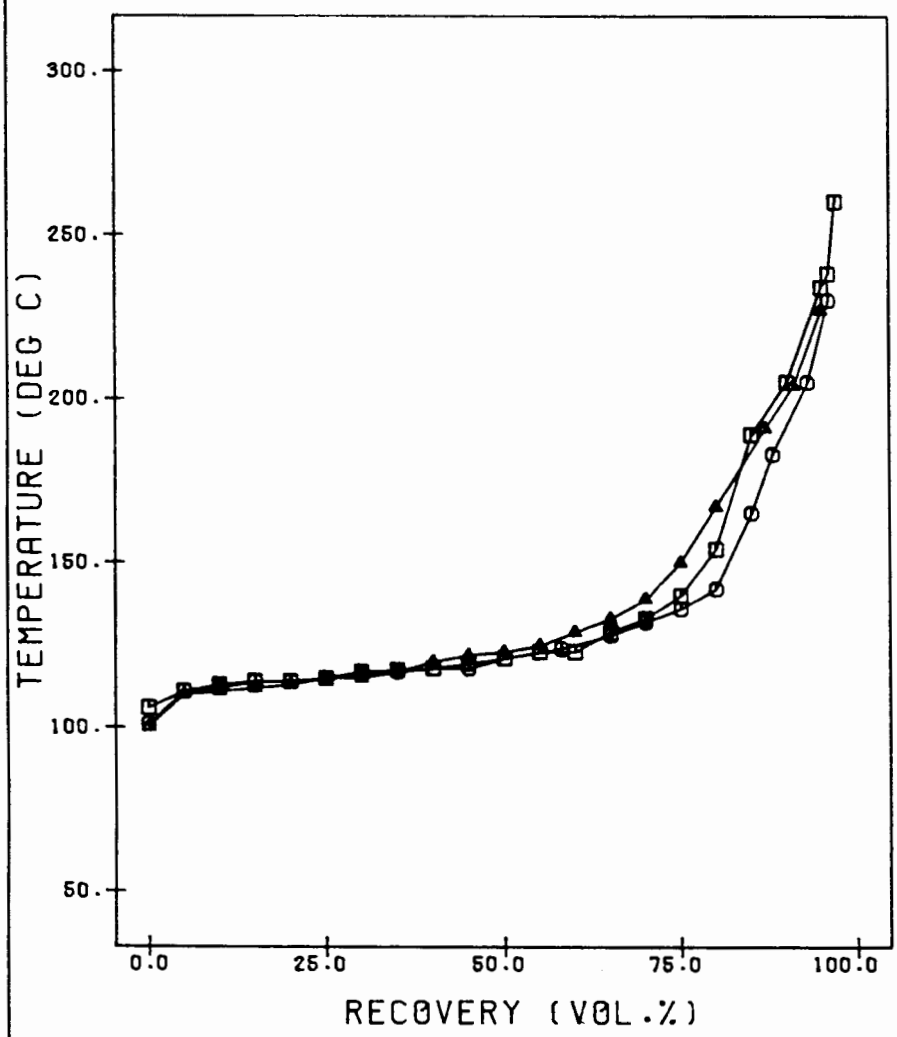

FIG. 4.4 4 ASTM-DISTILLATION:
EFFECT OF REGENERATION

□=FRESH RESIN
○=TREATED FOR CATIONIC FOULING
▲=TREATED FOR ORGANIC FOULING

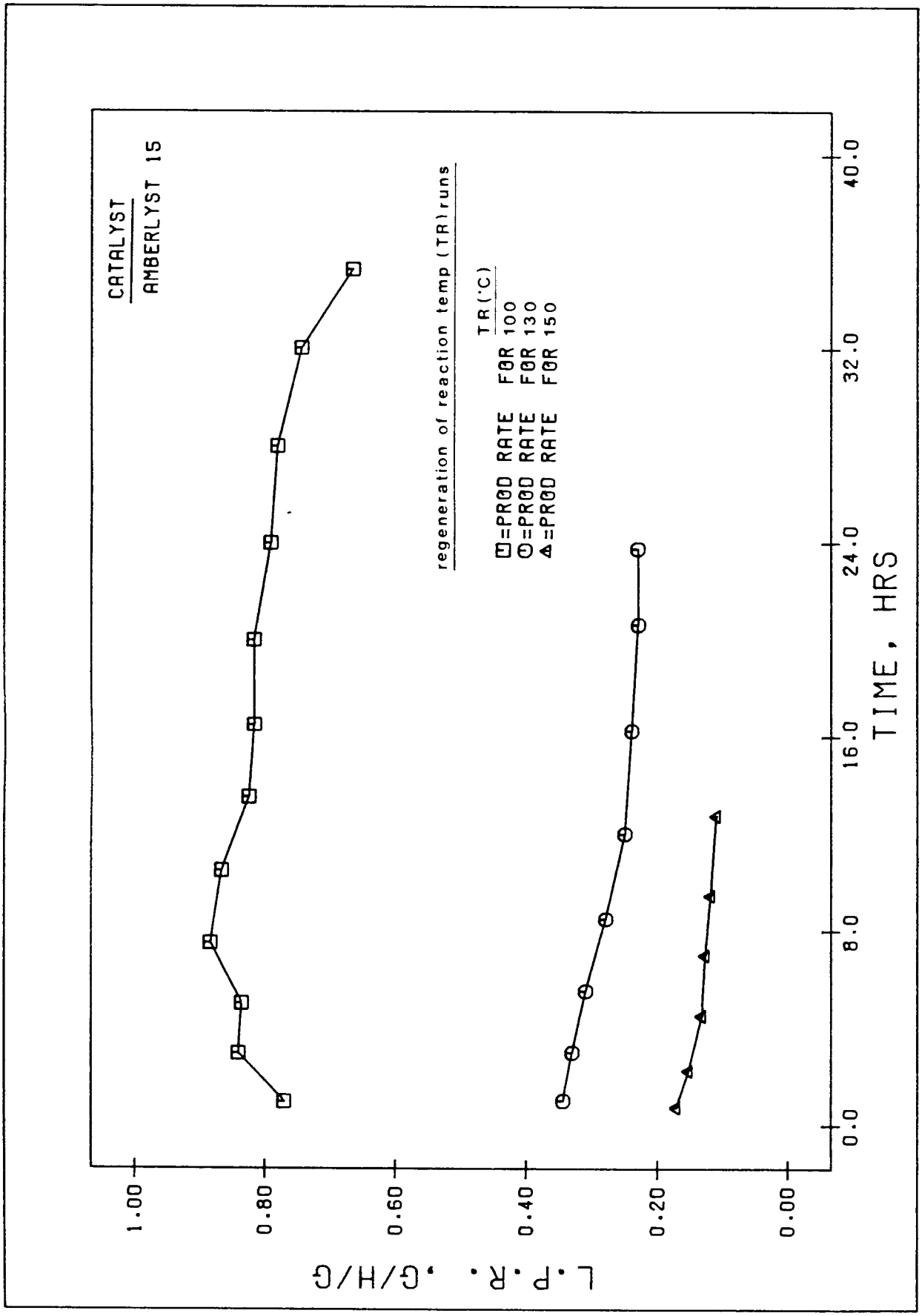

FIG.4.45 LIQUID PRODUCTION RATE (G/H/G) VS TIME (H)

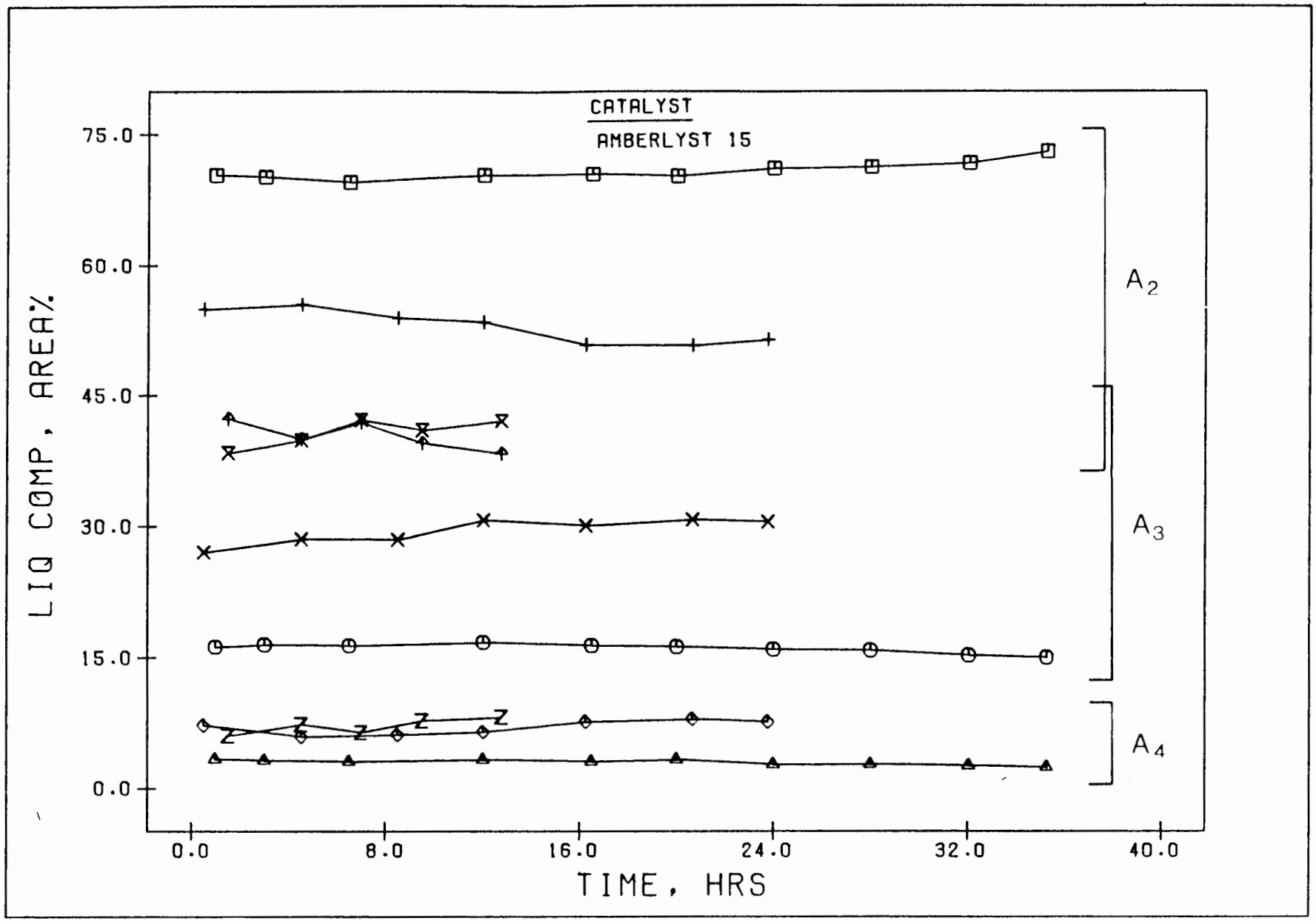

FIG. 4.46 LIQ PROD COMPOS (AREA%) VS TIME (H) regeneration of reaction temp. runs

	TR(°C)		TR(°C)		TR(°C)
⊡=DIMER	FOR	+=DIMER	FOR	↟=DIMER	FOR
⊖=TRIMER	FOR 100	×=TRIMER	FOR 130	⧖=TRIMER	FOR 150
▲=TETRAMER	FOR	◇=TETRAMER	FOR	Z=TETRAMER	FOR

15, with its macroporous structure and strongly acidic sulphonic groups, was chosen as the catalyst, due to its high L.P.R. A catalyst bead size of 300 to 500 microns was used because this gave a relative high L.P.R. while avoiding the problem of catalyst entrainment. The reaction temperature was set at 105°C, which allowed for a temperature rise due to exothermicity without causing thermal degradation of the catalyst, i.e. the deactivated catalyst could still be regenerated. Furthermore, the monomer was maintained in the gas phase, because this gave longer catalyst life. The pressure was thus set at 1.5 MPa. Finally, the feed rate was set at a WHSV of 1.

The catalyst operating under the above conditions, showed a very high L.P.R. This is shown in Fig. 4.47. The L.P.R. gradually decreases with reaction time, dropping almost linearly from a L.P.R. of 0.85 to 0.64g of product/hour/g of catalyst over a period of 140 hours.

The initial conversion is about 85%. This is more than the fraction of olefins in the feed. Fig. 4.48 shows the conversion as a function of time observed for this experiment. A detailed analysis of the gas utilization is shown in Fig. 4.49 where saturates, unsaturates consumed by reaction, and unsaturates produced by isomerization are shown.

Propene, isobutene and 1-butene are virtually completely converted, either by polymerization or by isomerization. Approximately 40% of the saturates are converted. This is most likely as a result of alkylation reactions. A more detailed study of the individual conversion of the saturates is shown in Fig. 4.50. From this it is clear that n-butane undergoes the highest conversion, followed by isobutane and propane.

With respect to cis- and trans-2-butene, Fig. 4.49 shows that for the first 75 hours they were disappearing by reaction, the rate of their disappearance diminishing with time. At times greater than approximately 75 hours they were actually being produced in the reaction process.

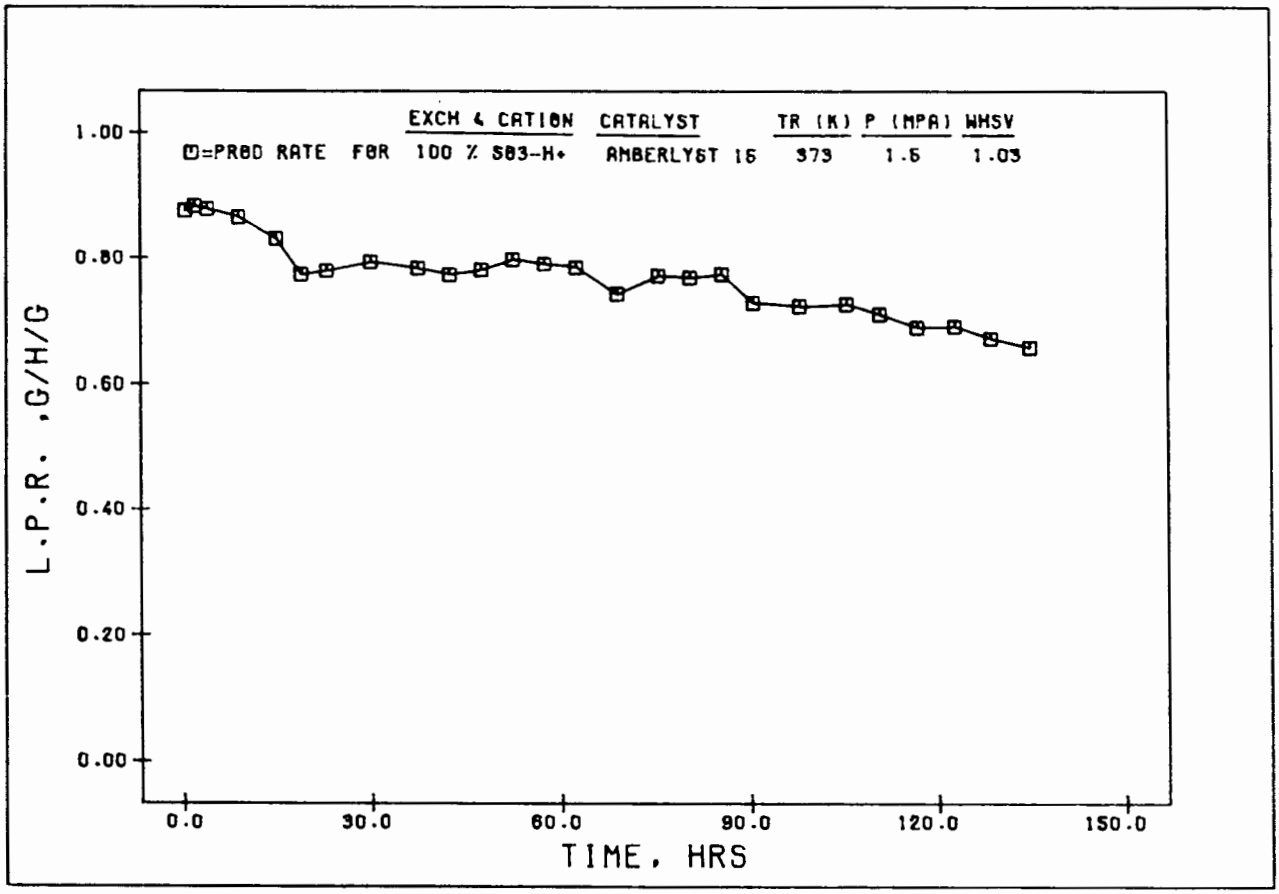

FIG. 4.47 LIQUID PRODUCTION RATE (G/H/G) VS TIME (H)

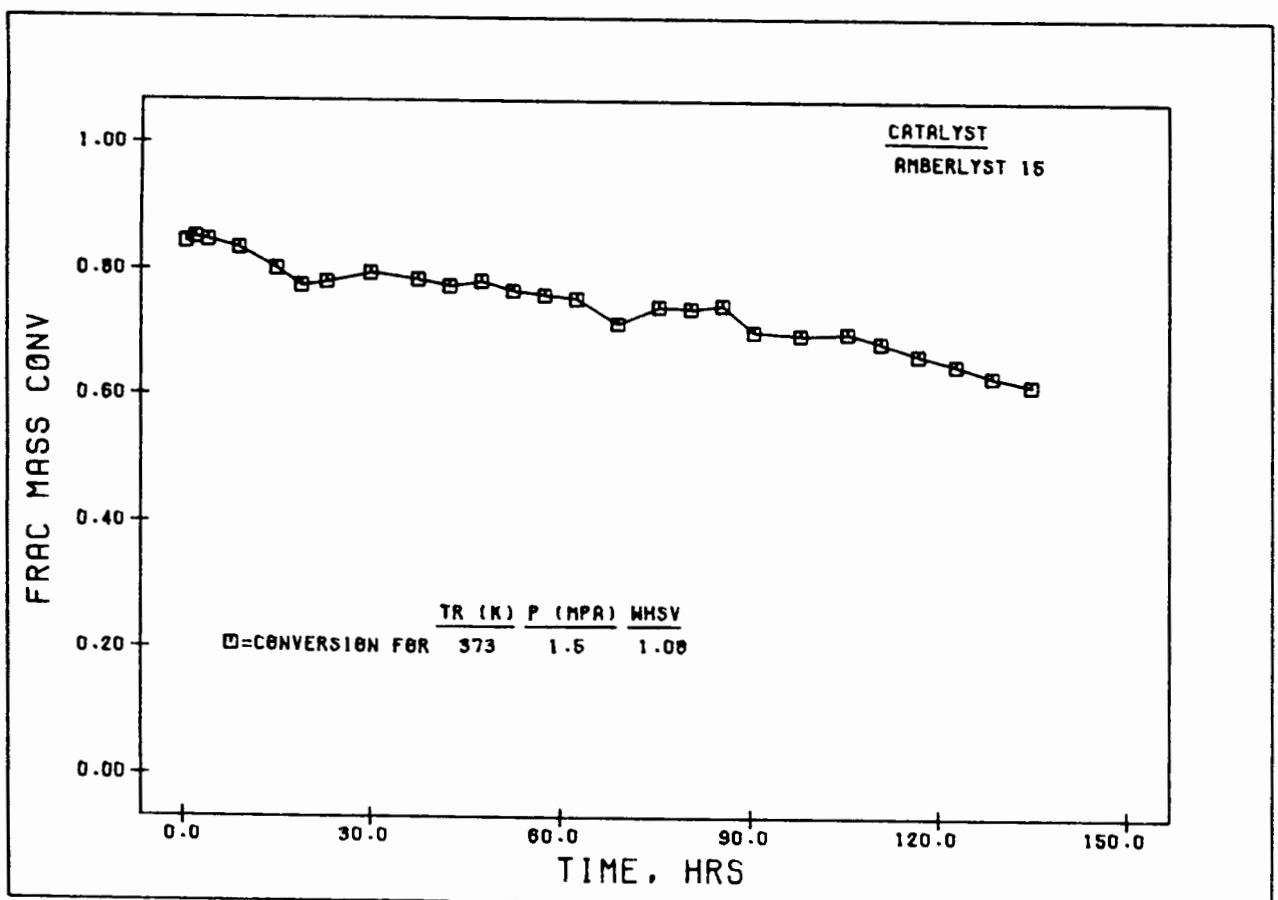

FIG. 4.48 FRACT CONV. FEED TO LIQ PROD VS TIME (H)

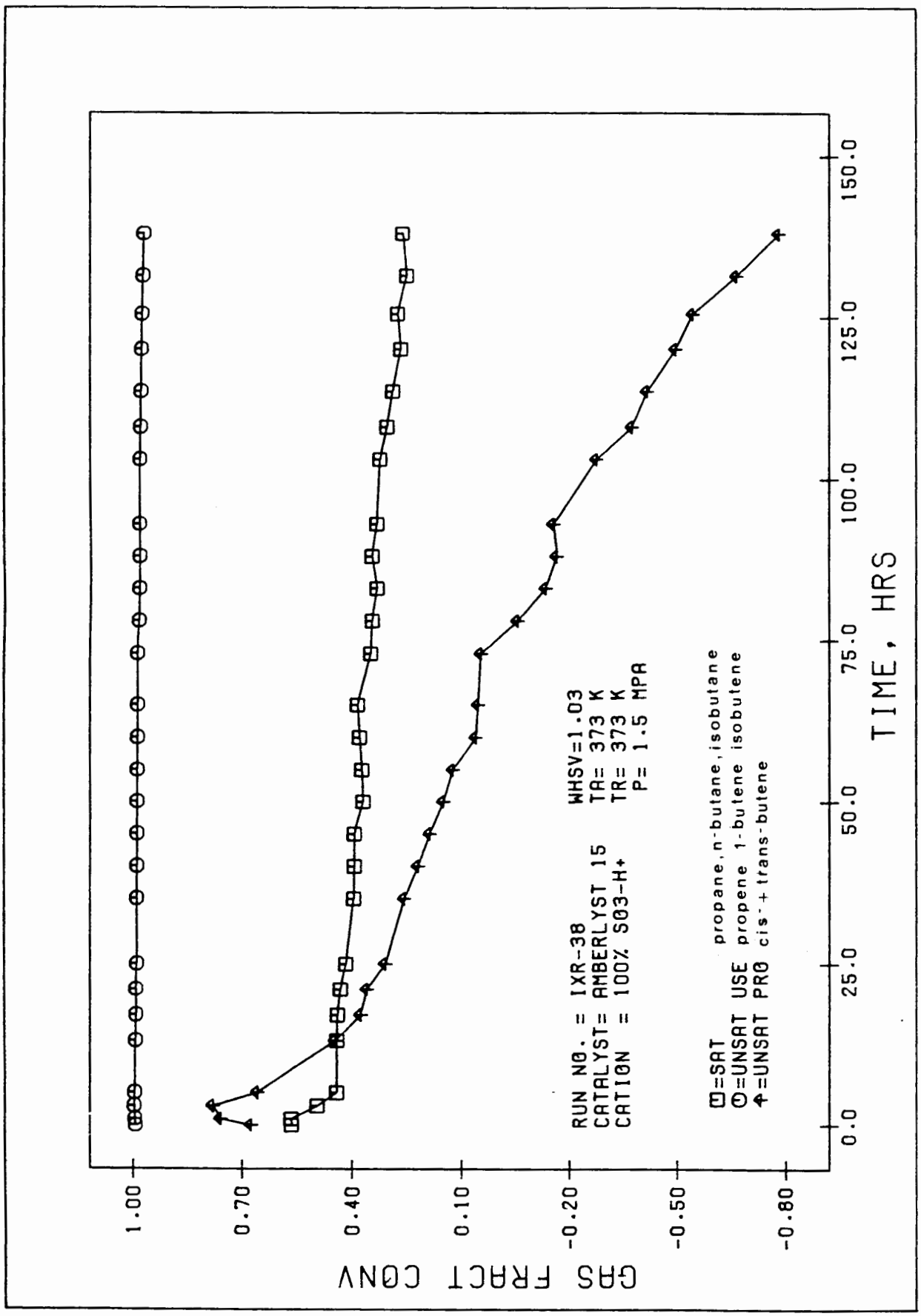

FIG.4.49 FEED GAS FRACT CONV VS TIME (H)

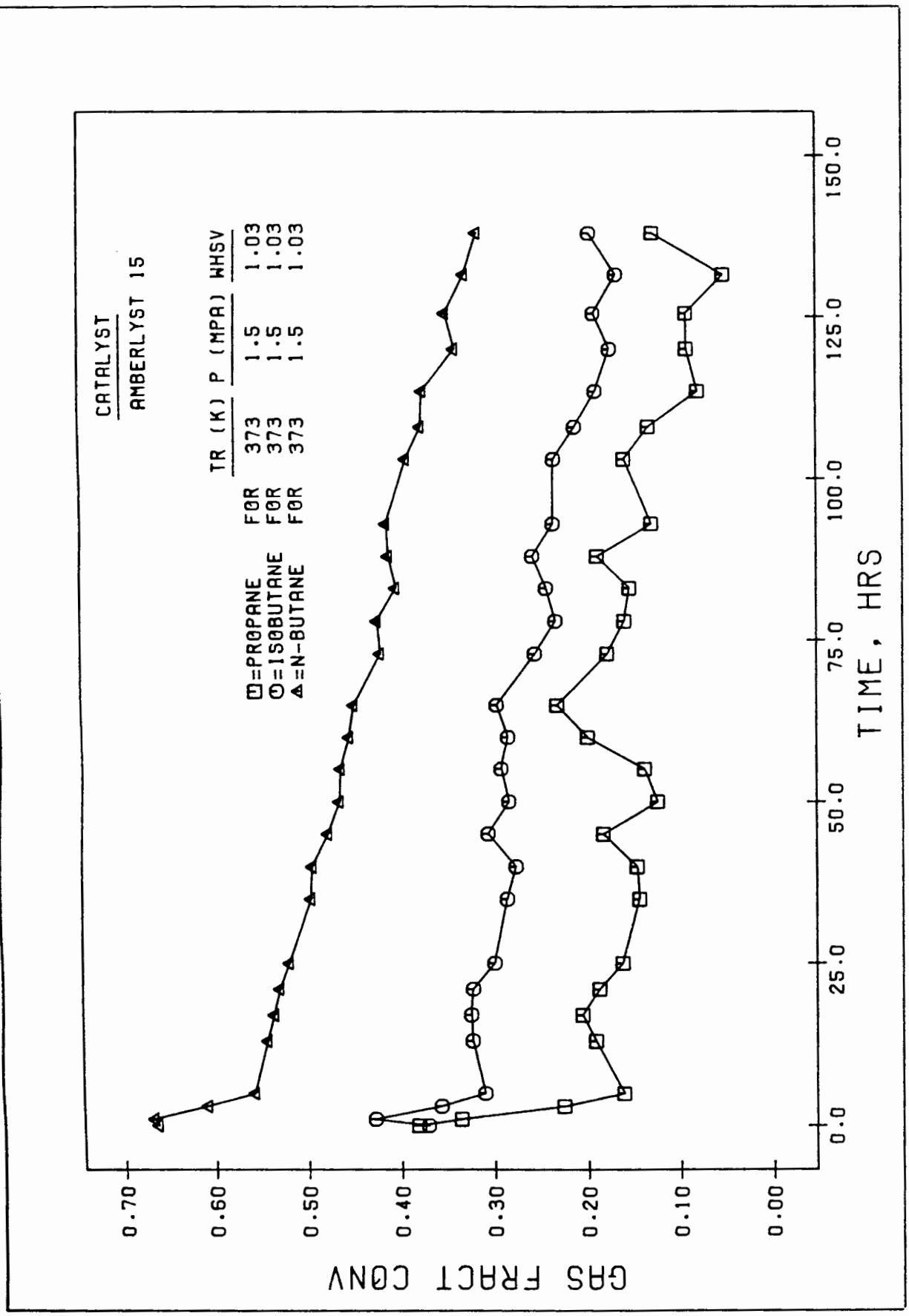

FIG.4.50 FEED GAS FRACT CONV VS TIME (H)

A closer look at the two components, i.e. cis- and trans-2-butene is shown in Fig. 4.51. They both seemed to be present in a ratio of about 1.6 trans-2-butene/cis-2-butene throughout a run. This has been experienced with all the other runs as well, and is most probably due to steric factors. A further indication of the activity of a catalyst is the temperature profile within the reactor bed. This is discussed in section 4.14.

The selectivity of the run is shown in Fig. 4.52. It confirms the previously found trends that mostly dimers are formed with much less trimers and tetramers and that as reaction time proceeds, the activity of the catalyst drops, and the fraction of dimer produced increases at the expense of the trimer and tetramer. This tendency is clearly demonstrated by a distillation. Fig. 4.53 shows the result of such distillations of the product obtained at various reaction times. It is readily seen that the reaction product becomes lighter at longer reaction times.

4.14 Temperature Profile within Catalyst Bed

For this study the catalyst bed was divided up into seven equal sections and temperatures were taken at the interfaces of these sections throughout the run. Fig. 4.54 shows such a temperature profile for the run described in section 4.13 as a function of time.

It is readily seen that a reaction front, indicated by a temperature peak, moves along the bed. As it slowly progresses from the top of the bed to the bottom, the temperature of the reaction front gradually decreases. This movement of the reaction front indicates that the bed is deactivated from the top downwards and as the temperature of the reaction front declines, the L.P.R. of the catalyst is reduced.

Also shown in the figure is that the upper 2/7th of the bed is deactivated within the first 18 hours after start-up. In contrast, the third, fourth and fifth section of the bed took 36.8 (1.11mm/hr), 34.2 (1.19 mm/hr) and 45.6 (0.89mm/hr) hours, respectively, to deactivate. The numbers in parentheses indicate the travelling speed of the reaction front.

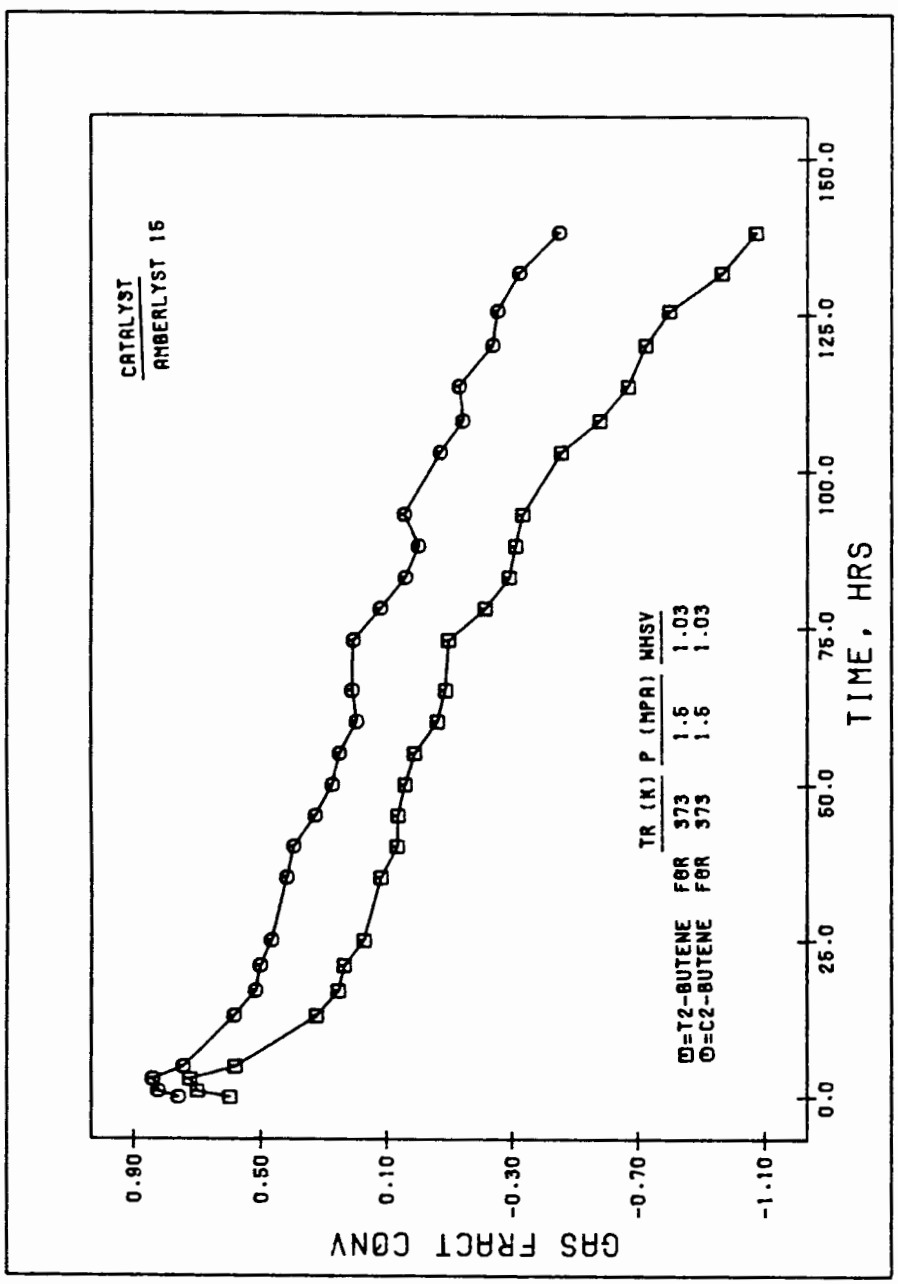

FIG.4.51 FEED GAS FRACT CONV VS TIME (H)

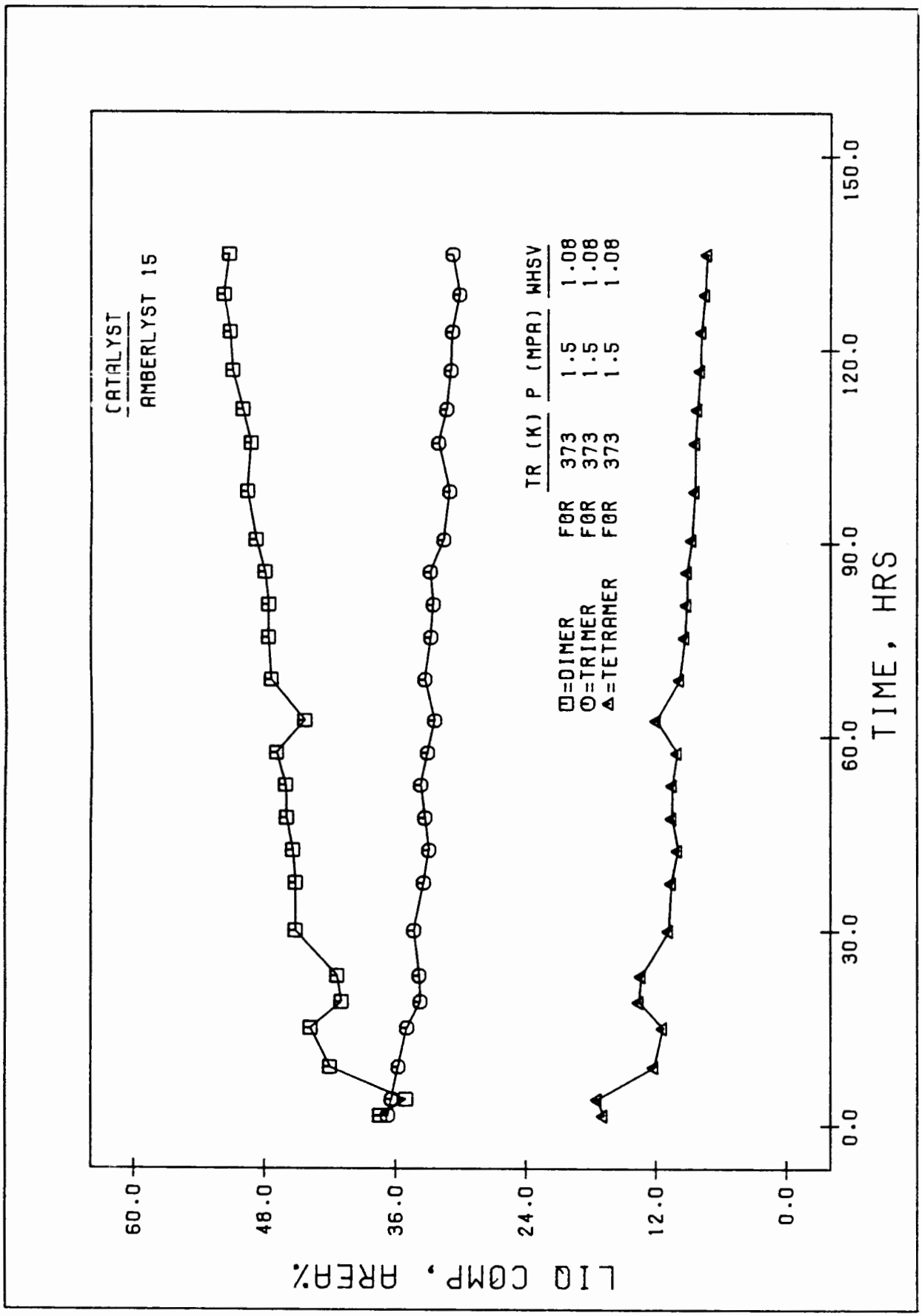

FIG.4.52 LIQ PROD COMPOS (AREA%) VS TIME (H)

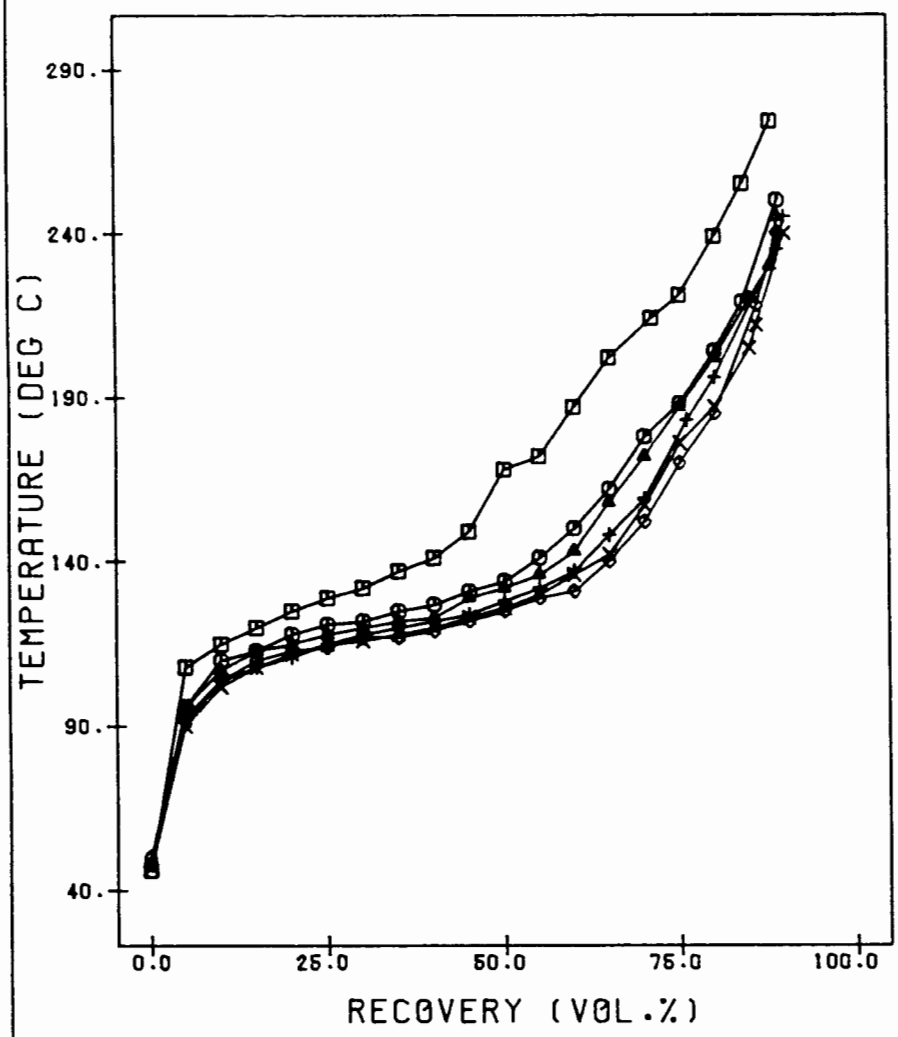

FIG.4.53 ASTM-DISTILLATION:
VARIATION OF PRODUCT SPECTRUM WITH TIME

PRODUCT SPECTRUM AT VARIOUS TIMES
□=T = 8.0 HR
○=T = 31.5 HR
▲=T = 58.5 HR
+=T = 81.5 HR
×=T = 111.5 HR
◇=T = 142.0 HR

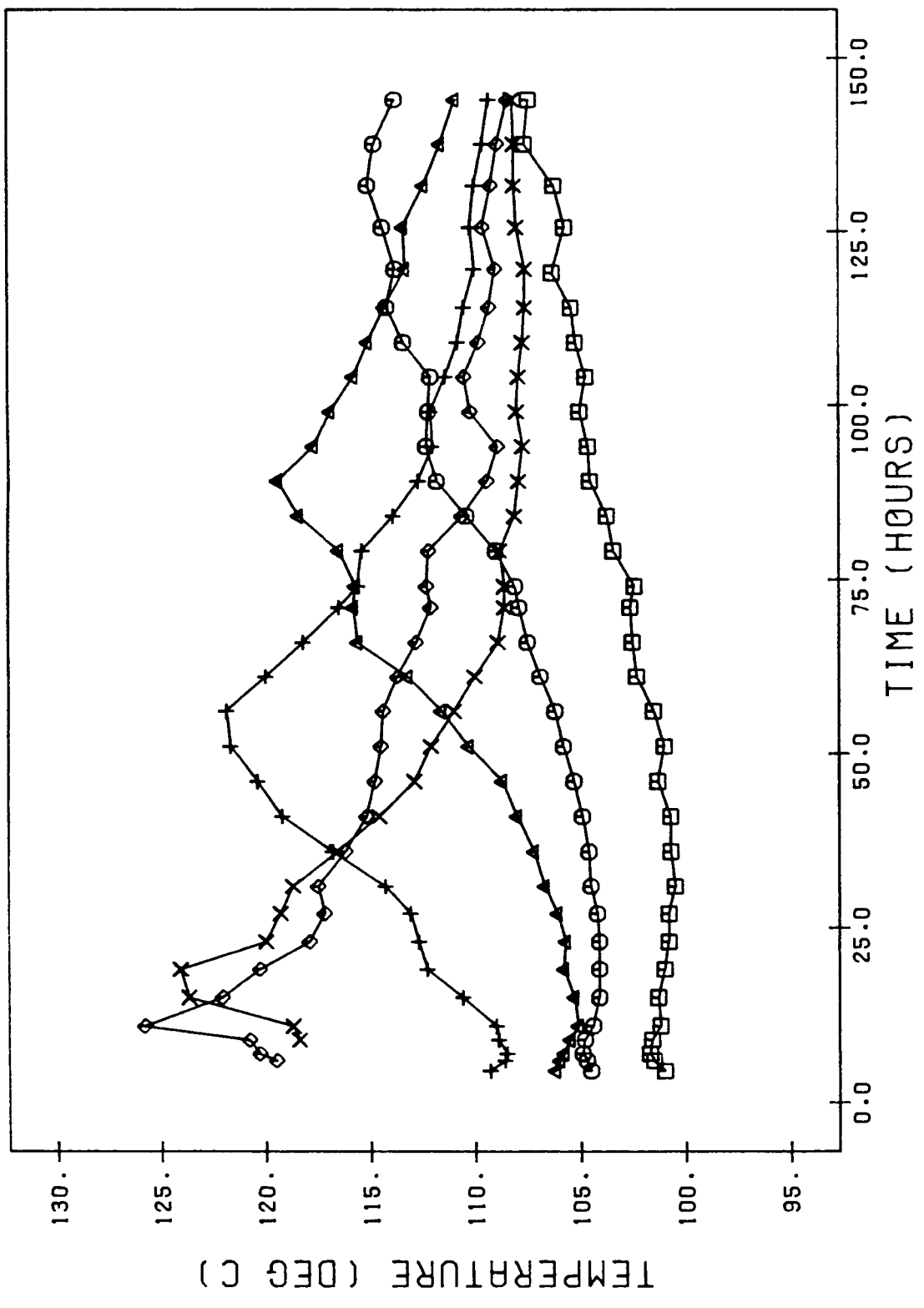

FIG. 4.54 TEMPERATURE PROFILE IN CATALYST BED

Similar studies on other runs have indicated that the depth of the reaction front is an indication of the activity of the catalyst. The high temperature runs at 130 and 150°C showed a much steeper reaction front with much higher travelling speeds of 4.43 and 7.53 mm/hr respectively. However, as shown elsewhere, deactivation for these runs was due to thermal degradation, while for the run in Fig. 4.54 it was most probably due to cationic fouling. For the high temperature runs at 130 and 150°C a significant drop in L.P.R. was observed after 24 hours and 15 hours (see Fig. 4.34) respectively, which can be shown to be the time when the reaction front reaches the bottom of the bed. For the run in Fig. 4.54 the reaction front has not yet reached the bottom of the bed.

4.15 Distillation

The results of the 100mℓ ASTM distillation carried out have been shown in previous sections.

Table 4.4 shows a summary of the bulk distillations separating the products into heavy and light fractions. The cut point was 180°C.

The trends can be summarised as follows:

i) Early stages of a run produce more higher boiling point product.
ii) Lower WHSV values produce more higher boiling point product.
iii) Catalyst bead size does not significantly affect the distribution between the two fractions.
iv) Both regeneration techniques, for cationic fouling and organic fouling, produce liquid having the same distribution as fresh catalyst.
v) Amberlyst 1010 tends to form more higher boiling point product than Amberlyst 15 and Duolite C26.
vi) Reaction temperature strongly affects product distribution with high reaction temperatures favouring the higher boiling point fraction.
vii) The phase of the reactants do not significantly affect the distribution.

Significance	Total weight (g)	Wt % −180°C (1 atm.)	Wt % +180°C (1 atm.)
WHSV = 0.85; initial fraction	1047.5	59.8	40.2
" middle fraction	983.6	69.3	30.7
" final fraction	860.3	69.3	30.7
" bulk fraction	2891.4	66.6	33.4
WHSV = 2.50	1053.8	83.4	16.6
WHSV = 1.70, reaction temp = 100°C, fresh resin 500-800 µm bead size Amberlyst 15. Reactant gas phase	1907.3	80.3	19.7
300-500µm bead size	1925.3	81.2	18.8
1000-1180µm bead size	1429.6	84.5	16.5
reg. : cationic fouling	566.8	81.2	18.8
reg. : organic fouling	647.7	80.4	19.6
Amberlyst 1010	358.4	66.2	33.8
Duolite C26	1937.5	84.8	15.2

Table 4.4 : Results of bulk distillation into light and heavy fractions

Significance	Total weight (g)	Wt % −180°C (1 atm)	Wt % +180°C (1 atm)
*Reaction temp = 130°C	1855.0	59.7	40.3
*Reaction temp = 150°C	992.3	44.2	55.8
Reactant : liquid phase	925.2	80.0	20.0
**Optimum conditions	3649.4	80.7	19.3

* This represents the product obtained by the reaction front reached the bottom of the bed

** For this distillation the cutpoint was 190°C, corresponding to about 180°C at the high altitude of Secunda.

Table 4.4 (Contd.) : Results of bulk distillation into light and heavy fractions

4.16 N.M.R.

The samples analysed for NMR were separated into two fractions, a low boiling point fraction (-180°C) representing the petrol fraction, and a high boiling point fraction (+180°C), representing the diesel fraction.

The presence of aromatics and olefins in the petrol fraction increases the R.O.N. value. Any alkyl groups need to be highly branched and a high ratio of methyl to methylene groups is desirable (≈ 1.0). On the other hand, high quality diesel is typically a saturated straight chain, and a CH_3/CH_2 ratio of about 0.5 is desirable.

N.M.R. was used to obtain an indication of the types of hydrocarbons present, the H/C ratio, and the extent of branching. The effect of reaction temperature and WHSV on the above factors was also examined. Fig. 4.55 and Fig. 4.56 show typical spectra of the petrol and light diesel fractions, respectively. The resonance peaks are also indicated.

Results of N.M.R. studies offer only an approximate guideline and a relative comparison between samples. Table 4.5 gives the results of the N.M.R. analysis for varying reaction conditions.

None of the samples showed any concentration of detectable aromatics. An analysis of the petrol fraction for saturated and unsaturated compounds showed that the extent of alkylation increases with decreasing WHSV and to a much lesser extent, with increasing reaction temperature.

For the petrol fraction, the H/C ratio increases with increasing reaction temperature, but is unaltered by changing the WHSV. The latter tendency also holds for the diesel fraction, except that reaction temperature does not affect this ratio.

Fig. 4.55 : Typical NMR spectrum of the -180°C fraction

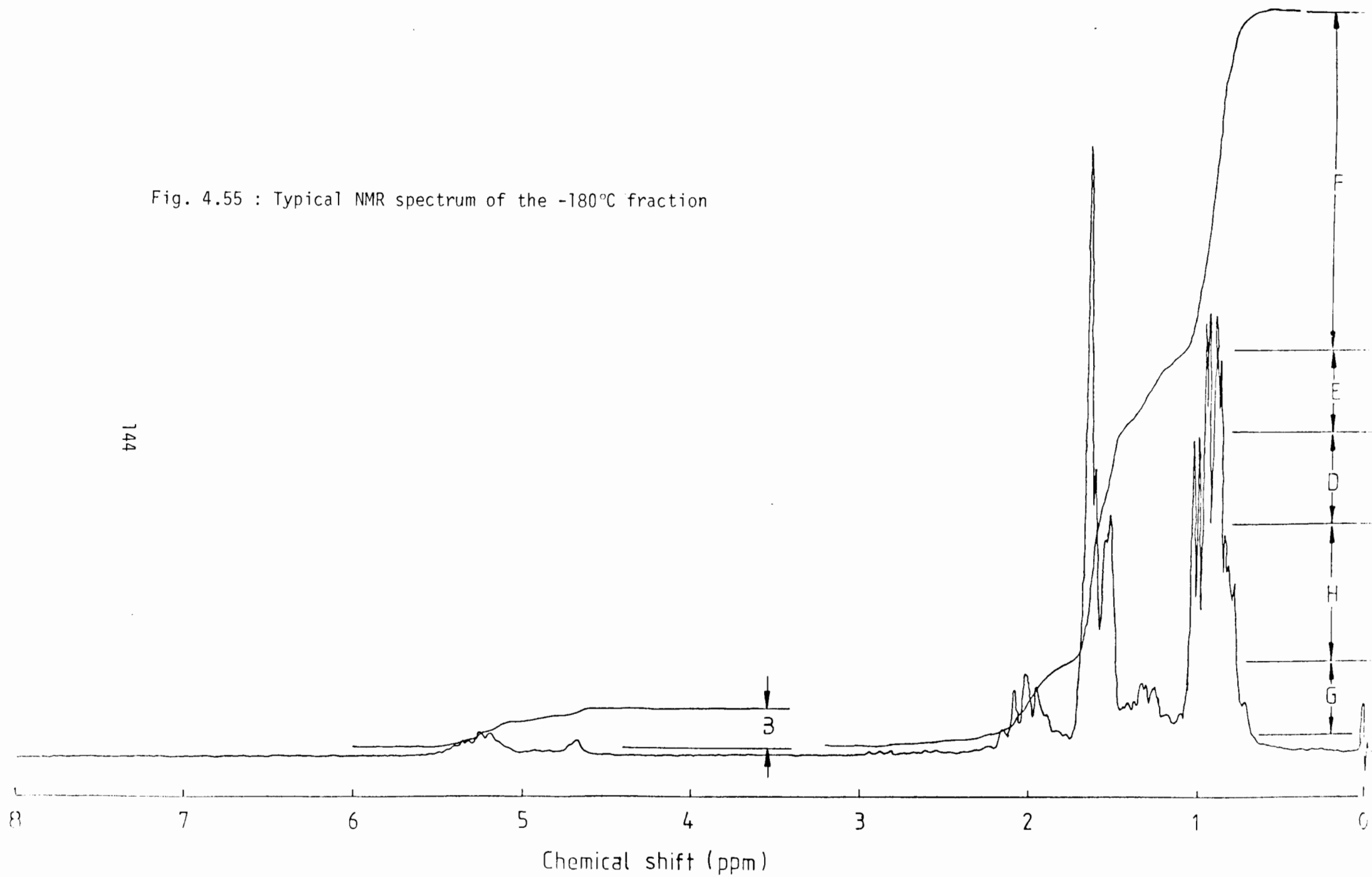

Fig. 4.56 : Typical NMR spectrum of the +180°C fraction

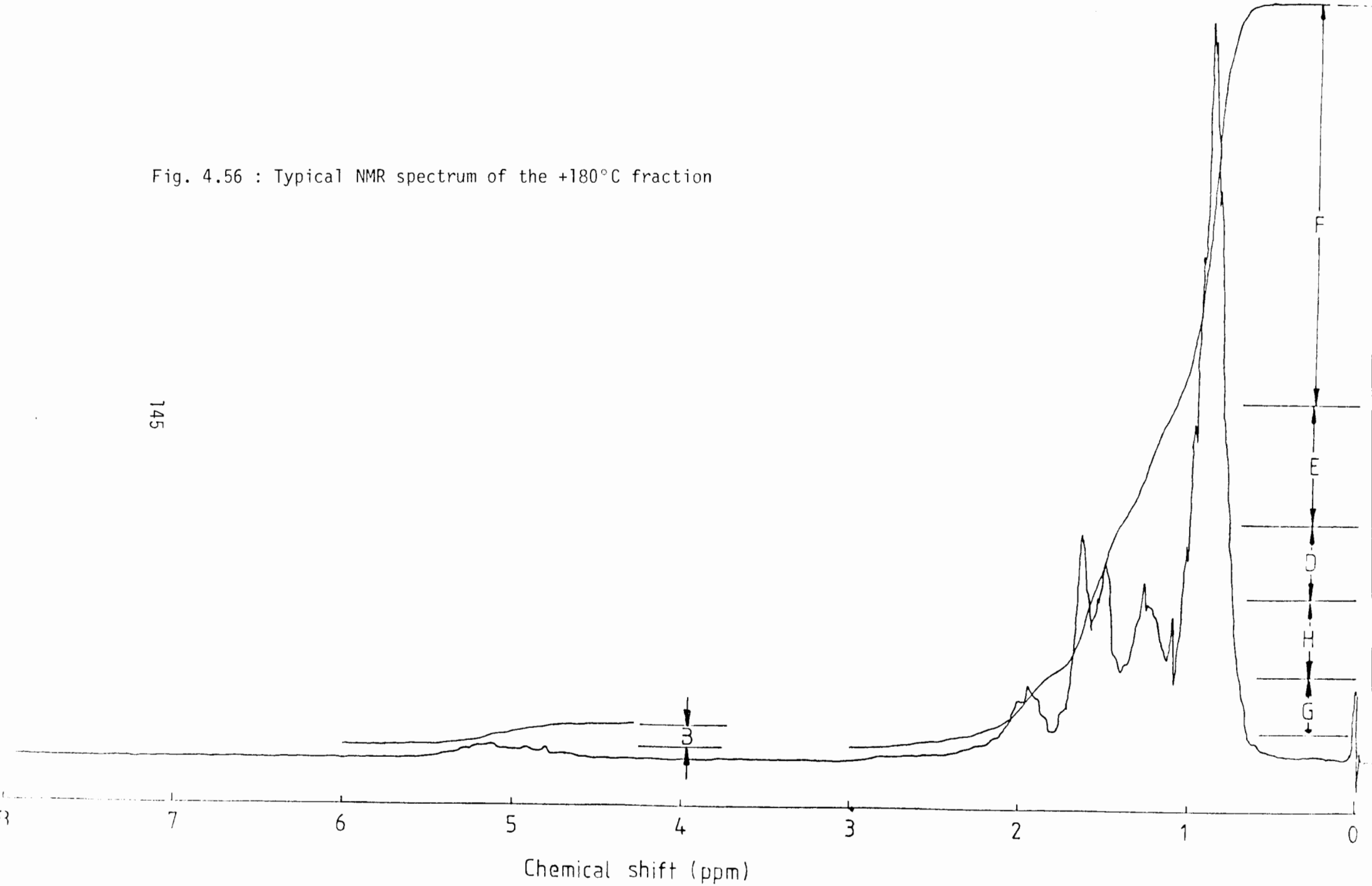

Fraction	Reaction temp °C	WHSV	Composition (vol %)			Ratio		
			Aromatics	Olefins	Saturates	H/C	CH_3/CH_2	Terminal C/chain C
-180°C	100	0.85	0.00	52.4	47.6	1.49	1.77	1.20
-180°C	100	2.50	0.00	62.7	37.3	1.48	1.60	1.11
-180°C	100	1.70	0.00	60.6	39.4	1.46	1.64	1.14
-180°C	130	1.70	0.00	58.3	42.7	1.52	1.94	1.30
-180°C	150	1.70	0.00	57.0	43.0	1.58	1.79	1.35
+180°C	100	0.85	0.00	-	-	1.64	1.83	1.49
+180°C	100	2.50	0.00	-	-	1.63	1.44	1.13
+180°C	100	1.70	0.00	-	-	1.63	1.70	1.37
+180°C	130	1.70	0.00	-	-	1.65	2.00	1.65
+180°C	150	1.70	0.00	-	-	1.64	2.06	1.69

Table 4.5 : Results of N.M.R. spectra

The degree of branching seems to be the most strongly affected by the reaction conditions. For the petrol fraction the CH_3/CH_2 ratio as well as the terminal C/chain C ratio increases with increasing WHSV and increasing reaction temperature. In particular the CH_3/CH_2 ratio for the run carried out at 130°C is very high. However the terminal C/chain C ratio follows the pattern indicated.

The CH_3/CH_2 ratio and terminal C/chain C ratio vary similarly for the petrol and diesel fraction.

4.17 Mass Spectroscopy

A typical gas chromatogram of the G.C.-mass spectrometer unit of the liquid product is shown in Fig. 4.57. The molecular weights of the compounds responsible for the peaks were determined by mass spectroscopy and are assigned in the figure. As a comparison to this a gas chromatogram of the liquid product obtained from the G.C. used for liquid product composition analysis is shown in Fig. 4.58. The grouping of the product into various polymers is also shown on both figures.

To get an estimate of the sensitivity of the mass spectrometer, two sample solutions were prepared. Apart from the typical liquid product, one sample contained 0.3% and the other 1% by volume of n-octane and n-dodecane, respectively. These standards were compared to the intensity of the only other C_8 and C_{12} detectable saturates in the sample. These occurred at a retention index of 44 and 52 for the octanes and at 149 for the dodecanes. n-Octane had a retention index of 60-61 and n-dodecane of 148-149. The only other detectable saturates were a small peak of saturated C_7 and C_{11}. These saturates were not separated by the G.C. from the unsaturates and therefore the peaks were superimposed. The intensity index used was the total ion current (T.I.C.). Table 4.6 shows the analysis of these samples. It indicates that the mass spectrometer still monitored the peaks at these intensities and that the concentration of saturates in the sample is less than that in the standards.

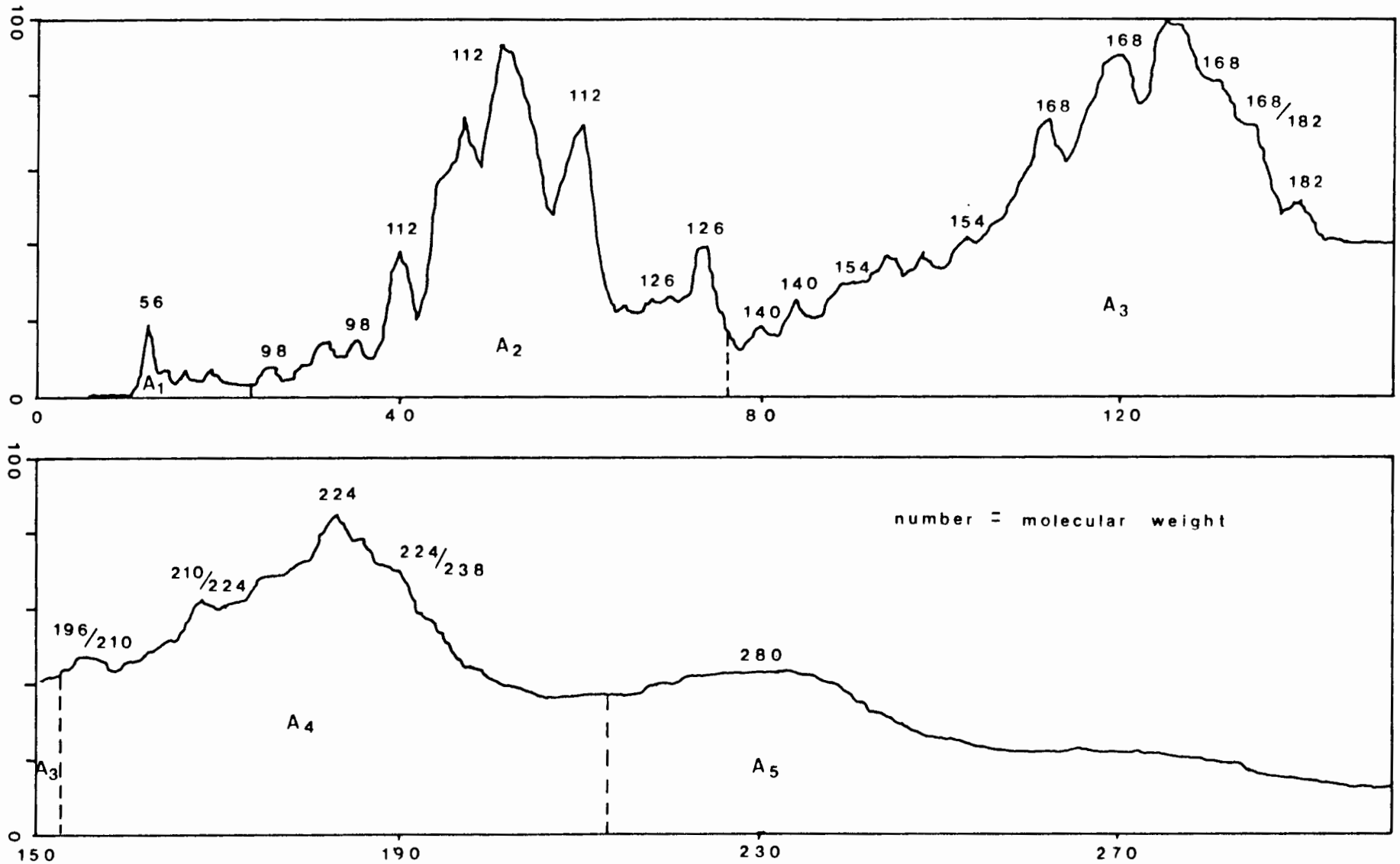

Fig. 4.57 : G.C. Spectrum of the G.C. - mass spectrometer unit of the liquid product

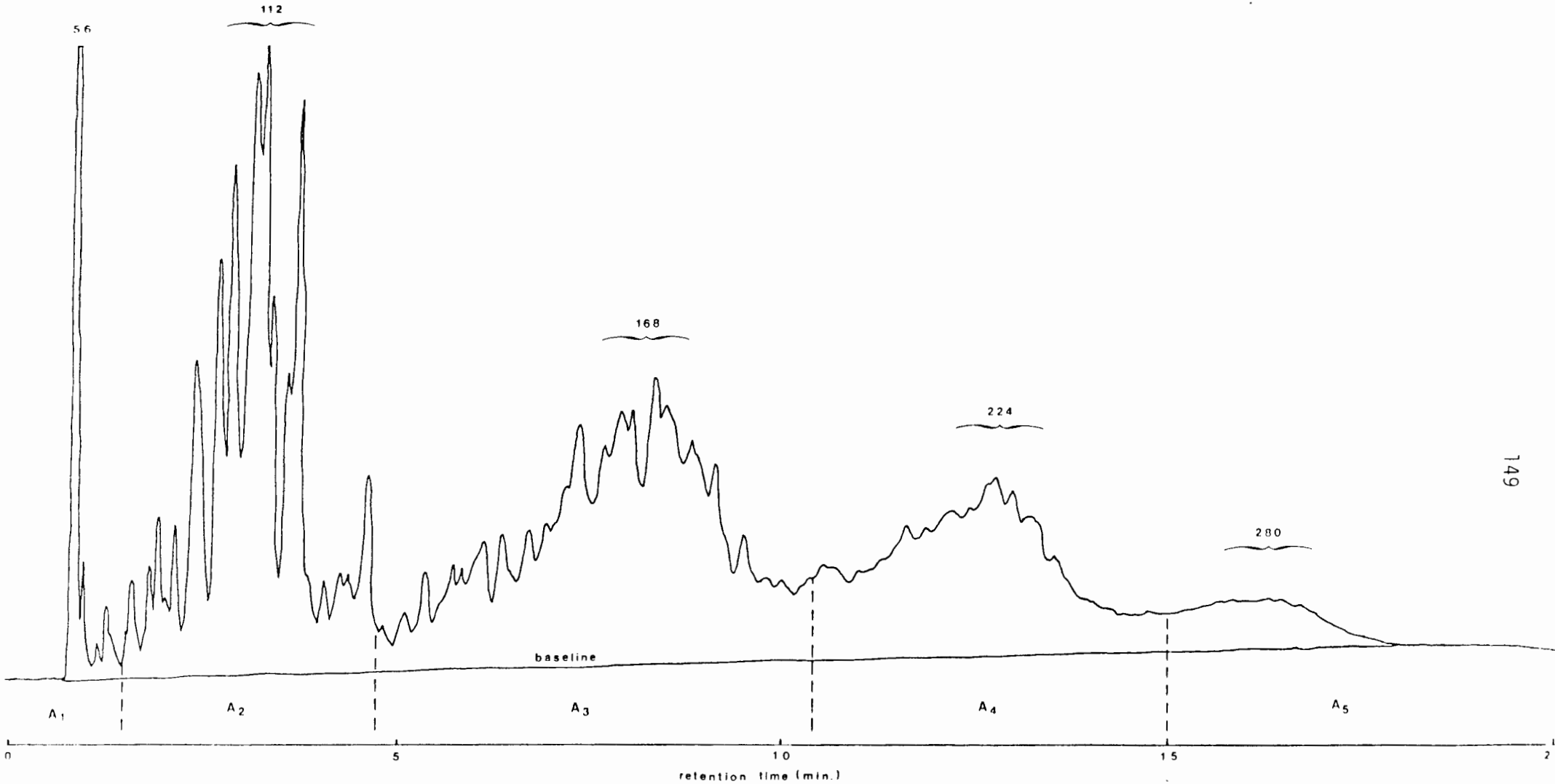

Fig. 4.58 : G.C. spectrum of the G.C. used for liquid product composition analysis

Sample	Retention Index	% T.I.C.
pure product	44	0.276
	52	0.109
	60	0
	61	0
	148	0
	149	0.133
product +	44	0.276
	52	0.111
0.33 vol % octane +	60	0.213
	61	0.230
0.33 vol % dodecane		
	148	0.406
	149	0.344
Product +	44	0.276
	52	0.105
1 vol % octane +	60	0.490
	61	0.504
1 vol % dodecane		
	148	0.730
	149	0.816

Table 4.6 : Sensitivity of mass spectrometer

4.18 Microanalysis

The samples tested were very volatile and this reduced the accuracy of the microanalysis. However the values obtained for hydrogen and carbon were between 99.5 and 100.5%. Thus the inaccuracy of the method was less than 0.5% and hence any oxygen which may have been present must have been less than 0.5%.

Table 4.7 shows the various compositions and the reaction conditions under which the samples were obtained.

WHSV (hr^{-1})	Reaction Temp. (°C)	Fraction Fraction	%H	%C
0.85	100	-180°C	14.2	85.8
		+180°C	14.0	86.0
1.73	100	-180°C	14.2	85.7
		+180°C	14.0	86.0
1.70	130	-180°C	14.2	85.8
		+180°C	14.0	86.0
1.70	150	-180°C	14.2	85.8
		+180°C	14.0	86.0

Table 4.7 : Results of microanalysis

4.19 D.W.C.

In determining the D.W.C., the mean of three readings was taken. The standard deviation in most cases was less than 3%. However, from batch to batch slight differences were observed. This was mainly due to the fact that the distilled water used for the analysis was not neutral. This also explains the slightly higher values obtained for the fresh resin than that quoted by the manufacturers.

Table 4.8 gives the D.W.C. of the three different ion exchange resins which were used in this work, before and after a run. Although the reaction time for all three runs was well over 40 hours (Fig. 4.5), only relatively low changes in capacity were observed.

Run no.	Resin	D.W.C.	
		Fresh	Used
06	Amberlyst 15	5.12	4.64
16	Amberlyst 1010	3.19	2.81
22	Duolite C26	5.01	4.86

Table 4.8 : D.W.C. of various ion exchange resin

Table 4.9 shows the effect of temperature on the D.W.C. The runs at 130°C and 150°C showed a much larger change in D.W.C. It is evident that the resin capacity is virtually completely restored upon regeneration for resins undergoing reactions at 100°C. However when regenerating the ion exchange resin which deactivated at 130°C and 150°C for cationic fouling, no change in capacity is observed, thus indicating that these sites have actually been destroyed.

Run no.	Remark	D.W.C.	
		Fresh	Used
06	Reaction temp: 100°C	5.12	4.64
19	Reaction temp: 130°C	4.98	3.29
21	Reaction temp: 150°C	4.92	3.69
09	Reg.run 06:Cationic fouling	4.95	4.44
10	Reg.run 06:Organic fouling	4.99	4.46
23	Reg.run 21:Cationic fouling	3.77	3.73
24	Reg.run 19: " fouling	3.36	3.50

Table 4.9 : D.W.C. of resins used at various temperatures and reactivation treatments

Table 4.10 shows the capacity of the various functionalized ion exchange resins, before and after a run. They also only show a relatively small drop over the whole run.

Run no.	% Functionalized	D.W.C.	
		Fresh	Used
26	100	5.01	4.86
28	96	4.84	3.71
25	89	4.46	3.98
36	82	4.14	3.81
37	59	2.93	2.14
27	37	1.87	1.13

Table 4.10 : D.W.C. of resins functionalized to various degrees

Table 4.11 shows the D.W.C. of cationic exchangers with phosphinic and phosphonic acid groups. Also shown is the capacity of the unfunctionalized matrix, indicating that it actually is almost inert.

Run No	Functionality	D.W.C.	
		Fresh	Used
-	raw beads	0.04	-
29	HPO_3-H^+	4.86	5.01
30	$PO_3^{2-}(H^+)_2$	9.33	7.15
38	HSO_3-H^+	5.12	3.37

Table 4.11 : D.W.C. of resins with various functional groups

4.20 A.S.T.M.

The results of bromine number tests are shown in Table 4.12 for the products obtained from various reaction conditions. Also shown in the table is the percentage olefinic content of the various samples. These calculations are based on the bromine reactive components in the product and the composition of the sample as obtained from the G.C. It is assumed that each hydrocarbon contains one unsaturated bond. It seems that the lighter fraction (-180°C) contains less olefins (between 43 and 69%) compared to the heavier fraction (+180°C)(between 62 and 83%).

Table 4.13 compares the R.O.N. values for various products obtained at different conditions. These values are seen to be relatively unaffected by the various reaction conditions and catalyst structures.

Table 4.14 gives the results of a full set of standard gasoline tests done on the -190°C fraction of the run described in section 4.13 and Table 4.15 those standard diesel tests for the +190°C fraction.

Reaction temp (°C)	WHSV (hr^{-1})	Bromine no.	% Unsaturation of sample	Fraction
100	0.85	47.94	68.9	-180°C
100	0.85	-	-	+180°C
100	1.73	40.84	59.7	-180°C
100	1.73	36.62	82.8	+180°C
130	"	-	-	-180°C
130	"	36.05	80.8	+180°C
150	"	28.71	43.1	-180°C
150	"	25.68	61.7	+180°C
105	1.03	48.6	71.4	-180°C

Table 4.12 : Bromine number tests

Significance	R.O.N. (M.O.N.)
Run time : Initial fraction	97.0
Middle fraction	97.3
Final fraction	97.0
Feed rate : WHSV = 0.85	97.0
WHSV = 1.73	97.0 (85.7)
WHSV = 2.53	98.0
Bead size : 300 - 500 micron	97.6
500 - 850 micron	97.7
1000 - 1180 micron	97.8
Regeneration : Cationic fouling	97.2
Organic fouling	97.3
Porosity : Amberlyst 15	97.7
Amberlyst 1010	98.0
Duolite C26	98.1
Reaction temp. : T = 100°C	97.7
T = 130°C	97.7
T = 150°C	97.1
Reaction pressure : p = 15 bar	97.7
p = 27 bar	96.0

Table 4.13 : Octane number of -180°C fraction

Automotive gasoline fuel tests (Contd)

Property	SABS specifications	Petrol fraction		Bayer process	
		unhydrogenated	hydrogenated	codimer	hydrogenated codimer
Sulphur content, % (m/m max	0.15	0.02		0.0004	0.0001
Copper corrosion, (3hr @ 50°C) max	1	1A		-	-
Vapor/liquid ratio, max (@ 55°C and 760mmHg)	20	<1		-	-
Water tolerance	pass	-		-	-
Total acidity, mg/KOH/g	0.03	-		-	-

Table 4.14 : Results of standard petrol tests

Automotive gasoline fuel tests

Property	SABS specifications	Petrol fraction		Bayer process	
		unhydrogenated	hydrogenated	codimer	hydrogenated codimer
Distillation					
a) Temperature, °C, for					
i)10% (vol/vol) evap.	65 max	109		109	110.3 (5%)
ii)50% (vol/vol) evap.	77 - 115	120		114	111.3
iii)90% (vol/vol) evap.	185 max	159		119	113.6 (95%)
b) Final boiling pt. °C	215 max	189		-	-
c) Residue % (vol/vol) max	2.0	0.5%		-	-
Vapour pressure (Reid) kPa (max.)	75	16		-	-
R.O.N.	87,93,98	99.0		99.8	99.1
M.O.N.	-	87.0		89.2	101.0
Induction period min. (min.)	240	90 >240**		> 480*	>480
Lead content,g/ℓ max	0.836	-		-	-
Existing gum, mg/100mℓ max	4	0.2		1	1
Potential gum,mg/100mℓ	4	1.2		-	-

* inhibited by 40mg/ℓ Kerobit bpd
** inhibited by ethyl 733

Table 4.14 : Results of standard petrol tests

Property	SABS Specifications		
	minimum	maximum	Diesel fraction
Distillation temp for			
Initial boiling point			
90%(vol/vol) recovery	-	357°C	
final boiling point	-	385°C	
Residue,%(vol/vol)			
Flash point	55°C	-	
Sulphur content, % m/m	-	0.5	
Cetane number	45		35
Copper corrosion at 100°C (3 hr)	-	1	
Cold filter plugging point, °C			
Carbon residue on 10% distillation residue % (m/m)	-	0.2	
Ash content, % (m/m)	-	0.01	
Water content,%(vol/vol)	-	0.05	
Sediment content, % (m/m)	-	0.01	
Viscosity @ 37.8°C, mm^2/s	1.8	5.8	

Table 4.15 : Results of standard diesel fuel tests

In Table 4.14 the results of the analysis of the petrol fraction are compared to the SABS specifications and to those typical of the commercial oligomerization process. They are also compared with values obtained for the hydrogenated and unhydrogenated product. The results of the diesel fraction are compared only to the SABS specifications.

Fig. 4.59 compares a 100mℓ distillation of a 93 octane petrol with the -190°C fraction of the run described in section 4.13. The latter fraction has a much narrower boiling point range.

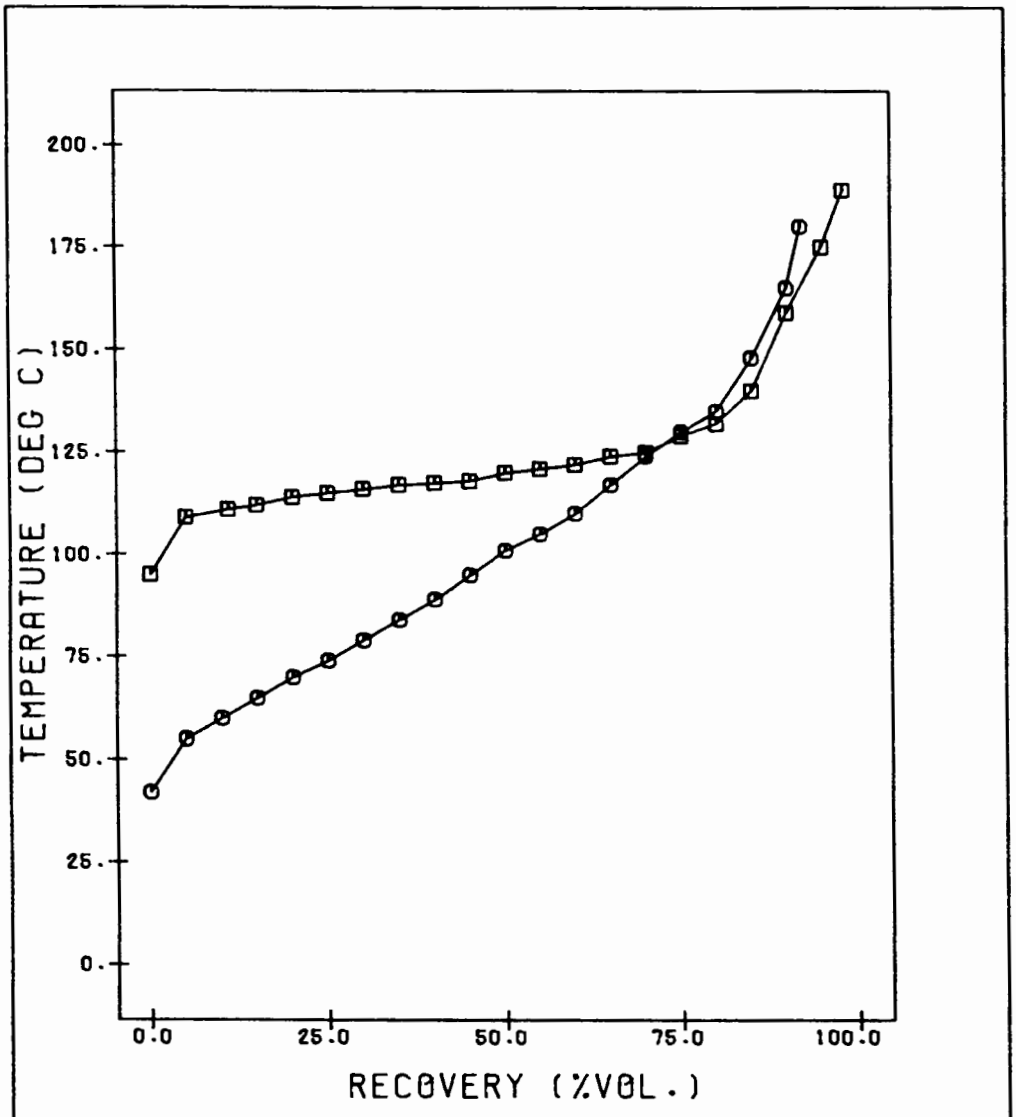

FIG.4.59 VOLATILITY DATA
93 OCTANE PETROL AND -190 DEG C FRACTION

□=-190 DEG C FRACTION
○=93 OCTANE PETROL

5. DISCUSSION

The reproducibility study (section 4.1) indicated that the experimental results obtained in this study are reliable. Once steady state was reached, both the selectivity and the L.P.R. showed little variation between runs at similar reaction conditions. The mass balance was within 5%.

The liquid product composition was expressed as integral polymeric groupings of C_4 hydrocarbons as shown in Figs. 4.57 and 4.58. Minor inaccuracies arose owing to polymers of intermediate carbon number. These were olefins (Fig. 4.57). They were probably formed as a result of true polymerization of the small quantities of propylene and pentene in the feed.

In most of the experiments the reactants were in the gas phase (Fig. 7.2). The product obtained, however, was in the liquid phase. Thus effectively a three phase system was studied.

Of particular interest in this study were the resins Amberlyst 15 and Amberlyst 1010, since comprehensive information on the physical characteristics of these resins was readily available. (Table 3.1). They had wide differences in physical properties and were produced by the same manufacturers, and hence one can assume that similar methods were used in their syntheses. Amberlyst 15 had most of its pores between 100 and 300Å, and a small internal surface area. On the other hand, Amberlyst 1010 had the major fraction of its pores between 50 and 100Å, and a larger internal surface area (Fig. 4.4). Both resins had the same volume of pores of size bigger than 35Å. Further, the run using a gelular resin showed that the active sites within the gelular phase of a resin bead were inaccessible for reactant molecules. In the dehydrated state, the hydrocarbon polymer chains of a gelular resin are as close as atomic forces allow and they separate to form micropores of diameters between 5 and 20Å only on the introduction of a swelling medium. Since the reactant molecules are non-polar, they are not effective as swelling agents,

severe diffusional limitations are expected in gelular resins. Therefore the acid sites within the gelular phase of the macro-reticular resins are not likely to take part in the reaction. This implies that although Amberlyst 15 had the larger total capacity, Amberlyst 1010 with its larger internal surface area had the larger numbers of accessible acid sites. Thus Amberlyst 1010 should show a larger L.P.R. if the latter is determined solely by the number of accessible acid sites. This, however, was not observed (Fig. 4.5). The only difference between the two cases, and thus the probable explanation for the higher L.P.R. of Amberlyst 15, is its larger pore sizes. Therefore macropore diffusional resistances are significant and are reduced when using resins with large pore sizes. Duolite C26 had a similar pore size distribution as Amberlyst 15 but had a lower total pore volume than both of the Amberlyst resins. Since it had a L.P.R. intermediate to the two Amberlyst resins, it follows that larger pore size is more important than pore volume. However, as the pore volume increased, so did the L.P.R. A further conclusion from the run using a gelular resin is that the external acid sites make a negligible contribution to the reaction being studied.

To confirm the above postulate of diffusional limitations, the effect of the catalyst bead size on the L.P.R. was studied, using Amberlyst 15 which had the largest mean pore size of the three resins. Since smaller beads have a larger ratio of surface area to volume (3/r), i.e. a reduced significance of the acid sites within the bead volume, and in addition require shorter diffusion times to the core of the bead under similar conditions, the relative effect of diffusional limitations is reduced.

Although a limited range of bead sizes of Amberlyst 15 was investigated, an increase in L.P.R. with decreasing bead size was nonetheless observed (Fig. 4.8), thereby indicating that transport limitations, either by liquid film diffusion or by matrix diffusion, are significant. No detectable changes in selectivity were observed in this size range.

The increased L.P.R. with decreasing catalyst bead size agrees with the observation made by Scharfe (41). A commercial butene oligomerization process utilizes as catalyst an ion exchange powder of less than 50 μm in diameter (36).

To determine the relative rates between liquid film and macropore diffusion, the effect of the acid site concentration was examined. The L.P.R. was dependent on the degree of functionalization (Fig. 4.11) and therefore it follows that liquid film diffusional resistance is not the controlling step in the reaction mechanism. Furthermore no linear proportionality was observed and the decrease in L.P.R. was much greater than the decrease in the number of acid sites. This implies either that more than one acid site is occupied by a reaction intermediate; or that there exist more than one type of acid site. The former proposal was rejected by Haag, who showed that the reaction follows a Langmuir-Rideal mechanism (24). This mechanism is based on a reaction between an adsorbed molecule and a free molecule (section 1.2.2.2.2). Furthermore Uematsu has already found by n-butalamine titrations an apparent heterogeneity in acid strength among the functional groups of sulphonic acid resins (26). He attributed this difference in acid strength to an inhomogeneous structure of the substrate resin and an induced heterogeneity by interactions of various groups.

The acid strength of the functional group of ion exchange resin is also important. This is evident from the fact that Duolite C26, functionalized with phosphonic acid groups to the same extent as in the case of sulphonic acid groups,showed no activity. The phosphonic acid strength as indicated by Hammett indicators was only slightly lower than that of sulphonic acid groups (Table 4.2). Therefore, it seems that a minimum acid strength of pKa= -2.4 is required to catalyse the reaction. When a similar study was carried out using a phosphinic acid group which has a dual functionality and an acid strength

range comparable to that of phosphonic acid, also no activity was observed. Previous work has shown that strong basic ion exchange resins are also ineffective in catalysing the reaction (94).

A comprehensive study of the effect of varying the reaction conditions was carried out. First, the effect of changing the WHSV was examined. As the WHSV was increased a drop in the overall conversion of the feed was observed. This may be due to a reduction in the space time of reactant molecules in the catalyst bed. At the same time, an increased WHSV causes an increased linear velocity of the feed molecules. This in turn reduces the liquid film around the bead particles and thus reduces any liquid film diffusional resistances. This phenomenon may be a reason for the observed increase in L.P.R. at increased WHSV. It seems, however, that the effect of reduced liquid film resistance is less significant than that of the reduced space time, since an overall drop in conversion was observed. Furthermore, an increased WHSV causes an increased reactant to catalyst ratio per unit time. As a result, more reactant molecules diffuse into the catalyst bead interior and make contact with active sites. This will cause an increased L.P.R. only if free active sites are available and if the rate is not controlled by the chemical reaction. Since L.P.R. increased (Fig. 4.12), not all acid sites were utilized and hence transportation limitations are more significant than rates of chemical reaction. Therefore high L.P.R. and optimum acid site utilization require large WHSV's. On the other hand, low WHSV's resulted in high conversion. Similarly, when co-feeding dimers, L.P.R. increased with decreasing recycle ratio. In decreasing the recycle ratio, the dimer feed rate was maintained constant while increasing the monomer feed rate. This results in an increase in WHSV of the monomer. However, for the equivalent monomer WHSV, the L.P.R. was greater in the absence of recycle (Fig. 4.26). It should be noted that there is negligible difference in the total volumetric flow rate in both the presence and the absence of recycle.

The co-feeding of the dimer causes an increase in liquid film around the bead particles. The effect of this increased film thickness is greater than that of the reduction of the space time as indicated by the fact that the monomer conversions were unaffected by the change in WHSV. In the absence of recycle, a strong dependence of monomer conversion on WHSV was observed (Fig. 4.27). At very high WHSV's the two situations, viz. with and without recycle, are comparable, since even in the absence of recycle a thick liquid film is formed as a result of high L.P.R. The increased liquid film has an additional effect of reducing the rate of monomer diffusion to the active sites, thereby lowering monomer concentrations at these sites. This increases the possibility of reaction between an adsorbed molecule and a free dimer. This is confirmed by the larger fraction of trimers formed at the expense of dimers in the case of recycle (Fig. 4.28).

An increase in reaction pressure thermodynamically favours the production of longer chain length polymers. At a reaction temperature of 100°C, the monomer is in the liquid phase at 2.7 MPa, and is in the gas phase at 1.5 MPa. The difference in L.P.R. for these two cases is shown in Fig. 4.29. Although both runs had the same initial L.P.R., the run with the monomer in the liquid phase showed a much faster rate of deactivation. The slightly longer chain length product for this run is probably due to its higher operating pressure.

The largest component of the liquid film surrounding the catalyst bead was the dimer which constituted the largest fraction of the product. To reduce the liquid film resistance, the dimer has to be in the gas phase. The only way this was possible was to increase the reaction temperature at atmospheric pressure. Since straight chain dimers boil at approximately 120°C, and branched dimers at 105°C (Appendix C), it was decided to carry out runs at reaction temperatures of 90°C,i.e. dimer in liquid phase, and 130 and 160°C, i.e. dimer in gas phase. A similar increase in initial L.P.R. was

observed with each incremental change in reaction temperature (Fig. 4.32). This means that the Arrhenius effect of temperature is more significant than that of reducing the liquid film by increasing temperature.

The product spectrum showed that the polymer chainlength decreased as the reaction temperature was changed from 90°C to 130°C, and then increased at higher reaction temperatures. Thermodynamically, the initial decrease in chainlength is to be expected but not the subsequent increase at the reaction temperature of 160°C. One explanation for this phenomenon is that at 90°C the liquid film retards the diffusion of monomer to the active sites, and thus increases the probability of the dimer reacting. The fast deactivation of the run at a reaction temperature of 160°C is due to thermal degradation of the catalyst. The effect of reaction temperature at 1.5 MPa is shown in Section 4.11. Over the range tested, i.e. from 100° to 150°C, the L.P.R. increased with increasing reaction temperature as is expected from kinetic considerations. Since the reaction is exothermic, this indicates that the equilibrium has not been attained. Moreover, as temperature was increased, longer chainlength polymers were formed, contrary to thermodynamic predictions. Hence at the temperatures being investigated, kinetic parameters such as activation energy and pore and liquid film diffusion coefficients are of greater importance.

Deactivation of ion exchange resin may either be due to poisoning, where the effectiveness of ion exchange material is reduced due to the irreversible adsorption of certain ionic species, or due to fouling, where the effectiveness of ion exchange resin is reduced due to accumulation of insoluble material on the surface and in the interior of the ion exchange particles. The side reactions causing deactivation can either be parallel to the main reaction, in which case deactivation is greatest at the top of the bed, or consecutive to the main reaction, in which case deactivation profile peaks at the bottom of the bed.

A study of the temperature profile within a catalyst bed showed that a reaction front moved down the bed. This suggests parallel fouling and most likely some component in the feed or an intermediate product deactivates the catalyst.

In section 4.12 the results of regenerating catalysts are given. In both cases, viz. regeneration for cationic fouling and organic fouling, the catalyst regained its initial activity. The slight discrepancies relative to the L.P.R. of the fresh catalyst are due to the lower WHSV's. Table 4.9 shows that the regeneration procedure resulted in the catalyst recovering its total initial acidity. The small difference between the D.W.C.'s is possibly due to the thermal destruction of some acid sites, which may have taken place during the start-up period of the run. Further, the results indicated that the product spectrum obtained from the regenerated runs was not significantly different from that obtained from the fresh catalyst.

The two methods of regeneration are principally the same, except that in the case of organically fouled resin more severe conditions of temperature, concentrations and treatment time were used, and these conditions would also regenerate cationically fouled resin. It may therefore be concluded that the major cause of deactivation is cationic fouling.

The catalyst from the two high temperature runs (130 and 160°C) was treated for cationic fouling. The L.P.R. of these two regenerated resins was compared to the L.P.R. of the resin treated for cationic fouling subsequent to reaction at 100°C (Fig. 4.45). The former two regenerated resins showed a significantly poorer performance than the latter.

This indicates that high reaction temperatures largely destroy the resin functionality. Confirmation for this was also obtained from total acidity tests which showed no effective difference in D.W.C. between used and regenerated resins (Table 4.9). The colour of the used resin was black, compared to the usual dark grey colour of resins used at moderate conditions.

A very important aspect of the selectivity can be explained on the basis of Fig. 1.7. Although this figure is specific to isobutylene, similar concentration-time profiles for the other reactants would be expected. The x-co-ordinate represents reaction time and this is equivalent to space time for a fixed-bed integral reactor. As mentioned previously, the figure shows that the monomer is selectively adsorbed onto the catalyst. This means that the reaction takes place between an adsorbed monomer and a free molecule, which is either another monomer or an already formed dimer, i.e. the product consists of mainly dimers with a few trimers. It also means that longer chain length polymers are formed only once all reactive monomers are converted and the catalyst starts to adsorb dimers. Therefore it is expected that a high conversion of monomer will produce a high boiling point product. The above phenomenon was observed in the present study. Firstly, during a 140 hour run (Section 4.13), it was observed that as time progressed, the conversion and L.P.R. decreased, and simultaneously the product distribution shifted towards lighter fractions (Fig. 4.53). Initially an almost complete conversion of unsaturated monomers occurred (Fig. 4.49). However, as the catalyst deactivated, the utilization of cis- and trans-2-butenes decreased and they began to compete for the active sites with the longer chain-length olefins further down the bed. This may have caused the decrease in the longer chain-length product fraction. The temperature of the reaction front decreased with time (Section 4.14) as did the L.P.R. and the conversion of monomer.

At the same time, the product spectrum shifted towards lighter fractions. This finding is consistent with the mechanism proposed by Haag for isobutylene oligomerization. Moreover, as time progressed, the effective catalyst bed depth, and hence space time, decreased, further causing the product spectrum to shift towards shorter polymers.

Secondly, a similar explanation can be offered for the shift in the product spectrum with decreasing WHSV. For example, the two runs carried out at a WHSV of 0.85 and 1.7 respectively, using Amberlyst 15 as catalyst showed that the run with a higher conversion, i.e. the WHSV of 0.85, yielded longer chain length products, while the run with the WHSV of 1.7 gave a lower conversion and lighter fractions.

The greater utilization of cis- and trans-2-butene demonstrated that the overall monomer conversion was nearly complete for the former run.

Both of the above examples illustrate that a high conversion level, and not a high L.P.R., ensures the shift to heavier fractions. This trend is further confirmed by the results of the two high temperature runs treated in Section 4.11. For these two runs, a sharp increase in the amount of cis- and trans-2-butene present in the tail gas was observed when the reaction front reached the bottom of the catalyst bed, and this was accompanied by a shift to lighter fractions in the product spectrum.

In studying the effect of degree of functionalization and regeneration of thermally degraded resins, it was found that at low conversions longer chain length products were formed. These conditions for low conversions represented higher ratios of monomer to active sites. Hence it may be postulated that there exists a greater potential for free monomer-adsorbed dimer interaction, as opposed to the case of low ratios of monomer to active sites which would result in greater monomer-active site interactions. Similar observations were made when using catalyst with higher pore diffusional resistances. This may be due to the difficulty of the dimer formed at the active site to diffuse out of the pore as well as the monomer to diffuse into the pore. This may increase the possibility of greater dimer-monomer interactions at active sites located in the pores.

The water content of the feed in this study was approximately 0.6%. This did not appear to have a significant inhibition effect on the fractional conversion. This observation is consistent with that of Rottmayer et al (63) who found in batch reactor studies that at water concentrations of less than 1%, conversions were 81% when studying iosbutene, and 56% in the case of 1-butene. Moreover in all runs the feed was dried over 3Å molecular sieves which tend to decrease the water concentration even further. The fact that this had no effect on conversions confirmed that the water content present in this feed is not significant. With respect to water content of the catalyst it is proposed that the pretreatment procedures used, were sufficiently adequate to remove most of the water absorbed in the matrix.

The degree of branching of the liquid product characterized by two ratios, CH_3/CH_2 and terminal C/chain C, was investigated by means of N.M.R. analysis. The CH_3/CH_2 ratio does not take the tertiary carbon $(R\text{-}\overset{R}{\underset{|}{C}}H\text{-}R)$ and vinylic carbons $(-C=CH-)$ into account and thus overestimates the degree of branching although, to be exact, the tertiary carbon should not be defined as a chain carbon. The second ratio, namely terminalC/chainC, is believed to reflect more accurately the degree of branching since it does not count the tertiary carbon. One deficiency of this approach, however, is that it does not distinguish between the $C = CH_2$ and $C = CH\text{-}R$ groups, thereby increasing the ratio slightly.

The ratios obtained were generally fairly large, indicating a high degree of branching in accordance with a carbonium ion mechanism. The carbonium ion formed is generally branched, because alkyl groups stabilize the positive charge. It should be recalled that branching reduces the quality of diesel and hence its cetane number. In this study, however, the above ratios for the high boiling point fraction were significantly larger than those for the low boiling point fraction. On the other hand, since branching increases the octane rating, petrol fractions of high quality were obtained from the same reaction products.

Lastly, the degree of branching was seen to increase with decreasing WHSV and with increasing temperature. However, these reaction conditions also produced longer polymers within the diesel and petrol fraction and hence it is expected to observe an increase in the degree of branching.

An attempt was made to identify the types of hydrocarbons present in the product stream. N.M.R. showed that no aromatic components were formed, as expected mechanistically. Similar findings were also reported by Scharfe (36). The various tests conducted to determine the presence of saturates gave conflicting evidence.

In the final run a G.C. analysis of the utilization of the gas components was performed (section 4.13). It showed a fairly steady conversion of about 40% by mass of the saturates in the gas stream. A simple mass balance together with an analysis of dissolved gases in the liquid product eliminated the possibility that these saturates dissolved as gases in the liquid product. Bromine number tests also showed the presence of saturates in the liquid product (Table 4.12).

One explanation which accounts for the conversion is that alkylation has taken place. n-Butane showed the highest fractional conversion, followed by isobutane and propane. The estent of alkylation appeared to increase with decreasing WHSV (Fig. 4.24) and increasing reaction temperature (Fig. 4.41). These trends were verified by N.M.R. analyses (see Table 4.5).

On the other hand the hydrogen to carbon ratio obtained from the microanalysis was very close to that of pure olefin (Table 4.7). Furthermore, no major peaks due to saturates could be identified by the mass spectrometer. Since this apparatus has a sufficient sensitivity to detect 0.33 vol % standard solutions, any saturates present must be present in lower concentrations. Those few peaks identified as saturates could not account for the mass conversion as indicated by the G.C. tail gas analysis.

The results of the standard fuel tests conducted on the petrol fraction indicated that the latter was of high quality having a R.O.N. of 99 and a M.O.N. of $\pm$ 87 because the fraction did not contain any dissolved gases and because the product consisted primarily of polymers of C_4-olefins . It showed a relatively low Reid vapour pressure and vapour/liquid ratio as well as high temperatures for 10% and 50% evaporation during distillation. The fraction had a relatively low volatility compared to a standard 93 R.O.N. petrol fraction, as can be seen from Fig 4.59. The volatility range of the experimentally obtained product can be increased by using a feed mixture of various carbon numbers.

The quality of the product, however, compares well with that produced in the commercial oligomerization process. Generally the octane number did not vary much with changing reaction conditions and catalyst structure (Table 4.13).

The diesel fraction was of poorer quality having a cetane number of only 35 owing to the high degree of branching as discussed above. Therefore this fraction is suitable only as a blending stock for high cetane number fuels. The cetane number of 35 is the same as that of the product from the phosphoric acid polymerization process. The diesel fraction was also of a relatively high volatility compared to typical diesel, as the former contained mainly trimers and tetramers and few higher polymers.

From the foregoing discussion it is evident that for the reaction being studied ion exchange resins have a very high L.P.R. This is best illustrated by the data of the run described in Sec 4.13. 74.2% by mass of feed, which contains 18% inerts, was converted over 144 hours. This means that 90.5% of the reactive feed was converted to liquid products. Similarly ion exchange resins showed a relatively slow rate of deactivation.

In the run referred to above a drop in L.P.R. of only 24,3% occurred over 144 hours.

One of the features of ion exchange resins is their selectivity towards producing lower chain length polymers.

The single most important parameter affecting selectivity was found to be the reaction temperature. This is best illustrated by the results of the bulk distillation. The weight fraction boiling above 180°C increased from 19.7% to 40.3% to 55.8% as the reaction temperature increased from 100°C to 130°C and 150°C. At the same time this fraction showed a tendency towards higher boiling point temperature ranges.

In using this catalyst to synthesize a typical diesel fraction, the thermal stability needs to be improved.

Research being done in this field is outlined in Sec 1.3.3.4. The possibility of a selective polymerization using a series of reactors should also be mentioned. Initially milder conditions could cause for example the polymerization of isobutylene to tetramers using a modified ion exchange resin (42), rather than having codimers formed and alkylation occurring, both of which reactions produce a less reactive dimer than does di-isobutylene. The same may hold for the

polymerization of n-butanes (37). Recycle and the use of superacid ion exchange resin could then be used to further upgrade the product.

During experimentation and data analysis a few disadvantages of the reactor system used became apparent. These may be specific to the catalyst used. They had an adverse effect on catalyst utilization, activity and selectivity. The temperature control of the reactor was inadequate. This was most apparent during start-up, when a selective cooling of various sections of the bed was required to counteract the formation of hotspots. Adequate control of this phenomenon, however, would be difficult.

It was also observed that the catalyst bed was non-isothermal. This again can be seen from the temperature profile (Sec 4.14), which showed a reaction front moving down the bed. In choosing reaction conditions this reaction front had to be taken into account to prevent the thermal destruction of acid sites and thereby ensure the regenerability of the resin. This therefore imposed a further restriction on the reaction temperature in addition to the already low upper temperature limit of ion exchange resin.

Since the reaction temperature is one of the most important factors affecting catalyst activity and selectivity, this temperature limitation presents a serious shortcoming of the reactor system. The temperature of the reaction front continuously decreased (Sec 4.14). This was a direct result of the decreasing catalyst activity and this caused an increase in the amount of unsaturates in the gaseous product. Moreover deactivation occurred as shown by the movement of the reaction front, from the top of the bed downwards (Sec.4.14), causing a decrease in the effective bed depth and therefore a lower monomer conversion. The implications of an increasing amount of unreacted

monomers on the selectivity have been discussed before. Furthermore, this unsteady catalyst L.P.R. would cause problems in a downstream upgrading of the products in an industrial plant due to decreasing liquid flowrate and changing product spectrum. Generally this is prevented by oversizing the reactor and by increasing the reaction temperature. The latter, however, is very restricted due to the upper temperature limit of resins.

In fixed bed reactors it is difficult to reduce the liquid film around the bead particles. From the discussion above, however, it has become apparent that there are film diffusional limitations which could, when overcome, increase the activity of the catalyst.

Decreasing bead size caused an increase in the L.P.R. However, a certain bead size is required in fixed bed reactors to prevent catalyst entrainment and to reduce pressure drop.

A possible reactor system which avoids the above disadvantages of the fixed bed reactor is the internal circulation reactor used for butane oligomerization in West Germany (36). The reactor system is shown in Fig. 1.13. It is an isothermal reactor and therefore allows operation at the upper temperature limit of ion exchange resins.

Since the only temperature increases are in the bulk liquid, these are easier to control and hence hotspots are not formed. Agitation ensures uniform temperatures throughout the reactor, allows reduction in liquid film diffusional limitations, and maintains the catalyst in suspension throughout the reactor. Bead sizes of much smaller diameter can be used. The reactor effluent is separated in a centrifuge, the underflow being returned to the reactor. Catalyst activity is maintained constant by adding a small amount of fresh catalyst while removing a similar quantity of spent catalyst.

The limitations of the internal circulation reactor are that the reactors are in the liquid phase and this has been found to cause faster deactivation (Sec. 4.9). Secondly it must be ensured that a low monomer concentration is maintained to prevent selective adsorption onto the acid sites.

An additional disadvantage of the use of ion exchange resins is their relative high costs compared to the catalyst of choice, phosphoric acid. Since ion exchange resins are, however, continuously regenerable, their costs are generally regarded as capital costs.

In conclusion,

(i) Ion exchange resins have a high L.P.R., a slow rate of deactivation and tend to selectively produce low chain length polymers.

(ii) The overall rate is influenced by macropore diffusion rates, although experimental results indicate that rates of liquid film diffusion and of chemical reaction cannot be neglected.

(iii) The catalyst structure influences mainly the L.P.R., causing the latter to increase with increasing macroporosity, increasing degree of functionalization and decreasing catalyst bead size. A minimum acid strength of $pk_A = -2.4$ is also required.

(iv) The reaction conditions influence L.P.R. and selectivity. The L.P.R. increases with increasing reaction temperature and increasing W.H.S.V. A tendency towards longer chain length products is observed with increasing reaction temperature and with reaction conditions which result in the complete conversion of monomers.

(v) Recycling liquid product results in reduced L.P.R., most probably due to increased liquid film diffusional resistances, and the production of larger fractions of trimers at the expense of dimers.

(vi) Ion exchange resins are regenerable when used at moderate reaction temperatures. Deactivation, which is parallel to the main reaction, is caused by cationic fouling. High temperatures cause thermal degradation of the active sites.

(vii) The liquid product is highly branched, resulting in high quality petrol and low quality diesel.

(viii) Some disadvantages of the reaction system used include inadequate temperature control, deactivation of catalyst bed and restrictions on agitation and catalyst bead sizes.

6. BIBLIOGRAPHY

1. Dutkuwicz, R K, Energy 1980 - An Energy Policy Discussion Document, The Energy Research Institute - U C T, February 1980.

2. Jager, B, Fischer Tropsch Synthesis, Paper delivered at Springs School in Coal Processing, September 1978.

3. Hoogendoorn, J C, The Sasol Story, Sasol, 1974.

4. Aalund, L R, Oil & Gas Journal, Technology, 71-77, April 1983.

5. Helfferich, F, Ion Exchange, McGraw-Hill, New York, 1962.

6. Pitochelli, A R, Ion Exchange Catalysis and Matrix Effects, Rohm and Haas Company, 1973.

7. Amberlite Ion Exchange Resins Laboratory Guide, Rohm and Haas Company, Philadelphia.

8. Chemical Processing by Ion Exchange, Rohm and Haas Company, Philadelphia.

9. Kunin, R, Helpful hints in Ion Exchange Technology, Rohm and Haas Company, Philadelphia, September 1981.

10. Amberlyst 15 - Synthetic resin catalyst, Technical Bulletin - Fluid Process Chemicals, Rohm and Haas Company, Philadelphia December 1980.

11. Ion Exchange in Non-Aqueous Media with Amberlyst Resins, Technical Bulletin - Fluid Process Chemicals, Rohm and Haas Company, Philadelphia, August 1979.

12. Cation Exchange Resin for Heterogeneous Catalysis. Selection - Description - Application, Technical Information, Bayer A G, Leverkusen.

13. Ion Exchange Resins as Catalysts, Technical Information, Bayer A G, Leverkusen.

14. Arnold, K H, Use of Cation Exchange Resins as Catalysts Illustrated by Examples from Petrochemistry, Bayer A G, Leverkusen, 1980.

15. Gates B C, Rodriquez W J, J of Catalysis, 31, 27, 1973.

16. Kunin, R, Ion Exchange Resin, Robert E Krieger Publishing Company, New York, 1972.

17. Schmerling L, Ipatieff V N, The Mechanism of the Polymerization of Alkenes, in Advances in Catalysis and related studies, Vol II, Academic Press Inc Publishers, New York, 1950.

18. Ublad A G, Mills G A, Heinemann H, Polymerization of Olefins in Emmett, Catalysis, Vol 5 New York, 1958.

19. Whitemore F C, Mechanism of the Polymerization of Olefins by Acid Catalysts, Industrial and Engineering Chemistry, Jan 1934.

20. Voge H H, May N C, J Am Chem Soc, 68, 550, 1946.

21. Turkewich J, Smith R V, J Chem Phys, 16, 466, 1948.

22. Hay R G, Coull J, Emmett P H, Ind Eng Chem, 71, 2809, 1949.

23. Haag W O, Pines H, J Am Chem Soc, 82, 2488, 1960

24. Haag W O, Chemical Engineering Progress - Symposium Series, Oligomerization of isobutylene on cation exchange resin, Vol 63, No 73, 140-147, 1967.

25. Gates B C, Johanson L N, Am Inst Chem Eng J, 17, 981, 1971.

26. Uematsu T, Bulletin of the Chemical Society of Japan, 45, 3329-3333, 1972.

27. Smith J M, van Ness H G, Introduction to Chemical Engineering Thermodynamics, 3rd edition, Tokyo, McGraw-Hill, 1975.

28. Atkins P W, Physical Chemistry, Oxford University Press, Oxford, 1978.

29. Tacke B, Süchting H, Landwirtsch Jahrb, 41, 717, 1911.

30. Rice F E, Osugi S, Soil Science, 5, 333, 1918.

31. Ruri A N, Dua A N, Soil Science, 46, 113, 1938.

32. I G Farbenindustrie, Ger Patent 882, 091, 1953.

33. Tabak, S A, Mobile olefins to gasoline and distillate process (MOGD), Natural Gas Utilization Symposium, Bangkok, 1984.

34. Nelson W L, Petroleum Refinery Engineering, 4th edition, McGraw-Hill, New York, 1958.

35. The Petroleum Handbook, 4th edition, Shell International Petroleum Company Limited, London, 1959.

36. Scharfe G, Hydrocarbon processing, April 1973.

37. United Kingdom Patent, 973555.

38. Krönig W, Scharfe G, Erdöl & Kohle - Erdgas-Petrochemie, 18, 852, 1965.

39. Gates B C, Albright R L et al, Chemtech, 46-53, 1983.

40. Krönig, W, Scharfe G, Erdöl & Kohle - Erdgas-Petrochemie, 19, 497-500, 1966.

41. Scharfe G, Private Communication.

42. U K Patent Specification 1143971.

43. Ancillotti F, Mauri M M, Pescarollo E, J Catalysis, 46 49-57 (1977).

44 Martinola F, Meyer A, Ion Exchange and Membranes, 2, 111-116, (1975).

45. Ihm S, Suh S, Oh I, J of Chem Eng Japan, 15, 3, 206-210 (1982).

46. Martinec A, Setinek K, Beranek L, J of Catalysis, 51, 86-95 (1978).

47. Widdecke H, Klein J, Chem Ing Tech, 53, 12, 954-957, (1981).

48. Gates B C, Schwab G M, J of Catalysis, 15, 430-434, (1969).

49. Setinek K, Beranek L, J of Catalysis, 17, 306-314, (1970).

50. Uematsu T, Tsukada K, Fujishima M, Hashimoto H, J of Catalysis 32, 369-375, (1974).

51. Misono M, Saito Y, Yoneda Y, J of Catalysis, 9, 135-145 (1967).

52. Gates B C, Wisnouskas J S, Heath H W, J of Catalysis, 24, 320-327 (1972).

53. Gates B C, Thornton R, J of Catalysis, 34, 275-287, (1974).

54. Wesley R B, Gates B C, J of Catalysis, 34, 288 (1974).

55. Reinicken R A, Gates B C, AICHE J, 20, 5, 933-940 (1974).

56. Sivanand S P, Kamath B V, Sigh R S, Chakrabarty D K, J of Catalysis, 69, 502-505, (1981).

57. Riesz P, Hammett L P, J Am Chem Soc, 76, 992 (1954).

58. Affrossman S, Murray J P, J Chem Soc (B), 1015 (1966).

59. Hepner F R, Trueblood K N, Lucas H J, J Amer Chem Soc, 74, 1333, (1952).

60. Diemer R B, Dooley K M, Gates B C, Albright R L, J of Catalysis, 74, 373-381, (1982).

61. Dooley K M, Williams J A, Gates B C, Albright R L, J of Catalysis, 74, 361-372 (1982).

62. Gicquel A, Torck B, J of Catalysis, 83, 9-18, (1983).

63. Rottmayer H H, Hartung H, Heublun G, Stackermann D, Z Chem, 23, 9, 335-337, 1983.

64. Davies C W, Thomas G G, J Chem Soc, 1607, (1952).

65. Haskell V C, Hammett L P, J Am Chem Soc, 71, 1287, 1949.

66. Bundel G, Hydration and Intermolecular Interaction: Infrared Investigations with Polyelectrolyte Membranes, Academie Press, New York, 1969.

67. Bundel G, Melzger H Z, Physik Chem (Frankfurt) 59, 225, 1968.

68. Klein J, Widdecke H, Erdöl & Kohle - Erdgas-Petrochemie, 36, 7, 307-310, Julie 1983.

69. Bothe N, Klein J, Widdecke H, Polymer 20, 849-854, 1979.

70. Frilette V J, Eriton N J, US Patent 3256250, 1966.

71. Costin C R, Rohm & Haas XN 1011, US Patent 4269943, 1981.

72. Döscher F, Klein J, Widdecke H, Makromal Chemie, 183, 93-102, 1982.

73. Magnotta V L, Gates B C, J of Polymer Science, 15, 1341-1347, 1977.

74. Fuentes G A, Bocgel J V, Gates B C, n-Butane Isomerization Catalysed by Supported Aluminium Chloride, Centre for Catalytic Science and Technology, University of Delaware.

75. Fuentes G A, Gates B C, J of Catalysis, 440-449, 1982.

76. Kluge H D, Moore F W, US Patent 2863823, 1959.

77. Kelly J T, US Patent, 2843642, 1958.

78. Huang T J, Yurchat S, US Patent 3855343, 1974.

79. Huang T J, Yurchak S, Isoparaffin/Olefin alkylation over Resin/Boron Trifluoride Catalysts, ACS Symposium Series, No 55, Industrial and Laboratory Alkylations, 1977.

80. Huang T J, Yurchak S, Am Chem Soc Proceedings, Division of Petroleum Chemistry, Preprints, 23, 3, 1021-1032, 1978.

81. Magnotta V L, Gates B C, J of Catalysis, 46, 266-274, 1977.

82. Fletcher J C Q, PhD Thesis, in preparation.

83. Duolite - Ion Exchange and absorbent resins, List of products, their properties and uses.

84. Zerolit, Testung Methods, Zerolit Limited, 1976.

85. United States Patent 2844546.

86. Foulds G, Final year project, UCT, 1983

87. Rootare H M, Prenzler C F, Surface Area from Mercury Porosimeter Measurements, J of Physical Chemistry, 71, 2733-6, 1967.

88. Dietz W A, J of Gas Chromatography, 68-71, Feb 1967.

89. Myers M E, Stollsteimer J, Wims A M, Analytical Chemistry, 47, 12, 1975.

90. Annual Book of ASTM Standards, Part 23, 1981

91. Annual Book of ASTM Standards, Part 24, 1981

92. Annual Book of ASTM Standards, Part 25, 1981

93. Annual Book of ASTM Standards, Part 47, 1981

94. Schumann W K, Final Year Project, UCT, 1982.

7. APPENDICES

A : Summary of the experiments and their significance

B : Operation of the high pressure reactors

C : Thermodynamic data

D : Catalyst treatment

- D1 : Detailed pretreatment procedure of catalysts
- D2 : Detailed reactivation procedure of catalysts
- D3 : Detailed procedure to determine dry weight capacity
- D4 : Preparation procedure for phosphonic and phosphinic functionalized resin

E : Analytical methods

- E1 : Typical gas chromatogram and gas component peak table
- E2 : Detailed procedure for determining the water content in the feed
- E3 : Standard fuel tests and their significance

Run number	Catalyst name	Temp (°C)	Pressure (bar)	WHSV	Particle size (microns)	% Exchange	Significance
1	Amberlyst 15	100	1.5	0.85	500 - 850	100	WHSV
2	Amberlyst 15	100	1.5	1.77	1000 - 1180	100	reproducibility
5	Amberlyst 15	100	1.5	1.70	500 - 850	100	gelular resin
6	Amberlyst 15	100	1.5	1.73	500 - 850	100	WHSV, particle size, temperature, regeneration, pressure, porosity
7	Amberlyst 15	100	1.5	1.79	300 - 500	100	particle size
8	Amberlyst 15	100	1.5	1.87	1000 - 1180	100	particle size, reproducibility
9	Amberlyst 15	100	1.5	1.58	500 - 850	Reg	regeneration-cationic fouling
10	Amberlyst 15	100	1.5	1.48	500 - 850	Reg	regeneration-organic fouling
11	Amberlyst 15	100	1.5	-	500 - 850	100	recycle
12	Amberlyst 15	96	0.1	1.70	500 - 850	100	temp at atmospheric pressure
14	Amberlyst 15	130	0.1	1.76	500 - 850	100	temp at atmospheric pressure
15	Amberlyst 15	160	0.1	1.88	500 - 850	100	temp at atmospheric pressure
16	Amberlyst 1010	100	1.5	1.68	500 - 850	100	porosity, WHSV
18	Amberlyst 15	100	1.5	2.53	500 - 850	100	WHSV
19	Amberlyst 15	150	1.5	1.61	500 - 850	100	temperature
21	Amberlyst 15	130	1.5	1.73	500 - 850	100	temperature
22	Duolite C26	100	1.5	1.69	500 - 850	100	porosity, WHSV, acid strength
23	Amberlyst 15	100	1.5	1.80	500 - 850	Reg	temperature regeneration (run 19)

Run number	Catalyst name	Temp (°C)	Pressure (MPa)	WHSV	Particle size	% Exchange	Significance
24	Amberlyst 15	100	1.5	1.57	500 - 850	Reg	temperature regeneration (run 21)
25	Duolite C26	100	1.5	1.15	unsieved	89	% functionalized
26	Duolite C26	100	1.5	1.11	unsieved	100	% functionalized, WHSV
27	Duolite C26	100	1.5	1.06	unsieved	37	% functionalized
28	Duolite C26	100	1.5	1.16	unsieved	96	% functionalized
29	Duolite C26 $HPO^{-}H+$	100	1.5	1.70	500 - 850	100	acid strength
30	Duolite C26 $PO_3^{2-}(H+)_2$	100	1.5	1.70	500 - 850	100	acid strength
33	Amberlyst 15	100	2.7	1.67	500 - 850	100	pressure
35	Amberlyst 1010	100	1.5	0.94	500 - 850	100	WHSV
36	Duolite C26	100	1.5	1.04	unsieved	82	% functionalized
37	Duolite C26	100	1.5	1.15	unsieved	60	% functionalized
38	Amberlyst 15	105	1.5	1.04	- 500	100	long run under typical reaction conditions

Table 7.1 : Summary of experiments and their significance

B : OPERATION OF THE HIGH PRESSURE REACTOR SYSTEM

1. PREPARING A RUN

1.1 Packing of reactor

For every run the reactor bed was packed in a similar way. This is shown in Fig. 7.1

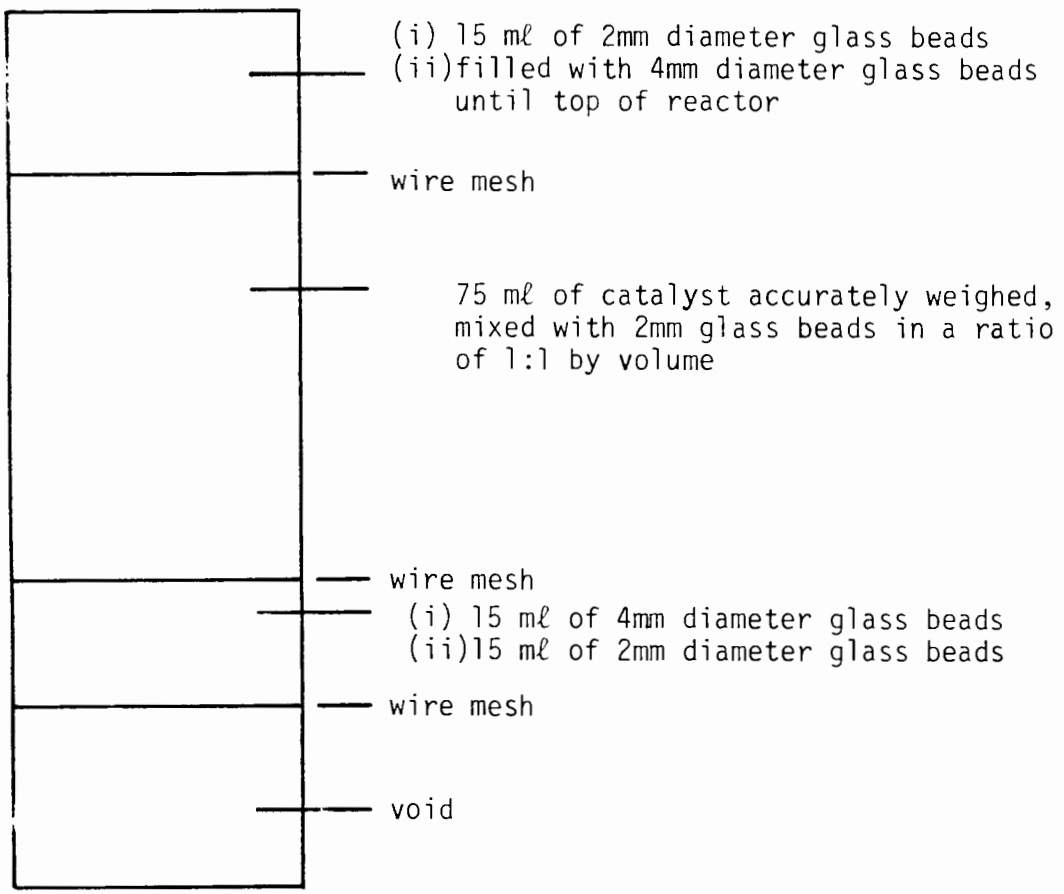

Fig. 7.1 : Packing of reactor bed

Four layers are distinguished. They are, from the bottom, :

i) A region of void space to prevent the catalyst from blocking the reactor exit.

ii) A layer of glass beads supported by a wire mesh which in turn supports the catalyst bed and prevents catalyst entrainment.

iii) The actual catalyst bed separated from the previous layer by a wire mesh. The bed itself consists of the catalyst mixed with 2mm diameter glass beads in a ratio of 1:1 by volume. The latter functions as a heat sink and as a catalyst dispersant and diluent.

iv) A layer of glass beads on top of the catalyst bed, separated by a wire mesh. The aim of this layer is to ensure plug flow of the feed, provide adequate preheating and prevent catalyst entrainment during sudden pressure drops.

The depth of each layer was accurately measured to enable temperature profiles to be plotted.

1.2 Purging of the System

Prior to start up, the reactor and downstream reactor line was purged with nitrogen for one hour at 100°C, and a LHSV of about 2000. This was done to remove any entrained air and moisture from the system. Thereafter the reactor was isolated under a nitrogen atmosphere and allowed to cool. Start-up was begun only after the reactor had returned to room temperature.

2 Start-up

Prior to introducing reactant into the system, the coolant system was allowed to operate for a sufficiently long time to ensure that the temperature reached steady state and that the temperature of the catch-pot was at 50°C. The back pressure regulator was set at the desired value. The feed cylinder was then opened and reactant introduced to the system. The reactant feed pump was started at a low pumpsetting while venting the line. The pump setting was then increased to close to its maximum and while the pressure increased to its setpoint, the system was vented intermittently.

Once the desired pressure was reached, the pumpsetting was altered to give the correct feed rate. It was found that the pump rate

was sensitive to both coolant and ambient temperatures. A gas sample was also taken to provide an analysis of the feed composition. When it was ensured that the correct feed rate was attained and no leaks were present in the system, the feed cylinder was changed and the temperature control started. Henceforward all events were recorded with time and the extent of the reaction was monitored by analysing the gas flow rate, gas composition and, later, reactant conversion to liquid product, until steady-state was attained at the desired reaction temperature and pressure. This sequence of start-up was followed, because it gave the maximum control over the reaction and, as is mentioned in the main section, was the critical stage for every run. Once steady state was reached the feed cylinder was changed again.

3 Steady state operation

The following readings were taken at selected time intervals:

- tail gas meter reading;
- reaction temperature and pressure;
- temperature profile down catalyst bed;
- G.C. analysis of a gas sample;
- G.C. analysis of a liquid sample; and
- liquid product flow rates

In addition to the above readings the feed gas cylinder was changed as required, noting the time and the mass of new and old cylinders, respectively.

4 Shut down

This was carried out in the following sequence:

- close feed cylinder;
- shut off temperature control;
- stop pump;
- take usual set of readings; and
- switch off water bath circulation system.

C : THERMODYNAMIC DATA

Fig. 7.2 shows a phase diagram of the feed used in this study. The critical temperatures and pressures of the feed components are shown in Table 7.2.

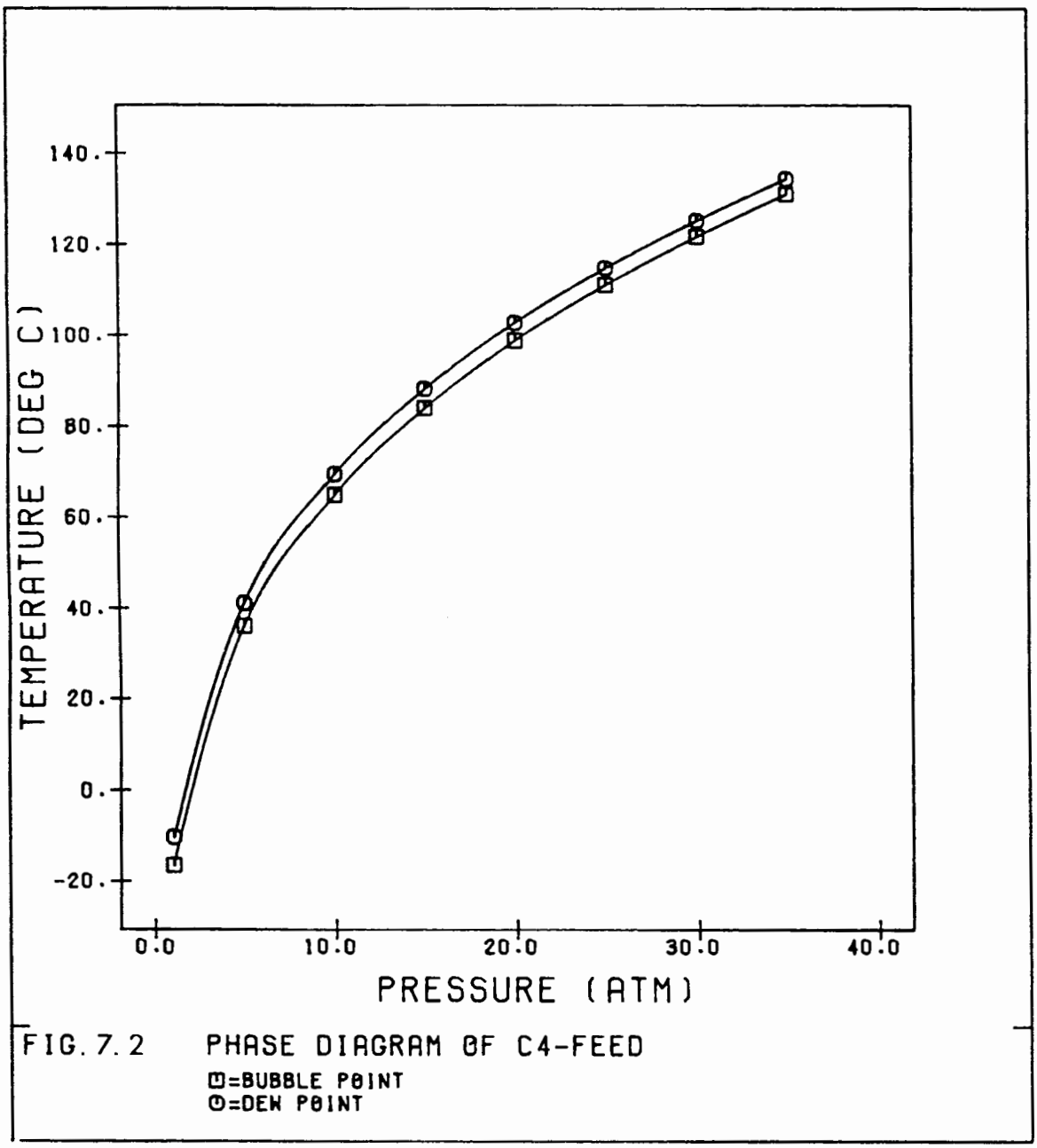

FIG. 7.2 PHASE DIAGRAM OF C4-FEED

Component	Critical Temp. (°C)	Critical Pres. (atm.)
propane	96.8	42.0
propylene	91.4	45.4
isobutane	135.0	36.0
n-butane	152.2	37.4
1-butene	145.0	39.0
isobutene	144.4	39.5
trans-2-butene	154.4	37.0
cis-2-butene	157.8	37.0

Table 7.2 Critical data of the feed components.

The boiling point of some C_8- hydrocarbons is shown in Table 7.3

Component	Boiling point
Octane	125.7
1-Octane	121.3
2.4.4, trimethyl-1-pentene	101.4
2.4.4, trimethyl-2-pentene	104.9

Table 7.3 : Boiling point of some C_8- hydrocarbons

D : CATALYST TREATMENT

D1 PRETREATMENT OF ION EXCHANGE RESINS

This was carried out in a 1000mm long, 25mm diameter glass column. Between 100 and 200 mℓ of resin was treated at a time. The exact procedure was as follows :

1. Elution with methanol. Three bed volumes of methanol were used. Prior to elution the resin bed was fluidized to remove any air pockets.

2. Exchange with 4% NaOH (1.043g mol/ℓ). A 100% excess of base was used (4) relative to the capacity of the resin, i.e.

$$\text{vol. NaOH (m}\ell\text{)} = 2 \times \frac{\text{cap. of resin (meq/m}\ell\text{) x vol. of cat.(m}\ell\text{)}}{1.043\text{(m mol/m}\ell\text{)}}$$

   This exchange was done over 30 minutes, although the conversion of the H+ to Na+ form is virtually complete in 20 seconds (4).

3. Washing with distilled water. This was continued until the effluent from the column was neutral to universal indicator paper.

4. Exchange with 14% H_2SO_4 (1.56g mol/ℓ). A 400% excess acid was used (4) relative to the capacity of the resin, i.e.

$$\text{vol. } H_2SO_4 \text{ (m}\ell\text{)} = 5 \times \frac{\text{cap of resin (meq/m}\ell\text{)xvol of cat (m}\ell\text{)}}{1.56 \text{ (m mol/m}\ell\text{)}}$$

   This exchange was done over 30 minutes, although the conversion of the Na^+ to H^+ form is virtually complete in 60 seconds (4).

5. Washing with distilled water. This was continued until the effluent from the column was neutral to universal indicator paper.

6. The resin was either stored in distilled water or dried at 100°C and atmospheric pressure for 24 hours for further use.

D2 : REACTIVATION OF FOULED ION EXCHANGE RESINS

2.1 Reactivation Procedure for Cationic Fouled Ion Exchange Resins

This is carried out in a 1000mm long, 25mm diameter glass column.

1. The sample is fluidized and rinsed with three bed volumes of methanol.

2. The sample is washed with distilled water, again using approximately three bed volumes.

3. 14% Sulphuric acid is passed through the catalyst bed at a rate of four bed volumes per hour until a total of two bed volumes of sulphuric acid has passed through the column.

4. The excess regenerant is rinsed off with distilled water until the pH of the effluent is above 4.

5. The sample is stored in distilled water or dried under the usual conditions.

2.2 Reactivation Procedure for Organically Fouled Ion Exchange Resins

This is carried out in a 500mℓ three-neck flask equipped with a mechanical stirrer, a reflux condenser and immersion thermometer.

1. Approximately 50g of used catalyst is added to the flask. To this 150mℓ of concentrated sulphuric acid (98%) is introduced and the content heated at 100°C under continuous agitation for eight hours.

2. The cooled resin is transferred to a 1000mm long, 25mm diameter glass column and the excess acid drained.

3. The sample is rinsed with distilled water until it is neutral to universal indicator paper.

4. The sample is stored in distilled water, or dried under the usual conditions.

D3 : METHOD FOR DETERMINING TOTAL ACID CAPACITY

1. The resin is dried to constant weight at 100 ± 5°C.

2. About 0.5g of the dry resin is weighed out into a conical flask containing 25mℓ of distilled water.

3. To this is added 10mℓ of 1 N NaOH measured by pipette.

4. The flask is then stoppered, and left to stand for four hours with occasional shaking.

5. The content of the flask is then back titrated with 0.5 N HCl using thymolphthalein indicator solution.

6. Capacity (meq/g) = $\frac{10N_1 - N_2 t}{W}$

where W = weight of dry resin (g)

N_1 = normality of standard NaOH

N_2 = normality of standard HCl

t = titre of standard HCl (mℓ)

The final capacity is the mean of three readings.

D4 : PREPARATION OF ION EXCHANGE RESINS CONTAINING PHOSPHONIC AND PHOSPHINIC FUNCTIONAL GROUPS

1. Reaction of resin matrix with phosphorus trihalide

50 Parts by weight of thoroughly dried beads of the resin matrix are placed into a vessel containing 268 parts by weight of phosphorus trichloride (dried by distillation), and then 60 parts by weight of an anhydrous aluminium chloride is added. This mixture is heated under continuous stirring and reflux at the boiling point of the phosphorus trichloride (73.5°C) for six hours. Anhydrous conditions are maintained by using a tube filled with molecular sieves in a flask fitted to a reflux condenser. Perchloroethylene, dried by distillation, is then added to serve as a heat transfer medium and essentially all of the phosphorus trichloride is removed by fractional distillation.

2. Hydrolysis

The dichlorophosphine derivative of the resin prepared as described above is added to a large excess of water and stirred, with resultant evolution of hydrogen chloride gas accompanied by generation of heat. The resin beads are then washed several times with water and then with a solution of 2N NaOH. Finally, the dichlorophosphine derivative of the resin is placed in a glass vessel containing 2N NaOh and is heated for two hours at 90°C, in order to complete the hydrolysis. The resin beads are then washed in an excess of 4N HCl and rinsed in distilled water until the pH is higher than 4. The D.W.C. is then determined.

3. Oxidation

One half of the bead product from the hydrolysis step is immersed in a flask containing an excess of 2N nitric acid.

The mixture is heated to 95°C and maintained at this temperature for two hours under continuous mixing. It is then allowed to cool before it is rinsed with distilled water until the pH is greater than 4. The D.W.C. is then determined.

E : ANALYTICAL METHODS

E1 : TYPICAL GAS CHROMATOGRAM AND GAS COMPONENT PEAK TABLE

Fig. 7.3 shows a typical gas chromatogram and the assignment of the various peaks.

Table 7.4 summarises these peaks and gives their approximate response time and their R.R.F. respectively.

Gas component	Approximate retention time	Relative response factor
propane	5.60	103.00
propene	6.60	100.00
isobutane	7.80	97.00
n-butane	8.30	97.00
1-butene	9.65	96.00
isobutene	9.90	96.00
trans-2-butene	10.20	96.00
cis-2-butene	10.50	96.00
$C_5's$	12.23	96.00
unknown	11.10, 13.20, 13.90, 14.70, 14.90, 15.30	96.00

Table 7.4 : Peak table of feed

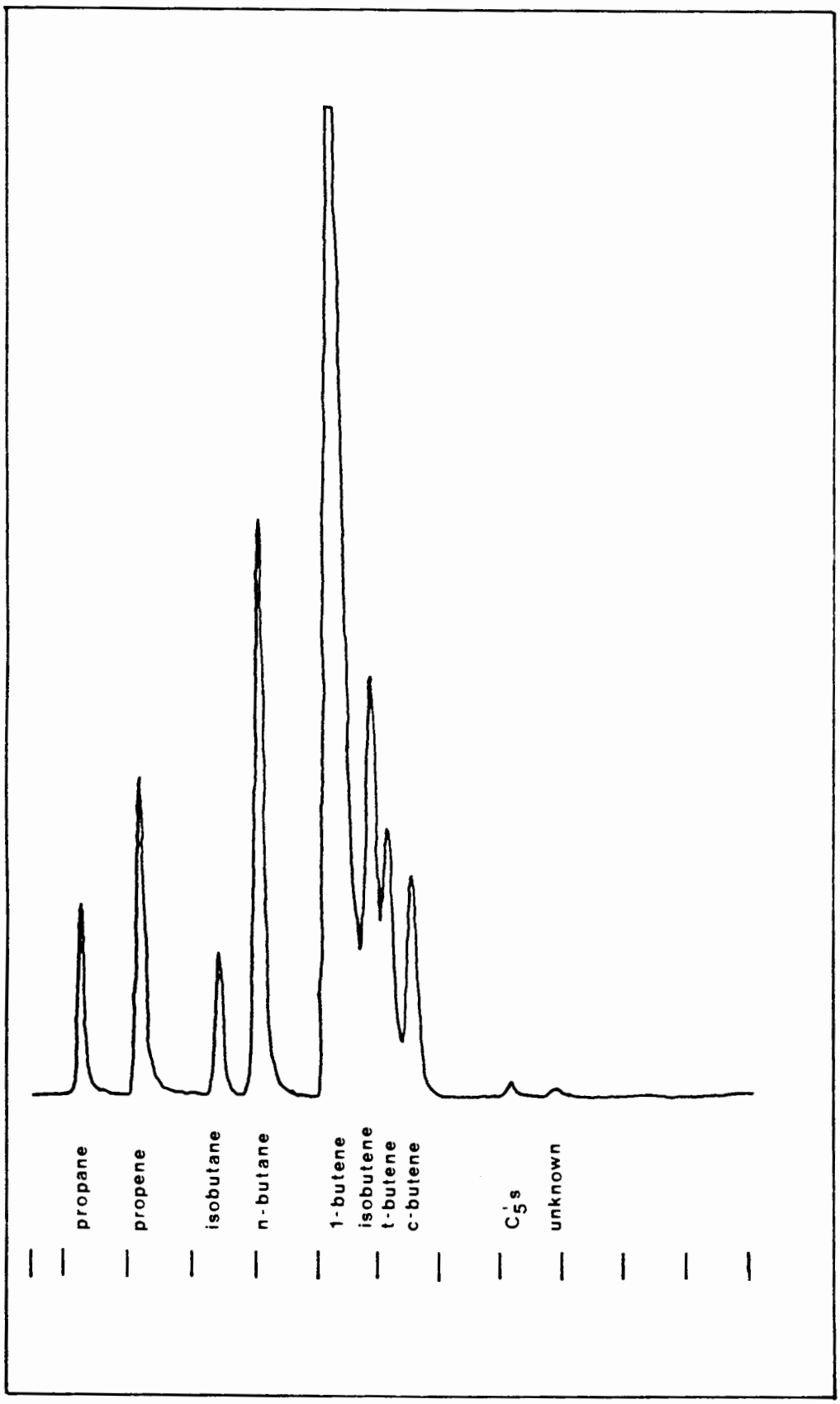

Fig. 7.3 : Typical feed gas chromatogram

E2 : DETERMINATION OF THE WATER CONTENT IN THE OLEFINIC FEED

1. Setting up a correlation between the T.C.D. response and the water concentration in the carrier gas stream.

All this work was carried out under anhydrous conditions. This was achieved by storing all liquids in volumentric flasks fitted with suba seals. Liquids were transferred with syringes. Methanol was used to dilute the water, since the retention time difference between these two components was the largest for the solvents tested, and for the columns available. Two 2300mm long, 3mm I.D. stainless steel columns packed with Poropak Q were used. The carrier gas was nitrogen. The water signal was found to tail-off significantly. Various temperature programs were tested and finally the following was used, because it gave the most distinct peaks:

Temp. of detector:	140°C
Temp. of injector:	150°C
Temp. of filament:	240°C (chosen to give the highest sensitivity without endangering the filament)
Temp. profile:	1 min @ 80°C; 5°C/min to 125°C; 5 min @ 125°C

The following procedure was adopted:

i) The methanol was dried over 3Å molecular sieves in a sealed flask.

ii) A standard with a water concentration of 58043 p.p.m. was prepared by mixing the corresponding amounts by weight of methanol and water.

iii) A pre-weighed amount of the standard as prepared in (ii) was diluted with methanol to give a standard of concentration 10063 p.p.m. water. Similarly standards of 1679,

331 and 118 p.p.m. water respectively were prepared. A sixth standard contained the dried methanol, which still contained detectable amounts of water.

iv) For each one of these samples six chromatograms were obtained. Fig. 7.4 shows a typical chromatogram. For each chromatogram the sample volume and the time range (Δt) over which the signal appeared was noted. This, together with the accurately measured carrier gas flow rate 'Q' enabled the following analysis to be made.

$$\text{moles } H_2O = \text{sample volume } (\mu\ell) \times \text{density } \left(\frac{0.7914\text{g solu}}{\text{m}\ell}\right)$$

$$\times \text{ concentration, p.p.m. } \left(\frac{\text{g } H_2O}{10^6\text{g solu}}\right)$$

$$\times \frac{1}{\text{molecular weight}} \quad \left(\frac{1\text{ mol}}{18\text{g } H_2O}\right)$$

$$\times \frac{10^{-3}\text{m}\ell}{1\ \mu\ell}$$

volume of N_2 (in which sample was detected)

$$= \Delta t(\text{min}) \times Q\ (\text{m}\ell/\text{min})$$

$\therefore$ concentration of H_2O in carrier/gas

$$= \text{moles } H_2O/\text{volume of } N_2$$

These calculations were carried out for each of the six chromatograms of the first five samples. The area counts were corrected by subtracting from each the area count per $\mu\ell$ of the pure methanol to allow for the residual water in the latter. Finally the mean was taken for both the water concentration and the area count for each sample.

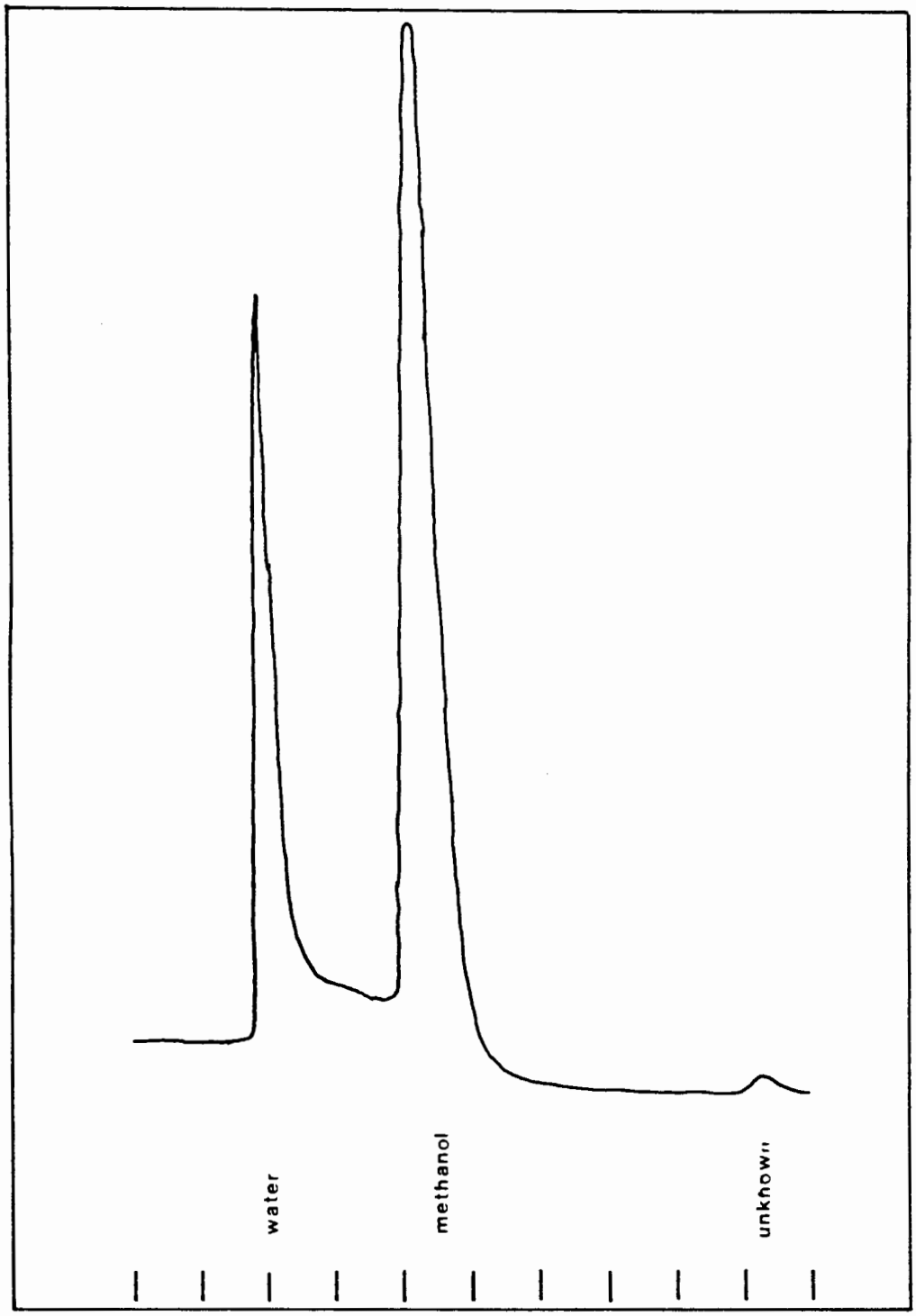

Fig. 7.4 : Typical water analysis chromatogram

v) These mean area counts, relating the detector response to the concentration of water in the carrier gas, are shown in Fig. 3.2. Due to the wide range of concentrations tested a logarithmic scale is used.

2. Determination of water content in olefinic feed by using the correlation in Fig. 3.2

The same system and conditions as in the previous section were used. However, this time a gas sample representing the olefinic feed was injected. Again the exact sample volume (ΔV), the time range over which the water signal appeared (Δt), and the carrier gas flow rate (Q) were noted. The chromatogram gave an area count which could be converted to water concentration in the carrier gas using the above correlation. From this the number of moles injected was calculated by:

$$\text{moles } H_2O = \text{conc.} \left(\frac{\text{moles } H_2O}{m\ell N_2}\right) \times Q\left(\frac{m\ell N_2}{\text{min}}\right) \times \Delta t(\text{min})$$

and the total number of moles injected by the equation:

$$\text{total number of moles} = \frac{p \times \Delta V}{RT} \quad \text{(ideal gas law)}$$

Therefore the concentration of water in the feed is given by:

$$\text{conc. } H_2O \text{ in feed (p.p.m.)} = \frac{\text{moles } H_2O}{\text{total number of moles}} \times \frac{\text{molecular weight of water}}{\text{molecular weight of feed}} \times 10^6$$

Two feed samples were tested, one of which was dried over 3Å molecular sieves and one which was not dried. The results are shown in Table 3.5

Finally, it was verified that the water content in the feed was below saturation pressure concentrations, i.e. no liquid water was present.

E3 : STANDARD FUEL TESTS AND THEIR SIGNIFICANCE

Table 7.5 gives the various test methods for motor gasoline and diesel fuel oils and the relevant ASTM/IP code.

Significance of specification for motor gasoline

Anti-knock performance and volatility define the general character of a fuel. All other requirements limit minor components of undesirable nature to such low concentrations that they have no adverse effect on engine performance.

1. Anti-knock Performance

The fuel-air mixture in the cylinder of a spark-ignition engine will, under certain conditions, burn spontaneously in localized areas instead of progressing from the spark. This may cause an audible knock. The anti-knock index is a measure of a gasoline's resistance to knock and depends on engine design, and operating and atmospheric conditions. Gasoline with an anti-knock index higher than that actually required for knock-free operation does not improve performance. Heavy and prolonged knocking may have an adverse effect in terms of power loss and possible damage to the engine. Two test methods for evaluating the anti-knock performance of motor fuels are recognized.

i) The Research Octane Number (R.O.N.) is determined by measuring the anti-knock performance under mild operating conditions, such as relatively low inlet mixture temperatures and relatively low engine speeds. It is indicative of fuel anti-knock performance in full-scale engines operating at wide open throttle and low- to medium engine speeds.

Test method	ASTM/IP code	
	Motor gasoline	Diesel fuel oil
Distillation	ASTM D86 / IP 123	ASTM D86 / IP 123
Vapour pressure (Reid)	ASTM D323 / IP 69	
R.O.N.	ASTM 2699	
M.O.N.	ASTM 2700	
Induction period	ASTM D525 / IP 40	
Existing gum	ASTM D381 / IP 131	
Potential gum	ASTM D873 / IP 138	
Sulphur content	ASTM D1266/ IP 107	ASTM D 129 / IP 61
Copper corrosion	ASTM D130 / IP 154	ASTM D 130 / IP 154
Vapour liquid ratio	ASTM D 2533	
Total acidity	ASTM D 3242	
Flash point		ASTM D 93/ IP 34
Cetane no.		ASTM D 613 / IP 41
Cold filter plugging point		IP 309
Carbon residue		ASTM D524 / IP 14
Ash content		ASTM D 482/ IP 4
Water content		IP 74
Sediment content		ASTM D 473 / IP 53
Viscosity		ASTM D 445 / IP 71
Anilene pt.		ASTM D 611 / IP 2

Table 7.5 : Standard fuel tests and their ASTM/IP code

ii) The motor octane number (M.O.N.) is determined by measuring the anti-knock performance under severe operating conditions, such as relatively high inlet mixture temperatures and relatively high engine speeds. It is indicative of fuel anti-knock performance in full-scale engines operating at wide open throttle and high engine speeds.

Correlating laboratory ratings of gasolines with their road ratings indicate the best relation of gasoline anti-knock performance to be the average of the research and motor octane numbers, (R.O.N. + M.O.N.)/2.

The octane number is expressed as a percentage of iso-octane, arbitrarily given an octane number of 100, in a blend with n-heptane (octane number 0) which matches the fuel under examination. Branched and/or aromatic molecules contribute towards a high octane number while straight chain hydrocarbons have a low octane number.

2. Volatility

In spark-ignition internal combustion engines, the gasoline is metered in liquid form through the carburettor where it is mixed with air and vapourized before entering the cylinders of the engine. Highly volatile gasolines may boil in fuel pumps, lines or carburettors and thereby cause a decrease in the fuel flow to the engine, resulting in a vapour lock, which means loss of power, rough engine operation or complete engine stoppage. Conversely, low volatile gasolines cause hard starting of cold engines, poor warm-up and acceleration, and unequal distribution of fuel to the individual cylinders.

Volatility limitations are established in terms of vapour liquid ratio, vapour pressure and distillation test results.

3. Vapour-Liquid ratio (V/L)

This is the ratio of the volume of vapour formed at atmospheric pressure to the volume of gasoline sampled. It increases with temperature for any given gasoline.

4. Distillation

This provides a measure of the volatility of the relative proportions of all the hydrocarbon components of a gasoline. The specifications designate the maximum temperatures at which 10%, 50%, and 90% of the fuel shall be evaporated and the maximum end point temperature.

The 10% evaporated temperature should be low enough to ensure ready starting under normal temperature conditions. The 50% evaporated temperature ensures good warm-up and acceleration qualities.

The 90% and maximum end point temperature should be low enough to preclude excessive dilution of the crankcase lubricating oil.

The vapour pressure, V/L ratio and distillation characteristics define and control starting, warm-up, acceleration, vapour lock, crankcase dilution, fuel economy and carburettor icing.

5. Corrosion

This test indicates whether or not the fuel will corrode the metal parts of fuel systems.

6. Existent gum

Gum is the sticky or hard non-volatile residue left on evaporation of gasoline. When present in excess, gum may cause manifold deposits and sticking of intake valves.

7. Sulphur

The limitation on sulphur content provides protection against engine wear, depletion of lubrication oil additives and corrosion of exhaust sytem parts.

8. Oxidation stability

Induction period is used as a measure of the oxidation stability of gasoline, that is, resistance to gum formation in storage.

9. Bromine number

This gives the number of grams of bromine that will react with 100g of the sample under the conditions of the test.

Significance of specifications of diesel fuel oils

1. Cetane number

This is a measure of the ignition quality of the fuel and influences combustion roughness. Increase in cetane number over values actually required does not materially improve engine performance. Accordingly, the cetane number specified should be as low as possible to ensure maximum fuel availability.

The cetane number of a fuel is the equivalent in ignition quality to the percentage by volume of cetane (cetane number by definition set equal to 100) in a mixture with α - methyl - naphthalene (cetane number by definition set equal to 0). Straight chain molecules are cetane number improvers, while branched and/or aromatic molecules reduce the cetane number.

2. Distillation

The fuel volatility requirements depend on engine design, size, nature of speed, load variations and starting and atmospheric conditions. Best fuel economy is generally obtained from the heavier types of fuels because of their higher heat content.

3. Viscosity

Minimum viscosity specifications are advantageous for some engines because of power loss due to injection pump and injector leakage. Maximum viscosity is limited by considerations involving engine design and size, and the characteristics of the injection system.

4. Carbon residue

This gives a measure of the carbon depositing tendency of a fuel oil when heated in a bulb under prescribed conditions.

5. Sulphur

The effect of sulphur content on engine wear and deposits depends largely on operating conditions.

6. Flash point

This is important in connection with fuel handling and storage and is not directly related to engine performance.

7. Cloud point

This defines the temperature at which a cloud or haze of waste crystals appears in the oil under prescribed test conditions and generally relates to the temperature at which wax crystals begin to precipitate from the oil in use.

8. Ash

Ash forming materials may be present in fuel oil in two forms: i) abrasive solids, and ii) soluble metallic soaps. The former contributes to injector, fuel pump, piston and ring wear and to engine deposits, while the latter contributes only to engine deposits.

9. Copper strip erosion

This serves as a measure of possible corrosion difficulties with copper, brass or bronze parts of the fuel system.

10. Anilene point

This is the minimum equilibrium solution temperature for equal volumes of anilene and sample.